(54) Title: ADAPTIVE FOCUSING AND NULLING HYPERTHERMIA ANNULAR AND MONOPOLE PHASED ARRAY APPLICATORS
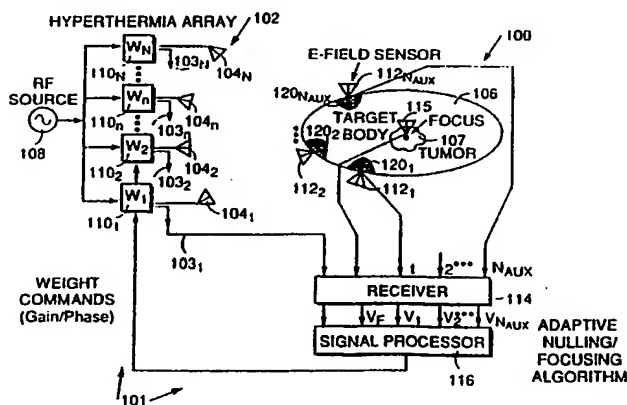
(57) Abstract

An R.F. hyperthermia phased array applicator uses adaptive nulling and focusing with non-invasive electric field probes (112) to control the electric field intensity at selected positions in and around a target body (106) to provide improved heating of solid tumors (107) during hyperthermia treatment. A gradient search or matrix inversion algorithm is used to control the amplitude and phase weighting for the phased array transmit elements (104) of the hyperthermia applicator. A 915 MHz monopole phased array hyperthermia applicator for heating brain tumors has an enclosed vessel including a plurality of monopole transmit antenna elements disposed as a circular arc array on a ground plane which has an aperture for positioning the tumor in proximity to the monopole antenna elements. Adaptive focusing with non-invasive electric field probes is used to maximize the electric field at the tumor site. Parallel plate microwave waveguides are used to direct R.F. energy from the monopole phased array to the tumor site. A microwave transmit and receive module generates amplitude and phase controlled transmit signals for exciting the monopole antenna elements, and receives passive microwave signals from the monopole antenna elements for taking non-invasive radiometry temperature measurements of the tumor site.

ADAPTIVE FOCUSING AND NULLING HYPERTHERMIA ANNULAR AND MONOPOLE PHASED ARRAY APPLICATORS

COPYRIGHT

Appendices A-D of the disclosure of this patent document contain
5   material which is subject to copyright protection. The copyright owner
has no objection to the facsimile reproduction by anyone of the patent
document or the patent disclosure, as it appears in the Patent and
Trademark Office patent file or records, but otherwise reserves all
copyright rights whatsoever.

10   ## BACKGROUND OF THE INVENTION

The successful treatment of deep-seated malignant tumors within a
patient is often a difficult task. The objective of the treatment is to reduce
in size or completely remove the tumor mass by one or more modalities
available at the treatment facility. Common treatment modalities are
15   surgery, chemotherapy, and x-ray therapy. One treatment modality used
alone or in conjunction with one of the above modalities is "tissue
heating", or hyperthermia. Hyperthermia can be considered as a form of
high fever localized within the body. A controlled thermal dose
distribution is required for hyperthermia to have a therapeutic value.
20   Typical localized-hyperthermia temperatures required for therapeutic
treatment of cancer are in the 43-45°C range. Normal tissue should be
kept at temperatures below 43°C during the treatment. Typically,
hyperthermia is induced in the body by radio-frequency (RF) waves,
acoustic (ultrasound) waves, or a combination of both. One of the most
25   difficult aspects of implementing hyperthermia, with either RF or
ultrasound waves, is producing sufficient heating at depth.
Multiple-applicator RF hyperthermia arrays are commonly used to provide a
focused near-field main beam at the tumor position. Ideally, a focal region

SUBSTITUTE SHEET

should be concentrated at the tumor site with minimal energy delivered to surrounding normal tissue.

In RF hyperthermia systems, the hyperthermia antenna beamwidth is proportional to the RF wavelength in the body. A small focal region

5   suggests that the RF wavelength be as small as possible. However, due to propagation losses in tissue, the RF depth of penetration decreases with increasing transmit frequency. One of the major side-effects in heating a deep-seated tumor with a hyperthermia antenna is the formation of undesired "hot spots" in surrounding tissue. This additional undesired

10 heating often produces pain, burns, and blistering in the patient, which requires terminating the treatment immediately. The patient does not receive anesthetics during the hyperthermia treatment in order to provide direct verbal feedback of any pain. Thus, techniques for reducing hot spots while maximizing energy delivered to the tumor site are desired in

15 hyperthermia treatment.

RF hyperthermia systems with electric field transmitting arrays, i.e., antenna arrays, in the frequency band of 60-2000 Mhz have been used to localize heating of malignant tumors within a target body. Phase control alone of the transmitting antennas of such an array has been used to

20 synthesize therapeutic RF radiation patterns within a target body. Theoretical studies of adaptive control of individual antenna phase and power (transmit weights) has been used to maximize the tumor temperature (or RF power delivered to the tumor) while minimizing the surrounding tissue temperature (or RF power delivered to the surrounding

25 tissue). Invasive temperature measuring techniques have been used to optimize the radiation pattern within a target body.

One commercially available hyperthermia annular phased-array antenna system is the Model BSD-2000, SIGMA-60 applicator, available from BSD Medical Corporation, Salt Lake City, Utah. This phased-array

30 system fully surrounds the patient, placing the patient at the center of an annular array of dipole transmit antennas. By fully surrounding the patient with an annular phased-array, it is possible to obtain constructive

SUBSTITUTE SHEET

interference (or signal enhancement) deep within the target volume. This hyperthermia system uses a 60 cm array diameter with eight uniformly spaced dipole elements operating over the frequency band 60-120 MHz. The eight dipoles are fed as four active pairs of elements. There are four

5   high-power amplifiers which drive the dipole pairs with up to 500 W average power per channel. Each of the four active channels has an electronically controlled variable-phase shifter for focusing the array. Temperature and electric-field probe sensors (both invasive and non-invasive) are used to monitor the treatment. A cool-water (5-40°C) bolus

10   between the patient and the phased-array is used to prevent excess heating of the skin surface. The water bolus is filled with circulating distilled water, which has a very low propagation loss.

SUMMARY OF THE INVENTION

In accordance with the invention, adaptive nulling and/or focusing

15   with non-invasive auxiliary probes is used to reduce or enhance the field intensity at selected positions in and around the target body while maintaining a desired focus at a tumor thereby avoiding or reducing the occurrences of "hot spots" while enhancing heating of the tumor during ultrasonic or R.F. hyperthermia treatment.

20   In general, in one aspect, the invention features a hyperthermia applicator having electric field radiators each coupled to a source of electric radiation through a controllable transmit weighting network to control the phase and amplitude of the electric field radiation transmitted by each radiator. The transmit weighting networks respond to feedback

25   signals from a controller coupled to electric field probes which receive the electric field radiation from the radiators. The controller adjusts the feedback signals in response to the received electric field radiation so that the electric field radiation is minimized at the electric field probes.

Preferred embodiments include a phased array of electric field

30   radiators, and an annular array of electric field radiators for surrounding the target.

SUBSTITUTE SHEET

-4-

The electric field probes include probes placed non-invasively around the perimeter of the target where the electric field energy is to be minimized. In one embodiment, the target is modeled as an ellipse and the electric field probes are placed at the front, back, and on both sides of the ellipse.

5   In another aspect, the invention also features a secondary electric field probe, and the controller adjusts the feedback signals in response to the electric field radiation received by the secondary electric field probe so that the electric field radiation is maximized at the secondary probe. Embodiments include placing the secondary probe at the desired focus of

10   the electric field radiation.

In yet another aspect, the invention features the controller performing either a matrix inversion algorithm or a gradient search algorithm to adjust the feedback signals controlling the transmit weighting networks in response to the electric field energy received by the electric

15   field probes.

In general, in another aspect, the invention features a hyperthermia applicator for heating a target inside a body, having electric field radiators each coupled to a source of electric radiation through a controllable transmit weighting network to control the phase and amplitude of the

20   electric field radiation transmitted by each radiator. The transmit weighting networks respond to feedback signals from a controller coupled to electric field probes placed outside the body which receive the electric field radiation from the radiators. The controller adjusts the feedback signals in response to the electric field radiation received outside the body

25   so that the electric field radiation is controlled at the target inside the body.

Preferred embodiments include a phased-array of electric field radiators, an annular array of electric field radiators for surrounding the target, and an array of monopole antenna elements for positioning nearby

30   the target.

In preferred embodiments of the monopole array, the monopole antenna elements are perpendicularly mounted to one side of an RF

SUBSTITUTE SHEET

reflecting groundplane. An RF reflecting screen is mounted perpendicular to the groundplane surface behind the monopole antenna elements to reflect RF energy from the monopole antenna elements toward the target. The ground plane includes an aperture for positioning the target on the

5   same side of the ground plane as the monopole antenna elements. An enclosure surrounds the monopole antenna elements and provides a vessel for enclosing a bolus of fluid, such as deionized water, between the monopole antenna elements and the body. In other preferred embodiments another ground plane is provided above the monopole

10   antenna elements to form a waveguide between the antenna elements and the target body. Further, multiple waveguides and monopole antenna arrays can be stacked.

In other preferred embodiments of the monopole array, the monopole array antenna elements resonate between 800 and 1000 MHz

15   and are arranged in a circular arc having a radius of between 5 and 20 cm. The body is a cranium and the target is a brain tumor. The radius of the monopole array circular arc is either the distance from the monopole antenna array to the center of the cranium, or to the target tumor.

In still other preferred embodiments, the electric field probes are

20   non-invasively placed along the perimeter of the body between the elements of the phased-array and the target. The controller adjusts the feedback signal, with a gradient search or matrix inversion algorithm, to minimize the difference in the electric field detected by adjacent electric field probes and thereby provide uniform electric field radiation into the

25   body.

In yet other preferred embodiments, the electric field probes are formed into an array non-invasively placed between the phased array and the target. The controller adjusts the feedback signal, with a gradient search or matrix inversion algorithm, to provide a particular electric field

30   pattern across the electric field probe array and thereby focus radiation into the target. The electric field probe array elements are placed symmetrically with respect to a bisector line which runs from the target to

SUBSTITUTE SHEET

the phased array to bisect the phased array. The controller adjusts the feedback signal to balance the electric field pattern with respect to the bisector line, and to minimize the difference in the electric field detected along the bisector line.

5   Thus, the present invention offers the advantages of allowing effective hyperthermia treatment to be applied to deep-seated tumors within the body while reducing or eliminating hot-spot formation on the surface of the body which interferes with the treatment. Another advantage is that hot spots are eliminated quickly by sensing and adjusting

10   the E-field radiation in the vicinity of the expected hot spot rather than by measuring the temperature rise of the tissue after heating has already occurred. Still another advantage is that the E-field sensing probes may be located on the surface of the target rather than having to be invasively placed within the target body. A further advantage is that the E-field

15   radiation can be focused on a target inside a body using E-field sensing probes non-invasively placed outside the body to maximize heating of the target tissue.

BRIEF DESCRIPTION OF THE DRAWINGS

The foregoing and other objects, features and advantages of the

20   invention will be apparent from the following more particular description of preferred embodiments of the invention, as illustrated in the accompanying drawings in which like reference characters refer to the same parts throughout different views. The drawings are not necessarily to scale, emphasis instead being placed upon illustrating the principles of the

25   invention.

FIG. 1 is a perspective view of an RF annular array hyperthermia system featuring the adaptive nulling of this invention.

FIG. 2 is a cross-sectional representation of the annular array of FIG. 1.

30   FIG. 3 is an analytical model of the cross-sectional representation of FIG. 2.

SUBSTITUTE SHEET

FIG. 4 is a simulated thermal profile of the analytical model of FIG. 3 without the adaptive nulling of this invention.

FIG. 5 is a simulated thermal profile of the analytical model of FIG. 3 with the adaptive nulling of this invention.

5   FIG. 6 is a schematic diagram of the adaptive hyperthermia array and array controller of FIG. 1.

FIG. 7 is a schematic diagram of an analytical model of an adaptive array for simulating the hyperthermia array of FIG. 1.

FIG. 8 is a block diagram detailing the sample matrix inversion

10   algorithm derived from the adaptive hyperthermia array model of FIG. 7.

FIG. 9 is a block diagram of the sample matrix inversion algorithm performed by the hyperthermia array controller of FIG. 6.

FIG. 10 is a scatter diagram of transmit weights used in deriving the gradient search adaptive hyperthermia algorithm.

15   FIG. 11 is a diagram showing the derivation of the gradient search directions.

FIG. 12 is a block diagram of the gradient search performed by the hyperthermia array controller of FIG. 6.

FIG. 13 is a schematic diagram of the analytical model of FIG. 7

20   redrawn to simplify derivation of method of moments analysis.

FIG. 14 is a schematic diagram of an equivalent circuit model for simulating an auxiliary probe.

FIG. 15 is a schematic diagram of a thermal conductivity model for simulating hyperthermia heating within a target.

25   FIG. 16(a) is a block diagram detailing the simulation model of the hyperthermia array of FIG. 1.

FIG. 16(b) is a table of values used in the simulation model of FIG. 16(a).

FIG. 17 is a schematic diagram of the transmit antenna array and

30   auxiliary probe array geometries for the simulation model of FIG. 16(a).

FIG. 18 is a diagram of the simulated E-field for the simulation model of FIG. 16(a) prior to adaptive nulling.

SUBSTITUTE SHEET

FIG. 19 is a diagram of the simulated profile in 1 dB steps for the E-field of FIG. 18.

FIGS. 20 and 21 are diagrams of the simulated E-field profile of FIG. 19 taken along the x- and z- axes, respectively.

5   FIG. 22 is a diagram of the simulated E-field for the simulation model of FIG. 16(a) after adaptive nulling.

FIGS. 23 and 24 are diagrams of the simulated E-field of FIGS. 18 and 22 taken along the x- and z- axes, respectively.

FIG. 25(a) is a diagram of the simulated E-field before and after

10   adaptive nulling taken longitudinally in the y direction along the x = 15, z = 0 cm line of the geometry shown in FIG. 25(b).

FIG. 26(a) is a diagram of the simulated E-field before and after adaptive nulling taken longitudinally along the y axis (x = 0, z = 0 cm) of the geometry shown in FIG. 26(b).

15   FIGS. 27(a) and 27(b) are graphs showing the transmit weight amplitude and phase, respectively, before and after adaptive nulling.

FIG. 28 is a graph showing the channel correlation matrix eigenvalues.

FIG. 29 is a diagram of the simulated target temperature profile for

20   the E-field of FIG. 18 prior to adaptive nulling.

FIGS. 30 and 31 are diagrams of the temperature profile of FIG. 29 taken along the x- and z- axes, respectively.

FIG. 32 is a diagram of the simulated target temperature profile for the E-field of FIG. 22 after adaptive nulling.

25   FIGS. 33 and 34 are diagrams of the temperature profile of FIGS. 29 and 32 taken along the x- and z- axes, respectively.

FIG. 35 is a diagram of the simulated target temperature profile for the E-field of FIG. 18 prior to adaptive nulling.

FIG. 36 is a diagram of the simulated target temperature profile for

30   the E-field of FIG. 22 after adaptive nulling.

FIGS. 37 and 38 are diagrams of the temperature profile of FIG. 36 taken along the x- and z- axis, respectively.

SUBSTITUTE SHEET

FIG. 39 is a cross-sectional view of an annular phased array hyperthermia system and saline phantom used for gathering experimental adaptive nulling and focusing data.

FIG. 40 is a diagram of the E-field amplitude measured at a single null site, the tumor site, and a reference site, versus gradient search iteration for the experimental hyperthermia system and phantom of FIG. 39.

FIG. 41 is a diagram of the simulated E-field power versus gradient search iteration at the single null site of FIG. 40.

FIG. 42 is a cross-sectional view of a beef phantom used in place of the saline phantom in the experimental system of FIG. 39.

FIG. 43 is a diagram of the E-field amplitude measured at a single null site, the tumor site, and a reference site, versus gradient search iteration for the experimental hyperthermia system of FIG. 39 using the beef phantom of FIG. 42.

FIG. 44 is a diagram of the measured temperature versus time at the beef phantom tumor site and the single null site of FIG. 42.

FIG. 45 is a diagram of the E-field amplitude measured at two null sites and the tumor site, versus gradient search iteration for the experimental hyperthermia system and phantom of FIG. 39.

FIG. 46 is a diagram of the E-field amplitude measured at a focus on the surface of the saline phantom versus gradient search iteration for the experimental hyperthermia system and phantom of FIG. 39.

FIG. 47 is a perspective view of an RF monopole array hyperthermia system for treating brain tumors, featuring the adaptive focusing of this invention.

FIG. 48 is a top-view of the monopole phased array hyperthermia system of FIG. 47

FIG. 49 is a cross-sectional side view of the RF monopole phased array hyperthermia system of FIG. 47.

FIG. 50 is a schematic diagram of the monopole phased array hyperthermia system of FIG. 47 and an array controller.

SUBSTITUTE SHEET

FIG. 51 is a schematic diagram of the monopole phased array geometries for the hyperthermia system of FIG. 47.

FIG. 52 is a schematic diagram of the monopole phased array and electric field probe array geometries for the hyperthermia system of FIG. 47.

FIG. 53 is a diagram of a simulated E-field pattern for the monopole phased array geometry of FIG. 52.

FIG. 54 is a diagram of the simulated E-field pattern of FIG. 53 taken parallel to the x- axis along the line z = 5.08 cm.

FIG. 55 is a diagram of the simulated temperature profile for the simulated E-field pattern of FIG. 53.

FIG. 56 is a schematic diagram of the monopole phased array hyperthermia system of FIG. 47 with an electric field probe array for generating uniform RF illumination over a large area of a target.

FIG. 57 show the monopole phased array system of FIG. 48 including the addition of a top ground plane surface forming a parallel plate waveguide.

FIGS. 58A shows a cross-sectional view of the wave guide of FIG. 57.

FIG. 58B shows a cross-sectional view of an alternative embodiment of the waveguide of FIG. 58A having diverging surfaces.

FIG. 58C shows a cross-sectional view of another alternative embodiment of the waveguide of FIG. 58A having flared surfaces forming a horn.

FIG. 59 shows a cross-sectional view of another alternative embodiment of the waveguide of FIG. 58A having multiple stacked monopole phased array antennas and associated stacked waveguides.

FIG. 60 is a block diagram of a microwave transmit and receive module for use with the monopole phased array system of FIG. 47.

SUBSTITUTE SHEET

DETAILED DESCRIPTION OF THE PREFERRED EMBODIMENT

Apparatus

Referring to FIG. 1, there is shown a hyperthermia annular phased-array system 100 having improved "hot spot" characteristics achieved by
5 utilizing the focused near-field adaptive nulling apparatus of this invention. An annular hyperthermia phased-array applicator 102, energized by a hyperthermia array controller 101, has a plurality of dipole transmit antenna elements 104 placed around a patient to be treated, or target body 106. The dipole antenna elements are uniformly disposed around the
10 patient. Each dipole antenna element is oriented parallel to the other dipole antennas and parallel to a longitudinal axis A-A passing through the center of a cylinder defined by applicator 102. The patient is positioned within the hyperthermia phased array applicator 102 such that the deep-seated tumor to be treated 107 is at the approximate center, or focus, of
15 the phased array applicator. A water-bolus 105 is provided between the patient and the phased array applicator to control the temperature of the patient's skin. Phased-array applicator 102 therapeutically illuminates the target body 106 with electric field (E-field) energy radiated by dipole antenna elements 104 focused on tumor 107 deep within the body.

20 An example of a deep-seated tumor is cancer of the prostate. The tumor volume often has a decreased blood flow which aids in heating the tumor, compared to normal tissue for which heat is carried away by normal blood flow. In practice, undesired high-temperature regions away from the focus can also occur on the skin and inside the volume of the
25 target body. For example, scar tissue, which has a decreased blood flow rate, will tend to heat up more rapidly than normal tissue having normal blood flow.

In the adaptive hyperthermia array of this invention, electric-field nulls are used to reduce the power delivered to potential hot spots.
30 Computer simulations, described herein, establish that non-invasive field probes, or sensors, 112 placed on the surface of the target can be used to eliminate hot spots interior to the target tissue. With the adaptive

SUBSTITUTE SHEET

hyperthermia phased-array described herein, RF energy nulls are adaptively formed to reduce the electric field energy delivered to these potential hot spots. As will be shown, the energy nulls achieved by the adaptive nulling apparatus of this invention are both invasive to the target, i.e., extend into

5 the target body, and non-invasive to the target, i.e., on the surface of the target.

Referring to FIG. 2, there is shown a schematic cross-sectional representation of an embodiment of an eight-element hyperthermia phased-array applicator 102 of FIG. 1. Phased-array applicator 102 has

10 transmit antennas 104_1 through 104_8, arranged symmetrically surrounding a human body target 106' at the prostate level.

An analytical model of the embodiment of FIG. 2 is shown in FIG. 3. Here, an elliptical phantom target 106 is used to model the prostate-level cross section of the human body 106'. The center 107 of the elliptical

15 phantom models the location of the prostate tumor to receive hyperthermia treatment, i.e., the focus of RF energy for the phased array applicator 102. Water bolus 105 is assumed to surround the target body 106, and is treated as a homogeneous medium for analysis purposes.

Four auxiliary RF E-field probes, or sensors, 112_1 through 112_4, i.e.,

20 receiving antennas, are placed around the perimeter of the target to model non-invasive probes placed on the skin of the human body target. Each auxiliary probe 112_1 through 112_4 has a corresponding null zone 120_1 through 120_4, respectively, centered at each auxiliary probe and extending into the elliptical target region 106. Each null zone indicates an area in

25 which undesired "hot spots" are reduced or eliminated. The width of each null zone is directly related to the strength of each null. The strength of each null (sometimes referred to as the amount of cancellation) is directly related to the signal-to-noise ratio at the probe position (SNR_p). A low SNR_p indicates a large amount of nulling (strong null), and a high SNR_p

30 indicates a small amount of nulling (weak null). The resolution, or minimum spacing, between the focus 107 and any null position is normally equal to the half-power beamwidth of the transmit antenna. Resolution

SUBSTITUTE SHEET

may be enhanced somewhat by using weak nulls whenever the separation between the null and focus is closer than the half-power beamwidth.

Referring to FIG. 4, there is shown the results of a simulation of the thermal distribution inside the target body 106 for the hyperthermia 5 ring array applicator 102 of the analytical model of FIG. 3, without adaptive nulling, transmitting into the target body. For simulation purposes, target body 106 is assumed to be a homogeneous elliptical region, and the RF energy from the array is focused at the center of the ellipse 107, simulating the tumor site. No adaptive nulling is used. The 10 contour lines of the thermal distribution represent isotherms having the indicated temperature in degrees Celsius (°C), and are spaced at 2°C intervals. The simulation shows that the focus is expected to have a temperature of approximately 46°C, while two undesired "hot spots" 122 and 124 to the left and right of the focus, respectively, are expected to 15 have temperatures of approximately 42°C.

FIG. 5 shows a simulated thermal distribution for the model of FIG. 3 where the adaptive nulling methods of this invention are applied. Comparison of FIG. 5 with FIG. 4 show that the "hot spots" 122 and 124 are essentially eliminated, no new "hot spots" have been produced within 20 the target body, and the peak temperature induced at the focus is still approximately 46°C.

Referring to FIG. 6, a generalized schematic of the non-invasive adaptive-nulling hyperthermia system of FIG. 3 includes hyperthermia transmitting phased array applicator 102 having a plurality of transmitting 25 antenna elements 104_n, where $n = 1,...,N$, surrounding target body 106 for focusing RF energy at focus 107 within the target body. Phased array applicator 102 is energized by an RF energy source 108 which is distributed to and drives each transmit antenna element 104_n through a corresponding transmit weighting function 110_n, each having a 30 corresponding weight w_n. Each weighting function w_n may affect the gain and phase of the RF energy fed to its corresponding antenna 104_n in the array, i.e., w_n represents a complex weighting function. Each weighting

SUBSTITUTE SHEET

-14-

function 110_n may be implemented by a voltage controlled RF amplifier and a voltage controlled RF phase shifter. An amplitude control voltage representing the amplitude component of transmit weight w_n is fed to the voltage controlled amplifier, and a phase control voltage representing the

5 phase of transmit weight w_n is fed to the voltage controlled phase shifter.

Target body 106 has a plurality of E-field auxiliary probes 112_m, where $m = 1,....,N_{aux}$, i.e., receiving antennas, positioned at various locations on the surface of the body for sampling the E-field at each particular location. Another receiving probe 115 may be placed at the

10 desired focus 107 of the array.

Receiving probes 112_m and 115 each drive an input to an RF receiver 114. The transmit amplitude and phase weights of each weighting function w_n are fed to the receiver 114 through lines 103_n and are used to find the transmit level of each transmit element 104_n. The

15 outputs of receiver 114 represent the auxiliary probe-received complex voltages $v_1, v_2 \cdots, v_{Naux}$, the focus probe-received complex voltage v_F, and the transmit level of the phased array. The receiver outputs drive the inputs of a signal processor 116, which applies a nulling algorithm to adjust the weighting functions w_n and thereby null, or minimize, the RF

20 signal received by each receiving probe 112_m, i.e., minimize the SNR_p at each probe.

To generate the desired field distribution in a clinical adaptive hyperthermia system, the receiving probes are positioned as close as possible to the focus (tumor site) and to where high temperatures are to

25 be avoided (such as near the spinal cord and scar tissue). For an annular array configuration the receiving probes can be located non-invasively on the surface (skin) of the target. Initially, the hyperthermia array is focused to produce the required field intensity at the tumor. An invasive probe may be used to achieve the optimum focus at depth. To avoid undesired

30 hot spots, it is necessary to minimize the power received at the desired null positions and to constrain the array transmit weights w_n to deliver a required amount of transmitted or focal region power.

SUBSTITUTE SHEET

Signal processor 116 performs either a sample matrix inversion (SMI) algorithm or a gradient search algorithm on the signals output from receiver 114 and updates the adaptive array weights w_n (with gain g and phase ϕ) to rapidly (within seconds) form the nulls at the auxiliary probes

5   before a significant amount of target heating takes place. With this adaptive system, it is possible to avoid unintentional hot spots in the proximity of the auxiliary probes and maintain a therapeutic thermal dose distribution at the focus (tumor).

Signal processor 116 may also perform a maximizing algorithm to

10   maximize energy at the focus 107. The focus probe 115 is invasively placed at the desired focus 107, and used to generate a maximum signal, or signal-to-noise ratio (SNR_F), at the tumor site. RF receiver 114 makes an amplitude and phase measurement on the output signal from invasive probe 115 for each transmit antenna element 104_n radiating one at a time.

15   Signal processor 116 processes these measurements and feeds back weight command signals to the transmit weighting functions 110_n to calibrate or phase align the transmit channels to thereby maximize the SNR_F, or RF power, at the invasive focal point probe. If receiver 114 makes amplitude-only measurements from invasive focus probe 115, then

20   a gradient search technique may be applied by the signal processor with all elements transmitting simultaneously to maximize the SNR_F at the invasive focal point probe.

Theoretical Formulation of Nulling Algorithms

FIG. 7 shows an analytical model of a hyperthermia phased-array

25   antenna system 200, paralleling the generalized hyperthermia phased-array antenna system 100 of FIG. 6, illustrating the principles of the near-field adaptive nulling technique of this invention. The phased-array antenna system 200 includes a hyperthermia transmitting antenna array 202 having a plurality of transmitting antennas 204_n, where n = 1,...,N for

30   focusing RF energy at a desired focus 207 in the near field of the antenna. Antenna array 202 is energized by an RF energy source 208 which drives a power divider 209. Power divider 209 has one output for driving each

SUBSTITUTE SHEET

antenna 204_n a corresponding transmit weighting function 210_n, each having a corresponding transmit weight w_n. It is assumed here that each weighting function w_n may affect the phase of the RF energy fed to its corresponding antenna 204_n in the array. A calibration E-field probe 212,

5   or focus probe antenna, is positioned at focus 207 for sampling the E-field at that location.

It is assumed that the hyperthermia phased-array antenna 200 is focused (as it normally is) in the near field and that a main beam 220 and possibly sidelobes 222 are formed in the target. In general, phase and

10 amplitude focusing is possible. It is assumed that phase focusing alone is used to produce the desired quiescent main beam, i.e., weighting functions w_n affects only the phase of the RF signal driving each antenna. The signal received by the calibration probe can be maximized by adjusting the phase weighting functions w_n so that the observed transmit antenna

15 element-to-element phase variation is removed, i.e., all transmit antennas appear to be in-phase when observed from the focus.

One way to achieve phase coherence at the focus in a numerical simulation is to choose a reference path length as the distance from the focus to the phase center 224 of the array. This distance is denoted r_F

20 and the distance from the focus to the nth array transmit antenna element is denoted r_n^F. The voltage received at the calibration probe 212 (located at focus 207) due to the nth array element may be computed using the "method of moments", as described below. To maximize the received voltage at the calibration probe output, it is necessary to apply the phase

25 conjugate of the signal observed at the calibration probe, due to each array transmit antenna element, to the corresponding element at the transmit array. The resulting near-field radiation pattern will have a main beam and sidelobes. The main beam will be pointed at the array focal point, and sidelobes will exist at angles away from the main beam.

30 Auxiliary probes can then be placed at the desired null positions in the quiescent sidelobe region. These sidelobes occur where tissue hot spots

SUBSTITUTE SHEET

-17-

are likely to occur, and they are nulled by one of the adaptive nulling algorithms described below.

Adaptive Transmit Array Formulation

Considering again the hyperthermia array and probe geometry
5   shown in FIG. 7, the hyperthermia transmit antenna array 202 typically contains N identical transmit antenna elements 204. The number of adaptive channels is denoted M, and for a fully adaptive array $M=N$. The ideal transmit weights w_n (a complex voltage gain vector) are assumed in the computer simulation, with $w = (w_1, w_2, ..., w_N)^T$ denoting the adaptive
10   channel weight vector as shown in FIG. 6. (Superscript T means transpose). To generate adaptive nulls, the transmit weights (phase and gain) are controlled by either the Sample Matrix Inversion (SMI) algorithm or a gradient search algorithm. The SMI algorithm has the flexibility to operate in either open- or closed-loop feedback modes; the gradient search
15   algorithm operates only in a feedback mode.

Sample Matrix Inversion (SMI) Algorithm

For the SMI algorithm, the fundamental quantities required to fully characterize the incident field for adaptive nulling purposes are the adaptive channel cross correlations. To implement this algorithm it is
20   necessary to know the complex received voltage at each of the auxiliary probes. For example, the moment-method formulation (described below) allows computation of complex-received voltage at each of the auxiliary probes.

FIG. 8 is a block diagram showing the SMI algorithm applied to the
25   adaptive hyperthermia phased-array of FIG. 7, and the derivation of performance measures to quantify computer simulation results. Four performance measures are used to quantify the computer simulations: electric-field distribution $E(x,y,z)$, channel correlation matrix eigenvalues λ_k, $k=1,...,N$, adaptive transmit weights w_a, and interference cancellation
30   C. The calculation of these performance measures is described in detail below.

SUBSTITUTE SHEET

-18-

Assuming a spherical wavefront is incident at an ith probe antenna 226 due to each of the N array transmit antenna elements 204_n (radiating one at a time with a unity-amplitude reference signal), the result is a set of probe-received complex voltages denoted $v_1^i, v_2^i \cdots, v_N^i$ after a gain

5   adjustment 250. The cross correlation R_{mn}^i of the received voltages due to the mth and nth transmit antenna (adaptive transmit channel) at the ith probe is given by

$$R_{mn}^i = E(v_m v_n^*) \qquad , \qquad (1)$$

where $*$ means complex conjugate and $E(\cdot)$ means mathematical expectation. (Note: for convenience, in Equation (1) the superscript i in v_m

10   and in v_n has been omitted.) Because v_m and v_n represent voltages of the same waveform but at different times, R_{mn}^i is also referred to as an autocorrelation function.

In the frequency domain, assuming the transmit waveform has a band-limited white noise power spectral density (as commonly assumed in

15   radar system analysis), Equation (1) can be expressed as the frequency average

$$R_{mn}^i = \frac{1}{B} \int_{f_1}^{f_2} v_m(f) v_n^*(f) df \qquad , \qquad (2)$$

where $B = f_2 - f_1$ is the nulling bandwidth, or bandwidth of frequencies applied by the hyperthermia treatment, and f is the transmit frequency of the hyperthermia array. It should be noted that $v_m(f)$ takes into account

20   the transmit wavefront shape, which is spherical for the hyperthermia application. For the special case of a continuous wave (CW) transmit waveform, as normally used in hyperthermia, the cross correlation reduces to

SUBSTITUTE SHEET

$$R_{mn}^{i} = v_m(f_o) v_n^*(f_o) \qquad (3)$$

where f_o is the transmit frequency of the hyperthermia array.

Next, the channel correlation matrix, or interference covariance matrix, denoted R is determined 252. (Note: in hyperthermia, interference
5 is used to refer to the signals received at the auxiliary probes. The undesired "hot spots" can be thought of as interfering with the therapy.) If there are N_{aux} independent desired null positions or auxiliary probes, the N_{aux}-probe channel correlation matrix is the sum of the channel correlation matrices observed at the individual probes. That is,

$$R = \sum_{i=1}^{N_{aux}} R_i + I \qquad , \qquad (4)$$

10 where R_i is the sample channel correlation matrix observed at the ith probe and I is the identity matrix used to represent the thermal noise level of the receiver for simulation purposes.

Prior to generating an adaptive null, the adaptive channel weight vector, w, is chosen to synthesize a desired quiescent radiation pattern.
15 When nulling is desired, the optimum set of transmit weights to form an adaptive null (or nulls), denoted w_a, is computed 254 by

$$w_a = R^{-1} w_q , \qquad (5)$$

where $^{-1}$ means inverse and w_q is the quiescent weight vector. During array calibration, the normalized quiescent transmit weight vector, with

SUBSTITUTE SHEET

transmit element 204_1 radiating, is chosen to be $w_q = (1,0,0,\cdots,0)^T$, i.e., the transmit channel weight of element 204_1 is unity and the remaining transmit channel weights are zero. Similar weight settings are used to calibrate the remaining transmit elements. For a fully adaptive annular

5 array focused at the origin in homogeneous tissue, the normalized quiescent weight vector is simply $w_q = (1,1,1,\cdots,1)^T$. Commonly, the weight vector is constrained to deliver a required amount of power to the hyperthermia array or to the tumor. For simplicity in the computer simulation used to analyze the hyperthermia array, the weights are

10 constrained such that

$$\sum_{n=1}^{N} |w_n|^2 = 1 \qquad , \qquad (6)$$

where w_n is the transmit weight for the nth element. It should be noted that in the computer simulations, the electric field due to the normalized weight vector is scaled appropriately to deliver the required amount of power to the tissue so that a desired focal-region temperature level is

15 achieved after t minutes. The summation of power received at the probes is given by

$$p = w^\dagger R w \qquad , \qquad (7)$$

where † means complex conjugate transpose. The signal-plus-noise-to-noise ratio for the auxiliary probe array, denoted SNR_p,

20 is computed as the ratio of the auxiliary probe array output power (defined in Equation (7)) with the transmit signal present, to the probe array output power with only receiver noise present, that is,

SUBSTITUTE SHEET

$$INR = \frac{w^\dagger R w}{w^\dagger w} \qquad (8)$$

Next, the adaptive array cancellation ratio indicative of the null strength, denoted C, is determined 255. C is defined here as the ratio of the summation of probe-received power after adaptation to the summation of probe-received power before adaptation (quiescent); that is,

$$C = \frac{P_a}{P_q} \qquad (9)$$

5   A large amount of cancellation indicated by a large value for C indicates a strong null, while a small amount of cancellation indicated by a small value for C indicates a weak null. Substituting Equation (7) into Equation (9) yields

$$C = \frac{w_a^\dagger R w_a}{w_q^\dagger R w_q} \qquad (10)$$

10   Next, the channel correlation matrix defined by the elements in Equations (2) or (3) is Hermitian (that is, $R = R^\dagger$), which, by the spectral theorem, can be decomposed 256 in eigenspace as

$$R = \sum_{k=1}^{M} \lambda_k e_k e_k^\dagger \qquad (11)$$

where λ_k, $k = 1, 2, \cdots, M$ are the eigenvalues of R, and e_k, $k = 1, 2, \cdots, M$ are the associated eigenvectors of R. The channel correlation matrix
15   eigenvalues $(\lambda_1, \lambda_2, \cdots, \lambda_M)$ are a convenient quantitative measure of the use of the adaptive array degrees of freedom. The amplitude spread between the largest and smallest eigenvalues is a quantitative measure of

SUBSTITUTE SHEET

-22-

the dynamic range of the interference (hot spot) signals. FIG. 9 is a block diagram of the sample matrix inversion algorithm implemented by the signal processor 116 of FIG. 6. Receiver 114 generates probe-received complex voltage vector $v_1^i, v_2^i \cdots, v_N^i$ for the ith auxiliary probe. The

5 signal processor generates 280 the transmit channel correlations R_{mn}^i defined by equation (3), and sums 282 them to form the channel correlation matrix R defined by equation (4). Next, the signal processor multiplies 284 the inverse of the channel correlation matrix R^{-1} by the quiescent transmit weight vector w_q to form the new adapted transmit

10 weight vector w_a containing the adapted transmit weights fed back to the transmit weight networks 110_n of FIG. 6.

Gradient Search Algorithm

Under conditions where only the probe received voltage amplitude is measured, it is appropriate to consider a gradient search algorithm to

15 minimize the interference power at selected positions. The gradient search is used to control the transmit weights w_n iteratively such that the RF signal received by the probe array is minimized. The transmit array weights (gain and phase) are adaptively changed in small increments and the probe array output power is monitored to determine weight settings

20 that reduce the output power most rapidly to a null.

Consider J sets of N transmit weights that are applied to adaptive hyperthermia phased array applicator 102 of FIG. 6. In terms of adaptive nulling, the optimum transmit weight settings (from the collection of J sets of N transmit weights) occur when the SNR_P is minimized. Equivalently,

25 the total interference power received by the auxiliary probe array, denoted p^{rec}, is to be minimized. For notational convenience let a figure of merit F denote either the SNR_P or p^{rec} and employ a gradient search to find the optimum transmit weights to minimize F, that is,

$$F_{opt} = \min(F_j) \quad j=1,2,\cdots,J \ . \tag{12}$$

-23-

The transmit weight settings for which F_{opt} occurs yields the closest approximation to the optimal transmit weights determined by using the sample matrix inverse approach described above.

FIG. 10 shows an amplitude and phase scatter diagram for the N
5   complex transmit weights w_n at the jth configuration, i.e., the jth set of weights tried. The nth transmit weight in the jth configuration of transmit weights is denoted

$$w_{nj} = A_{nj} e^{j\phi_{nj}} ,\tag{13}$$

where A_{nj} is the transmit weight amplitude distributed over the range A_{min} to A_{max} and ϕ_{nj} is the transmit weight phase distributed over the range $-\pi$
10   to π radians.

Referring also to FIG. 11, it is desired to find the values of amplitude and phase for each of the N transmit weights such that the figure of merit F (SNR_P or p^{rec}) is minimized. When the figure of merit is minimized, adaptive radiation pattern nulls will be formed at the auxiliary
15   probe positions.

Assuming an initial setting of the N transmit weights such as those selected to focus the radiation pattern on a tumor, the weights are adjusted by dithering them until the optimum figure of merit is achieved. It is desired to find the collective search directions for the N transmit
20   weights such that F decreases most rapidly. That is, weights are selected so that the directional derivative is minimized at (A_j, ϕ_j), where A_j and ϕ_j are vectors representing the transmit amplitude weights and transmit phase weights, respectively, for the jth configuration.

The directional derivative of F_j is expressed in terms of the
25   amplitude and phase changes of the transmit weights as

SUBSTITUTE SHEET

-24-

$$D(F_j) = \sum_{n=1}^{N} \left(\frac{\partial F_j}{\partial A_{n}} r_{An_j} + \frac{\partial F_j}{\partial \Phi_{n}} r_{\phi n_j} \right) \tag{14}$$

where ∂ means partial derivative, and r_{An_j}, $r_{\phi n_j}$ are the (A, Φ) directions for which F_j is decreasing most rapidly. The directions r_{An_j}, $r_{\phi n_j}$ are constrained by

$$\sum_{i=1}^{N} (r_{An_j}^2 + r_{\phi n_j}^2) = 1 \ . \tag{15}$$

It is desired to minimize $D(F_j)$ subject to the above constraint equation.
5   Using Lagrange multipliers it is possible to construct the Lagrangian function

$$L_j = \sum_{n=1}^{N} \left(\frac{\partial F_j}{\partial A_{n}} r_{An_j} + \frac{\partial F_j}{\partial \Phi_{n}} r_{\phi n_j} \right) + G[1 - \sum_{n=1}^{N} (r_{An_j}^2 + r_{\phi n_j}^2)] \tag{16}$$

where G is a constant to be determined. The requirement that L_j be an extremum implies

$$\frac{\partial L_j}{\partial r_{An_j}} = \frac{\partial F_j}{\partial A_{n}} - 2Gr_{An_j} = 0 \ , n=1,2,\cdots,N \tag{17}$$

and

$$\frac{\partial L_j}{\partial r_{\phi n_j}} = \frac{\partial F_j}{\partial \Phi_{n}} - 2Gr_{\phi n_j} = 0 \ , n=1,2,\cdots,N \tag{18}$$

10   or that

SUBSTITUTE SHEET

$$r_{A_{nj}} = \frac{1}{2G} \frac{\partial F_j}{\partial A_{nj}} \qquad (19)$$

and

$$r_{\Phi_{nj}} = \frac{1}{2G} \frac{\partial F_j}{\partial \Phi_{nj}} \, . \qquad (20)$$

Squaring equations (19) and (20) and invoking equation (15) yields

$$\sum_{j=1}^{N} (r_{A_{nj}}^2 + r_{\Phi_{nj}}^2) = 1 = \frac{1}{4G^2} \sum_{n=1}^{N} [(\frac{\partial F_j}{\partial A_{nj}})^2 + (\frac{\partial F_j}{\partial \Phi_{nj}})^2] \qquad (21)$$

thus,

$$G = \pm \frac{1}{2} \sqrt{\sum_{n=1}^{N} [(\frac{\partial F_j}{\partial A_{nj}})^2 + (\frac{\partial F_j}{\partial \Phi_{nj}})^2]} \qquad . \qquad (22)$$

SUBSTITUTE SHEET

Substituting this expression for G in equations (19) and (20) gives

$$r_{A_{n'}} = -\frac{\dfrac{\partial F_I}{\partial A_{n'}}}{\sqrt{\displaystyle\sum_{n=1}^{N}\left[\left(\dfrac{\partial F_I}{\partial A_{n'}}\right)^2 + \left(\dfrac{\partial F_I}{\partial \Phi_{n'}}\right)^2\right]}} \qquad (23)$$

and

$$r_{\Phi_{n'}} = -\frac{\dfrac{\partial F_I}{\partial \Phi_{n'}}}{\sqrt{\displaystyle\sum_{n=1}^{N}\left[\left(\dfrac{\partial F_I}{\partial A_{n'}}\right)^2 + \left(\dfrac{\partial F_I}{\partial \Phi_{n'}}\right)^2\right]}} \qquad (24)$$

The minus sign was chosen corresponding to the direction of maximum function decrease. This choice of minus sign in equation (22) enforces

5   nulls in the hyperthermia array radiation pattern. Alternatively, if the positive sign in equation (22) is selected, then the gradient directions can be used to maximize the figure of merit for the purposes of focusing at an invasive probe at the tumor site, i.e., maximize the SNR_F. This may be used, for example, to determine the quiescent transmit weight vector w_q.

10   Thus, two gradient searches may be performed to optimize the radiation pattern of the hyperthermia array. The first to produce a peak or focused radiation pattern at the tumor, and the second to form the desired nulls at the auxiliary probes. Furthermore, these two gradient searches may be implemented as a single, combined gradient search constrained to

15   maximize the radiation pattern at the focus and minimize the radiation pattern at the desired nulls. The combined gradient search is implemented by minimizing the figure of merit defined as the ratio of the power received at the auxiliary probes to the power received by the probe at the focus.

SUBSTITUTE SHEET

-27-

The partial derivatives

$$\frac{\partial F_j}{\partial A_{nj}}, \frac{\partial F_j}{\partial \Phi_{nj}}; \quad n=1,2,\cdots,N \tag{25}$$

represent the gradient directions for maximum function decrease. Since the figure of merit F cannot be expressed here in analytical form, the partial derivatives are numerically evaluated by using finite differences.
5   Thus, we write

$$\frac{\partial F_j}{\partial A_{nj}} = \frac{\Delta F_{A_{nj}}}{2\Delta A_{nj}} \tag{26}$$

and

$$\frac{\partial F_j}{\partial \Phi_{nj}} = \frac{\Delta F_{\bullet_{nj}}}{2\Delta \Phi_{nj}} \tag{27}$$

where as shown in FIG. 2 the figure of merit differences are

$$\Delta F_{A_{nj}} = F_j(A_{nj} + \Delta A_{nj}; \Phi_{nj}) - F_j(A_{nj} - \Delta A_{nj}; \Phi_{nj}) \tag{28}$$

and

$$\Delta F_{\bullet_{nj}} = F_j(A_{nj}; \Phi_{nj} + \Delta \Phi_{nj}) - F_j(A_{nj}; \Phi_{nj} - \Delta \Phi_{nj}) \tag{29}$$

and ΔA_{nj} and $\Delta \Phi_{nj}$ are assumed to be small increments.
10   We will assume that the increments ΔA_{nj} and $\Delta \Phi_{nj}$ are independent of the configuration number and element number, that is,

SUBSTITUTE SHEET

$$\Delta A_{nj} = \Delta A \qquad (30)$$

and

$$\Delta \Phi_{nj} = \Delta \Phi \qquad . \qquad (31)$$

Substituting equations (26), (27), (30) and (31) in equations (23) and (24) gives the desired result for the search directions

$$r_{Anj} = -\frac{\dfrac{\Delta F_{Anj}}{\Delta A}}{\sqrt{\sum_{n=1}^{N} [(\dfrac{\Delta F_{Anj}}{\Delta A})^2 + (\dfrac{\Delta F_{\Phi nj}}{\Delta \Phi})^2]}} \qquad (32)$$

5   and

$$r_{\Phi nj} = -\frac{\dfrac{\Delta F_{\Phi nj}}{\Delta \Phi}}{\sqrt{\sum_{n=1}^{N} [(\dfrac{\Delta F_{Anj}}{\Delta A})^2 + (\dfrac{\Delta F_{\Phi nj}}{\Delta \Phi})^2]}} \qquad . \qquad (33)$$

Equations (32) and (33) are used to compute the new amplitude and phase settings of the (j+ 1)th transmit weight configuration according to

SUBSTITUTE SHEET

$$A_{n,j+1} = A_{nj} + \Delta A r_{Anj} \qquad\qquad (34)$$

and

$$\Phi_{n,j+1} = \Phi_{nj} + \Delta \Phi r_{\Phi nj} \; . \qquad\qquad (35)$$

In practice, it may be necessary to keep one of the transmit weights fixed (in amplitude and in phase) during the gradient search to guarantee convergence.

5   FIG. 12 is a block diagram of the gradient search algorithm implemented by the signal processor 116 of FIG. 6. Each of the N transmit antennas 104_n of phased array applicator 102 (FIG. 6) is driven through its corresponding weighting network 110_n which applies complex transmit weights w_{nj} at the jth configuration of the weights. The transmit

10   antennas induce a voltage across the ith probe antenna 112_i at the corresponding input to receiver 114 (FIG. 6). Receiver 114 amplifies the signal received from the ith probe by gain a_i to produce voltage amplitude vector $|v_{1j}^i|, |v_{2j}^i|, \cdots, |v_{Nj}^i|$ at the receiver output.

     The voltage amplitude vector is input to signal processor 116 which

15   performs the gradient search. For any initial configuration ($j = 1$) of the transmit weights w_{nj}, the signal processor causes each weight to be dithered by a small amount in amplitude, ΔA_{nj}, and phase, $\Delta \Phi_{nj}$. Each transmit weight is dithered independent of the other transmit weights, which remain in their jth configuration state. Received voltage vectors

20      $|v_{1j}^i|, |v_{2j}^i|, \cdots, |v_{Nj}^i|$, i.e., are stored and used to calculate the resulting figure of merit F_{nj} 300 for each dithered condition, the figure of merit being the power received by the auxiliary prove array. The figure of merit is a rectangular matrix of dimension N x 4, where the dimensionality of four is due to the plus and minus dithering of both of the amplitude and

25   phase. The figure of merit differences ΔF_{Anj} and $\Delta F_{\Phi nj}$ caused by

SUBSTITUTE SHEET

-30-

dithering the amplitude and phase, respectively, are calculated according
to equations (28) and (29). The gradient search directions r_{Anj} and $r_{\varphi nj}$,
based upon minimizing the auxiliary probe array received power, are then
determined 302 from the figure of merit differences according to equations

5   (32) and (33), respectively. The resulting search directions are used to
update 304 transmit weights w_{nj} to the $(j+1)$th configuration transmit
weights $w_{n,(j+1)}$ according to equations (34) and (35). The transmit
weights $w_{n,(j+1)}$ are sent to update the transmit weighting networks 110_n,
and the process is repeated. The final adaptive weight vector w_a is

10   achieved when the $(j+1)$th transmit weight configuration has converged.
Convergence is expected to occur within several hundred iterations
depending on the dither step size ΔA and $\Delta \Phi$.

It is understood that other forms of gradient searches exist which
can be used to update the transmit weights toward convergence. Another

15   such gradient search approach, where the step sizes ΔA and $\Delta \Phi$ are
computed at each iteration, is described by D.J. Farina and R.P. Flam, "A
Self-normalizing Gradient Search Adaptive Array Algorithm", IEEE
Transactions on Aerospace and Electronic Systems, November 1991, Vol.
27, No. 6, pp 901-905.

20   **COMPUTER SIMULATION OF ADAPTIVE NULLING HYPERTHERMIA**
Moment-Method Formulation

Referring again to FIG. 8, a method of moments formulation 258 is
used to compute the probe-received voltages in Equation (2) due to the
transmitting hyperthermia phased-array antenna in an infinite

25   homogeneous conducting medium. The medium is described by the three
parameters μ, ϵ, and σ, which are discussed below. The formulation given
here is analogous to that developed under array-receiving conditions for an
adaptive radar. The software used to analyze a hyperthermia array is
based on the receive-array analogy but the theory presented below is

30   given in the context of a transmit array.

SUBSTITUTE SHEET

An antenna analysis code (WIRES) originally developed by J.H. Richmond is capable of analyzing antenna or radar cross section problems. See, J.H. Richmond, "Computer program for thin-wire structures in a homogeneous conducting medium", Ohio State University, ElectroScience

5 Laboratory, Technical Report 2902-12, August 1973; and, J.H. Richmond, "Radiation and scattering by thin-wire structures in a homogeneous conducting medium (computer program description)", IEEE Trans. Antennas Propagation, Vol. AP-22, no. 2, p.365, March 1974. WIRES was modified to analyzing the near-field and far-field adaptive nulling

10 performance of thin-wire phased arrays in free space. A new version of the thin-wire code that can analyze adaptive hyperthermia arrays in an infinite homogeneous conducting medium was written to conduct the adaptive hyperthermia simulation discussed below. The new version of the thin-wire code is attached as Appendix A.

15 WIRES is a moment-method code that uses the electric field integral equation (EFIE) to enforce the boundary condition of the tangential electric field being zero at the surface of the antenna of interest. The moment-method basis and testing functions used in this code are piecewise sinusoidal.

20 Appendix B lists sample input and output files for the adaptive hyperthermia simulation. The first data file was used to generate the E-field results for a four auxiliary probe system, and the second data file was used to generate the E-field results for a two auxiliary probe system. The corresponding output files give the values for the array mutual

25 coupling, quiescent and adaptive transmit weights, channel correlation matrix, eigenvalues, and cancellation.

Referring to FIG. 13, there is shown the hyperthermia phased-array antenna system 200 of FIG. 7, redrawn to simplify the following method of moments analysis. The RF source 208, power divider 209 and weights

30 210_n of FIG. 7, are modeled as a plurality of RF signal generators 250_1 through 250_N, feeding its corresponding transmit antenna element 204_1 through 204_N. Each generator 250_1 through 250_N has a corresponding

SUBSTITUTE SHEET

amplitude and phase weight denoted by w_1 through w_N, and a known output impedance Z_L. The jth probe 226 (i.e., the same as the ith probe 226 of FIG. 7, with different notation) is modeled as a dipole antenna having an overall length L_p and an open-circuit voltage $v_j^{o.c.}$ induced by

5   the RF energy transmitted from the antenna array 200.

The open-circuit voltage at the jth probe antenna 226 is computed from the array terminal currents and from Z_n^j, the open-circuit mutual impedance between the nth array element and the jth probe antenna. Let $v_{n,j}^{o.c.}$ represent the open-circuit voltage at the jth probe due to the nth

10   transmit-array element. Here, the jth probe can denote either the focal point calibration probe (calibration probe 212 of FIG. 7) or one of the auxiliary probes used to null a sidelobe. The number of auxiliary probes is denoted by N_{aux}.

Referring also to FIG. 14, the jth probe 226 is modeled as a voltage

15   source 260, having an output voltage $v_j^{o.c.}$, driving a first impedance 262, representing the input impedance Z_{IN} of the jth probe, in series with a second impedance 264, representing the termination impedance Z_r of the jth probe. The jth probe receive current i_j^{rec} flows through these two impedances. The output voltage of the jth probe v_j^{rec} appears across the

20   termination impedance Z_r.

Referring again to FIG. 13, next, let Z denote the open-circuit mutual impedance matrix (with dimensions $N \times N$ for the N-element array). The open-circuit mutual impedance between array elements 204_m and 204_n is denoted $Z_{m,n}$. It is assumed that multiple interaction between the

25   hyperthermia array and the auxiliary probe can be neglected. Thus, the hyperthermia array terminal current vector I can be computed in terms of the transmit weights w as

$$I = [Z + Z_L I]^{-1} w \quad . \tag{36}$$

-33-

Next, let Z_n^j be the open-circuit mutual impedance between the jth probe and the nth array element. The induced open-circuit voltage $v_{n,j}^{o.c.}$ at the jth receive probe, due to the nth array element transmit current i_n, can then be expressed as

$$v_{n,j}^{o.c.} = Z_n^j \cdot i_n \qquad (37)$$

5   In matrix form, the induced open-circuit probe-voltage matrix $v_{probe}^{o.c.}$ is

$$v_{probe}^{o.c.} = Z_{probe,array} i \qquad (38)$$

or

$$v_{probe}^{o.c.} = Z_{probe,array} [Z + Z_L]^{-1} W \qquad (39)$$

where $Z_{probe,array}$ is a rectangular matrix of order $N_{aux} \times N$ for the open-circuit mutual impedance between the probe array and the hyperthermia array. Note that the jth row of the matrix $Z_{probe,array}$ is

10   written as $(Z_1^j, Z_2^j, \cdots, Z_N^j)$, where $j = 1, 2, \cdots, N_{aux}$. The receive voltage matrix is then computed by the receiving circuit equivalence theorem for an antenna. The receive-antenna equivalent circuit is depicted in FIG. 14, where it is readily determined that

$$v_{probe}^{rec} = v_{probe}^{o.c.} \frac{Z_r}{Z_{in} + Z_r} \qquad (40)$$

SUBSTITUTE SHEET

-34-

where Z_{in} is the input impedance of the probe. It should be noted that the v_{probe}^{rec} matrix is a column vector of length N_{aux} and v_j^{rec} is the jth element of the matrix. The probe-receive current matrix is given by

$$i_{probe}^{rec} = v_{probe}^{o.c.} \frac{1}{Z_{in} + Z_r} \qquad (41)$$

The jth element of the column vector i_{probe}^{rec} is denoted i_j^{rec}, $j = 1, 2, \cdots,$
5   N_{aux}. Finally, the power received by the jth probe is

$$p_j^{rec} = \frac{1}{2} Re(v_j^{rec} \cdot i_j^{rec*}) \qquad (42)$$

where Re means real part. Substituting Equations (40) and (41) into Equation (42) yields

$$p_j^{rec} = \frac{1}{2} |v_j^{o.c.}|^2 \frac{Re(Z_r)}{|Z_{in} + Z_r|^2} \qquad (43)$$

The total interference power received by the auxiliary probe array is given by
10

$$p^{rec} = \sum_{j=1}^{J_{aux}} p_j^{rec} \qquad (44)$$

SUBSTITUTE SHEET

-35-

The incident electric field E is related to the open-circuit voltage $v^{o.c.}$ by the effective height h of the probe antenna as

$$v^{o.c.} = hE \qquad (45)$$

If the length L_p of the probe antenna 226 is approximately 0.1λ or less, the current distribution is triangular and the effective height is $h = 0.5L_p$.
5 Thus, for a short-dipole probe the open-circuit voltage can be expressed as

$$v^{o.c.} = \frac{L_p}{2}E \qquad (46)$$

It then follows from Equation (46) that the E field for a short-dipole probe at position (x,y,z) is given by

$$E(x,y,z) = \frac{2v^{o.c.}(x,y,z)}{L_p} \qquad (47)$$

Finally, the quiescent and adapted E-field radiation patterns are computed using the quiescent and adapted weight vectors w_q and w_a, respectively,
10 in Equations (39) and (47). The moment-method expansion and testing functions are assumed to be sinusoidal. The open-circuit mutual impedances in Equation (39) between thin-wire dipoles in a homogeneous conducting medium are computed based on subroutines from the moment-method computer code developed by J.H. Richmond. In
15 evaluating Z_n^j for the jth auxiliary probe, double precision computations are used.

SUBSTITUTE SHEET

-36-

As mentioned previously, the array is calibrated (phased focused) initially using a short dipole at the focal point. To accomplish this numerically, having computed v_{focus}^{rec}, the transmit array weight vector **w** will have its phase commands set equal to the conjugate of the

5　corresponding phases in v_{focus}^{rec}. Transmit antenna radiation patterns are obtained by scanning (moving) a dipole probe with half-length l in the near-field and computing the receive probe-voltage response.

The received voltage matrix for the jth probe (denoted v_j^{rec}) is computed at K frequencies across the nulling bandwidth. Thus,

10　$v_j^{rec}(f_1), v_j^{rec}(f_2), \cdots, v_j^{rec}(f_K)$ are needed. For the purposes of this computer simulation, the impedance matrix is computed at K frequencies and is inverted K times. The probe channel correlation matrix elements are computed by evaluating Equation (2) numerically, using Simpson's rule numerical integration. For multiple auxiliary probes, the channel

15　correlation matrix is evaluated using Equation (4). Adaptive array radiation patterns are computed by superimposing the quiescent radiation pattern with the weighted sum of auxiliary-channel-received voltages.

Wave Propagation in Conducting Media

To gain insight into the effect of a lossy medium, e.g.. the target

20　body, on the propagation of an electromagnetic wave, it is useful to review certain fundamental equations which govern the field characteristics. In a conducting medium, Maxwell's curl equations in time-harmonic form are

$$\nabla \times H = J + j\omega\epsilon E \tag{48}$$

and

$$\nabla \times E = -j\omega\mu H \tag{49}$$

SUBSTITUTE SHEET

where E and H are the electric and magnetic fields, respectively, J is the conduction current density, $\omega = 2\pi f$ is the radian frequency, ϵ is the permittivity of the medium, and μ is the permeability of the medium. The permittivity is expressed as $\epsilon = \epsilon_r \epsilon_o$, where ϵ_r is the dielectric constant

5 (relative permittivity) and ϵ_o is the permittivity of free space. Similarly, $\mu = \mu_r \mu_o$, where μ_r is the relative permeability and μ_o is the permeability of free space. For a medium with electrical conductivity σ, J and E are related as

$$J = \sigma E \qquad (50)$$

Substituting Equation (50) into Equation (48) yields

$$\nabla \times H = (\sigma + j\omega\epsilon)E \qquad (51)$$

From Equations (48) and (49), the vector wave equation in terms of E is

10 derived as

$$\nabla^2 E - \gamma^2 E = 0 \qquad (52)$$

It is readily shown that

$$\gamma = \pm\sqrt{j\omega\mu(\sigma + j\omega\epsilon)} = \pm j\omega\sqrt{\mu\epsilon}\sqrt{1 - j\frac{\sigma}{\omega\epsilon}} \qquad (53)$$

The quantity $\sigma/\omega\epsilon$ is referred to as the loss tangent. It is common to express the complex propagation constant as

SUBSTITUTE SHEET

-38-

$$\gamma = \alpha + j\beta \tag{54}$$

where α is the attenuation constant and β is the phase constant. The constants α and β are found by setting Equation (53) equal to Equation (54) and then squaring both sides, equating the real and imaginary parts, and solving the pair of simultaneous equations, with the result

$$\alpha = \frac{\omega\sqrt{\mu\epsilon}}{\sqrt{2}}\left[\sqrt{1+(\frac{\sigma}{\omega\epsilon})^2}-1\right]^{1/2} \tag{55}$$

5   and

$$\beta = \frac{\omega\sqrt{\mu\epsilon}}{\sqrt{2}}\left[\sqrt{1+(\frac{\sigma}{\omega\epsilon})^2}+1\right]^{1/2} \tag{56}$$

The wavelength λ in the lossy dielectric is then computed from

$$\lambda = \frac{2\pi}{\beta} \tag{57}$$

The intrinsic wave impedance η is given by

$$\eta = \sqrt{\frac{j\omega\mu}{\sigma+j\omega\epsilon}} = \sqrt{\frac{\mu}{\epsilon}}\frac{1}{\sqrt{1-j\frac{\sigma}{\omega\epsilon}}} \tag{58}$$

SUBSTITUTE SHEET

The instantaneous power density of the electromagnetic field is given by Poynting's vector, denoted P,

$$P = \frac{1}{2} E \times H^*$$

(59)

which has units of (W/m^2). The time-average power flow density is equal to the real part of the complex Poynting's vector. The time-average power dissipation per unit volume P_d (W/m^3) is derived from Maxwell's equations, with the result

$$P_d = \frac{1}{2} E \cdot J^* = \frac{1}{2} \sigma |E|^2$$

(60)

The specific absorption rate (SAR) is the power dissipated or absorbed per unit mass (W/kg) of the medium (tissue), or

$$SAR = \frac{P_d}{\rho} = \frac{\sigma}{2\rho} |E|^2$$

(61)

where ρ is the density of the medium in kg/m^3.

It is convenient to have a simple equation for computing the propagation loss between any two points in the near field of an isolated transmitting antenna. Thus, mutual coupling effects are ignored for the time being. Consider a time-harmonic source radiating a spherical wave into an infinite homogeneous conducting medium. For an isotropic

SUBSTITUTE SHEET

radiator, and suppressing the $e^{j\omega t}$ time dependence, the electric field as a function of range r can be expressed as

$$E(r) = E_o \frac{e^{-\gamma r}}{r} \tag{62}$$

where E_0 is a constant.

For a source at the origin, the amplitude of the electric field at range
5   r_1 is given by

$$|E(r_1)| = E_o \frac{e^{-\alpha r_1}}{r_1} \tag{63}$$

and at range r_2 by

$$|E(r_2)| = E_o \frac{e^{-\alpha r_2}}{r_2} \tag{64}$$

The total propagation loss between ranges r_1 and r_2 is found by taking the ratio of Equations (64) and (63), or

$$\frac{|E(r_2)|}{|E(r_1)|} = \frac{r_1}{r_2} e^{-\alpha(r_2 - r_1)} \tag{65}$$

The field attenuation A_σ in dB from range r_1 to range r_2 due to the lossy
10   dielectric is simply

SUBSTITUTE SHEET

$$A_s = 20\log_{10}(e^{-\alpha(r_2-r_1)}) \tag{66}$$

Similarly, the *1/r* attenuation loss A_r in dB is

$$A_r = 20\log_{10}\frac{r_1}{r_2} \tag{67}$$

Thermal Modeling of an Inhomogeneous Target

A thermal analysis computer program called the transient thermal analyzer (TTA), developed by Arthur D. Little, Inc., has been used to
5 accomplish the thermal modeling of homogeneous muscle tissue surrounded by a constant-temperature water bolus.

The TTA program uses the finite-difference technique to solve a set of nonlinear energy balance equations. Consider a system of interconnected nodes that model an inhomogeneous volume for which the
10 temperature T_i of the *i*th node is to be determined. The heat-balance equation, which is solved by TTA, is expressed as

$$\sum_{j=1}^{N} Q_{i,j} - P_i(t) + M_i \frac{dT_i}{dt} = 0 \tag{68}$$

where $Q_{i,j}$ is the net outward heat flow from node *i* in the direction of node *j*, $P_i(t)$ is the power into node *i* at time *t*, and M_i is the thermal mass (mass times specific heat) of node *i*.
15 FIG. 15 shows an electric circuit analog 400 which is used to model the two-dimensional thermal characteristics of the material volume 402 which simulates the target body as a plurality of uniformly distributed nodes 406 spaced Δl apart. With reference to the *i*th node 406_i, but

SUBSTITUTE SHEET

-42-

applying generally to the other nodes, power P_i in watts is delivered 404_i to the ith node. Capacitor 408_i, having thermal capacitance denoted C_i (with units Joules/°C), is used to model the thermal capacitance at the ith node. Resistor 410_{ij}, having heat resistance denoted $R_{i,j}$ (with units

5   °C/W), is used to model the heat resistance between ith node 406_i and the jth node 406_j.

With a spacing of Δl between nodes (assuming cubic cells), the values of $R_{i,j}$, C_i and P_i are computed as

$$R_{i,j} = \frac{1}{k_{i,j} \Delta l} \tag{69}$$

where $k_{i,j}$ is the thermal conductivity (with units W/m°C) between nodes i

10   and j;

$$C_i = \rho_i C_{p_i} (\Delta l)^3 \tag{70}$$

where C_{p_i} is the specific heat at the ith node and ρ_i is the density (kg/m³) at the ith node; and

$$P_i = (SAR)_i \rho_i (\Delta l)^3 \tag{71}$$

where $(SAR)_i$ is the SAR for the ith node, which is given by

$$(SAR)_i = \frac{\sigma_i}{2\rho_i} |E_i|^2 \tag{72}$$

SUBSTITUTE SHEET

where σ_i is the electrical conductivity of the ith node and $|E_i|$ is the magnitude of the electric field delivered by the hyperthermia array to the ith node. It should be noted that in substituting Equation (72) into Equation (71), the density ρ_i cancels. Thus, an equivalent approach to computing the power delivered to the ith node is written in terms of the time-average power dissipated per unit volume of the ith node (denoted P_{di}) as

$$P_i = P_{di}(\Delta l)^3 \qquad (73)$$

FIG. 16 is a block diagram showing how TTA is used in the hyperthermia simulation described herein. First, the method of moments 500, controlled by the SMI nulling algorithm 502, is used to compute the electric field radiation pattern throughout a homogeneous region, simulating muscle tissue, inside an annular phased array 501. These E-field simulations assume that the signal received by a short-dipole probe within the region is due to a transmitting phased array embedded in an infinite homogeneous lossy dielectric (muscle tissue).

The resulting E-Field power distribution is then read 504 into the TTA program 506, which computes the temperature distribution inside an elliptical muscle-tissue target surrounded with a constant-temperature water bolus 507. Because the RF wavelengths in the target and water bolus are similar, the E-field simulations are believed to give a reasonable approximation to the field distribution inside the elliptical target. The computed temperature distribution is output 508 from the TTA for further analysis or display.

The E-field calculation in the assumed infinite homogeneous medium introduces additional field attenuation not present in a clinical hyperthermia system with an annular array transmitting through a water bolus into a patient. As mentioned earlier, the water bolus has very little RF propagation loss. In addition, the transmit array weights are normalized

SUBSTITUTE SHEET

-44-

according to Equation (6). Thus, no attempt is made to compute the absolute E-field strength in volts/meter in the elliptical target. Instead, the peak power in the elliptical target is adjusted (by a scale factor) to produce a desired maximum focal-region temperature (T_{max}) after t minutes. It

5   should be noted that an approximate absolute scale factor could be computed by making an initial computer simulation with an infinite homogeneous water bolus and then matching the target boundary field to the infinite homogeneous muscle tissue simulation.

The computer simulation model is related, in part, to the

10 hyperthermia annular phased-array antenna system shown in FIG. 1. The simulated array is assumed to have a 60-cm array diameter with eight uniformly spaced dipole elements which operate over the frequency band 60-120 MHz. The eight elements of the array are assumed to be fully adaptive, whereby seven independent nulls can be formed while

15 simultaneously focusing on a tumor.

It is further assumed for the purpose of this simulation that the adaptive radiation pattern null-width characteristics in a homogeneous target are similar to the characteristics observed in an inhomogeneous target. The null-width characteristics are directly related to the RF

20 wavelength, and, only a 5 percent change in wavelength occurs between the assumed muscle tissue and water bolus. With this assumption, the transmit array may be simulated as embedded in homogeneous tissue, which allows direct use of the thin-wire moment-method formulation discussed above.

25   After computing the two-dimensional E-field distribution in the homogeneous medium, we then consider only an elliptical portion of the homogeneous region and use the ellipse as the homogeneous target. In the thermal analysis, the elliptical target is surrounded with a constant 10°C water bolus. The E-field amplitude is scaled to produce a 46°C

30 peak temperature, at time $t=20$ minutes, at the center of the elliptical phantom. The initial temperature of the phantom is assumed to be 25°C (room temperature).

SUBSTITUTE SHEET

All computer simulations assume a 120 MHz operating frequency with initially four auxiliary nulling probes, i.e., $N_{aux}=4$. The parameters used in the electrical and thermal analyses are summarized in Table 1. These parameters are for a frequency of 100 MHz, but is assumed that

5   similar values of the parameters will exist at 120 MHz. It should be noted that although the relative dielectric constants of phantom muscle tissue and distilled water are very similar, the electrical conductivities are vastly different. The relevant thermal characteristics---density, specific heat, and thermal conductivity---are very similar for phantom muscle tissue and

10   distilled water.

SIMULATION RESULTS

Electric Field for Array in Homogeneous Tissue

Substituting the values $f=120$ MHz, $\sigma=0.5$ S/m, and $\epsilon_r=73.5$ into Equation (53) yields $\gamma_m = 10.0 + j23.8$ for the muscle tissue. With $\beta_m =$

15   23.8 radians/m, the wavelength in the phantom muscle tissue is $\lambda_m=26.5$ cm. The attenuation constant for the muscle tissue is $\alpha_m=10.0$ radians/m. Similarly, for distilled water $\gamma_w = 0.0021 + j22.5$, so the wavelength is $\lambda_w=27.9$ cm. The attenuation constant for the distilled water medium is $\alpha_w=0.0021$ radians/m. The propagation loss in the

20   phantom muscle tissue is $20log_{10}e^{-10.0}$, or -0.87 dB/cm. Similarly, the propagation loss in the distilled water is found to be -0.0002 dB/cm. Thus, the total loss due to propagation through 15 cm of distilled water is 0.003 dB. For 15 cm of muscle tissue the corresponding loss is 13.1 dB. The wave impedance in the muscle tissue is computed from Equation (58)

25   as $\eta_m = 33.9 + j14.2 \ \Omega$, and similarly in the distilled water $\eta_w = 42.1 + j0.004 \ \Omega$.

FIG. 17 shows the geometry used in the simulations, which parallels the array shown in FIG. 3. A 60-cm-diameter ring phased array applicator 102 of eight perfectly conducting center-fed dipoles, 104_1 through 104_8,

30   uniformly surrounds a fictitious elliptical target zone 106 with major axis 30 cm and minor axis 20 cm. The length of each dipole array element

104_n at 120 MHz in the infinite homogeneous muscle tissue is $\lambda/2$, or 13.25 cm. The array focus 107 is assumed at the origin ($x=0$, $y=0$, $z=0$) and four auxiliary short-dipole probes, 112_1 through 112_4, with length 1.27 cm (0.05λ) are positioned at (x,y,z) coordinates at (15 cm, 0,
5   0), (-15 cm, 0, 0), (0, 0, 10 cm), and (0, 0, -10 cm), respectively, i.e., the auxiliary E-field probes are located every 90° in azimuth on the perimeter of the target. In rectangular coordinates, each dipole is oriented along the $\hat{y}$ direction and the feed terminals of each dipole are located at $y=0$.

The moment-method computer simulations were run on a Sun
10   3/260 workstation. The total CPU time for a complete moment-method run is 19.2 minutes. This CPU time includes computing the quiescent and adaptive radiation patterns on a 41 by 41 grid of points. The CPU time without radiation pattern calculations is 33 seconds.

FIG. 18 shows the two-dimensional radiation pattern in the plane
15     $y=0$, before nulling, at 120 MHz with uniform amplitude and phase illumination. The calculated data are collected on a 41 by 41 grid of points over a square region, with side length 76.2 cm, centered at the focus 107. The spacing between data points is 1.905 cm, or 0.072λ, and the contour levels are displayed in 10-dB steps. The E-field data are
20   computed for the case of a 1.27-cm short-dipole observation probe. The positions of the eight dipole radiators 104_1 through 104_8 are clearly evident by the -20 dB contours surrounding each element. The radiation pattern is symmetric because of the symmetry of the array and the assumed homogeneous medium.

25   FIG. 19 shows finer contour levels (1-dB steps) for the quiescent radiation pattern of FIG. 18. Here, it is evident that the focused main beam of the ring array is increasing in amplitude as the observation point moves closer to the focus. Away from the main beam region, the pattern amplitude is seen to increase as the observation position moves toward
30   the array perimeter.

FIG. 20 shows the quiescent radiation pattern of FIG. 18 cut at $z=0$. The large amplitude that occurs at ±30 cm, i.e., at the position of

SUBSTITUTE SHEET

the phased array applicator 102, is due to the E-field probe's close
proximity to the transmitting elements 104_1 and 104_5. The large
attenuation that occurs from the array diameter to the focus is due to the
1/r attenuation loss and the loss in the uniform homogeneous muscle

5   tissue. FIG. 21 shows the radiation pattern of FIG. 18 cut at $x=0$. Here,
the pattern is identical to the pattern of FIG. 20 due to the symmetry of
the array. In both FIGS. 20 and 21 the boundary of the fictitious elliptical
target zone 106 is indicated. The target zone of FIG. 20 is larger than that
of FIG. 21 since the major axis of elliptical target 106 lies along the x-axis,

10   and the minor axis of target 106 lies along the z-axis.

The increasing radiation pattern amplitude near the left and right
sides of the elliptical target of FIG. 20 is shown to produce hot spots in
the thermal distribution. Because the top (anterior) and bottom (posterior)
of the elliptical target of FIG. 21 are not as strongly illuminated as to the

15   left and right sides of the elliptical target of FIG. 20, no quiescent hot
spots occur at the top or bottom.

Further, FIG. 20 shows that the ring-array half-power beamwidth in
the target region is approximately 13 cm, or approximately one-half the
wavelength (26.5 cm) in the phantom muscle tissue. The adaptive nulling

20   resolution or closest allowed spacing between a strong adaptive null and
the main beam has been shown to be equal to the half-power beamwidth
of the antenna. Thus, the closest allowed null position is 13 cm from the
focus. Since the target width is 30 cm across the major axis, two nulls
can be formed at $(x = \pm 15$ cm, $z=0)$ at the left and right side of the target

25   without disturbing the focus. However, if two strong nulls are formed at
the posterior and anterior $(x=0, z= \pm 10$ cm) of the target the focus will
be compromised. In practice, the water bolus surrounding the target
would restrict the placement of short-dipole probes 112_n to the surface of
the target. Thus, only weak nulls can be formed at $(x=0, z= \pm 10$ cm) so

30   that the focus will not be affected by the adaptive nulling process. That
is, the effect of the two minor axis nulls is to keep the $z= \pm 10$ cm E-field
from increasing beyond the quiescent values.

SUBSTITUTE SHEET

Next, adaptive radiation patterns are computed with four auxiliary dipole probes 112_1 through 112_4 positioned as shown in FIG. 17. The value of the receiving gain for auxiliary dipole probes 112_1 and 112_2 is adjusted to produce a SNR > 35 dB. This amount of SNR results in

5   greater than 35 dB of nulling in the direction of auxiliary dipole probes 112_1 and 112_2. In contrast, the gain values for auxiliary dipole probes 112_3 and 112_4 are turned down to produce about a 3 dB SNR. Thus, only about 3 dB of nulling will occur at probe positions 112_3 and 112_4 as the adaptive algorithm reduces the interference to the noise level of the

10   receiver. The reason for choosing these null strengths will become apparent with the data that follow.

FIG. 22 shows the two-dimensional radiation pattern after nulling with four auxiliary probes 112_1 through 112_4. Two strong adaptive nulls at $x = \pm 15$ cm occur as expected, and weak nulling occurs at $z = \pm 10$ cm,

15   also as expected.

The two strong nulls in the $z = 0$ cut are quantified in FIG. 23, where greater than 35 dB of interference nulling or pattern reduction occurs at $x = \pm 15$ cm. The peak level at the focus 107 is adjusted to 0 dB for both the quiescent and adaptive patterns. Two weak adaptive nulls

20   are seen in the $x = 0$ radiation pattern cut shown in FIG. 24. The weak nulls in effect in the adaptive patterns reduce variation from the quiescent radiation pattern.

FIG. 25(a) shows the two-dimensional radiation pattern before and after nulling taken longitudinally along a line parallel to the y-axis and

25   passing through probe 112_1 as shown in FIG. 25(b), i.e., $x = 15$ cm, $z = 0$. This radiation pattern clearly shows that a strong adaptive null also extends in the y direction from the E-field probe being nulled.

FIG. 26(a) shows the two-dimensional radiation pattern before and after nulling taken along the y-axis and passing through the focus 107 as

30   shown in FIG. 26(b), i.e., $x = 0$, $z = 0$. This radiation pattern clearly shows that the E-field at the focus remains virtually the same in the y direction before and after adaptive nulling at the E-field probes 112_1 through 112_4.

SUBSTITUTE SHEET

FIG. 27(a) shows the transmit array amplitude weights before (solid line) and after (broken line) nulling, and FIG. 27(b) shows the transmit array phase weights before (solid line) and after (broken line) nulling. As shown, the adaptive transmit weights exhibit a 5-dB dynamic range in FIG.

5   27(a).

FIG. 28 shows the channel correlation matrix eigenvalues before (solid line) and after (broken line) nulling. There are two large eigenvalues, λ_1 and λ_2, and two weak (non-zero) eigenvalues, λ_3 and λ_4, shown in FIG. 28. These eigenvalues are directly associated with the two high-SNR

10   auxiliary probes 112_1 and 112_2, and the two weak-SNR auxiliary probes 112_3 and 112_4, respectively. Note that the 0-dB level in FIG. 28 is equal to the receiver noise level. The probe-array output power before and after adaptive nulling is 31.4 dB and 0.9 dB, respectively, as calculated from equation (10). This difference in power before and after nulling indicates

15   that the adaptive cancellation is -30.5 dB.

Temperature Distribution in Elliptical Phantom

To simulate the temperature distribution in the target body resulting from the calculated E-fields, the transient thermal analysis (TTA) software is used to compute the temperature distribution in an elliptical phantom

20   surrounded with a constant-temperature water bolus. The 41 X 41 two-dimensional E-field radiation pattern data of FIGS. 18 through 24 are used as the power source for the thermal node network. Two node spacings are considered. First, the node spacing $\Delta x = \Delta z = \Delta l = 1.905$ cm (coarse grid) is used to obtain thermal data. Then, the node spacing is

25   decreased by a factor of two to $\Delta l = 0.9525$ cm (fine grid) to check convergence. The coarser spacing is shown to be adequate.

The scale factors used to convert the normalized E-field distributions to a power level that induces a 46°C peak temperature at $t = 20$ minutes are 94.1 dB and 96.0 dB for the quiescent and adaptive patterns,

30   respectively. These scale factors are determined empirically. From Equations (68) through (73) and the parameter values given in Table 1, all resistors $R_{i,j}$ in the phantom muscle tissue had a value of 96.5°C/W and

SUBSTITUTE SHEET

-50-

all resistors $R_{i,j}$ in the water bolus had a value of 87.2°C/W. The value of the capacitors C_i in the phantom muscle tissue is 23.6 J/°C. Capacitors are not used in the water-bolus region in the input to the transient thermal analysis software. Instead, a constant temperature of 10°C is enforced at

5   each water-bolus node. With a 41 X 41 grid, a total of 3280 resistors and 1681 capacitors are used in the thermal simulation. The CPU time required to compute this temperature distribution is under four minutes.

FIG. 29 shows the two-dimensional temperature distribution produced at time $t=20$ minutes in the elliptical phantom muscle tissue

10   target 106 without adaptive nulling. To generate FIG. 29, the power source used in the transient thermal analysis is the quiescent radiation pattern given in FIG. 18. The initial temperature (at time $t=0$) is 25°C. Notice the occurrence of two hot spots 122 and 124 on the left and right sides of the elliptical phantom, respectively. The peak temperature at

15   focus 107 is 46°C, which is achieved by scaling the normalized quiescent E-field as described earlier. The two hot spots 122 and 124 are quantified in the $z=0$ temperature pattern cut shown in FIG. 30, and have a peak temperature at each hot spot of approximately 41°C. The temperature profile for $x=0$ in FIG. 31 shows no hot spots. As any undesired hot spot

20   is a potential source for compromising the therapy session, adaptive nulling is used to reduce the sidelobes corresponding to the hot spots.

FIG. 32 shows the simulated two-dimensional thermal distribution at time $t=20$ minutes, with adaptive nulling at four auxiliary probes 112_1 through 112_4 in effect. The focal-spot diameter at focus 107 with

25   adaptive nulling is equivalent to the focal-spot diameter before adaptive nulling, shown in FIG. 29. Hot spots on the left and right sides of the target 106 are eliminated. FIG. 33 shows a comparison of the temperature distribution before (solid line) and after (broken line) nulling along the major axis ($z=0$) of the target ellipse 106. Similarly, FIG. 34

30   shows the temperature distribution before (solid line) and after (broken line) nulling along the minor axis ($x=0$) of the target ellipse 106.

SUBSTITUTE SHEET

-51-

The convergence of the previous thermal simulations was verified by increasing the density of E-field observation probe positions by a factor of two, with a new spacing between points of 0.9525 cm, still with a 41 X 41 grid. The ring array operates as before at 120 MHz, and there are

5   four auxiliary probes 112_1 through 112_4 laid out as shown in FIG. 17. As the auxiliary positions are the same, the adaptive weights and channel correlation matrix eigenvalues in FIGS. 27 and 28, respectively, remain the same. From the parameter values in Table 1, all resistors $R_{i,j}$ in the finer-grid muscle-tissue phantom had a value of 193.0°C/W and all

10   resistors $R_{i,j}$ in the water bolus had a value of 174.4°C/W. The value of the capacitors C_j in the phantom muscle-tissue is 2.95 J/°C. Again, a constant temperature of 10°C is enforced at each water-bolus node. The E-field scaling factors to raise the focal-point temperature to 46°C before and after nulling are 76.5 dB and 78.4 dB, respectively. The finer-grid

15   two-dimensional thermal distributions before and after nulling are shown in FIGS. 35 and 34, respectively. Although the temperature contours are smoother, the general agreement between these patterns and the coarser-grid patterns in FIGS. 29 and 32 are evident. Similarly, one-dimensional thermal pattern cuts with the finer grid are shown in

20   FIGS. 37 (x axis) and 38 (z axis), and good agreement with the coarse-grid patterns of FIGS. 33 and 35, respectively, is observed. In particular, the finer detail in FIG. 37 shows that the hot spots 122 and 124 are at approximately 42°C compared to 41°C observed for the coarse grid of FIG. 33. Thus, convergence of the coarse-grid thermal patterns is

25   demonstrated.

Elliptical Array

An elliptical phased-array hyperthermia applicator, having a 70 cm major axis and a 60 cm minor axis, was also analyzed by computer simulation. The computer simulation parameters were the same as those

30   applied to the analysis of the annular array. Generally, the computer simulations show that reduced hot spot temperatures are observed along the major axis of the elliptical phantom, without adaptive nulling, while

SUBSTITUTE SHEET

small increases in hot spot temperatures occur along the minor axis. Certain tumor geometries may be heated more efficiently with an elliptical array than with an annular array.

EXPERIMENTAL RESULTS

5   Experimental data have been gathered from a commercial annular phased-array hyperthermia system modified to perform a gradient search algorithm to produce an adaptive null (or focus) at one or more auxiliary E-field probe positions. The results confirm that a strong null can be formed at the surface of the target body without significantly affecting the power

10   delivered at the focus of the hyperthermia system.

FIG. 39 shows a cross-sectional view of the experimental system 700, which is a modified BSD-2000 SIGMA-60 annular phased-array hyperthermia applicator, available from BSD Medical Corporation, Salt Lake City, Utah. The annular array antenna 702 of the system is 59 cm in

15   diameter and includes eight uniformly spaced dipole antennas 704_1 through 704_8, excited with a four channel transmitter at 100 MHz. Each of the four transmit channel signals are distributed by separate coaxial cables from the hyperthermia controller (not shown) to a two-way power divider having two outputs. The two outputs of each two-way power

20   divider drive a pair of dipole antenna elements through a pair of coaxial cables.

A cylindrical phantom target body 706 is supported by a patient sling 705 which centrally locates the phantom within the annular array so that the longitudinal axes of the phantom and the annular array correspond

25   to each other. Phantom target 706 is a 28 cm diameter X 40 cm long polymer bottle filled with saline solution (0.9% NaCl), which simulates a human subject. A deionized water-filled bladder 705 provides a water bolus between the annular array and the target phantom.

Single Adaptive Null

30   Three E-field probes are used to monitor the amplitude of the E-field at various sites in and around the phantom for this experiment. The first E-field probe 715 (BSD Medical Corp. Model EP-500) is located inside the

SUBSTITUTE SHEET

phantom at the center, or focus, 707 of the array which simulates the tumor site. This probe monitors the amplitude of the E-field at the tumor site as the null is formed at the null site. The second E-field probe 720 (BSD Medical Corp. Model EP-100) is taped onto the outside surface of

5   the phantom at the desired null location which simulates an E-field probe taped to a patient's skin. The probe is used to monitor the amplitude of the E-field at the null site as the null is formed by the gradient search algorithm. The third E-field probe 721 (BSD Medical Corp. Model EP-400) is taped onto the outside surface of the phantom diametrically opposite

10   the location of the null site probe 720. This probe is used to monitor the amplitude of the E-field away from the null and focus sites and provides an E-field amplitude reference for the experiment.

The transmit array amplitude and phase control software and the electric field probe monitoring software supplied with the BSD-2000

15   system were modified to incorporate a gradient search feedback routine for adaptive nulling and adaptive focusing. Pascal source code listings and sample output of the adaptive nulling and focusing gradient search feedback routines are attached hereto as Appendicies C and D, respectively.

20   Fig. 40 graphically illustrates the results of this experiment, showing the measured E-field probe amplitude, in dB, versus the gradient search iteration number. The dB values are obtained by computing $10log_{10}(probe$ $output\ signal)$ and normalizing the resulting values to 0 dB at iteration 0. It is evident from this graph that the gradient search formed a strong E-

25   field amplitude null at the null site, on the order of -15 to -20 dB with respect to the reference site, in less than 50 iterations. (The apparent rise in the E-field amplitude at the null site between iterations 45 and 50 is most likely due to noise associated with the convergence calculations). Furthermore, the measured E-field amplitude at the tumor site was reduced

30   by no more than -5 dB with respect to the initial reference level. Fig. 41 shows a graphic illustration of the power, in dB, calculated at the null site versus gradient search iteration. It is evident from this graph that the

SUBSTITUTE SHEET

gradient search causes the null site power to monotonically decrease with each iteration, achieving an approximately 12 dB reduction in power within 50 iterations.

It should be noted that for at least the first 30 iterations of the
5   gradient search, there is good agreement between the computer simulations, presented above, and these experimental measurements. After approximately 30 iterations, however, the results of the computer simulations differ from the experimental measurements. One reason for this difference is that the computer simulations herein described do not
10 attempt to accurately model all the characteristics of the BSD-2000 system used for the experiments. For example, the simulations do not account for phase shifter non-linearities, A/D convertor errors, or D/A convertor errors associated with the system which will affect the experimental measurements, especially at the relatively low signal levels
15 present after 30 iterations. Thus, it is not expected that the computer simulations and the experimental results will necessarily behave the same where the signals or computations are most affected by measurement system noise.

Single Adaptive Null- Beef Phantom

20   Referring to Fig. 42, in another experiment, a single adaptive null was produced in a beef phantom 706' used in place of the saline phantom 706 of Fig. 39 to better simulate human tissue. Beef phantom 706' was a 24 lbs. hind leg cut having a front face width of 38 cm, a front face height of 23 cm and a thickness of 15 cm. The E-field probe positions
25 used with the beef phantom are analogous to the E-field probe positions used with the saline phantom. That is, the first E-field probe 715' (BSD Medical Corp. Model EP-500) is located inside the beef phantom at the center, or focus, 707' of the array which simulates the tumor site. This probe monitors the amplitude of the E-field at the tumor site as the null is
30 formed at the null site. The second E-field probe 720' (BSD Medical Corp. Model EP-100) is taped onto the outside surface of the beef phantom at the desired null location which simulates an E-field probe taped to a

SUBSTITUTE SHEET

-55-

patient's skin. This probe is used to monitor the amplitude of the E-field at the null site as the null is formed by the gradient search algorithm. The third E-field probe 721' (BSD Medical Corp. Model EP-400) is taped onto the outside surface of the beef phantom diametrically opposite the location
5   of the null site probe 720'. This probe is used to monitor the amplitude of the E-field away from the null and focus sites and provides an E-field amplitude reference for the experiment.

Fig. 43 graphically illustrates the results of the beef phantom experiment, showing the measured E-field probe amplitude, in dB, versus
10 the gradient search iteration number. Again, the dB values are obtained by computing $10log_{10}(probe\ output\ signal)$ and normalizing the resulting values to 0 dB at iteration 0. It is evident from this graph that the gradient search formed a strong E-field amplitude null at the null site 720', on the order of -18 to -20 dB with respect to the reference site, in less
15 than 50 iterations. Furthermore, the E-field amplitude at the tumor site was reduced by no more than -2 dB with respect to the initial reference level. It should be noted that these results are very similar to the results obtained with the saline phantom (Fig. 40).

Fig. 44 shows a comparison between the temperature rise at the
20 beef phantom tumor site 707' and the null site 720' during nulling. A thermocouple probe was located at each of the tumor and null sites, and the RF power was applied in four intervals of 15 minutes power on and 5 minutes power off for a total experiment time of 80 minutes. The gradient search performed 10 iterations during the 15 minute power on portion of
25 each interval. Temperature measurements were taken during the 5 minute power off portion of each interval, i.e., one measurement for each 10 iterations. The experimental data shows that the tumor site was initially at about 26°C and the null site was initially at about 27°C before applying RF power. After 40 minutes (30 minutes power on and 10 minutes power
30 off) the temperature of the tumor site has risen 4°C to about 30°C, while the null site has risen only 1°C to about 28°C. After 80 minutes (60 minutes power on and 20 minutes power off) the temperature of the

SUBSTITUTE SHEET

-56-

tumor site has risen 8°C to about 34°C, while the temperature of the null site has risen only 3°C to about 30°C. Thus, an approximate differential of about 4°C is attained between the tissue temperature of a deep-seated target and the temperature of a single surface null site in a beef phantom.

5   <u>Two Adaptive Nulls</u>

In another experiment, two adaptive nulls on the surface of the saline-filled cylindrical phantom were generated and measured. This experiment used the same configuration as shown in Fig. 39 with the one E-field probe 715 (BSD Medical Corp. Model EP-500) located inside the

10   phantom 706 at the center, or focus, 707 of the array simulating the tumor site. Two E-field probes 720 and 721 (BSD Medical Corp. Model EP-100) were located on the outside surface of the phantom at diametrically opposite positions representing the two non-invasive null sites. Probe 715 monitored the E-field amplitude at the tumor site while

15   probes 720 and 721 monitored the E-field amplitude at the null sites.

FIG. 45 graphically illustrates the results of this experiment, showing the measured E-field probe amplitude, in dB, versus the gradient search iteration number. Again, the dB values are obtained by computing $10log_{10}$(probe output signal) and normalizing the resulting values to 0 dB

20   at iteration 0. It is evident from this graph that the gradient search formed two strong adaptive E-field amplitude nulls at the null sites, on the order of -10 to -20 dB with respect to the reference site, in about 50 iterations. In particular, at iteration number 50 the null strength at probe 720 (probe site 2) is approximately -18.0 dB and the null strength at probe 721 (probe site

25   3) is approximately -11.8 dB. Furthermore, the E-field amplitude at the tumor site 715 (probe site 1) was held close to a constant value (0 dB) throughout the 50 iterations.

<u>Adaptive Focusing</u>

In another experiment, adaptive phase focusing was used to

30   maximize the E-field amplitude at a selected location different from focus 707 of the saline-filled cylindrical phantom 706 of FIG. 39. In this case,

SUBSTITUTE SHEET

the selected focus site was at E-field probe 720 (BSD Medical Corp. Model EP-100) located on the outside surface of the cylindrical phantom.

FIG. 46 graphically illustrates the results of this experiment, showing the measured E-field probe amplitude, in dB, versus the gradient
5 search iteration number for 30 iterations. Again, the dB values are obtained by computing $10log_{10}(probe\ output\ signal)$ and normalizing the resulting values to 0 dB at iteration 0. The initial phase weights applied to the transmit elements of the array were equal, nominally producing an E-field focused at the center of the array 707. The gradient search was
10 used to adjust the phases of the array transmit weights to maximize the E-field amplitude at probe site 720, i.e., refocus the array at probe 720. The transmit weight amplitudes were held constant over the 30 iterations. As shown, the gradient search converged in about 10 iterations and the power at probe 720 increased by about 0.9 dB compared to its initial
15 value. This result demonstrates that adaptive focusing can be used successfully to optimize the peak power delivered to a tumor site.

Clinical Application

A modified BSD-2000 Sigma 60 system can be used as a clinical adaptive hyperthermia system for implementing the adaptive nulling and
20 focusing techniques of this invention. An unmodified BSD-2000 hyperthermia system uses four transmit channels to energize the eight transmit elements (in pairs) of the annular array, and eight EP-400 (or EP-100) non-invasive E-field probes to monitor clinical hyperthermia treatments. The eight E-field probes can provide feedback signals to the
25 controller performing the adaptive nulling and/or focusing algorithms. Theoretically, three independent adaptive nulls (and/or peaks) can be formed by adaptively adjusting the phases and gains of the four transmit channels. Any three of the eight E-field probes can provide the feedback signals required to produce a null (or peak) at the corresponding probe.
30 Various treatment protocols are possible for selecting desired null sites, depending on the particular patient and case history. One protocol

SUBSTITUTE SHEET

would place the eight E-field probes around the circumference of the patient to measure the E-field strength at each probe before nulling and thereby identify the strongest electric fields on the surface of the patient indicating potentially serious hot spots. Adaptive nulling would then be
5 applied to minimize the electric field at the three probes having the strongest electric fields before nulling. Alternatively, if the patient can localize a painful hot spot during treatment, adaptive nulling would be applied to minimize the electric field at the E-field probe closest to the identified hot spot.

10   The number of adaptive nulls required will vary with patient and pathology. In some situations it is possible that more than three independent adaptive nulls will be required to achieve a therapeutic thermal distribution in the patient. In such a case, an extension of the four transmit channel BSD-2000 system to an eight transmit channel
15 configuration will allow up to seven independent adaptive nulls and an adaptive focus to be formed.

MONOPOLE ARRAY EMBODIMENT

FIGS. 47-49 show an embodiment of a non-invasive RF monopole
20 phased-array hyperthermia system 400 for treating malignant brain tumors. Hyperthermia system 400 features a monopole phased-array transmit antenna 402 having a plurality of monopole transmit antenna elements 404 placed in proximity to the cranium 406 of a patient to be treated for a malignant brain tumor 407. Hyperthermia system 400 also
25 features improved focusing characteristics through using one or more non-invasive electric field probes 412 placed on or near the patient's cranium, in conjunction with the near-field adaptive focusing and nulling apparatus and methods of this invention.

Monopole phased-array 402 is used to therapeutically heat the brain
30 tumor 407, typically located 1-3 cm below the skin surface of the cranium 406, by adaptively focusing the RF electric field energy radiated by the monopole radiator elements 404 into the tumor 407. In practice, it is

SUBSTITUTE SHEET

dangerous, and often impossible, to invasively place an E-field probe into the brain tumor site to facilitate adaptive focusing of the RF energy into the tumor. "Hot spots" are not typically a problem with the monopole hyperthermia array described since the side lobes generated by a phased-

5   array in this near-field geometry are much lower than those generated by the annular phased-array described above. Thus, the monopole phased-array receives its major benefit by applying the adaptive focusing of this invention to more precisely focus energy into the tumor site. However, the adaptive nulling of this invention may also be used if "hot spots" do

10   develop through the use of the monopole array.

The monopole phased array antenna 402 is mounted inside an water-tight enclosure 430 having a generally circular top and bottom surface 432 and 434, respectively, and a cylindrical or conical side surface 436 connecting the top and bottom surfaces. The enclosure is made from

15   non-conductive plastic material, such as plexiglas, but may also be fashioned from any material which acts as an electrical insulator and will not interfere with the RF radiation patterns generated by the monopole phased-array inside the enclosure.

The bottom surface 434 has a central elliptical aperture 438 which

20   accommodates a portion of the patient's cranium 406 to allow tumor 407 to be disposed within the interior of enclosure 430 adjacent to the monopole phased-array 402. A flexible silicone rubber membrane 440 covers the aperture to maintain the water-tight integrity of the enclosure. The enclosure 430 can be filled with chilled de-ionized water 442 for

25   cooling the patient's skin during hyperthermia treatment. The de-ionized water can be temperature controlled and circulated through the enclosure 430 to maximize the cooling effect.

Bottom surface 434 also includes an RF conducting ground plane 444 mounted co-planar with the bottom surface and which acts as an RF

30   reflector for monopole antenna elements 404. This ground plane may be fashioned out of a metal sheet, metal foil, metal mesh, or any other RF conductive material which can be fashioned to cover the area of bottom

surface 434. The ground plane may also be imbedded into the bottom surface by, for instance, laminating the ground plane between two layers of insulating material.

The monopole radiator elements 404 are each mounted
5   perpendicularly onto bottom surface 434 so that they may be energized from outside the enclosure, yet remain insulated from the ground plane 444. In one preferred embodiment, each monopole radiator element 404 is a 1/4 wavelength long straight wire radiator threadably attached on one end into a connector mounted onto surface 434 and insulated from ground
10   plane 444. It is understood that another form of a monopole antenna element, other than a straight wire radiator, can also be used. For instance, helical monopole, conical monopole, and sleeve monopole antenna elements are also appropriate for use as monopole array elements of the present invention.

15   Each monopole element is energized through a coaxial cable fed through the bottom surface 434 to the connector. The bottom surface may also be provided with extra monopole connectors which allow repositioning of the monopole radiator elements within the enclosure. Repositioning allows the user to change the geometry of the monopole
20   phased-array antenna as well as position the antenna adjacent to the tumor location to maximize the therapeutic effect.

An RF reflecting screen 446 (FIGS. 48 and 49) can be placed behind the monopole antenna elements 404 to direct more of the radiated RF energy toward the cranium, i.e., energy which would otherwise be lost
25   through the side of the water-tight enclosure. Reflecting screen 446 is typically positioned in the water bolus approximately 1/4 wavelength behind the monopole antenna elements and has a cylindrical reflecting surface extending perpendicularly from the ground screen to a height of approximately twice the wavelength of the radiated energy. Alternatively,
30   the reflecting surface of the screen can be curved toward the target to further enhance radiation of the target. The reflecting screen is constructed from high frequency RF conducting mesh which allows water

SUBSTITUTE SHEET

to freely flow through it, and is electrically connected to the ground screen using good high frequency RF construction practices.

Each monopole radiator element 404 is configured as a 1/4 wavelength radiator to resonate at approximately 915 MHz which is

5 effective for heating tumors 1 to 3 cm, or more, beneath the surface of the patient's skull. The monopole phased-array can include a varying number of radiator elements spatially arranged in a variety of patterns. The spacing between the monopole antenna elements is typically between 1/2 to 1 wavelength. Furthermore, the number and location of the non-

10 invasive electric field probes 412 can also vary depending on the hyperthermia focusing patterns desired.

In the adaptive hyperthermia monopole phased-array of this invention, non-invasive E-field probes are used in conjunction with the adaptive focusing apparatus and techniques of this invention to maximize

15 the RF power delivered to the tumor site inside the cranium. Computer simulations, presented herein, show that the optimum focused (e.g., with an invasive E-field probe) phased array can produce an RF energy pattern with maximum electric field strength at the tumor site and no undesired hot spots within the cranial target.

20 With the adaptive hyperthermia monopole phased-array described herein, RF energy peaks are adaptively formed to maximize the electric field energy delivered to the target focus. As shown, the focused energy peak achieved by the adaptive focusing apparatus of this invention is invasive to the cranial target extending into the tumor region.

25 Referring to FIG. 50, the adaptive-focusing monopole phased-array hyperthermia system of this invention can be described in terms corresponding to the generalized annular phased-array system schematic diagram of FIG. 6. Specifically, monopole transmit elements 404_n of hyperthermia transmitting antenna array 402 correspond respectively to

30 the dipole transmit elements 104_n of annular phased array applicator 102 of FIG. 6. Furthermore, the plurality of E-field auxiliary probes 412_m, correspond to the E-field probes 112_m of FIG. 6. It is apparent that the

SUBSTITUTE SHEET

monopole phased-array hyperthermia system herein described does not take advantage of an electric field probe placed at the tumor 407, analogous to the receiving probe 115 used with the annular phased array applicator 102 of FIG. 6, to maximize the focus radiated energy into the

5 tumor. Use of a probe at the focus would in most cases require a surgical procedure to invasively place the probe within the patient's brain.

The receiver 114, signal processor 116, RF source 108, and weighting functions 110_n (FIG. 6) operate with the monopole array as described above with regard to the annular array, except that the signal

10 processor 116 performs an adaptive focusing algorithm described below, which is related to the adaptive nulling algorithm. That is, signal processor 116 performs either a sample matrix inversion (SMI) algorithm or a gradient search algorithm on the signals output from receiver 114 and updates the adaptive array weights w_n (with gain g and phase ϕ) to

15 rapidly (within seconds) focus energy at the tumor 407.

Referring to FIGS. 51 and 52, there is shown an analytical model of an embodiment of an eight-element, 915 MHz hyperthermia monopole phased-array 402 of FIG. 47. Phased-array 402 has transmit antennas 404_1 through 404_8, arranged adjacent to an elliptical phantom target 406

20 representing the cross section of the human cranium at the tumor level. The focus 407 of the elliptical phantom models the location, approximately 2.0 cm below the surface of the cranium, of the brain tumor to receive hyperthermia treatment, i.e., the focus of RF energy for the phased array 402. Water bolus 442 is assumed to surround the target body 406, and is

25 treated as a homogeneous medium for analysis purposes.

The monopole radiator elements 404_1 through 404_8 are arranged as a 120° circular arc array of uniformly spaced elements having a constant radius of 12.7 cm relative to the geometric center of the cranium C, i.e., at x = 0.0 cm, z = 0.0 cm. The tumor site, or focus 407 of the RF

30 energy, is assumed to be at x = 0.0 cm, z = 5.08 cm for simulation purposes. (In an alternative preferred embodiment the monopole array elements form a circular arc having a geometric center at focus 407

SUBSTITUTE SHEET

(target) rather than at the center of the cranium C. This has the advantage that less phase focusing should be required to maximize the energy delivered to the focus, and thus the required number of gradient search iterations is reduced.)

5   Six auxiliary RF E-field probes, or sensors, 412_1 through 412_6 (i.e., receiving antennas) are placed on and near the perimeter of the elliptical target to model non-invasive E-field probes placed on and near the skin of the cranial target. Auxiliary probes 412_1, 412_2, and 412_3 are uniformly spaced in an arc row, between the arc array and the cranial target, having

10   a constant radius of approximately 4.0 cm relative to the desired focus 407. Auxiliary probes 412_4, 412_5 and 412_6 are placed on the target skin adjacent to focus 407. Specifically, the first arc row of electric field probes 412_1 through 412_3 may be denoted as probes L_1, M_1, and R_1, respectively, and the row of electric field probes 412_4 through 412_6 may

15   be denoted as probes L_2, M_2, and R_2, respectively. The electric field probes are arranged so that corresponding probes on the two rows are located along a radial line extending from the desired focus at tumor site 407 and are spaced 1/4 to 1/2 wavelength apart. That is, probe pair (L_1,L_2) is located along radial r_L, probe pair (M_1,M_2) is located along radial

20   r_M and, probe pair (R_1,R_2) is located along radial r_R.

The gains and phases of the monopole elements are adaptively adjusted as described below to focus the energy output from the monopole phased-array into the tumor site 407 located several centimeters below the surface of the cranium. From the phased-array geometry of Fig.

25   52 it is observed that an electric field focused at tumor 407 will be balanced and symmetric with respect to the line $x=0$. Furthermore, the electric field is attenuated in the water bolus external to the cranium in the direction away from the transmit array. To achieve a focus interior to the cranium at the tumor site 407 it is assumed that the amplitude difference

30   between the electric field adjacent to the skin surface of the cranium and the field approximately one quarter wavelength exterior to the skin surface of the cranium must be constrained to a desired value. This desired value

-64-

is typically a minimum to avoid "hot spots" on the skin surface. Similarly the amplitude of the electric field in the transverse direction should be balanced to minimize the electric field variation between the left and right electric field probes with respect to the middle electric field probes, i.e.,

5   maintain electric field symmetry with respect to the x-axis. The electric field differences in the radial direction may be denoted by

$$\Delta A_{L12} = |A_{L1} - A_{L2}| \quad , \tag{74}$$

$$\Delta A_{M12} = |A_{M1} - A_{M2}| \quad , \tag{75}$$

$$\Delta A_{R12} = |A_{R1} - A_{R2}| \quad . \tag{76}$$

where A denotes the amplitude of the electric field measured by the specified field probe, $\hat{p}$ is a unit vector in the radial direction which bisects the transmit monopole array and $\hat{t}$ is a transverse unit vector as shown in

10   FIG. 52. The electric field differences in the transverse direction for the first row may be denoted by

$$\Delta A_{LM1} = |A_{L1} - A_{M1}| \quad , \tag{77}$$

and,

$$\Delta A_{RM1} = |A_{R1} - A_{M1}| \quad , \tag{78}$$

and the electric field differences in the transverse direction for the second row may be denoted by

-65-

$$\Delta A_{LM2} = |A_{L2} - A_{M2}| \quad , \quad \text{(79)}$$

and,

$$\Delta A_{RM2} = |A_{R2} - A_{M2}| \quad . \quad \text{(80)}$$

A figure of merit F can be defined as

$$F = \alpha(\Delta A_{L12} + \Delta A_{M12} + \Delta A_{R12})$$
$$+ \Delta A_{LM1} + \Delta A_{RM1} + \Delta A_{LM2} + \Delta A_{RM2} \quad , \quad \text{(81)}$$

where α is a scale factor used to adjust the effect of the electrical field gradient caused by attenuation in the radial direction between the phased-
5   array antenna and the target. The figure of merit F involves seven constraints which are easily taken into account by the eight transmit element phased-array described. The gradient search algorithm described above is used to minimize the figure of merit F.

FIG. 53 shows a simulated two-dimensional quiescent radiation
10   pattern in the plane $y = 0$ *for the eight element* monopole arc array of FIG. 52 operating at 915 MHz before adaptive focusing, i.e., with uniform amplitude and phase illumination. This radiation pattern was calculated using the moment-method described above, and the calculations assume an infinite homogeneous conducting medium simulating phantom brain
15   tissue, i.e., $\epsilon_r = 50.0$, $\sigma = 1.3$. The focus of the array is at $x = 0.0$, $z = 5.0$ cm. The positions of the eight monopole radiators 404_1 through 404_8 are clearly evident by the *-10* dB contours surrounding each element. The radiation pattern is symmetric because of the symmetry of the array and the assumed homogeneous medium.
20   FIG. 54 shows the quiescent radiation pattern of FIG. 53 cut at $z = 5.0$ cm, which is through the tumor site 407 assumed to be at $x = 0.0$,

SUBSTITUTE SHEET

$z = 5.0$ cm. The focused main beam is centered at $x = 0.0$ as desired. The half-power beamwidth is approximately 2.0 cm, which is close to 1/2 wavelength for the full ring array.

FIG. 55 shows a simulated two-dimensional thermal pattern
5 expected for the quiescent radiation pattern of FIG. 53 at time $t = 20$ minutes. This simulation assumes that the elliptical phantom brain tissue is surrounded by a 10°C constant temperature water bolus and that the initial temperature of the brain tissue phantom is 25°C.

FIG. 56 shows a configuration of the monopole phased-array
10 hyperthermia system of this invention configured to uniformly heat a large intra-cranial tumor target 407'. In this case, a set of auxiliary E-field probes 412 are uniformly spaced along the skin surface of the cranium between the monopole radiator elements 404 and the tumor site 407'. Here, seven E-field probes 412_1 through 412_7 are used, denoted P_1
15 through P_7 respectively, but the quantity of probes required will vary according to the tumor size and location. The gains and phases of the monopole elements are adaptively adjusted to uniformly distribute the electric field energy at the E-field probes 412_1 through 412_7. From the geometry of FIG. 56 it is observed that a uniform electric field at the E-
20 field probes will produce a substantially uniform electric field inside tumor 407' to induce uniform heating of the tumor.

To achieve a uniform electric field distribution across all the E-field probes, and thus uniform heating of the tumor 407', the amplitude difference between any two adjacent E-field probes on the skin surface of
25 the cranium must be minimized. The electric field differences between adjacent E-field probes may be written as

$$\Delta A_{P12} = |A_{P1} - A_{P2}| \quad , \qquad (82)$$

$$\Delta A_{P23} = |A_{P2} - A_{P3}| \quad , \qquad (83)$$

$$\Delta A_{P34} = |A_{P3} - A_{P4}| \quad , \qquad (84)$$

SUBSTITUTE SHEET

$$\Delta A_{P45} = |A_{P4} - A_{P5}| \qquad , \qquad (85)$$

$$\Delta A_{P56} = |A_{P5} - A_{P6}| \qquad , \qquad (86)$$

and,

$$\Delta A_{P67} = |A_{P6} - A_{P7}| \qquad , \qquad (87)$$

where A denotes the amplitude of the electric field measured by the specified field probe. A figure of merit F may be defined as

$$F = \Delta A_{P12}^2 + \Delta A_{P23}^2 + \Delta A_{P34}^2 + \Delta A_{P45}^2 + \Delta A_{P56}^2 + \Delta A_{P67}^2 \qquad . \qquad (88)$$

The figure of merit F involves six constraints on measured differences and
5   an additional constraint on total power radiated by the transmit array, all
of which are easily taken into account by the eight transmit element
phased-array described. The gradient search algorithm described above is
used to minimize the figure of merit F and thereby achieve a uniform
electric field distribution across the E-field probes.

10   It should be noted that this approach for achieving a uniform electric
field distribution to effect uniform heating within a large mass is not
limited to the monopole array heating of a brain tumor, and for example
can be similarly implemented with the annular phased-array hyperthermia
applicator of FIG. 1 for uniformly heating a large mass in other areas of the
15 body.

        FIGS. 57 and 58A show an alternative preferred embodiment of the
monopole phased array applicator 400 of FIG. 48 including the addition of
a top ground plane surface 450 positioned above the monopole antenna
elements 404_n and extending from the reflecting screen 446 toward the
20 target body parallel to ground plane surface 442. The top ground plane
surface 450 combines with ground plane surface 442 to form a parallel

SUBSTITUTE SHEET

plate waveguide region 452 between the monopole antenna elements and the target body 406. The spacing between the parallel plates (i.e., between surfaces 442 and 450) can be used to adjust the radiation pattern in the direction perpendicular to the parallel plates. The spacing

5   between the parallel plates is typically between 1/2 and 5 wavelengths. FIGS. 58B and 58C show alternative preferred embodiments of the parallel plate waveguide of FIG. 58A having non-parallel waveguide surfaces, and flared waveguide surface forming a horn, respectively.

FIG 59 shows a preferred embodiment of a stacked waveguide
10   phased array applicator having multiple stacked parallel plates 450, 454, and 456 forming respective stacked waveguide regions 452, 458, and 460, each having a corresponding set of monopole phased array antenna elements 404_n, $404_n'$, $404_n''$.

FIG. 60 shows a block diagram of a preferred embodiment of a 915
15   MHz transmit and receive (T/R) module 800 for use with the monopole phased array hyperthermia system 400 (FIG. 47), specifically for use in transmit amplifier/phase shift network 110 of FIG. 50. Generally, the T/R module 800, as well as the monopole hyperthermia system 400, is not restricted to operate at 915 MHz, and is adaptable for operation anywhere
20   within the industrial, scientific, medical (ISM) frequency band of 902 to 928 MHz.

The transmit function of the T/R module 800 is used to energize a monopole transmit antenna element 404_n (FIG. 50) of the monopole hyperthermia array 402 with a 915 MHz signal, having controlled phase
25   and gain, for the purposes of heating the target 407. Each monopole transmit antenna element 404_n of the array 402 is connected to a corresponding T/R module and therefore the quantity of T/R modules required depends on the quantity of monopole antenna elements 404_n in the array.

30   With regard to the generation of the 915 MHz transmit signal, having controlled phase and gain, a tunable oscillator 802, tunable from 180 to 206 MHz, is used to produce a transmit signal having a 193 MHz

SUBSTITUTE SHEET

center frequency. The 193 MHz transmit signal is input to a dual-stage voltage-variable attenuator 804 which covers an attenuation range of 0 to -40 dB (-60 dB off state) determined by a 12 bit analog control voltage. The other port of mixer 808 is driven with a constant frequency 1108

5   MHz phase-controlled signal generated by a phase-controlled local oscillator 810.

Phase-controlled local oscillator 810 is excited with a 277 MHz signal generated by a fixed frequency local oscillator 812. The output of the 277 MHz local oscillator 812 is input to a voltage-variable phase

10   shifter which shifts the phase of the 277 MHz signal from 0 to 90°, determined by a 12 bit analog control voltage. The phase-shifted 277 MHz signal is input to a X4 frequency multiplier 816 which quadruples the signal to 1108 MHz and extends the phase control range to 0 to 360°. The output of the frequency multiplier passes through a 1108 MHz

15   bandpass filter 818, having a 50 MHz bandwidth, to remove undesired harmonics. The 1108 MHz output of the bandpass filter is then amplified to saturation by an amplifier 820 to produce a relatively constant input power to the input port of mixer 808 independent of the commanded phase shift.

20   The upconverted, gain and phase-controlled 915 MHz signal output from mixer 808 passes through a 915 MHz bandpass filter 822, having a 50 MHz bandwidth, to remove undesired harmonics generated in mixer 808. The output signal of bandpass filter 822 passes through another T/R switch 824 which, when in the transmit position (T), connects the

25   bandpass filter output signal to drive the input of a power amplifier 826 having an average CW output power of up to, or greater than, 100 watts. The output signal of the power amplifier 826 passes through another T/R switch 828 which, when in the transmit position (T), connects the amplified 915 MHz transmit signal to the input of another 915 MHz

30   bandpass filter 830, having a 50 MHz bandwidth, which removes unwanted harmonics generated in the power amplifier. Finally, the 915 MHz transmit signal output from bandpass filter 830 is connected by a

transmission line 832 to a monopole antenna element 404_n of the monopole hyperthermia array 402.

The receive function of the T/R module 800 can be used for passive microwave radiometry for non-invasively sensing the temperature of the

5   target tissue 407 (FIG. 50) with the monopole antenna elements 404_n of array 402. To operate in a non-invasive microwave radiometry mode, the transmit power is turned off as desired for a period of several seconds during which the elements of the monopole hyperthermia array act as passive receive antennas.

10   In this case, the three T/R switches 806, 824, and 828 are set to the receive (R) position. The 915 MHz center-frequency passive signal received by the monopole antenna element 404_n is filtered by bandpass filter 830, amplified by a low-noise amplifier 834, and again filtered by bandpass filter 822. The output of bandpass filter 822 is mixed with the

15   1108 MHz controlled-phase local oscillator signal by mixer 808, the output of which is input to a lowpass filter 836. Lowpass filter 836 has a 350 MHz high frequency cutoff which provides a 193 MHz center frequency receive signal for input to a second mixer 838. A variable frequency local oscillator, tunable over a 150-176 MHz range, has an output signal tuned

20   to 163 MHz which is amplified by an amplifier 841 and input to another port of mixer 838 to mix with the 193 MHz center frequency receive signal. The output of mixer 838 contains a 30 MHz center frequency receive signal which is input to a 30 MHz bandpass filter 842, having a 5 MHz bandwidth, to remove unwanted out of band signals. The filtered 30

25   MHz center frequency receive signal is then passed through a voltage controlled 0 to -40 dB attenuator 844 whose output signal 846 is controlled by a 12 bit analog voltage level.

The 30 MHz center frequency receive signal 846 can be analyzed with a commercial network analyzer, such as a Hewlett Packard 8510

30   analyzer, or can be combined with the output of the other T/R modules (i.e., receive signals from the other monopole antenna elements) in a commercial analog power combiner at the 30 MHz frequency.

SUBSTITUTE SHEET

Alternatively, the 30 MHz receive signal 846 can be mixed with a 28.5 MHz local oscillator and downconverted to a baseband offset frequency of 1.5 MHz. The resulting baseband signal is lowpass filtered with a cutoff frequency of 2.0 MHz, and sampled with a high speed digital to analog

5   convertor at 4.5 MHz (i.e., above the Nyquist sampling limit for the bandlimited signal). The frequency spectrum of the baseband signal is then computed using digital signal processing techniques (see, J.R. Johnson, et al., "An Experimental Adaptive Nulling Receiver Utilizing the Sample Matrix Inversion Algorithm with Channel Equalization", IEEE

10   Transactions on Microwave Theory and Techniques, Vol. MTT-39, No. 5, pp. 798-808, May 1991). It should further be noted that the T/R module 800 can be used as a receiver 114 (FIG. 50) for the E-field probes 412 if the low-noise amplifier 834 is bypassed.

SUBSTITUTE SHEET

APPENDIX A

```
*** Copyright MIT Lincoln Laboratory 1991.  All rights reserved.
*************************makefile for moment method software********
****file sdipjamhyperMake*****
EXECUTABLE = sdipjamhyper.out
OBJS = sdipjamhyper.o dzabgnloss.o \
       dpack2.o zabgnloss.o pack2.o fwgh.o \
       chebaf.o wwquan.o taylor.o \
       eigenv.o reordr.o ydipsubloss.o \
       plothyper.o contek.o plabel.o \
       conturek.o circsubloss.o
# use tabs for continues
IL = /usr/lib/f68881/libm.il
FLAGS = -O1 -v -f68881
$(EXECUTABLE): $(OBJS)
        dislink -lF77 $(FLAGS) -o $(EXECUTABLE) $(OBJS) $(IL)

sdipjamhyper.o: /home/ajf/hyperthermia/sdipjamhyper.f
        f77 $(FLAGS) -c /home/ajf/hyperthermia/sdipjamhyper.f $(IL)

plothyper.o: /home/ajf/hyperthermia/plothyper.f
        f77 $(FLAGS) -c /home/ajf/hyperthermia/plothyper.f $(IL)

dzabgnloss.o: /home/ajf/hyperthermia/dzabgnloss.f
        f77 $(FLAGS) -c /home/ajf/hyperthermia/dzabgnloss.f $(IL)

dpack2.o: /home/ajf/monjam/dpack2.f
        f77 $(FLAGS) -c /home/ajf/monjam/dpack2.f $(IL)

contek.o: /home/ajf/monjam/contek.f
        f77 $(FLAGS) -c /home/ajf/monjam/contek.f $(IL)

plabel.o: /home/ajf/monjtr/plabel.f
        f77 $(FLAGS) -c /home/ajf/monjtr/plabel.f $(IL)
```

SUBSTITUTE SHEET

```
conturek.o: /home/ajf/hyperthermia/conturek.f
    f77 $(FLAGS) -c /home/ajf/hyperthermia/conturek.f $(IL)
zabgenloss.o: /home/ajf/hyperthermia/zabgenloss.f
    f77 $(FLAGS) -c /home/ajf/hyperthermia/zabgenloss.f $(IL)

pack2.o: /home/ajf/monjam/pack2.f
    f77 $(FLAGS) -c /home/ajf/monjam/pack2.f $(IL)

fwgh.o: /home/ajf/monjam/fwgh.f
    f77 $(FLAGS) -c /home/ajf/monjam/fwgh.f $(IL)

chebaf.o: /home/ajf/monjam/chebaf.f
    f77 $(FLAGS) -c /home/ajf/monjam/chebaf.f $(IL)

wwquan.o: /home/ajf/monjam/wwquan.f
    f77 $(FLAGS) -c /home/ajf/monjam/wwquan.f $(IL)

taylor.o: /home/ajf/monjam/taylor.f
    f77 $(FLAGS) -c /home/ajf/monjam/taylor.f $(IL)

eigenv.o: /home/ajf/monjam/eigenv.f
    f77 $(FLAGS) -c /home/ajf/monjam/eigenv.f $(IL)
reordr.o: /home/ajf/monjam/reordr.f
    f77 $(FLAGS) -c /home/ajf/monjam/reordr.f $(IL)

ydipsubloss.o: /home/ajf/hyperthermia/ydipsubloss.f
    f77 $(FLAGS) -c /home/ajf/hyperthermia/ydipsubloss.f $(IL)

circsubloss.o: /home/ajf/hyperthermia/circsubloss.f
    f77 $(FLAGS) -c /home/ajf/hyperthermia/circsubloss.f $(IL)

******file sdipjamhyper.f*************
C***PROGRAM SDIPJAMHYPER.F --- ANALYZES FINITE ARRAYS OF DIPOLES
C***IN LOSSY DIELECTRIC OR FREE SPACE.
```

```
C***THE DIPOLES ARE ASSUMED TO BE ORIENTED PARALLEL
C***TO THE PLANE OF THE GRID FOR A PLANAR ARRAY, OR THEY CAN BE
C***ARRANGED IN AN ANNULAR (RING) ARRAY CONFIGURATION.
C***RECEIVING CONDITIONS ARE ASSUMED.
C***DOUBLE-PRECISION VERSION
      PARAMETER (NUMCHN=8)
      PARAMETER (NUMAUX=8)
      PARAMETER (NUMJAM=7)
      PARAMETER (NUMELM=8)
      PARAMETER (NUMFRQ=5)
      PARAMETER (NUMNPT=1681)
      COMPLEX PS(1825),CZ(900),VA(NUMELM),Z(NUMELM,NUMELM)
      COMPLEX VTA(NUMELM),VREFA,VRECVA(NUMELM)
      COMPLEX VCW(NUMELM),VRECVX(NUMELM),CJ,CSUMA,VXA
CC***THE ABOVE MATRICES ARE DIMENSIONED BY THE NUMBER OF ELEMENTS
      COMPLEX *16 COVNF(NUMCHN,NUMCHN),COVNFI(NUMCHN,NUMCHN)
      COMPLEX *16 COVAAJ(NUMCHN,NUMCHN),CINVCN(NUMCHN,NUMCHN)
      COMPLEX *16 VCHA(NUMCHN,NUMFRQ)
      COMPLEX *16 VMAJMA(NUMJAM,NUMFRQ)
      COMPLEX *16 VAUXJA(NUMAUX,NUMJAM,NUMFRQ)
      COMPLEX *8 VAXCWA(NUMAUX,NUMNPT)
C***NOTE DIMENS.  VCHA(NCHAN,NFREQ),VMAJMA(NJAM,NFREQ)
                  VAUXJA(NAUX,NJAM,NFREQ),VAXCWA(NAUX,NPTS)
C
      COMPLEX *8 VXMANA(NUMNPT),ETASP,GAMSP
      COMPLEX *16 EIGVAN(NUMCHN),EIGVEN(NUMCHN,NUMCHN)
      COMPLEX *16 WANA(NUMCHN,1)
      COMPLEX *16 WTCTR(1,NUMCHN),WQSLC(NUMCHN,1)
      COMPLEX *16 WQNA(NUMELM,1),CMPROD(1,NUMCHN),WAN(NUMCHN,1)
      COMPLEX *16 WANDMA(NUMELM,1)
      COMPLEX *16 CWTA(NUMELM,1),ETADP,GAMDP
      DIMENSION ACALPH(NUMELM),RWTA(NUMELM),RWTB(NUMELM)
      DIMENSION VXADB(NUMNPT),VXAPH(NUMNPT)
      DIMENSION XC(NUMNPT),YC(NUMNPT),ZC(NUMNPT)
      DIMENSION THSD(1),PHSD(1),THCT(1),PHCT(1)
      DIMENSION XJAMIN(NUMJAM),YJAMIN(NUMJAM),ZJAMIN(NUMJAM)
```

SUBSTITUTE SHEET

```
      DIMENSION XJAM(NUMJAM),YJAM(NUMJAM),ZJAM(NUMJAM)
      DIMENSION PWRJDB(NUMJAM)
      DIMENSION PCHADB(NUMNPT)
      REAL *8 CNDB,PHASEN,DPDCR,WKE(144),EVLDBN
      REAL *8 PREALN,PIMAGN
      REAL *8 QINRDB,AINRDB,CANCDB,EXCPCB
      REAL *8 QINRAA,AINRAA
      REAL *8 CNCLNA,ELSGDB,ELSGDG,AWSGDB,AWSGDG
      REAL *8 SUMC,SUMAA,AVECAN,AVCAA,SAVE,SAVESR
      REAL *4 RX(100),RY(100),RZ(100),FM(41,41),DMF(41,41)
      REAL *4 AUXADB(NUMAUX),VATENA(NUMAUX)
      INTEGER IAUXA(NUMAUX),LTMP(NUMCHN),MTMP(NUMCHN)
      CHARACTER DATNAM*35, OUTNAM*35
      COMMON/A/DX,DY,NCOLX,NROWY,NEL,HZ,HL,ARAD,ZLOAD,ZCHAR
      COMMON /B/ NGEN,IGEN,THETAS,PHIS,IMUT,IBLTSL,IPATRN
      COMMON /D/ FGHZ,RLAMDA,IWL,IS,NSCANS
      COMMON /DEG/ THDR,THDMIN
      COMMON /PLT/ INEAR,IPLOTM
      COMMON/XLYL/XL,YL
      COMMON/NEAR/IANTX,IANTY,NPOWER,IPCONN,IPCONF,IPCUTF
      COMMON/NEAR2/IPCFX,IPCFY,IPCFZ
      COMMON /P/XN,YN,ZN,RLSX,RLSY,RLSZ,NCOLXN,NROWYN,NCOLZN
      COMMON /P2/EDGET,ICOMB,PUNFLX,PUNFLY
      COMMON /CHEBY/ ICHEB,SLLDB
      COMMON /GROUND/ IGRNDP
      COMMON /NORM/ IENORM,BIGNDB
      COMMON /NORMAL/ INRNOR
      COMMON/PCENTR/PCDXIN
      COMMON /WRITE/ IWR
      COMMON /SPLOSS/ ETASP,GAMSP
      COMMON /DPLOSS/ ETADP,GAMDP
      COMMON /F/ FHZ,ER3,SIG3,TD3
      COMMON /CIRCLE/ ICIRC,RADIUS,HLS
      NAMELIST/DIPOLE/NCOLX,NROWY,HZIN,HLIN,ARADIN,ZLOAD,NGEN,IGEN,
     1DXIN,DYIN,IMUT,NSCANS,THSD,PHSD,THSINC,IBLTSL,IPATRN,ER3,SIG3,TD3,
```

```
     2NPHCT,PHCT,NTHPT,ZCHAR,IWL,FCHZ,BWFHZ,NFREQ,THDR,THDMIN,ICIRC,
     3XNIN,YNIN,ZNIN,NCOLZN,NROWYN,NCOLXN,NFCOLX,NFROWY,IPCONN,IPCONF,IPCUTF,IPOL,HLSIN,
     4IANTX,IANTY,NPOWER,NFCOLX,NFROWY,IPCONN,IPCONF,IPCUTF,IPOL,HLSIN,
     5IPCFX,IPCFY,IPCFZ,ITEK,IGRNDP,IGAIN,ICHEB,IWR,IENORM,BIGNDB,
     6NXDUM,NYDUM,NPDX,EDGTDB,RLSXIN,RLSYIN,RLSZIN,ISLC,INUNIF,
     7XFOCIN,ZFOCIN,XJAMIN,YJAMIN,ZJAMIN,IATTEN,AUXADB,INRNOR,
     8NJAMS,PWRCDB,PWRJDB,NAUX,IAUXA,IAUXB,ITLTPR,ITLTDP,
     9IQUAN,IRNERR,ELERDB,ELERDG,AWERDB,AWERDG,NBMOD,NBADWT,NRAN,SLLDB
C**NOTE; IF IWL=0 (INCHES), IWL=2 (METERS)
         WRITE(6,2959)
2959     FORMAT(1X,'ENTER INPUT DATA FILE NAME (typ. sdipjamhyper.data)')
         READ(5,*) DATNAM
         OPEN(4,FILE=DATNAM,FORM='FORMATTED')
         WRITE(6,3959)
3959     FORMAT(1X,'ENTER OUTPUT DATA FILE NAME (typ sdipjamhyper.output)')
         READ(5,*) OUTNAM
         OPEN(8,FILE=OUTNAM,FORM='FORMATTED')
         CALL GETCP2(CPU1)
         PI=3.141592654
         DCR=PI/180.
         DPDCR=DCR
         CJ=(0.,1.)
         CINMTR=0.0254
         IGRNDP=1
         IGAIN=0
         ZLOAD=0.0
         ICHEB=0
         IWR=0
         IENORM=1
         EXCPCB=-1.0D0
         IQUAN=0
         NRAN=1
         TILTPR=0.0
         TILTDP=0.0
         IATTEN=0
```

SUBSTITUTE SHEET

```
        IPOL=1
        ER3=1.0
        SIG3=0.0
        TD3=-1.0
        ICIRC=0
        CRADIN=0.0
        HLSIN=0.0
        ISLC=1
        INUNIF=0
        INRNOR=0
        READ(4,DIPOLE)
        IF(NFREQ.EQ.1) BWFHZ=0.0
        IF(ISLC.EQ.0) WRITE(6,81100)
81100   FORMAT(1X,'FULLY ADAPTIVE ARRAY')
        IF(ISLC.EQ.0.AND.ICHEB.EQ.0) INUNIF=1
        IF(ICIRC.EQ.1) WRITE(6,7000)
7000    FORMAT(1X,'RING ARRAY GEOMETRY')
        FHZ=FCHZ
        IXZ=0
        IXY=0
        IF(NROWYN.EQ.1) IXZ=1
        IF(NCOL2N.EQ.1) IXY=1
        IF(IPOL.EQ.2) IPRCOM=0
        IF(IPRCOM.EQ.0) WRITE(6,7898)
7898    FORMAT(1X,'NO PROBE COMPENSATION')
        WRITE(6,9276)IGRNDP
9276    FORMAT(1X'GROUND PLANE PARAMETER, IGRNDP=',I4)
CC      DO 1615 IX=1,NAUX
CC      IF(IATTEN.EQ.0) AUXADB(IX)=0.0
CC      WRITE(6,2318)IX,AUXADB(IX)
C2318   FORMAT(1X,'IX,AUXADB(IX)=',I4,2X,F12.2)
CC      VATENA(IX)=10.**(AUXADB(IX)/20.)
C1615   CONTINUE
        IF(NJAMS.GT.1) WRITE(8,2009)XJAMIN(1),YJAMIN(1),ZJAMIN(1)
2009    FORMAT(1X,'XJAMIN(1),YJAMIN(1),ZJAMIN(1)=',3F12.3)
```

SUBSTITUTE SHEET

```fortran
      WRITE(6,6987) BWFHZ,NFREQ
6987  FORMAT(1X,'BWFHZ,NFREQ=',E12.5,2X,I5)
      IF(ITEK.EQ.0)CALL COMPRS
      IF(ITEK.EQ.1)CALL TEKALL(4014,480,0,1,0)
      IF(INEAR.EQ.0) CALL PRNTDA
      IF(IMUT.EQ.0) ZLOAD=1.0
      IF(ITLTPR.EQ.1) TILTPR=45.
      IF(ITLTDP.EQ.1) TILTDP=45.
      CTPR=COS(TILTPR*DCR)
      STPR=SIN(TILTPR*DCR)
      CTDP=COS(TILTDP*DCR)
      STDP=SIN(TILTDP*DCR)
      FGHZ=FCHZ/1.0E9
      NEL=NCOLX*NROWY
      RNEL=NEL
      XLIN=DXIN*(NCOLX-1)
      YLIN=DYIN*(NROWY-1)
      NACOLX=NCOLX-NPDX-2*NXDUM
      NAROWY=NROWY-2*NYDUM
      NAEL=NACOLX*NAROWY
      PCDXIN=NPDX*DXIN
      NAUXP1=NAUX+1
      NAUXP2=NAUX+2
      IF(ISLC.EQ.1)  NMAX=NAUXP1
      IF(ISLC.EQ.0)  NMAX=NEL
      NMAXP1=NMAX+1
      ELSGDB=ELERDB*SQRT(3.)
      ELSGDG=ELERDG*SQRT(3.)
      AWSGDB=AWERDB*SQRT(3.)
      AWSGDG=AWERDG*SQRT(3.)
      INITRN=1
      IF(ISLC.EQ.0)  THEN
      NAUX=NEL
      NAUXP1=NAUX+1
      NAUXP2=NAUX+2
```

CC

```
        DO 79130 I=1,NEL
        IAUXA(I)=I
        WRITE(6,76767)I,IAUXA(I)
76767   FORMAT(1X,'I,IAUXA(I)=',2I5)
79130   CONTINUE
        ENDIF
        DO 1615 IX=1,NAUX
        IF(IATTEN.EQ.0) AUXADB(IX)=0.0
        WRITE(6,2318)IX,AUXADB(IX)
2318    FORMAT(1X,'IX,AUXADB(IX)=',I4,2X,F12.2)
        VATENA(IX)=10.**(AUXADB(IX)/20.)
1615    CONTINUE
30      CONTINUE
        NR=1
        IF(NGEN.EQ.1) NSCANS=0
        ICC=NEL
        ICC1=ICC
        IF(IBLTSL.EQ.1) ICC1=NROWY
        IF(IWL.EQ.1)GO TO 50
        WRITE(8,40)FGHZ
40      FORMAT(/,1X,'FGHZ=',F15.7)
C**********************************************************
C******COMPUTE FREE SPACE LAMBDA*********
C*****ALL UNITS HAVE TO BE IN METERS
        RLAMDA=2.997925E10/FCHZ/2.54
C***PARAMETER CONVERSIONS TO PROPER UNITS
55      CONTINUE
        IF(IWL.EQ.2) GO TO 50
        DX=DXIN*CINMTR
        DY=DYIN*CINMTR
        HL=HLIN*CINMTR
        HLS=HLSIN*CINMTR
        ARAD=ARADIN*CINMTR
        H2=H2IN*CINMTR
        RLSX=RLSXIN*CINMTR
```

SUBSTITUTE SHEET

```
      RLSY=RLSYIN*CINMTR
      RLSZ=RLSZIN*CINMTR
      XN=XNIN*CINMTR
      YN=YNIN*CINMTR
      ZN=ZNIN*CINMTR
      XFOC=XFOCIN*CINMTR
      ZFOC=ZFOCIN*CINMTR
      XL=XLIN*CINMTR
      YL=YLIN*CINMTR
      PCDX=PCDXIN*CINMTR
      RADIUS=CRADIN*CINMTR
50    CONTINUE
      WRITE(8,60)DX,DY,HL,ARAD
60    FORMAT(1X,'DX,DY,HL,ARAD=',2X,4F14.5)
C
C***COMPUTE CALIBRATION CONSTANTS (PHASE ONLY) TO
C***MAXIMIZE GAIN (FOCUS ANTENNA) TO NEAR FIELD RANGE
C
C***PHASE CENTER 'A' VOLTAGE EXCITATION
      XOA=-XL/2.+NXDUM*DX+(NACOLX-1)/2.*DX
      YP=0.0
      IF(ICIRC.EQ.0) WRITE(6,24690)
24690 FORMAT(1X,'CALLING NFDPX2')
      IF(ICIRC.EQ.0)
     2CALL NFDPX2(CTPR,STPR,CTDP,STDP,XFOC,YP,ZFOC,XOA,0,VA,VREFA)
      IF(ICIRC.EQ.1)
     2CALL NFDPC2(XFOC,YP,ZFOC,XOA,0,VA,VREFA)
C***SAVE INCIDENT VOLTAGES
      DO 65 IV=1,NEL
      VTA(IV)=VA(IV)
      WRITE(6,3757)IV,VTA(IV)
      WRITE(8,3757)IV,VTA(IV)
3757  FORMAT(1X,'IV,VTA=',I4,2X,2E12.4)
65    CONTINUE
      WRITE(6,9876)VTA(2)
```

SUBSTITUTE SHEET

```
9876    FORMAT(1X,'VTA(2)=',2E12.4)
        NB=NCOLX
        IDMB=NROWY
        IDM=NEL
        ICC=NEL
        IBLT=IBLTSL
        IDM1=IDMB
        IF(IBLT.EQ.0) IDM1=NEL
        I2=1
8889    CONTINUE
        CALL ZMATRX(CTDP,STDP,IBLTSL,ICC1,ICC,CZ,Z)
C***SOLVE SYSTEM OF EQUATIONS FOR THE UNKNOWN CURRENTS
        IF(IBLT.EQ.1) GO TO 240
        ISYM=0
        I12=1
        WRITE(6,9876)VTA(2)
        WRITE(6,6110)
6110    FORMAT(1X,'CALL CROUT')
        CALL CROUT(Z,VA,ICC1,ICC,ISYM,IWR,I12,NEL)
        I12=2
        WRITE(6,9876)VTA(2)
        GO TO 255
240     IENTRY=4
        CALL BLTSOL(CZ,VA,PS,NCOLX,IDMB,IENTRY)
        IENTRY=3
255     WRITE(8,270)
270     FORMAT(1X,'CURRENTS')
        IF(NEL.LT.40) CALL CNORM(VA,NEL)
        WRITE(6,280)
280     FORMAT(1X,'AFTER CURRENTS SOLUTION')
C****VA ARE CURRENTS (AMPERES) NOW
C*
C***COMPUTE RECEIVED VOLTAGES
        DO 285 IC=1,NEL
        WRITE(6,7531)ZLOAD
```

SUBSTITUTE SHEET

```
7531    FORMAT(1X,'ZLOAD=',F12.5)
        WRITE(6,1134)IC,VTA(IC)
        VRECVA(IC)=VA(IC)*ZLOAD
        WRITE(6,1174)IC,VRECVA(IC)
1134    FORMAT(1X,'IC,VTA=',I4,2X,2E12.4)
1174    FORMAT(1X,'IC,VRECVA=',I4,2X,2E12.4)
        WRITE(6,1135)IC,VA(IC)
1135    FORMAT(1X,'IC,VA=',I4,2X,2E12.4)
        VRADB=20.*ALOG10(CABS(VRECVA(IC)))
        VRAPH=ATAN2(AIMAG(VRECVA(IC)),REAL(VRECVA(IC)))/DCR
C***COMPUTE CALIBRATION CONSTANTS (PHASE ONLY)
        ACALPH(IC)=-VRAPH
285     CONTINUE
        DO 7777 IC=1,NEL
        WRITE(6,6667)IC,ACALPH(IC)
CC      WRITE(8,6667)IC,ACALPH(IC)
6667    FORMAT(1X,'IC,ACALPH=',I4,2X,F10.2,' DEGS')
7777    CONTINUE
C***COMPUTE NEAR FIELD PATTERN OF FOCUSED ARRAY
C
C***COMPUTE BEAMFORMER WEIGHTS (I.E. TAPER)
        IF(INUNIF.EQ.0)
2       CALL VRCVWT(NACOLX,NAROWY,NXDUM,NYDUM,EDGTDB,RWTA,RWTB)
        DO 1199 IC=1,NEL
        IF(INUNIF.EQ.1.AND.ISLC.EQ.0) RWTA(IC)=1./SQRT(RNEL)
        WRITE(6,5111)IC,RWTA(IC)
        WRITE(8,5111)IC,RWTA(IC)
5111    FORMAT(1X,'IC,RWTA=',I4,2X,E12.5)
1199    CONTINUE
        DO 5333 KC=1,NEL
        CWTA(KC,1)=RWTA(KC)*CEXP(CJ*ACALPH(KC)*DCR)
5333    CONTINUE
        IF(IQUAN.EQ.1)
2       CALL ADQUAN(NEL,CWTA,NBMOD,IRNERR,INITRN,ELSGDB,ELSGDG)
        BIGWDB=-299.0
```

SUBSTITUTE SHEET

```
      DO 91020 I=1,NEL
      WRITE(6,61910)I,CWTA(I,1)
      WRITE(8,61910)I,CWTA(I,1)
61910 FORMAT(1X,'I,CWTA(I,1)=',I4,2X,2E12.5)
      CWTADB=20.*DLOG10(CDABS(CWTA(I,1)))
      IF(CWTADB.GT.BIGWDB) BIGWDB=CWTADB
91020 CONTINUE
      DO 91120 I=1,NEL
      CWTADB=20.*DLOG10(CDABS(CWTA(I,1)))-BIGWDB
      CWTADG=DATAN2(DIMAG(CWTA(I,1)),DREAL(CWTA(I,1)))/DCR
      WRITE(6,35990)I,CWTADB,CWTADG
      WRITE(8,35990)I,CWTADB,CWTADG
35990 FORMAT(1X,'I=',I4,2X,'CWTADB,CWTADG=',1X,2F14.5)
91120 CONTINUE
      INITRN=2
C****PERFORM NEAR FIELD SCAN WITH CW RADIATING DIPOLE
      IF(INEAR.EQ.0) GO TO 390
      WRITE(6,350)
      WRITE(6,360)XNIN,YNIN,ZNIN,RLSXIN,RLSYIN,RLSZIN,NCOLXN,NROWYN,
     2NCOLZN
      WRITE(6,320)IWL
320   FORMAT(1X,'IWL=',I4)
      WRITE(6,330)
330   FORMAT(1X,'CHANGE NEAR FIELD SCAN PARAMETERS?, ICHANG=1')
      READ(5,*,END=370)ICHANG
      IF(ICHANG.EQ.0) GO TO 370
      WRITE(6,350)
350   FORMAT(1X,'XN,YN,ZN,RLSXIN,RLSYIN,RLSZIN,NCOLXN,NROWYN,NCOLZN=')
      READ(5,*)XNIN,YNIN,ZNIN,RLSXIN,RLSYIN,RLSZIN,NCOLXN,NROWYN,NCOLZN
      WRITE(6,360)XNIN,YNIN,ZNIN,RLSXIN,RLSYIN,RLSZIN,NCOLXN,NROWYN,
     2NCOLZN
360   FORMAT(1X,6F10.3,2X,3I5)
      IF(IWL.EQ.2) GO TO 370
      XN=XNIN*CINMTR
      YN=YNIN*CINMTR
```

SUBSTITUTE SHEET

```
        ZN=ZNIN*CINMTR
        RLSX=RLSXIN*CINMTR
        RLSY=RLSYIN*CINMTR
        RLSZ=RLSZIN*CINMTR
370     CONTINUE
C**ALL DIMENSIONS IN METERS
        NELN=NCOLXN*NROWYN
        NPTSN=NELN*NCOLZN
C***SET DEFAULT VALUES FOR DXN,DYN,DZN
        DXN=0.0
        DYN=0.1
        DZN=0.0
        IF(NCOLXN.GT.1)DXN=RLSX/(NCOLXN-1)
        IF(NROWYN.GT.1)DYN=RLSY/(NROWYN-1)
        IF(NCOLZN.GT.1)DZN=RLSZ/(NCOLZN-1)
        IC=0
        BIGNDB=-299.0
        DO 3000 ICOLZN=1,NCOLZN
        ZPOS=ZN+DZN*(ICOLZN-1)
        DO 3000 IROWYN=1,NROWYN
        Y=YN+DYN*(IROWYN-1)
        DO 3000 ICOLXN=1,NCOLXN
        CALL GETCP2(CPU2)
        CPUSUB=CPU2-CPU1
        WRITE(6,7319)CPUSUB
7319    FORMAT(1X,'CPU SUBTOTAL=',F14.2)
        IC=IC+1
        X=XN+DXN*(ICOLXN-1)
        XC(IC)=X
        YC(IC)=Y
        ZC(IC)=ZPOS
        WRITE(6,6969)IC,XC(IC),YC(IC),ZC(IC)
6969    FORMAT(1X,'IC,XC,YC,ZC=',I4,2X,3F12.3)
        IF(ICIRC.EQ.0)
2CALL NFDPX2(CTPR,STPR,CTDP,STDP,X,Y,ZPOS,0.0,0,VCW,VREFCW)
```

SUBSTITUTE SHEET

```
      IF(ICIRC.EQ.1)
     2CALL NFDPC2(X,Y,2POS,0.0,0,VCW,VREFCW)
      IF(IMUT.EQ.0) GO TO 4255
C***SOLVE EACH SYSTEM OF EQUATIONS FOR THE UNKNOWN CURRENTS
      IF(IBLT.EQ.1) GO TO 4040
      I12=2
      WRITE(6,6110)
      CALL CROUT(Z,VCW,ICC1,ICC,ISYM,IWR,I12,NEL)
      GO TO 4255
 4040 IENTRY=3
      CALL BLTSOL(CZ,VCW,PS,NCOLX,IDMB,IENTRY)
 4255 CONTINUE
C***COMPUTE RECEIVED VOLTAGES FOR PRESENT SCAN
      DO 3285 IIIC=1,NEL
      VRECVX(IIIC)=VCW(IIIC)*ZLOAD
 3285 CONTINUE
C***STORE AUX. CHANNEL VOLTAGES
      DO 1681 IAX=1,NAUX
C**MODIFICATION TO INCLUDE AUX. ATTEN.
      VAXCWA(IAX,IC)=VRECVX(IAUXA(IAX))*VATENA(IAX)
CC    WRITE(6,3231)IAX,IC,XC(IC),VAXCWA(IAX,IC)
 3231 FORMAT(1X,'IAX,IC,XC,VAXCWA(IAX,IC)=',2I4,2X,F12.3,2X,2E12.5)
 1681 CONTINUE
C***PERFORM BEAM FORMATION
      CSUMA=(0.,0.)
      DO 5444 KC=1,NEL
      CSUMA=CSUMA+VRECVX(KC)*CWTA(KC,1)
 5444 CONTINUE
      VXA=CSUMA
      IF(CABS(VXA).EQ.0.)VXA=(1.E-10,0.)
      VXADB(IC)=20.*ALOG10(CABS(VXA))
      IF(VXADB(IC).GT.BIGNDB) BIGNDB=VXADB(IC)
      VXAPH(IC)=ATAN2(AIMAG(VXA),REAL(VXA))/DCR
      VXMANA(IC)=10.**(VXADB(IC)/20.)*CEXP(CJ*VXAPH(IC)*DCR)
CC    WRITE(6,4457)IC,VXMANA(IC)
```

SUBSTITUTE SHEET

```
4457   FORMAT(1X,'IC,VXMANA=',I4,2X,2E12.5)
       WRITE(6,6429)IC,XC(IC),VXADB(IC)
6429   FORMAT(1X,'IC,X,VXADB=',I4,2X,F10.2,2X,F12.2)
3000   CONTINUE
       IF(IENORM.EQ.0) GO TO 2500
       WRITE(6,3765)BIGNDB
3765   FORMAT(1X,'BIGNDB=',F12.2)
       DO 3020 IC=1,NPTSN
CC     WRITE(6,3343)IC,VXADB(IC)
       VXADB(IC)=VXADB(IC)-BIGNDB
CC     WRITE(6,3343)IC,VXADB(IC)
3020   CONTINUE
2500   WRITE(6,3030)
3030   FORMAT(1X,'WANT TO PLOT NEAR FIELD CUTS, IPLOTN=1')
       READ(5,*)IPLOTN
C***NEXT LINE ADDED TO AVOID RUN TIME ERROR
       IF(IPCONN.EQ.1) IPLOTN=0
       IF(IPCONN.EQ.0) THEN
       WRITE(30,18889)
       WRITE(30,18888)XN,NCOLXN,DXN,ZN,NCOLZN,DZN
       WRITE(30,4547)
4547   FORMAT(1X,'IZ,IX,VXADB(IC)')
       ENDIF
       IPP=0
       DO 7788 IZ=1,NCOLZN
       DO 7788 IY=1,NROWYN
       DO 7788 IX=1,NCOLXN
       IPP=IPP+1
       DO 7788 IPP=1,NPTSN
CC     WRITE(6,3343)IPP,VXADB(IPP)
CC
3343   FORMAT(1X,'IPP,VXADB=',I4,2X,F12.2)
       IF(IPCONN.EQ.0) WRITE(30,*) IZ,IX,VXADB(IPP)
7788   CONTINUE
3040   IF((NCOLXN.GT.1.OR.NROWYN.GT.1).AND.IPLOTN.EQ.1)
      1CALL PLOTTR(NCOLXN,NROWYN,NCOLZN,XC,YC,ZC,NPTSN,VXADB,VXAPH,
```

SUBSTITUTE SHEET

```
      2VXADB,VXAPH)
       IF(NELN.EQ.1.AND.IPLOTN.EQ.1)
      1CALL PLOTAX(NPTSN,ZC,VXADB,VXAPH,VXADB,VXAPH)
       IF(IPCONN.EQ.0) GO TO 3939
C***THIS SECTION FOR CONTOUR PLOTS
       NCLXN2=NCOLXN+2
       NRWYN2=NROWYN+2
       NCLZN2=NCOLZN+2
       DO 3777 IX=1,NCOLXN
       RX(IX)=(XN+DXN*(IX-1))/CINMTR
3777   CONTINUE
       DO 3008 IY=1,NROWYN
       RY(IY)=(YN+DYN*(IY-1))/CINMTR
3008   CONTINUE
       DO 3009 IZ=1,NCOLZN
       RZ(IZ)=(ZN+DZN*(IZ-1))/CINMTR
3009   CONTINUE
       IC=0
       IF(IXZ.EQ.1) WRITE(30,18889)
18889  FORMAT(1X,'XN,NCOLXN,DXN,ZN,NCOLZN,DZN=')
       IF(IXZ.EQ.1) WRITE(30,18888) XN,NCOLXN,DXN,ZN,NCOLZN,DZN
18888  FORMAT(1X,E14.5,I5,2X,E14.5,2X,E14.5,I5,2X,E14.5)
       IF(IXZ.EQ.1) WRITE(30,4546)
4546   FORMAT(1X,'IZ,IX,FM(IZ,IX)')
       DO 3022 IZ=1,NCOLZN
       DO 3022 IY=1,NROWYN
       DO 3022 IX=1,NCOLXN
       IC=IC+1
       IF(IXY.EQ.1) FM(IY,IX)=VXADB(IC)
       IF(IXZ.EQ.1) FM(IZ,IX)=VXADB(IC)
       IF(IXZ.EQ.1.AND.IPCONN.EQ.1) WRITE(30,*) IZ,IX,FM(IZ,IX)
3022   CONTINUE
       IF(IXY.EQ.1)
      2CALL PLCONT(NCOLXN,NROWYN,NCLXN2,NRWYN2,RX,RY,FM,DMF,-50.,
      310.,5,1)
```

SUBSTITUTE SHEET

```
      IF(IX2.EQ.1)
     2CALL PLCONT(NCOLXN,NCOLZN,NCLXN2,NCLZN2,RX,RZ,FM,DMF,-50.,
     310.,5,1)
3939  CONTINUE
CC    WRITE(25,*)NCOLXN
      DO 1767 IDDD=1,NCOLXN
CC    WRITE(25,*)VXADB(IDDD)
1767  CONTINUE
      WRITE(6,3050)
3050  FORMAT(1X,'PLOT NEAR FIELD AGAIN?, IPLA=1')
      READ(5,*)IPLA
      IF(IPLA.EQ.1) GO TO 3040
390   CONTINUE
      ISTOP=0
      IF(ISTOP.EQ.1) GO TO 9999
C***CALL PRNTDA (PRINT PARAMETERS)
C370    CALL PRNTDA
      IF(IPATRN.EQ.0) GO TO 440
410   WRITE(6,420)
420   FORMAT(1X,'ISYLMBL FOR PLOTTING, LT. 0 THEN NOT USED')
      READ(5,*)ISYMBL
      WRITE(6,430)
430   FORMAT(1X,'WANT TO PLOT PATTERNS AGAIN?, IPFNA=1')
      READ(5,*)IPFNA
      IF(IPFNA.EQ.1) GO TO 410
440   CONTINUE
C***THIS SECTION FOR COVARIANCE MATRIX COMPUTATION
      IF(NJAMS.EQ.0) GO TO 9999
      DO 7999 ICH=1,NMAX
      DO 7999 JCH=1,NMAX
      COVNF(ICH,JCH)=DCMPLX(0.0D0,0.0D0)
7999  CONTINUE
8888  IF(NJAMS.EQ.0) GO TO 4444
C***THIS SECTION FOR JAMMER COVARIANCE MATRIX
      FMINHZ=FCHZ-BWFHZ/2.
```

SUBSTITUTE SHEET

```
      DELFHZ=0.0
      IF(NFREQ.GT.1) DELFHZ=BWFHZ/(NFREQ-1)
      DO 600 IFR=1,NFREQ
      FHZ=FMINHZ+DELFHZ*(IFR-1)
      FGHZ=FHZ/1.0E9
C***COMPUTE FREE SPACE WAVELENGTH AT EACH FREQUENCY
      RLAMDA=2.997925E10/FHZ/2.54
C***NOTE: GAMMA= ALPHA +J BETA
C***      AND RLAMDA=2 PI/ BETA      (REF. HAYT PG. 334)
C***THUS NEED TO COMPUTE GAMMA, AND ETA FOR EACH FREQ.
      IF(IWL.EQ.2) GO TO 8789
      DX=DXIN*CINMTR
      DY=DYIN*CINMTR
      HL=HLIN*CINMTR
      ARAD=ARADIN*CINMTR
      HZ=HZIN*CINMTR
8789  CONTINUE
      CALL ZMATRX(CTDP,STDP,IBLTSL,ICC1,ICC,CC2,2)
C***COMPUTE ELEMENT INDUCED VOLTAGES DUE TO JAMMER SOURCES
      CALL VJAMMR(NJAMS,NEL,PWRJDB,ICC1,ICC,PS,CZ,Z,CWTA
     1,NB,IDMB,NAUX,IAUXA,ZLOAD,XJAMIN,YJAMIN,ZJAMIN,
     2IFR,NFREQ,CTPR,STPR,CTDP,STDP,VMAJMA,VMAJMA,VAUXJA)
      WRITE(6,1234)IFR,VMAJMA(1,1,IFR),VAUXJA(1,1,IFR)
      WRITE(8,1234)IFR,VMAJMA(1,1,IFR),VAUXJA(1,1,IFR)
1234  FORMAT(1X,'IFR,VMAJMA,VAUXA=',I4,2X,4E11.4)
600   CONTINUE
C***FORM RECEIVED VOLTAGE MATRIX
C***VRECVM(MAIN A, AUX A1, AUX A2,... AUX AN :)
      DO 9001 IJAM=1,NJAMS
      DO 9002 IFR=1,NFREQ
      IF(ISLC.EQ.1) VCHA(1,IFR)=VMAJMA(IJAM,IFR)
CC    WRITE(6,6789)IJAM,IFR,VMAJMA(IJAM,IFR)
6789  FORMAT(1X,'IJAM,IFR,VMAJMA(IJAM,IFR)=',2I4,2X,2E12.5)
      DO 9003 IA=1,NAUX
      IAP1=IA+1
```

SUBSTITUTE SHEET

```
      IF(ISLC.EQ.1) VCHA(IAP1,IFR)=VAUXJA(IA,IJAM,IFR)*VATENA(IA)
      IF(ISLC.EQ.0) VCHA(IA,IFR)=VAUXJA(IA,IJAM,IFR)*VATENA(IA)
      WRITE(6,8876)IJAM,IFR,IA,VAUXJA(IA,IJAM,IFR)
      WRITE(8,8876)IJAM,IFR,IA,VAUXJA(IA,IJAM,IFR)
8876  FORMAT(1X,' IJAM,IFR,IA,VAUXJA=',3I4,2X,2E12.4)
9003  CONTINUE
9002  CONTINUE
      DO 5555 KKK=1,4
      DO 5555 LLL=1,NFREQ
CCC   WRITE(6,6655)KKK,LLL,VCHA(KKK,LLL)
5555  CONTINUE
      WRITE(6,5533)
5533  FORMAT(1X,'NOW COMPUTE JAMMER COVARIANCE MATRIX')
C***COMPUTE COVARIANCE MATRIX FOR JTH JAMMER SOURCE
      IF(NFREQ.GT.1) CALL COVSWC(VCHA,VCHA,NMAX,NFREQ,BWFHZ,COVAAJ)
      DO 9005 ICH=1,NMAX
      DO 9005 JCH=1,NMAX
      COVNF(ICH,JCH)=COVNF(ICH,JCH)+COVAAJ(ICH,JCH)
CC    WRITE(6,2299)ICH,JCH,COVNF(ICH,JCH)
9005  CONTINUE
9001  CONTINUE
C***ADD RECEIVER NOISE TO DIAGONAL ELEMENTS
4444  DO 8006 ICH=1,NMAX
      COVNF(ICH,ICH)=COVNF(ICH,ICH)+1.0D0
8006  CONTINUE
      DO 2727 I=1,NMAX
      DO 2727 J=1,NMAX
      IF(CDABS(COVNF(I,J)).EQ.0.0D0) GO TO 2727
      CNDB=10.*DLOG10(CDABS(COVNF(I,J)))
      PREALN=DREAL(COVNF(I,J))
      PIMAGN=DIMAG(COVNF(I,J))
      PHASEN=DATAN2(PIMAGN,PREALN)/DCR
      WRITE(8,4411)I,J,CNDB,PHASEN
      IF(I.EQ.1)WRITE(6,4411)I,J,CNDB,PHASEN
4411  FORMAT(1X,'I,J,CNDB,PHASEN=',2I4,2X,2F12.2)
```

```
2727  CONTINUE
C***COMPUTE COVARIANCE MATRIX INVERSE
      DO 8007 ICH=1,NMAX
      DO 8007 JCH=1,NMAX
      COVNFI(ICH,JCH)=COVNF(ICH,JCH)
8007  CONTINUE
      CALL DCMINV(COVNFI,LTMP,MTMP,NMAX,NMAX)
C***CHECK MATRIX INVERSION ACCURACY    (CINVERSE*C=I)
      CALL CMMULT(COVNFI,COVNF,NMAX,NMAX,NMAX,CINVCN)
      DO 8008 ICH=1,NMAX
      DO 8008 JCH=1,NMAX
      IF(ICH.EQ.1)WRITE(6,8009)ICH,JCH,CINVCN(ICH,JCH)
8009  FORMAT(1X,'ICH,JCH,CINVCN=',2I4,2X,2E12.5)
8008  CONTINUE
C***COMPUTE EIGENVALUES (ALSO EIGENVECTORS AND PERFORMANCE INDEX)
      IJOB=2
      CALL EIGCC(COVNF,NMAX,NMAX,IJOB,EIGVAN,EIGVEN,NMAX,WKE,IER)
      WRITE(6,155)IER
155   FORMAT(1X,'AFTER COMPUTE EIGENVALUES,  IER=',I5)
      DO 200 I=1,NMAX
      WRITE(6,300)I,EIGVAN(I)
300   FORMAT(1X,'I,EIGVAN=',2X,I4,2E10.3)
200   CONTINUE
      DO 205 I=1,NMAX
      EVLDBN=10.*DLOG10(CDABS(EIGVAN(I)))
      WRITE(8,207)I,EVLDBN
      WRITE(6,207)I,EVLDBN
207   FORMAT(1X,'I,EVLDBN=',I4,2X,2F12.3)
205   CONTINUE
C***  CALL PRNTDA
C***FILL-IN SIDELOBE CANCELLER QUIESCENT WEIGHTS
      DO 8985 I=1,NMAX
      WQSLC(I,1)=DCMPLX(0.0D0,0.0D0)
8985  CONTINUE
      WQSLC(1,1)=DCMPLX(1.0D0,0.0D0)
```

SUBSTITUTE SHEET

```
          DO 7769 I=1,NMAX
          WRITE(6,1212)I,WQSLC(I,1)
          WRITE(8,1212)I,WQSLC(I,1)
1212      FORMAT(1X,'I,WQSLC=',I4,2X,2E12.5)
7769      CONTINUE
C***COMPUTE QUIESCENT INR
          IF(ISLC.EQ.1) CALL INRTIO(WQSLC,COVNF,NMAX,WTCTR,CMPROD,QINRDB)
          IF(ISLC.EQ.0) CALL INRTIO(CWTA,COVNF,NMAX,WTCTR,CMPROD,QINRDB)
          QINRAA=10.*DLOG10(CDABS(COVNF(1,1)))
C***COMPUTE AVERAGE CANCELLATION
          SUMC=0.0
          SUMAA=0.0
          DO 1829 IR=1,NRAN
C***ZERO-OUT ADAPTIVE WEIGHTS INITIALLY
          DO 57 I=1,NMAX
          WAN(I,1)=DCMPLX(0.0D0,0.0D0)
57        CONTINUE
C***COMPUTE ADAPTIVE ARRAY WEIGHTS
          IF(ISLC.EQ.1) CALL CMMULT(COVNFI,WQSLC,NMAX,NMAX,1,WAN)
          IF(ISLC.EQ.0) CALL CMMULT(COVNFI,CWTA,NMAX,NMAX,1,WAN)
C***QUANTIZE AND RANDOMIZE ADAPTIVE WEIGHT SETTINGS
          IF(IQUAN.EQ.1.AND.NBADWT.LT.20)
2         CALL ADQUAN(NMAX,WAN,NBADWT,IRNERR,INITRN,AWSGDB,AWSGDG)
C***NORMALIZE FULLY ADAPTIVE WEIGHTS
          IF(ISLC.EQ.0) THEN
          SAVE=0.0D0
          DO 33345 I=1,NEL
          SAVE=SAVE+CDABS(WAN(I,1))**2
33345     CONTINUE
          SAVESR=DSQRT(SAVE)
          DO 44456 I=1,NEL
          WAN(I,1)=WAN(I,1)/SAVESR
          WANDB=20.*DLOG10(CDABS(WAN(I,1)))
          IF(IR.EQ.1) WRITE(6,3599)I,WANDB
          IF(IR.EQ.1) WRITE(8,3599)I,WANDB
```

```
3599    FORMAT(1X,'I=',I4,2X,'WANDB=',1X,F12.3)
44456   CONTINUE
        ENDIF
C****TO PRINT NORMALIZED WEIGHTS
        BIGWDB=-299.0
        DO 9102 I=1,NMAX
        IF(IR.EQ.1) WRITE(6,6191)I,WAN(I,1)
        IF(IR.EQ.1) WRITE(8,6191)I,WAN(I,1)
6191    FORMAT(1X,'I,WAN(I,1)=',I4,2X,2E12.5)
        WANDBM=20.*DLOG10(CDABS(WAN(I,1)))
        IF(WANDBM.GT.BIGWDB) BIGWDB=WANDBM
9102    CONTINUE
        DO 9112 I=1,NMAX
        WANDB=20.*DLOG10(CDABS(WAN(I,1)))-BIGWDB
        WANDG=DATAN2(DIMAG(WAN(I,1)),DREAL(WAN(I,1)))/DCR
        IF(IR.EQ.1) WRITE(6,35991)I,WANDB,WANDG
        IF(IR.EQ.1) WRITE(8,35991)I,WANDB,WANDG
35991   FORMAT(1X,'I=',I4,2X,'WANDB,WANDG=',1X,2F14.5)
9112    CONTINUE
C***COMPUTE ADAPTED INR
        CALL INRTIO(WAN,COVNF,NMAX,WTCTR,CMPROD,AINRDB)
C***COMPUTE CANCELLATION
        CANCDB=AINRDB-QINRDB
        WRITE(6,3007)QINRDB,AINRDB,CANCDB
        WRITE(8,3007)QINRDB,AINRDB,CANCDB
3007    FORMAT(1X,'INR= QUI,ADAP ,CANCEL=',2X,3F10.3,2X,' DB')
        SUMC=SUMC+CANCDB
C***COMPUTE ADAPTED INR CH. A
        DO 2255 I=1,NMAX
        WANDMA(I,1)=WAN(I,1)
        IF(I.GT.NMAX) WANDMA(I,1)=(0.0D0,0.0D0)
2255    CONTINUE
        CALL INRTIO(WANDMA,COVNF,NMAX,WTCTR,CMPROD,AINRAA)
C***CANCELLATION CH. A
        CNCLNA=AINRAA-QINRAA
```

SUBSTITUTE SHEET

WO 93/00132

PCT/US92/05464

-94-

```
         WRITE(6,3738)QINRAA,AINRAA,CNCLNA
         WRITE(8,3738)QINRAA,AINRAA,CNCLNA
3738     FORMAT(1X,'SIDELOBE CANCELLER CH. A INR= QUI,ADAP,CAN=',2X,3F10.3)
         SUMAA=SUMAA+CNCLNA
1829     CONTINUE
         AVECAN=SUMC/NRAN
         WRITE(6,4456)CANCDB,NRAN,AVECAN
4456     FORMAT(1X,'CANCDB,NRAN,AVECAN=',F12.5,2X,I5,2X,F12.5)
         WRITE(8,4456)CANCDB,NRAN,AVECAN
         AVECAA=SUMAA/NRAN
         WRITE(6,2220)AVECAA
         WRITE(8,2220)AVECAA
2220     FORMAT(1X,'AVE. CANEL. CH. A, =',2X,F12.5)
C***SECTION TO COMPUTE ADAPTIVE ARRAY RADIATION PATTERNS
CC       IF(INEAR.EQ.0.OR.IANGLP.EQ.0) GO TO 9990
         IF(INEAR.EQ.0) GO TO 9990
         BIGADB=-299.
         IC=0
         DO 8919 IZ=1,NCOLZN
         DO 8919 IY=1,NROWYN
         DO 8919 IX=1,NCOLXN
         IC=IC+1
         CSUMA=(0.,0.)
         IF(ISLC.EQ.1) CSUMA=CSUMA+DCONJG(WAN(1,1))*VXMANA(IC)
         DO 7921 IAX=1,NAUX
         IAXP1=IAX+1
         IF(ISLC.EQ.1) CSUMA=CSUMA+DCONJG(WAN(IAXP1,1))*VAXCWA(IAX,IC)
         IF(ISLC.EQ.0) CSUMA=CSUMA+DCONJG(WAN(IAX,1))*VAXCWA(IAX,IC)
7921     CONTINUE
         IF(CABS(CSUMA).EQ.0.) CSUMA=(1.E-10,0.)
         PCHADB(IC)=20.*ALOG10(CABS(CSUMA))
         IF(PCHADB(IC).GT.BIGADB) BIGADB=PCHADB(IC)
         WRITE(6,4999) IC,PCHADB(IC)
8919     CONTINUE
C***NORMALIZE ADAPTIVE PATTERNS
```

SUBSTITUTE SHEET

```
      IF(IXZ.EQ.1)  WRITE(31,18889)
      IF(IXZ.EQ.1)  WRITE(31,18888)XN,NCOLXN,DXN,ZN,NCOLZN,DZN
      IF(IXZ.EQ.1)  WRITE(31,4546)
      IC=0
      DO 3459 IZ=1,NCOLZN
      DO 3459 IY=1,NROWYN
      DO 3459 IX=1,NCOLXN
      IC=IC+1
      PCHADB(IC)=PCHADB(IC)-BIGADB
      IF(IPCONN.EQ.0) WRITE(31,*)IZ,IX,PCHADB(IC)
      IF(IPCONN.EQ.0) GO TO 3459
      IF(IXY.EQ.1)  FM(IY,IX)=PCHADB(IC)
      IF(IXZ.EQ.1)  FM(IZ,IX)=PCHADB(IC)
      IF(IXZ.EQ.1.AND.IPCONN.EQ.1) WRITE(31,*) IZ,IX,FM(IZ,IX)
 3459 CONTINUE
      WRITE(25,*)NCOLXN
      DO 1879 IDDD=1,NCOLXN
      WRITE(25,*)PCHADB(IDDD)
 1879 CONTINUE
      IF((NCOLXN.GT.1.OR.NROWYN.GT.1).AND.IPLOTN.EQ.1.AND.IPLOTN.EQ.1.AND.IANGLP.EQ.0)
     2CALL PLOTTR(NCOLXN,NROWYN,NCOLZN,XC,YC,ZC,NPTSN,PCHADB,PCHADB,
     3PCHADB,PCHADB)
      IF(IPCONN.EQ.1.AND.IXY.EQ.1)
     2CALL PLCONT(NCOLXN,NROWYN,NCLXN2,NRWYN2,RX,RY,
     3FM,DMF,-50.,10.,5,1)
      IF(IPCONN.EQ.1.AND.IXZ.EQ.1)
     2CALL PLCONT(NCOLXN,NCOLZN,NCLXN2,NCLZN2,RX,RZ,
     3FM,DMF,-50.,10.,5,1)
 9990 CONTINUE
 9999 CONTINUE
      CALL DONEPL
      CALL GETCP2(CPUL)
      CPUTOT=CPUL-CPU1
      WRITE(6,2006)CPUTOT
 2006 FORMAT(1X,'TOTAL CPU TIME=',F15.2)
```

SUBSTITUTE SHEET

```
      STOP
      END
C***SUBROUTINE TO COMPUTE IMPEDANCE MATRIX
      SUBROUTINE ZMATRX(CTDP,STDP,IBLTSL,ICC1,ICC,CZ,Z)
      COMPLEX Z(ICC1,ICC),CZ(1)
      COMMON/A/DX,DY,NCOLX,NROWY,NEL,HZ,HL,ARAD,ZLOAD,ZCHAR
      COMMON /GROUND/ IGRNDP
      COMMON /CIRCLE/ ICIRC,RADIUS,HLS
      NB=NCOLX
      IDMB=NROWY
C***COMPUTE MUTUAL IMPEDANCES Z(1,1),Z(1,2),Z(1,3),....,Z(1,NEL).
CC    CALL RGDZMN(IGRNDP,ICC1,ICC,Z)
CC    CALL RGDZAB(CTDP,STDP,IGRNDP,ICC1,ICC,Z)
      IF(ICIRC.EQ.0) CALL RGDZA2(CTDP,STDP,IGRNDP,ICC1,ICC,Z)
      IF(ICIRC.EQ.1) CALL CADZA2(CTDP,STDP,IGRNDP,ICC1,ICC,Z)
      WRITE(8,10) NEL,NCOLX,NROWY
10    FORMAT(1X,'NEL,NCOLX,NROWY=',3I5)
      ICOUNT=0
      DO 20 I=1,NCOLX
      DO 20 J=1,NROWY
      ICOUNT=ICOUNT+1
      WRITE(6,80) I,J,Z(1,ICOUNT)
80    FORMAT(1X,'I,J,Z(1,ICOUNT)=',2I4,2X,2E12.5)
20    CONTINUE
      IDM=NEL
      ICC=NEL
C***FILL THE IMPEDANCE MATRIX
      IF(NCOLX.LE.1) GO TO 70
      IBLT=IBLTSL
      IDM1=IDMB
      IF(IBLT.EQ.0) IDM1=NEL
      IF(NROWY.GT.1) GO TO 40
C***FILL TOEPLITZ MATRIX
      DO 30 I=2,NEL
      DO 30 J=I,NEL
```

SUBSTITUTE SHEET

```
      K=1+J-I
      Z(I,J)=Z(1,K)
30    CONTINUE
      GO TO 50
40    CALL BTOEPL(IBLT,NB,IDMB,IDM1,IDM,Z)
50    CONTINUE
      IF(IBLT.EQ.0) GO TO 70
      DO 60 I=1,IDMB
      DO 60 J=1,IDM
      IC=(J-1)*IDMB+I
      CZ(IC)=Z(I,J)
CC    WRITE(8,7878)I,J,Z(I,J)
7878  FORMAT(1X,'I,J,Z(I,J)=',2I4,2X,2E12.5)
60    CONTINUE
70    CONTINUE
      RETURN
      END
C***SUBROUTINE TO COMPUTE RECEIVE BEAMFORMER WEIGHTS
      SUBROUTINE VRCVWT(NACOLX,NAROWY,NXDUM,NYDUM,EDGTDB,WA,WB)
      DIMENSION WA(1),WB(1)
      DIMENSION WT(180)
      COMMON/A/DX,DY,NCOLX,NROWY,NEL,HZ,HL,ARAD,ZLOAD,ZCHAR
      COMMON /CHEBY/ ICHEB,SLLDB
      PI=3.141592654
      TPI=2.*PI
      DCR=PI/180.
      SLLDB=40.
CC    TAP=10.**(EDGTDB/20.)
      WRITE(6,*)TAP
      AMP=(1.-TAP)/2.
      NPDX=NCOLX-NACOLX-2*NXDUM
      AXL=DX*(NACOLX-1)
      AYL=DY*(NAROWY-1)
      IF(TAP.NE.1.0)FX=AXL/2.*PI/ACOS(TAP)
      IF(TAP.NE.1.0)FY=AYL/2.*PI/ACOS(TAP)
```

```
20      WRITE(6,20)
        FORMAT(1X,'BEFORE CALL CHEBWT')
30      WRITE(6,30)SLLDB
        FORMAT(1X,'SLLDB=',2X,F10.2)
        IF(ICHEB.EQ.1)CALL CHEBWT(NACOLX,SLLDB,WT,RLOSS)
        WRITE(6,40)
40      FORMAT(1X,'AFTER CHEBWT')
        DO 1000 IC=1,NEL
        WA(IC)=0.0
        WB(IC)=0.0
1000    CONTINUE
C***COMPUTE EFFECTIVE DIPOLE CENTER COORDS. FOR BOTH PHASE CENTERS
        X0=-AXL/2.
        Y0=-AYL/2.
        IC=0
        DO 80 I=1,NACOLX
        DO 80 J=1,NAROWY
        IC=IC+1
        X=X0+DX*(I-1)
        Y=Y0+DY*(J-1)
        TAPERX=1.0
        TAPERY=1.0
        IF(ICHEB.EQ.1) GO TO 70
        IF(TAP.NE.1.0)TAPERX=COS(PI*X/FX)
        IF(TAP.NE.1.0.AND.FY.NE.0.0)TAPERY=COS(PI*Y/FY)
        TAPER=TAPERX*TAPERY
        WT(IC)=TAPER
70      CONTINUE
80      CONTINUE
C***TRANSFORM FROM SUB-APERTURES TO FULL ARRAY
        IBGNA=NXDUM*NROWY+NYDUM
        IBGNB=IBGNA+NPDX*NROWY
        IC=0
        DO 1010 IX=1,NACOLX
        DO 1010 IY=1,NAROWY
```

```
        IC=IC+1
        IA=IBGNA+(IX-1)*NROWY+IY
        IB=IBGNB+(IX-1)*NROWY+IY
        WA(IA)=WT(IC)
        WB(IB)=WT(IC)
1010    CONTINUE
        RETURN
        END
C***SUBROUTINE TO COVARIANCE MATRIX BASED ON NUMERICAL INTEGRATION
C***IN THE FREQUENCY DOMAIN ACCORDING TO SIMPSON'S RULE
        SUBROUTINE COVSWC(VA,VB,NCHAN,NFREQ,BWFHZ,COVAB)
        COMPLEX *16 VA(NCHAN,NFREQ),VB(NCHAN,NFREQ)
        COMPLEX *16 COVAB(NCHAN,NCHAN),CSUM,DCABF
        REAL *8 SWC(101)
        DELTAF=BWFHZ/(NFREQ-1)
        CALL SIMWC(NFREQ,SWC)
        DO 10 ICH=1,NCHAN
        DO 10 JCH=1,NCHAN
        CSUM=(0.0D0,0.0D0)
        DO 20 IFR=1,NFREQ
        DCABF=VA(ICH,IFR)*DCONJG(VB(JCH,IFR))
        CSUM=CSUM+DCABF*SWC(IFR)
CC      WRITE(6,6767)IFR,CSUM
6767    FORMAT(1X,'IFR,CSUM=',I4,2X,2E12.5)
20      CONTINUE
        COVAB(ICH,JCH)=DELTAF/2.*CSUM
C***NEW LINE TO NORMALIZE COVAB
        COVAB(ICH,JCH)=COVAB(ICH,JCH)/BWFHZ
CC      WRITE(6,4567)ICH,JCH,COVAB(ICH,JCH)
4567    FORMAT(1X,'ICH,JCH,COVAB(ICH,JCH)=',2I4,2X,2E12.5)
10      CONTINUE
        RETURN
        END
C***SUBROUTINE TO GENERATE SIMPSON'S 1/3 RULE WEIGHTING COEF.
C***INTGERAL F(X)DX=(DELTAX/3.)*(F(1)+4*F(2)+2*F(3)+4*F(4)+...+F(OOD))
```

SUBSTITUTE SHEET

-100-

```
C*** THE SERIES 1 4 2 4 2 4 .....1 ARE SIMPSON'S COEF.
      SUBROUTINE SIMWC(NCOEF,SWC)
      REAL *8 SWC(NCOEF)
      DO 10 N=1,NCOEF
      XNN=FLOAT(N)
      NN=N/2
      TT=XNN/2.
      DIF=TT-FLOAT(NN)
      NC=2
      IF(DIF.EQ.0.) NC=4
      IF(N.EQ.1.OR.N.EQ.NCOEF) NC=1
      SWC(N)=NC
   10 CONTINUE
      RETURN
      END
C***SUBROUTINE TO COMPUTE RECEIVED VOLTAGES DUE TO JAMMER SOURCES
      SUBROUTINE VJAMMR(NJM,NEL,PWRJDB,ICC1,ICC,PS,CZ,Z,CWTA
     1,NB,IDMB,NAUX,IAUXA,ZLOAD,XJAMIN,YJAMIN,ZJAMIN,
     2IFR,NFR,CTPR,STPR,CTDP,STDP,VMAINA,VAUXA)
      COMPLEX *16 CWTA(NEL,1)
      COMPLEX PS(1),CZ(1),Z(ICC1,ICC)
      COMPLEX VJM(180),VREFJM
      COMPLEX CJ,CSUMA
      COMPLEX *16 VMAINA(NJM,NFR)
      COMPLEX *16 VAUKA(NAUX,NJM,NFR)
      DIMENSION PWRJDB(1),PWRJ(10)
      DIMENSION XJAMIN(1),YJAMIN(1),ZJAMIN(1)
      INTEGER IAUXA(1)
      COMMON/PCENTR/PCDXIN
      COMMON /B/ NGEN,IGEN,THETAS,PHIS,IMUT,IBLTSL,IPATRN
      COMMON /D/ FGHZ,RLAMDA,IWL,IS,NSCANS
      COMMON /WRITE/ IWR
      COMMON /CIRCLE/ ICIRC,RADIUS,HLS
      PI=3.141592654
      DCR=PI/180.
```

SUBSTITUTE SHEET

```
      CJ=(0.,1.)
      CINMTR=0.0254
      ISYM=0
C***CONVERT DB TO POWER (RELATIVE TO NOISE)
      DO 10 II=1,NJM
      PWRJ(II)=10.**(PWRJDB(II)/10.)
      WRITE(6,66)II,PWRJ(II)
      WRITE(8,66)II,PWRJ(II)
66    FORMAT(1X,'II,PWRJ IN POWER=',I4,2X,E12.5)
10    CONTINUE
      IF(IFR.GT.1) GO TO 55
      WRITE(6,20)IWL
      DO 5544 IJAM=1,NJM
      WRITE(6,40)
      WRITE(6,50)XJAMIN(IJAM),YJAMIN(IJAM),ZJAMIN(IJAM)
5544  CONTINUE
20    FORMAT(1X,'IWL=',I4)
      WRITE(6,30)
30    FORMAT(1X,'CHANGE NEAR FIELD JAMMER POSITIONS (INCHES)?, ICH=1')
      READ(5,*)ICH
      IF(ICH.EQ.0) GO TO 55
      DO 8887 IJAM=1,NJM
      WRITE(6,40)
40    FORMAT(1X,'XJAMIN,YJAMIN,ZJAMIN,=')
      READ(5,*,END=55)XJAMIN(IJAM),YJAMIN(IJAM),ZJAMIN(IJAM)
      WRITE(6,50)XJAMIN(IJAM),YJAMIN(IJAM),ZJAMIN(IJAM)
50    FORMAT(1X,5F10.3,2X,2I5)
8887  CONTINUE
55    CONTINUE
      PCDX=PCDXIN*CINMTR
      WRITE(6,4757)IFR
4757  FORMAT(1X,'FREQ. INDEX, IFR=',I4)
60    CONTINUE
C**ALL DIMENSIONS IN METERS
      DO 180 IPHACN=1,1
```

SUBSTITUTE SHEET

```
2223    WRITE(6,2223)IPHACN
        FORMAT(1X,'IPHACN=',I4)
        XREFDP=-PCDX/2.+(IPHACN-1)*PCDX
C***PERFORM JAMMER SOURCE SCAN
        DO 180 IJAM=1,NJM
        X=XJAMIN(IJAM)*CINMTR+PCDX*(IPHACN-1)
        Y=YJAMIN(IJAM)*CINMTR
        ZPOS=ZJAMIN(IJAM)*CINMTR
        WRITE(6,6688)X,Y,ZPOS,XREFDP
6688    FORMAT(1X,'X,Y,ZPOS,XREFDP (METERS)=',4F12.4)
        IF(ICIRC.EQ.0)
       2CALL NFDPX2(CTPR,STPR,CTDP,STDP,X,Y,ZPOS,XREFDP,1,VJM,VREFJM)
        IF(ICIRC.EQ.1)
       2CALL NFDPC2(X,Y,ZPOS,XREFDP,1,VJM,VREFJM)
C***NORMALIZE INCIDENT JAMMER POWER
        DO 70 INORM=1,NEL
        VJM(INORM)=VJM(INORM)/VREFJM*SQRT(PWRJ(IJAM))
        WRITE(6,77)INORM,VJM(INORM)
77      FORMAT(1X,'INORM,VJM(INORM) VOLTAGE=',I4,2X,2E12.5)
70      CONTINUE
        IF(IMUT.EQ.0) GO TO 90
C***SOLVE EACH SYSTEM OF EQUATIONS FOR THE UNKNOWN CURRENTS
        IF(IBLTSL.EQ.1) GO TO 80
        I12=1
        IF(IJAM.GT.1.OR.IPHACN.GT.1) I12=2
        WRITE(6,6110)
6110    FORMAT(1X,'CALL CROUT IN VJAMMER')
        CALL CROUT(Z,VJM,ICC1,ICC,ISYM,IWR,I12,NEL)
        GO TO 90
        IENTRY=4
80      IF(IJAM.GT.1.OR.IPHACN.GT.1) IENTRY=3
        CALL BLTSOL(CZ,VJM,PS,NB,IDMB,IENTRY)
        IF(NEL.LT.40) CALL CNORM(VJM,NEL)
90      CONTINUE
C***COMPUTE RECEIVED VOLTAGES FOR PRESENT SOURCE POSITION
```

```
        DO 100 IEL=1,NEL
        VJM(IEL)=VJM(IEL)*ZLOAD
CC      WRITE(6,4456)IEL,VJM(IEL)
4456    FORMAT(1X,'IEL,VJM(IEL) RECEIVED VOLT.=',I4,2X,2E12.5)
100     CONTINUE
C***PERFORM BEAM FORMATION FOR MAIN A
C***PHASE CENTER A
        CSUMA=(0.0D0,0.0D0)
        DO 110 KC=1,NEL
        CSUMA=CSUMA+VJM(KC)*CWTA(KC,1)
110     CONTINUE
        VMAINA(IJAM,IFR)=CSUMA
        WRITE(6,2222)IJAM,IFR,VMAINA(IJAM,IFR)
2222    FORMAT(1X,'IJAM,IFR,VMAINA= (AFTER B.F.)',2I4,2X,2E12.5)
C***COMPUTE AUXILIARY CHANNEL VOLTAGES
        DO 7000 IAUX=1,NAUX
        VAUXA(IAUX,IJAM,IFR)=VJM(IAUXA(IAUX))
7000    CONTINUE
180     CONTINUE
        DO 9000 IJAM=1,NJAMS
CCC     WRITE(6,4433)IJAM,IFR,VMAINA(IJAM,IFR)
4433    FORMAT(1X,'VJAMMR:IJAM,IFR,VMAINA=',2I4,2X,2E12.5)
        DO 9001 IAUX=1,NAUX
        WRITE(6,3333)IAUX,IJAM,IFR,VAUXA(IAUX,IJAM,IFR)
3333    FORMAT(1X,'VJAMMR:IAUX,IJAM,IFR,VAUXA=',3I4,2X,2E12.5)
9001    CONTINUE
9000    CONTINUE
        RETURN
        END
C***SUBROUTINE TO COMPUTE INTERFERENCE TO NOISE RATIO
        SUBROUTINE INRTIO(WT,COV,NEL,WTCTR,CMPROD,DBINR)
        IMPLICIT REAL *8 (A-H,O-Z)
        COMPLEX *16 WT(NEL,1),COV(NEL,NEL),WTCTR(1,NEL)
        COMPLEX *16 CMPROD(1,NEL),CPROD1(1,1),CPROD2(1,1),CINR
        COMMON /NORMAL/ INRNOR
```

SUBSTITUTE SHEET

```
2222        WRITE(12,2222)
            FORMAT(1X,'INSIDE INRTIO SUBROUTINE')
CC          DO 110 I=1,NEL
445         WRITE(12,445)I,WT(I,1)
            FORMAT(1X,'I,WT(I,1)=',2X,I4,2X,2E12.5)
110         CONTINUE
            CALL CONJTR(WT,NEL,1,WTCTR)
CC          DO 111 I=1,NEL
666         WRITE(12,666)I,WT(I,1),WTCTR(1,I)
            FORMAT(1X,'I,WT,WTCTR=',2X,I4,2X,4E12.5)
111         CONTINUE
            CALL CMMULT(WTCTR,COV,1,NEL,NEL,CMPROD)
            CALL CMMULT(CMPROD,WT,1,NEL,1,CPROD1)
            CALL CMMULT(WTCTR,WT,1,NEL,1,CPROD2)
            WRITE(6,333)CPROD1(1,1),CPROD2(1,1)
            WRITE(8,333)CPROD1(1,1),CPROD2(1,1)
333         FORMAT(1X,'CPROD1,CPROD2=',4E12.5)
C***INR NORMALIZED
CC          INRNOR=0
            WRITE(6,7739)INRNOR
            WRITE(8,7739)INRNOR
7739        FORMAT(1X,'INR NORMALIZATION PARAMETER, INRNOR=',I4)
            IF(INRNOR.EQ.1) CINR=CPROD1(1,1)/CPROD2(1,1)
C***INR NOT NORMALIZED FOR INRNOR=0
            IF(INRNOR.EQ.0) CINR=CPROD1(1,1)
            DBINR=10.*DLOG10(CDABS(CINR))
            RETURN
            END
            SUBROUTINE CMMULT(A,B,L,M,N,C)
            COMPLEX *16 A(L,M),B(M,N),C(L,N)
            DO 20 I=1,L
            DO 20 J=1,N
            C(I,J)=DCMPLX(0.0D0,0.0D0)
            DO 20 K=1,M
            C(I,J)=C(I,J)+(A(I,K)*B(K,J))
```

SUBSTITUTE SHEET

```
20      CONTINUE
        RETURN
        END
C***SUBROUTINE TO COMPUTE CONJUGATE TRANSPOSE OF A MATRIX
        SUBROUTINE CONJTR(A,L,M,ACTR)
        COMPLEX *16 A(L,M),ACTR(M,L)
        DO 10 I=1,M
        DO 10 J=1,L
        ACTR(I,J)=DCONJG(A(J,I))
CC      WRITE(12,7766)I,J,A(J,I),ACTR(I,J)
7766    FORMAT(1X,'I,J,A(J,I),ACTR(I,J)=',2X,2I4,2X,4E12.5)
10      CONTINUE
        RETURN
        END
        SUBROUTINE DCMINV(A,L,M,IDM,NEQ)
        COMPLEX *16 A(IDM,IDM),BIGA,HOLD,DET
        INTEGER L(IDM),M(IDM)
        N=NEQ
        DET=DCMPLX(1.0D0,0.0D0)
        DO 80 K=1,N
        L(K)=K
        M(K)=K
        BIGA=A(K,K)
        DO 20 J=K,N
        DO 20 I=K,N
10      IF(CDABS(BIGA)-CDABS(A(I,J)))15,19,19
15      BIGA=A(I,J)
        L(K)=I
        M(K)=J
19      CONTINUE
20      CONTINUE
        J=L(K)
        IF(J-K)35,35,25
25      CONTINUE
        DO 30 I=1,N
```

```
         HOLD=-A(K,I)
         A(K,I)=A(J,I)
         A(J,I)=HOLD
   30    I=M(K)
   35    IF(I-K)  45,45,38
   38    CONTINUE
         DO 40 J=1,N
         HOLD=-A(J,K)
         A(J,K)=A(J,I)
         A(J,I)=HOLD
   40    CONTINUE
   45    CONTINUE
         DO 55 I=1,N
   50    IF(I-K)50,55,50
         A(I,K)=A(I,K)/(-BIGA)
   55    CONTINUE
         DO 65 I=1,N
         DO 65 J=1,N
   60    IF(I-K)60,64,60
   62    IF(J-K)62,64,62
         A(I,J)=A(I,K)*A(K,J)+A(I,J)
   64    CONTINUE
   65    CONTINUE
         DO 75 J=1,N
   70    IF(J-K)70,75,70
         A(K,J)=A(K,J)/BIGA
   75    CONTINUE
         DET=DET*BIGA
         A(K,K)=1.0D0/BIGA
   80    CONTINUE
         K=N
  100    K=K-1
         IF(K)150,150,105
  105    I=L(K)
         IF(I-K)120,120,108
  108    CONTINUE
```

```
        DO 110 J=1,N
        HOLD=A(J,K)
        A(J,K)=-A(J,I)
110     A(J,I)=HOLD
120     J=M(K)
        IF(J-K)100,100,125
125     CONTINUE
        DO 130 I=1,N
        HOLD=A(K,I)
        A(K,I)=-A(J,I)
130     A(J,I)=HOLD
        GO TO 100
150     RETURN
        END
C***SUBROUTINE CNORM
C***COMPUTES A NORMALIZED COMPLEX COLUMN VECTOR SUCH THAT THE
C***MAXIMUM ELEMENT HAS UNITY MAGNITUDE.
C
C***PRINTS MAGNITUDE AND PHASE OF NORMALIZED VECTOR
C
        SUBROUTINE CNORM(V,N)
C***    V IS THE INPUT COMPLEX COLUMN VECTOR
C***    N IS THE LENGTH OF V
        COMPLEX V(1),SS
        CNOR=0.0
        DO 10 K=1,N
        SA=CABS(V(K))
        IF(SA.GT.CNOR) CNOR=SA
10      CONTINUE
        IF(CNOR.LE.0.) CNOR=1.0
        DO 30 K=1,N
        SS=V(K)
        SA=CABS(SS)
        SNOR=SA/CNOR
        PHR=0.
```

SUBSTITUTE SHEET

```
        IF(SA.GT.0.) PHR=ATAN2(AIMAG(SS),REAL(SS))
        PH=57.29578*PHR
20      WRITE(8,20) K,SNOR,SA,PH
        FORMAT(1X,I5,F10.6,3X,E15.3,F10.0)
30      CONTINUE
        RETURN
        END
        SUBROUTINE GETCP2(RCPU)
        REAL ETIME,TARRAY(2),RCPU
        TIME=ETIME(TARRAY)
        RCPU=TARRAY(1)
        RETURN
        END
C***SUBROUTINE TO COMPUTE INDUCED VOLTAGE BETWEEN PROBE AND
C***DIPOLE ARRAY ELEMENTS
C***RING ARRAY
        SUBROUTINE NFDPC2(XP,YP,ZP,XREF,IREF,V,VREF)
C***DISTANCES ARE IN METERS
        COMPLEX V(1),VD,VR1,VREF
        COMPLEX *16 DZABG
        COMMON/A/DX,DY,NCOLX,NROWY,NEL,HZ,HL,ARAD,ZLOAD,ZCHAR
        COMMON /CIRCLE/ ICIRC,RADIUS,HLS
C***NOTE: AA,BB,... FOR PROBE    11,22,.... FOR DIPOLE
        PI=3.1415926535
        DCR=PI/180.
C***PROBE DIMENSIONS
        XAA=XP
        XBB=XP
        XCC=XP
        YAA=YP-HLS
        YBB=YP
        YCC=YP+HLS
785     ZAA=ZP
        ZBB=ZP
        ZCC=ZP
```

```
      IC=0
C****CIRCULAR DIPOLE ARRAY ELEMENTS
      DELPHI=360./NEL
      DO 10 IX=1,NEL
      PHI=DELPHI*(IX-1)
      XD=RADIUS*COS(PHI*DCR)
      ZD=RADIUS*SIN(PHI*DCR)
      DIST=SQRT((XP-XD)**2+(ZP-ZD)**2)
      IF(DIST.LT.ARAD) XD=XD+ARAD
      X11=XD
      X22=XD
      X33=XD
      Y11=YP-HL
      Y22=YP
      Y33=YP+HL
      Z11=ZD
      Z22=ZD
      Z33=ZD
9446  IC=IC+1
CC    WRITE(6,2233)IX,IY,XD,YD
2233  FORMAT(1X,'IX,IY,XD,YD=',2X,2I4,2X,2F12.5)
CC    WRITE(6,7854)XAA,XBB,XCC,YAA,YBB,YCC,ZAA,ZBB,ZCC
7854  FORMAT(1X,'XYZABC=',9E12.5)
CC    WRITE(6,7855)X11,X22,X33,Y11,Y22,Y33,Z11,Z22,Z33
7855  FORMAT(1X,'XYZ123=',9E12.5)
      CALL DSZABG(XAA,XBB,XCC,YAA,YBB,YCC,ZAA,ZBB,ZCC,X11,X22,X33,
     2Y11,Y22,Y33,Z11,Z22,Z33,DZABG)
      VD=DZABG
CC    WRITE(6,33)IC,VD
33    FORMAT(1X,'IC,VD=',2X,I5,2E12.5)
      V(IC)=VD
      VAMPDB=20.*ALOG10(CABS(V(IC)))
      VPHASE=ATAN2(AIMAG(V(IC)),REAL(V(IC)))*180./3.141592654
CC    WRITE(6,4455)IC,VAMPDB,VPHASE
4455  FORMAT(1X,'IC,VAMDB,VPHASE=',2X,I4,2X,2F12.2)
```

SUBSTITUTE SHEET

```
10      CONTINUE
C***COMPUTE REFERENCE VOLTAGE (FICTITIOUS ELEMENT AT XREF,  Y=0)
C***SET XREF=RADIUS, THIS MAKES ELEMENT 1 THE REFERENCE
        XREF=RADIUS
C***SET XREF=ARAD,  (REF.  CLOSE TO THE ORIGIN)
        XREF=ARAD
        X11=XREF
        X22=XREF
        X33=XREF
        Y11=-HL
        Y22=0.0
        Y33=HL
        Z11=0.0
        Z22=0.0
        Z33=0.0
9267    CALL DSZABG(XAA,XBB,XCC,YAA,YBB,YCC,ZAA,ZBB,ZCC,X11,X22,X33,
       2Y11,Y22,Y33,Z11,Z22,Z33,DZABG)
        VR1=DZABG
        VREF=VR1
99      RETURN
        END
C***SUBROUTINE TO COMPUTE MUT. IMPED.  BETWEEN STRAIGHT DIPOLES
C***ARRANGED IN A RING ARRAY (CIRCLE)
        SUBROUTINE CADZA2(CTDP,STDP,IGRNDP,ICC1,ICC,2)
        COMPLEX ZMA,ZABG,Z(ICC1,ICC)
        COMMON /A/ DX,DY,NCOLX,NROWY,NEL,HZ,HL,ARAD,ZLOAD,ZCHAR
        COMMON /CIRCLE/ ICIRC,RADIUS,HLS
C***ALL DIMENSIONS IN METERS
        PI=3.1415926535
        DCR=PI/180.
C***FIXED POSITION FOR ELEMENT 1
        XAA=RADIUS
        XBB=RADIUS
        XCC=RADIUS
        YAA=-HL
```

SUBSTITUTE SHEET

```
      YBB=0.0
      YCC=HL
      ZAA=0.0
      ZBB=0.0
      ZCC=0.0
      Y11=YAA
      Y22=YBB
      Y33=YCC
C***VARIABLE POSITION FOR RING ARRAY ELEMENTS
      DELPHI=360./NEL
      IC=0
      DO 20 I=1,NEL
      IC=IC+1
      PHI=DELPHI*(I-1)*DCR
      XD=RADIUS*COS(PHI)
      ZD=RADIUS*SIN(PHI)
      X11=XD
      X22=XD
      X33=XD
      IF(I.EQ.1)  X11=X11+ARAD
      IF(I.EQ.1)  X22=X22+ARAD
      IF(I.EQ.1)  X33=X33+ARAD
      Z11=ZD
      Z22=ZD
      Z33=ZD
CC    WRITE(6,87)IC
87    FORMAT(1X,'IC=',I5)
CC    WRITE(6,88)XAA,XBB,XCC,YAA,YBB,YCC,ZAA,ZBB,ZCC
88    FORMAT(1X,'XYZABC=',9E12.4)
CC    WRITE(6,89)X11,X22,X33,Y11,Y22,Y33,Z11,Z22,Z33
89    FORMAT(1X,'XYZ123=',9E12.4)
      ZMA=ZABG(XAA,XBB,XCC,YAA,YBB,YCC,ZAA,ZBB,ZCC,X11,X22,X33,
     2Y11,Y22,Y33,Z11,Z22,Z33)
      Z(1,IC)=ZMA
      IF(IC.EQ.1) Z(1,1)=Z(1,1)+ZLOAD
```

SUBSTITUTE SHEET

```
20    CONTINUE
      DO 40 I=1,NEL
      IF(I.LT.9)WRITE(6,30)I,Z(1,I)
      WRITE(8,30)I,Z(1,I)
30    FORMAT(1X,'Z(1,',I4,')=',2E12.5)
40    CONTINUE
      RETURN
      END
**********file zabgenloss.f*******************
C***PROGRAM TO CALCULATE MUTUAL IMPEDANCE BETWEEN TWO DIPOLES
C***WITH ARBITRARY LENGTH AND ORIENTATION.  A PIECEWISE-
C***SINUSOIDAL CURRENT DISTRIBUTION IS ASSUMED.
      COMPLEX FUNCTION ZABG(X1,X2,X3,Y1,Y2,Y3,Z1,Z2,Z3,XA,XB,XC,YA,YB,YCZAB00040
     2,ZA,ZB,ZC)
      COMPLEX P11,P12,P21,P22,Q11,Q12,Q21,Q22,R11,R12,R21,R22
      COMPLEX S11,S12,S21,S22,JCOM,GAM,CGDS,SGDS,SGDT,ETA,EP3
      COMPLEX EGDS,EGDT
      COMMON /F/ FHZ,ER3,SIG3,TD3
C***ALL DIMENSIONS IN METERS
      PI=3.141592654
      TPI=2.*PI
      B=TPI
      JCOM=(0.,1.)
      E0=8.854E-12
      U0=1.2566E-6
      OMEGA=TPI*FHZ
      IF(SIG3.LT.0.)EP3=ER3*E0*CMPLX(1.,-TD3)
      IF(TD3.LT.0.)EP3=CMPLX(ER3*E0,-SIG3/OMEGA)
      ETA=CSQRT(U0/EP3)
      GAM=OMEGA*CSQRT(-U0*EP3)
      AM=0.0001
      IF(CABS(GAM*AM).GT.0.06) WRITE(6,7923)AM
7923  FORMAT(1X,'CABS(GAM*AM)  IS GREATER THAN 0.06,  AM=',E14.5)
      INT=0
      XBA=XB-XA
```

```
      YBA=YB-YA
      ZBA=ZB-ZA
      X21=X2-X1
      Y21=Y2-Y1
      Z21=Z2-Z1
      DS=SQRT(XBA*XBA+YBA*YBA+ZBA*ZBA)
      DT=SQRT(X21*X21+Y21*Y21+Z21*Z21)
CC    DSK=B*DS
CC    DTK=B*DT
CC    CGDS=CMPLX(COS(DSK),0.0)
CC    SGDS=CMPLX(0.0,SIN(DSK))
CC    SGDT=CMPLX(0.0,SIN(DTK))
C***FOR LOSSY MEDIUM THE NEXT LINES ARE APPROPRIATE
      EGDS=CEXP(GAM*DS)
      EGDT=CEXP(GAM*DT)
      CGDS=(EGDS+1./EGDS)/2.
      SGDS=(EGDS-1./EGDS)/2.
      SGDT=(EGDT-1./EGDT)/2.
CC    WRITE(6,1345)XA,XB,YA,YB,ZA,ZB
1345  FORMAT(1X,'XYZAB=',6E14.5)
CC    WRITE(6,1346)X1,X2,Y1,Y2,Z1,Z2
1346  FORMAT(1X,'XYZ12=',6E14.5)
      CALL GGS(XA,YA,ZA,XB,YB,ZB,X1,Y1,Z1,X2,Y2,Z2,AM,
     2DS,CGDS,SGDS,DT,SGDT,INT,ETA,GAM,P11,P12,P21,P22)
      CALL GGS(XA,YA,ZA,XB,YB,ZB,X2,Y2,Z2,X3,Y3,Z3,AM,
     2DS,CGDS,SGDS,DT,SGDT,INT,ETA,GAM,Q11,Q12,Q21,Q22)
      CALL GGS(XB,YB,ZB,XC,YC,ZC,X1,Y1,Z1,X2,Y2,Z2,AM,
     2DS,CGDS,SGDS,DT,SGDT,INT,ETA,GAM,R11,R12,R21,R22)
      CALL GGS(XB,YB,ZB,XC,YC,ZC,X2,Y2,Z2,X3,Y3,Z3,AM,
     2DS,CGDS,SGDS,DT,SGDT,INT,ETA,GAM,S11,S12,S21,S22)
      ZABG=P22+Q21+R12+S11
CC    WRITE(6,7898)ZABG
7898  FORMAT(1X,'EXITING ZABG WITH ZABG=',2E14.5)
      RETURN
      END
```

```
**********file dzabgnloss.f********
C****DOUBLE PRECISION VERSION
C***PROGRAM TO CALCULATE MUTUAL IMPEDANCE BETWEEN TWO DIPOLES
C***WITH ARBITRARY LENGTH AND ORIENTATION.  A PIECEWISE-
C***SINUSOIDAL CURRENT DISTRIBUTION IS ASSUMED.
      SUBROUTINE DSZABG(SX1,SX2,SX3,SY1,SY2,SY3,SZ1,SZ2,SZ3,
     2SXA,SXB,SXC,SYA,SYB,SYC,SZA,SZB,SZC,DZABG)
      IMPLICIT REAL*8  (A-H,O-Z)
      COMPLEX*16 P11,P12,P21,P22,Q11,Q12,Q21,Q22,R11,R12,R21,R22
      COMPLEX*16 S11,S12,S21,S22,JCOM,GAM,CGDS,SGDS,SGDT,ETA
      COMPLEX*16 DZABG,EP3,EGDS,EGDT
      REAL*4  SX1,SX2,SX3,SY1,SY2,SY3,SZ1,SZ2,SZ3
      REAL*4  SXA,SXB,SXC,SYA,SYB,SYC,SZA,SZB,SZC
      REAL*4  FHZ,ER3,SIG3,TD3
      COMMON /F/ FHZ,ER3,SIG3,TD3
      JCOM=(0.D0,1.D0)
      PI=3.141592653589800
      TPI=2.0D0*PI
      B=TPI
      E0=8.854D-12
      U0=1.2566D-6
      OMEGA=TPI*FHZ
CC    WRITE(6,2843)OMEGA
2843  FORMAT(1X,'OMEGA=',E12.5)
      IF(SIG3.LT.0.0D0)EP3=ER3*E0*DCMPLX(1.0D0,-TD3)
      IF(TD3.LT.0.0D0)EP3=DCMPLX(ER3*E0,-SIG3/OMEGA)
CC    WRITE(6,7755)ER3,E0,EP3
7755  FORMAT(1X,'ER3,E0,EP3=',4E12.5)
      ETA=CDSQRT(U0/EP3)
      GAM=OMEGA*CDSQRT(-U0*EP3)
C**COMPUTE GAMMA BY EQUATION IN HAYT PAGE 333
CC    GAM=JCOM*OMEGA*CDSQRT(U0*EP3)*CDSQRT(1.D0-JCOM*SIG3/(OMEGA*EP3))
CC    WRITE(6,8888)GAM
8888  FORMAT(1X,'HYAT GAM=',2E12.5)
      AM=0.0001D0
```

SUBSTITUTE SHEET

```
      INT=0
      X1=SX1
      X2=SX2
      X3=SX3
      Y1=SY1
      Y2=SY2
      Y3=SY3
      Z1=SZ1
      Z2=SZ2
      Z3=SZ3
      XA=SXA
      XB=SXB
      XC=SXC
      YA=SYA
      YB=SYB
      YC=SYC
      ZA=SZA
      ZB=SZB
      ZC=SZC
      XBA=XB-XA
      YBA=YB-YA
      ZBA=ZB-ZA
      X21=X2-X1
      Y21=Y2-Y1
      Z21=Z2-Z1
      DS=DSQRT(XBA*XBA+YBA*YBA+ZBA*ZBA)
      DT=DSQRT(X21*X21+Y21*Y21+Z21*Z21)
      DSK=B*DS
      DTK=B*DT
CC    CGDS=DCMPLX(DCOS(DSK),0.0D0)
CC    SGDS=DCMPLX(0.0D0,DSIN(DSK))
CC    SGDT=DCMPLX(0.0D0,DSIN(DTK))
CC    EGDS=CDEXP(GAM*DS)
CC    EGDT=CDEXP(GAM*DT)
      CGDS=(EGDS+1.0D0/EGDS)/2.0D0
```

SUBSTITUTE SHEET

-116-

```
      SGDS=(EGDS-1.0D0/EGDS)/2.0D0
      SGDT=(EGDT-1.0D0/EGDT)/2.0D0
      CALL DGGS(XA,YA,ZA,XB,YB,ZB,X1,Y1,Z1,X2,Y2,Z2,AM,
     2DS,CGDS,SGDS,DT,SGDT,INT,ETA,GAM,P11,P12,P21,P22)
      CALL DGGS(XA,YA,ZA,XB,YB,ZB,X2,Y2,Z2,X3,Y3,Z3,AM,
     2DS,CGDS,SGDS,DT,SGDT,INT,ETA,GAM,Q11,Q12,Q21,Q22)
      CALL DGGS(XB,YB,ZB,XC,YC,ZC,X1,Y1,Z1,X2,Y2,Z2,AM,
     2DS,CGDS,SGDS,DT,SGDT,INT,ETA,GAM,R11,R12,R21,R22)
      CALL DGGS(XB,YB,ZB,XC,YC,ZC,X2,Y2,Z2,X3,Y3,Z3,AM,
     2DS,CGDS,SGDS,DT,SGDT,INT,ETA,GAM,S11,S12,S21,S22)
      DZABG=P22+Q21+R12+S11
      WRITE(6,8899)DZABG
CC
8899  FORMAT(1X,'EXITING  DZABG,  DZABG=',2E14.5)
      RETURN
      END
```

SUBSTITUTE SHEET

APPENDIX B

***Input data file for adaptive nulling with four auxiliary probes.
***sdipjamhyper data file, filename sdipjamhyper.datacirconicrr4
&DIPOLE NCOLX=8,NROWY=1,HZIN=0.001,HLIN=2.6,
DXIN=6.888,DYIN=6.888,ARADIN=0.0039,
ICIRC=1,CRADIN=11.81,HLSIN=0.25,
IWL=0,FCHZ=120.0E6,BWFHZ=1.0E0,NFREQ=5,IWR=0,
NPDX=0,NXDUM=0,NYDUM=0,ER3=73.5,SIG3=0.5,TD3=-1.0,
ZLOAD=50.0,ZCHAR=0.0,NGEN=8,IGEN=0,
NSCANS=1,
THSINC=5.0,
IMUT=1,IBLTSL=0,
IENORM=1,ICHEB=0,SLLDB=20.,EDGTDB=0.,
IPATRN=1,IPRCOM=1,IANGLP=0,
NPHCT=0,NTHPT=499,
THDR=180.,THDMIN=-90.,
NCOLXN=121,NROWYN=1,NCOLZN=1,
RLSYIN=0.0,RLSZIN=0.0,
NCOLXN=117,NROWYN=1,NCOLZN=1,
INEAR=1,
IPOL=2,IGRNDP=0,
ITLTPR=0,ITLTDP=0,
NFCOLX=1,NFROWY=1,
IANTX=1,IANTY=0,NPOWER=0,
IPCONN=1,IPCONF=0,IPCUTF=0,IPCFX=0,IPCFY=0,IPCFZ=0,
ITEK=0,
IQUAN=0,IRNERR=0,ELERDB=0.02,ELERDG=0.2,NBMOD=12,
NRAN=1,NBADWT=32,AWERDB=0.0,AWERDG=0.0,
NAUX=7,IAUXA(1)=1,2,3,4,5,6,7,
IATTEN=1,
NJAMS=7,ISLC=0,AUXADB(1)=8*0.0,
PWRJDB(1)=40.,40.,15.,15.,3*-99.0,
YJAMIN(1)=7*0.0,

```
XFOCIN=0.0,ZFOCIN=0.0,
XJAMIN(1)=5.9,-5.9,2*0.0,3*-0.0,
ZJAMIN(1)=0.0,0.0,4.0,-4.0,3*0.0
YNIN=0.0,
NCOLXN=101,NTHPT=101,
XNIN=-15.,ZNIN=-15.,RLSXIN=30.,RLSZIN=30.,NCOLXN=41,NCOLZN=41,
&END
```

```
***Output data file for adaptive nulling with four auxiliary probes.
***sdipjamhyper data file, filename sdipjamhyper.datacirconicrr4
XJAMIN(1),YJAMIN(1),ZJAMIN(1)=     5.900    0.000    0.06604    0.00010
FGHZ=    0.1200000        0.17496        0.17496    0.000
DX,DY,HL,ARAD=
IV,VTA=   1    0.5916E-02  0.2211E-02
IV,VTA=   2    0.5916E-02  0.2211E-02
IV,VTA=   3    0.5916E-02  0.2211E-02
IV,VTA=   4    0.5916E-02  0.2211E-02
IV,VTA=   5    0.5916E-02  0.2211E-02
IV,VTA=   6    0.5916E-02  0.2211E-02
IV,VTA=   7    0.5916E-02  0.2211E-02
IV,VTA=   8    0.5916E-02  0.2211E-02
********array mutual impedance matrix (first row)********
Z(1,  1)= 0.91705E+02 0.12403E+02
Z(1,  2)=-0.33552E-01 0.19136E+00
Z(1,  3)=-0.14488E-01-0.54125E-02
Z(1,  4)= 0.29420E-02 0.13780E-02
Z(1,  5)= 0.15283E-02-0.11371E-02
Z(1,  6)= 0.29420E-02 0.13780E-02
Z(1,  7)=-0.14488E-01-0.54125E-02
Z(1,  8)=-0.33552E-01 0.19136E+00
NEL,NCOLX,NROWY=   8   8   1
CURRENTS
1  1.000000        0.683E-04   13.
2  1.000000        0.683E-04   13.
3  1.000000        0.683E-04   13.
4  1.000000        0.683E-04   13.
5  1.000000        0.683E-04   13.
6  1.000000        0.683E-04   13.
7  1.000000        0.683E-04   13.
8  1.000000        0.683E-04   13.
IC,RWTA=   1    0.35355E+00
IC,RWTA=   2    0.35355E+00
```

SUBSTITUTE SHEET

```
IC,RWTA=   3    0.35355E+00
IC,RWTA=   4    0.35355E+00
IC,RWTA=   5    0.35355E+00
IC,RWTA=   6    0.35355E+00
IC,RWTA=   7    0.35355E+00
IC,RWTA=   8    0.35355E+00
I,CWTA(I,1)=  1   0.34510E+00-0.76830E-01
I,CWTA(I,1)=  2   0.34510E+00-0.76830E-01
I,CWTA(I,1)=  3   0.34510E+00-0.76830E-01
I,CWTA(I,1)=  4   0.34510E+00-0.76830E-01
I,CWTA(I,1)=  5   0.34510E+00-0.76830E-01
I,CWTA(I,1)=  6   0.34510E+00-0.76830E-01
I,CWTA(I,1)=  7   0.34510E+00-0.76830E-01
I,CWTA(I,1)=  8   0.34510E+00-0.76830E-01
******ring array weights before nulling (amp,phase)**************
I=  1   CWTADB,CWTADG=   0.00000   -12.55098
I=  2   CWTADB,CWTADG=   0.00000   -12.55099
I=  3   CWTADB,CWTADG=   0.00000   -12.55098
I=  4   CWTADB,CWTADG=   0.00000   -12.55097
I=  5   CWTADB,CWTADG=   0.00000   -12.55098
I=  6   CWTADB,CWTADG=   0.00000   -12.55097
I=  7   CWTADB,CWTADG=   0.00000   -12.55097
I=  8   CWTADB,CWTADG=   0.00000   -12.55098
                                   -12.55097
Z(1,  1)= 0.91705E+02 0.12403E+02
Z(1,  2)=-0.33552E-01 0.19136E+00
Z(1,  3)=-0.14488E-01-0.54125E-02
Z(1,  4)= 0.29420E-02 0.13780E-02
Z(1,  5)= 0.15283E-02-0.11371E-02
Z(1,  6)= 0.29420E-02 0.13780E-02
Z(1,  7)=-0.14488E-01-0.54125E-02
Z(1,  8)=-0.33552E-01 0.19136E+00
NEL,NCOLX,NROWY=   8   8   1
II,PWRJ IN POWER=  1   0.10000E+05
II,PWRJ IN POWER=  2   0.10000E+05
II,PWRJ IN POWER=  3   0.31623E+02
```

SUBSTITUTE SHEET

```
II,PWRJ IN POWER=    4    0.31623E+02
II,PWRJ IN POWER=    5    0.12589E-09
II,PWRJ IN POWER=    6    0.12589E-09
II,PWRJ IN POWER=    7    0.12589E-09
*****covariance matrix************************************
I,J,CNDB,PHASEN=    1    1    36.35      0.00
I,J,CNDB,PHASEN=    1    2    31.68     91.33
I,J,CNDB,PHASEN=    1    3    24.99   -117.95
I,J,CNDB,PHASEN=    1    4    20.88      6.26
I,J,CNDB,PHASEN=    1    5    20.72     -0.14
I,J,CNDB,PHASEN=    1    6    20.88      6.26
I,J,CNDB,PHASEN=    1    7    24.99   -117.95
I,J,CNDB,PHASEN=    1    8    31.68     91.33
I,J,CNDB,PHASEN=    2    1    31.68    -91.33
I,J,CNDB,PHASEN=    2    2    27.05      0.00
I,J,CNDB,PHASEN=    2    3    20.23    155.55
I,J,CNDB,PHASEN=    2    4     8.12    177.91
I,J,CNDB,PHASEN=    2    5    20.90     -6.14
I,J,CNDB,PHASEN=    2    6     8.28    177.98
I,J,CNDB,PHASEN=    2    7    20.24    155.46
I,J,CNDB,PHASEN=    2    8    27.04      0.00
I,J,CNDB,PHASEN=    3    1    24.99    117.95
I,J,CNDB,PHASEN=    3    2    20.23   -155.55
I,J,CNDB,PHASEN=    3    3    16.67      0.00
I,J,CNDB,PHASEN=    3    4    20.26   -155.49
I,J,CNDB,PHASEN=    3    5    25.01    117.95
I,J,CNDB,PHASEN=    3    6    20.27   -155.41
I,J,CNDB,PHASEN=    3    7    16.52      0.00
I,J,CNDB,PHASEN=    3    8    20.24   -155.46
I,J,CNDB,PHASEN=    4    1    20.88     -6.26
I,J,CNDB,PHASEN=    4    2     8.12   -177.91
I,J,CNDB,PHASEN=    4    3    20.26    155.49
I,J,CNDB,PHASEN=    4    4    27.08      0.00
I,J,CNDB,PHASEN=    4    5    31.71    -91.33
I,J,CNDB,PHASEN=    4    6    27.07      0.00
```

```
I,J,CNDB,PHASEN=    4   7    20.27     155.41
I,J,CNDB,PHASEN=    4   8     8.28    -177.98
I,J,CNDB,PHASEN=    5   1    20.72       0.14
I,J,CNDB,PHASEN=    5   2    20.90       6.14
I,J,CNDB,PHASEN=    5   3    25.01    -117.95
I,J,CNDB,PHASEN=    5   4    31.71      91.33
I,J,CNDB,PHASEN=    5   5    36.38       0.00
I,J,CNDB,PHASEN=    5   6    31.71      91.33
I,J,CNDB,PHASEN=    5   7    25.01    -117.95
I,J,CNDB,PHASEN=    5   8    20.90       6.14
I,J,CNDB,PHASEN=    6   1    20.88      -6.26
I,J,CNDB,PHASEN=    6   2     8.28    -177.98
I,J,CNDB,PHASEN=    6   3    20.27     155.41
I,J,CNDB,PHASEN=    6   4    27.07       0.00
I,J,CNDB,PHASEN=    6   5    31.71     -91.33
I,J,CNDB,PHASEN=    6   6    27.08       0.00
I,J,CNDB,PHASEN=    6   7    20.26     155.49
I,J,CNDB,PHASEN=    6   8     8.12    -177.91
I,J,CNDB,PHASEN=    7   1    24.99     117.95
I,J,CNDB,PHASEN=    7   2    20.24    -155.46
I,J,CNDB,PHASEN=    7   3    16.52       0.00
I,J,CNDB,PHASEN=    7   4    20.27    -155.41
I,J,CNDB,PHASEN=    7   5    25.01     117.95
I,J,CNDB,PHASEN=    7   6    20.26    -155.49
I,J,CNDB,PHASEN=    7   7    16.67       0.00
I,J,CNDB,PHASEN=    7   8    20.23    -155.55
I,J,CNDB,PHASEN=    8   1    31.68     -91.33
I,J,CNDB,PHASEN=    8   2    27.04       0.00
I,J,CNDB,PHASEN=    8   3    20.24     155.46
I,J,CNDB,PHASEN=    8   4     8.28     177.98
I,J,CNDB,PHASEN=    8   5    20.90      -6.14
I,J,CNDB,PHASEN=    8   6     8.12     177.91
I,J,CNDB,PHASEN=    8   7    20.23     155.55
I,J,CNDB,PHASEN=    8   8    27.05       0.00
*********eigenvalues*******************************
```

SUBSTITUTE SHEET

```
I,EVLDBN=    1        37.437
I,EVLDBN=    2        37.195
I,EVLDBN=    3         2.771
I,EVLDBN=    4         3.103
I,EVLDBN=    5         0.000
I,EVLDBN=    6         0.000
I,EVLDBN=    7         0.000
I,EVLDBN=    8         0.000
CPROD1,CPROD2= 0.13839E+04-0.85265E-13 0.10000E+01 0.00000E+00
INR NORMALIZATION PARAMETER, INRNOR=   1
I=    1  WANDB=   -12.318
I=    2  WANDB=    -8.734
I=    3  WANDB=    -7.602
I=    4  WANDB=    -8.734
I=    5  WANDB=   -12.318
I=    6  WANDB=    -8.734
I=    7  WANDB=    -7.602
I=    8  WANDB=    -8.734
I,WAN(I,1)=    1   0.11307E+00-0.21414E+00
I,WAN(I,1)=    2   0.34937E+00 0.10851E+00
I,WAN(I,1)=    3   0.32832E+00-0.25671E+00
I,WAN(I,1)=    4   0.34937E+00 0.10851E+00
I,WAN(I,1)=    5   0.11307E+00-0.21414E+00
I,WAN(I,1)=    6   0.34937E+00 0.10851E+00
I,WAN(I,1)=    7   0.32832E+00-0.25671E+00
I,WAN(I,1)=    8   0.34937E+00 0.10851E+00
**********adaptive array weights (amp.,phase)**********
I=    1  WANDB,WANDG=   -4.71576   -62.16515
I=    2  WANDB,WANDG=   -1.13211    17.25469
I=    3  WANDB,WANDG=    0.00000   -38.02192
I=    4  WANDB,WANDG=   -1.13210    17.25474
I=    5  WANDB,WANDG=   -4.71576   -62.16529
I=    6  WANDB,WANDG=   -1.13210    17.25474
I=    7  WANDB,WANDG=    0.00000   -38.02193
I=    8  WANDB,WANDG=   -1.13210    17.25469
```

```
********cancellation********************
CPROD1,CPROD2= 0.12271E+01 0.12185E-13 0.10000E+01 0.00000E+00
INR NORMALIZATION PARAMETER, INRNOR=    1
INR= QUI,ADAP ,CANCEL=     31.411     0.889    -30.522    DB
CANCDB,NRAN,AVECAN=    -30.52207      1       -30.52207
***Input data file for adaptive nulling with two auxiliary probes.
***sdipjamhyper data file, filename sdipjamhyper.datacirconicrr3
&DIPOLE NCOLX=8,NROWY=1,HZIN=0.001,HLIN=2.6,
 DXIN=6.888,DYIN=6.888,ARADIN=0.0039,
 ICIRC=1,CRADIN=11.81,HLSIN=0.25,
 IWL=0,FCHZ=120.0E6,BWFHZ=1.0E0,NFREQ=5,IWR=0,
 NPDX=0,NXDUM=0,NYDUM=0,ER3=73.5,SIG3=0.5,TD3=-1.0,
 ZLOAD=50.0,ZCHAR=0.0,NGEN=8,IGEN=0,
 NSCANS=1,
 THSINC=5.0,
 IMUT=1,IBLTSL=0,
 IENORM=1,ICHEB=0,SLLDB=20.,EDGTDB=0.,
 IPATRN=1,IPRCOM=1,IANGLP=0,
 NPHCT=0,NTHPT=499,
 THDR=180.,THDMIN=-90.,
 RLSYIN=0.0,RLSZIN=0.0,
 NCOLXN=117,NROWYN=1,NCOLZN=1,
 INEAR=1,
 IPOL=2,IGRNDP=0,
 ITLTPR=0,ITLTDP=0,
 NFCOLX=1,NFROWY=1,
 IANTX=1,IANTY=0,NPOWER=0,
 IPCONN=1,IPCONF=0,IPCUTF=0,IPCFX=0,IPCFY=0,IPCF2=0,
 ITEK=0,
 IQUAN=0,IRNERR=0,ELERDB=0.02,ELERDG=0.2,NBMOD=12,
 NRAN=1,NBADWT=32,AWERDB=0.0,AWERDG=0.0,
 NAUX=7,IAUXA(1)=1,2,3,4,5,6,7,
 IATTEN=1,
 INRNOR=1,
 NJAMS=7,ISLC=0,AUXADB(1)=8*0.0,
```

SUBSTITUTE SHEET

```
PWRJDB(1)=40.,40.,5*-99.0,
YJAMIN(1)=7*0.0,
XFOCIN=0.0,ZFOCIN=0.0,
XJAMIN(1)=5.9,-5.9,2*0.0,2*-4.0,1*0.0,
ZJAMIN(1)=0.0,0.0,4.0,-4.0,3.0,-3.0,1*0.0
YNIN=0.0,
NCOLXN=101,NTHPT=101,
XNIN=-15.,ZNIN=-15.,RLSXIN=30.,RLSZIN=30.,NCOLXN=41,NCOLZN=41,
&END
***Output data file for adadptive nulling with two auxiliary probes.
***sdipjamhyper data file, filename sdipjamhyper.datacirconicrr3
XJAMIN(1),YJAMIN(1),ZJAMIN(1)=          5.900      0.000      0.000

FGH2=      0.1200000
DX,DY,HL,ARAD=          0.17496    0.17496    0.06604    0.00010
IV,VTA=    1      0.5916E-02  0.2211E-02
IV,VTA=    2      0.5916E-02  0.2211E-02
IV,VTA=    3      0.5916E-02  0.2211E-02
IV,VTA=    4      0.5916E-02  0.2211E-02
IV,VTA=    5      0.5916E-02  0.2211E-02
IV,VTA=    6      0.5916E-02  0.2211E-02
IV,VTA=    7      0.5916E-02  0.2211E-02
IV,VTA=    8      0.5916E-02  0.2211E-02
*********array mutual impedance matrix (first row)********
Z(1,  1)= 0.91705E+02 0.12403E+02
Z(1,  2)=-0.33552E-01 0.19136E+00
Z(1,  3)=-0.14488E-01-0.54125E-02
Z(1,  4)= 0.29420E-02 0.13780E-02
Z(1,  5)= 0.15283E-02-0.11371E-02
Z(1,  6)= 0.29420E-02 0.13780E-02
Z(1,  7)=-0.14488E-01-0.54125E-02
Z(1,  8)=-0.33552E-01 0.19136E+00
NEL,NCOLX,NROWY=    8      8      1
CURRENTS
  1  1.000000         0.683E-04      13.
```

```
2    1.000000              0.683E-04    13.
3    1.000000              0.683E-04    13.
4    1.000000              0.683E-04    13.
5    1.000000              0.683E-04    13.
6    1.000000              0.683E-04    13.
7    1.000000              0.683E-04    13.
8    1.000000              0.683E-04    13.
IC,RWTA=   1    0.35355E+00
IC,RWTA=   2    0.35355E+00
IC,RWTA=   3    0.35355E+00
IC,RWTA=   4    0.35355E+00
IC,RWTA=   5    0.35355E+00
IC,RWTA=   6    0.35355E+00
IC,RWTA=   7    0.35355E+00
IC,RWTA=   8    0.35355E+00
I,CWTA(I,1)=   1    0.34510E+00-0.76830E-01
I,CWTA(I,1)=   2    0.34510E+00-0.76830E-01
I,CWTA(I,1)=   3    0.34510E+00-0.76830E-01
I,CWTA(I,1)=   4    0.34510E+00-0.76830E-01
I,CWTA(I,1)=   5    0.34510E+00-0.76830E-01
I,CWTA(I,1)=   6    0.34510E+00-0.76830E-01
I,CWTA(I,1)=   7    0.34510E+00-0.76830E-01
I,CWTA(I,1)=   8    0.34510E+00-0.76830E-01
*******ring array weights before nulling (amp,phase)****************
I=  1    CWTADB,CWTADG=    0.00000   -12.55098
I=  2    CWTADB,CWTADG=    0.00000   -12.55099
I=  3    CWTADB,CWTADG=    0.00000   -12.55098
I=  4    CWTADB,CWTADG=    0.00000   -12.55097
I=  5    CWTADB,CWTADG=    0.00000   -12.55098
I=  6    CWTADB,CWTADG=    0.00000   -12.55097
I=  7    CWTADB,CWTADG=    0.00000   -12.55098
I=  8    CWTADB,CWTADG=    0.00000   -12.55097
Z(1,  1)= 0.91705E+02  0.12403E+02
Z(1,  2)=-0.33552E-01  0.19136E+00
Z(1,  3)=-0.14488E-01-0.54125E-02
```

SUBSTITUTE SHEET

```
Z(1,    4)=  0.29420E-02 0.13780E-02
Z(1,    5)=  0.15283E-02-0.11371E-02
Z(1,    6)=  0.29420E-02 0.13780E-02
Z(1,    7)=-0.14488E-01-0.54125E-02
Z(1,    8)=-0.33552E-01 0.19136E+00
NEL,NCOLX,NROWY=    8    8    1
II,PWRJ IN POWER=   1  0.10000E+05
II,PWRJ IN POWER=   2  0.10000E+05
II,PWRJ IN POWER=   3  0.12589E-09
II,PWRJ IN POWER=   4  0.12589E-09
II,PWRJ IN POWER=   5  0.12589E-09
II,PWRJ IN POWER=   6  0.12589E-09
II,PWRJ IN POWER=   7  0.12589E-09
*****covariance matrix*******************************
I,J,CNDB,PHASEN=   1   1   36.35     0.00
I,J,CNDB,PHASEN=   1   2   31.68    91.33
I,J,CNDB,PHASEN=   1   3   24.98  -117.94
I,J,CNDB,PHASEN=   1   4   20.88     6.28
I,J,CNDB,PHASEN=   1   5   20.72    -0.14
I,J,CNDB,PHASEN=   1   6   20.88     6.28
I,J,CNDB,PHASEN=   1   7   24.98  -117.94
I,J,CNDB,PHASEN=   1   8   31.68    91.33
I,J,CNDB,PHASEN=   2   1   31.68   -91.33
I,J,CNDB,PHASEN=   2   2   27.05     0.00
I,J,CNDB,PHASEN=   2   3   20.24   155.47
I,J,CNDB,PHASEN=   2   4    8.24   177.97
I,J,CNDB,PHASEN=   2   5   20.90    -6.17
I,J,CNDB,PHASEN=   2   6    8.24   177.97
I,J,CNDB,PHASEN=   2   7   20.24   155.47
I,J,CNDB,PHASEN=   2   8   27.04     0.00
I,J,CNDB,PHASEN=   3   1   24.98   117.94
I,J,CNDB,PHASEN=   3   2   20.24  -155.47
I,J,CNDB,PHASEN=   3   3   16.62     0.00
I,J,CNDB,PHASEN=   3   4   20.27  -155.41
I,J,CNDB,PHASEN=   3   5   25.01   117.93
```

```
I,J,CNDB,PHASEN=    3    6    20.27    -155.41
I,J,CNDB,PHASEN=    3    7    16.52       0.00
I,J,CNDB,PHASEN=    3    8    20.24    -155.47
I,J,CNDB,PHASEN=    4    1    20.88      -6.28
I,J,CNDB,PHASEN=    4    2     8.24    -177.97
I,J,CNDB,PHASEN=    4    3    20.27     155.41
I,J,CNDB,PHASEN=    4    4    27.08       0.00
I,J,CNDB,PHASEN=    4    5    31.71     -91.33
I,J,CNDB,PHASEN=    4    6    27.07       0.00
I,J,CNDB,PHASEN=    4    7    20.27     155.41
I,J,CNDB,PHASEN=    4    8     8.24    -177.97
I,J,CNDB,PHASEN=    5    1    20.72       0.14
I,J,CNDB,PHASEN=    5    2    20.90       6.17
I,J,CNDB,PHASEN=    5    3    25.01    -117.93
I,J,CNDB,PHASEN=    5    4    31.71      91.33
I,J,CNDB,PHASEN=    5    5    36.38       0.00
I,J,CNDB,PHASEN=    5    6    31.71      91.33
I,J,CNDB,PHASEN=    5    7    25.01    -117.93
I,J,CNDB,PHASEN=    5    8    20.90       6.17
I,J,CNDB,PHASEN=    6    1    20.88      -6.28
I,J,CNDB,PHASEN=    6    2     8.24    -177.97
I,J,CNDB,PHASEN=    6    3    20.27     155.41
I,J,CNDB,PHASEN=    6    4    27.07       0.00
I,J,CNDB,PHASEN=    6    5    31.71     -91.33
I,J,CNDB,PHASEN=    6    6    27.08       0.00
I,J,CNDB,PHASEN=    6    7    20.27     155.41
I,J,CNDB,PHASEN=    6    8     8.24    -177.97
I,J,CNDB,PHASEN=    7    1    24.98     117.94
I,J,CNDB,PHASEN=    7    2    20.24    -155.47
I,J,CNDB,PHASEN=    7    3    16.52       0.00
I,J,CNDB,PHASEN=    7    4    20.27    -155.41
I,J,CNDB,PHASEN=    7    5    25.01     117.93
I,J,CNDB,PHASEN=    7    6    20.27    -155.41
I,J,CNDB,PHASEN=    7    7    16.62       0.00
I,J,CNDB,PHASEN=    7    8    20.24    -155.47
```

```
I,J,CNDB,PHASEN=   8   1       31.68    -91.33
I,J,CNDB,PHASEN=   8   2       27.04      0.00
1 I,J,CNDB,PHASEN=   8   3       20.24    155.47
I,J,CNDB,PHASEN=   8   4        8.24    177.97
I,J,CNDB,PHASEN=   8   5       20.90     -6.17
I,J,CNDB,PHASEN=   8   6        8.24    177.97
I,J,CNDB,PHASEN=   8   7       20.24    155.47
I,J,CNDB,PHASEN=   8   8       27.05      0.00
********eigenvalues*********************

I,EVLDBN=  1      37.195
I,EVLDBN=  2      37.437
I,EVLDBN=  3       0.000
I,EVLDBN=  4       0.000
I,EVLDBN=  5       0.000
I,EVLDBN=  6       0.000
I,EVLDBN=  7       0.000
I,EVLDBN=  8       0.000
CPROD1,CPROD2= 0.13835E+04-0.56843E-13 0.10000E+01 0.00000E+00
INR NORMALIZATION PARAMETER, INRNOR=  1
I=  1  WANDB=  -14.003
I=  2  WANDB=   -8.939
I=  3  WANDB=   -6.886
I=  4  WANDB=   -8.939
I=  5  WANDB=  -14.003
I=  6  WANDB=   -8.939
I=  7  WANDB=   -6.886
I=  8  WANDB=   -8.939
I,WAN(I,1)=  1    0.48427E-01-0.19349E+00
I,WAN(I,1)=  2    0.35635E+00 0.26440E-01
I,WAN(I,1)=  3    0.43481E+00-0.12564E+00
I,WAN(I,1)=  4    0.35635E+00 0.26441E-01
I,WAN(I,1)=  5    0.48427E-01-0.19349E+00
I,WAN(I,1)=  6    0.35635E+00 0.26441E-01
I,WAN(I,1)=  7    0.43481E+00-0.12564E+00
I,WAN(I,1)=  8    0.35635E+00 0.26441E-01
```

SUBSTITUTE SHEET

```
**********adaptive array weights (amp.,phase)**********
I= 1  WANDB,WANDG=    -7.11720      -75.94859
I= 2  WANDB,WANDG=    -2.05298        4.24348
I= 3  WANDB,WANDG=     0.00000      -16.11658
I= 4  WANDB,WANDG=    -2.05297        4.24352
I= 5  WANDB,WANDG=    -7.11719      -75.94872
I= 6  WANDB,WANDG=    -2.05298        4.24352
I= 7  WANDB,WANDG=     0.00000      -16.11658
I= 8  WANDB,WANDG=    -2.05297        4.24348
**********cancellation**********
CPROD1,CPROD2= 0.10001E+01-0.63768E-14 0.10000E+01 0.00000E+00
INR NORMALIZATION PARAMETER, INRNOR= 1
INR= QUI,ADAP ,CANCEL=   31.410     0.000    -31.410    DB
CANCDB,NRAN,AVECAN=  -31.40966     1    -31.40966
```

SUBSTITUTE SHEET

APPENDIX C

```
{ COPYRIGHT M.I.T. LINCOLN LABORATORY 1991, ALL RIGHTS RESERVED}
{ PROGRAM NULLGS.P (PASCAL VERSION BY ALAN J. FENN)}
{ THIS SUBROUTINE PERFORMS A GRADIENT SEARCH FOR THE}
{ ADAPTIVE NULLING WEIGHTS (AMPLITUDE AND PHASE)}
{ BASED ON MINIMIZING THE POWER RECEIVED BY AN E-FIELD PROBE}
{ AT A DESIRED NULLING POSITION. }
PROGRAM NULLGS (INPUT,OUTPUT) ;

{ PROGRAM INPUT OR FIXED PARAMETERS}

    NCHAN IS THE NUMBER OF ADAPTIVE TRANSMIT CHANNELS (=4)}
    NETUMOR IS THE NUMBER OF E-FIELD TUMOR-SITE PROBES (=1)}
    NEPROBE IS THE NUMBER OF E-FIELD NULLING PROBES (=1)}
    JSMAX IS THE MAXIMUM NUMBER OF GRADIENT ITERATIONS (=200)}
    NBSETWT IS THE NUMBER OF BITS USED IN SETTING THE TRANSMIT WEIGHTS (=8)}
    NBMEAWT IS THE NUMBER OF BITS USED IN MEASURING THE TRANSMIT WEIGHTS (=12)}
    NBPROBE IS THE NUMBER OF BITS USED IN MEASURING THE E-FIELD PROBE POWER (=12)}
    PROGRAM OUTPUT}

    IWTAMP8 IS THE ADAPTIVE NULLING WEIGHT VECTOR AMPLITUDE}
    IWTPHA8 IS THE ADAPTIVE NULLING WEIGHT VECTOR PHASE}

This computer program is intended to be used in the following manner:}
Initially, the hyperthermia phased array should be turned on and the}
transmit weights are set to some nominal values.  Assume that there are}
two E-field probes, one invasive at the desired tumor position and}
one noninvasive on the skin surface.  The output power of the two E-field}
probes should be measured and be printed, saved, or displayed on the screen }
for reference purposes.}

{ DECLARE INTEGER AND REAL ARRAYS WITH APPROPRIATE DIMENSIONS}

VAR
```

```
IWTAMP12  : ARRAY [1..4] OF INTEGER;
IWTPHA12  : ARRAY [1..4] OF INTEGER;
IWTAMP8   : ARRAY [1..4] OF INTEGER;
IWTPHA8   : ARRAY [1..4] OF INTEGER;
IWORKAM8  : ARRAY [1..4] OF INTEGER;
IWORKPH8  : ARRAY [1..4] OF INTEGER;
DFANJ     : ARRAY [1..4] OF REAL;
DFPNJ     : ARRAY [1..4] OF REAL;
RANJ      : ARRAY [1..4] OF REAL;
RPNJ      : ARRAY [1..4] OF REAL;

{ DECLARE INTEGER AND REAL VARIABLES}

MAXAMP8,NBSETWT,NBMEAWT,NBPROBE                    : INTEGER;
MSBMEAWT,MSBSETWT,MSBPROBE                         : INTEGER;
I,K,N,MDELAMP,MDELPHA,ITER,JSMAX                   : INTEGER;
NCHAN,IAMPP8,IPHAP8,IAMPM8,IPHAM8                  : INTEGER;
NAMPINC,NPHAINC,NEWMAXA8                           : INTEGER;
NETUMOR,NEPROBE                                    : INTEGER;

FAC12TO8,FACDEN,SUMDF
TPOWER,DNPOWER,TAPOWER,DNAPOWER                    : REAL;
PWR_TPA,PWR_NPA,PWR_TMA,PWR_NMA                    : REAL;
PWR_TPP,PWR_NPP,PWR_TMP,PWR_NMP                    : REAL;
RMSBMEAW,RMSBSETW,RNAMPINC,RNPHAINC                : REAL;
RMAXAMP8                                           : REAL;

{ NOTE: Define  MEASUREPOWER Procedure}

PROCEDURE MEASUREP (IA1,IA2,IA3,IA4,IP1,IP2,IP3,IP4 : INTEGER ;
         VAR  POWER : REAL) ;  {E-FIELD PROBE POWER MEASUREMENT PROCEDURE}

VAR
   IA01,IA02,IA03,IA04,IP01,IP02,IP03,IP04 : INTEGER ;
   POWERA,POWERP                           : REAL     ;
```

SUBSTITUTE SHEET

```
BEGIN

    {8-bit weight data}

    IA01 := 71 ;
    IA02 := 85 ;
    IA03 := 91 ;
    IA04 := 125 ;

    IP01 := 1 ;
    IP02 := 100 ;
    IP03 := 74 ;
    IP04 := 42 ;

{ Polynomial Function Definition }

POWERA := SQR(IA1-IA01)+SQR(IA2-IA02)+SQR(IA3-IA03)+SQR(IA4-IA04) ;
POWERP := SQR(IP1-IP01)+SQR(IP2-IP02)+SQR(IP3-IP03)+SQR(IP4-IP04) ;

POWER := POWERA + POWERP    {    ;    }

END;

PROCEDURE MEASIW (VAR  IWA1,IWA2,IWA3,IWA4,IWP1,IWP2,IWP3,IWP4 : INTEGER) ;

{THIS PROCEDURE MEASURES THE INITIAL WEIGHTS}
{artificially sets them for now}

BEGIN

    {12-bit data}

    IWA1 := 2000 ;
    IWA2 := 2000 ;
```

SUBSTITUTE SHEET

```
    IWA3 := 2000 ;
    IWA4 := 2000 ;

    IWP1 := 1 ;
    IWP2 := 1 ;
    IWP3 := 1 ;
    IWP4 := 1        {  ;  }

END;

PROCEDURE SETWTS ;   {procedure to set weights}

BEGIN

{NON-FUNCTIONING FOR NOW}

END;

BEGIN   {BEGIN THE MAIN PROGRAM}

{  FIXED DATA FOR SYSTEM}

    NCHAN := 4 ;

{ NUMBER OF BITS TO SET WEIGHTS, MEASURE WEIGHTS, MEASURE E-FIELD PROBE}
    NBSETWT:=8 ;
    NBMEAWT:=12 ;
    NBPROBE:=12 ;

    NETUMOR:=1 ;
    NEPROBE:=1 ;
    JSMAX   :=25 ;    {number of iterations in gradient search}
```

SUBSTITUTE SHEET

```
WRITELN('enter number of iterations in gradient search') ;

READLN (JSMAX) ;

WRITELN('JSMAX=',JSMAX) ;

{ END OF DATA}

{ MEASURE INITIAL E-FIELD POWER AT TUMOR SITE (RECEIVE PROBE CHANNEL 1)}
{ CALL MEASUREPOWER( measure TPOWER, the E-field probe power at the tumor site)}
{ MEASURE INITIAL E-FIELD POWER AT DESIRED NULL POSITION (RECEIVE PROBE CHANNEL 2)}
{ CALL MEASUREPOWER( measure DNPOWER, the E-field probe power at the desired null pos.)}

{ MEASURE TRANSMIT WEIGHTS AMPLITUDE (IWTAMP12) AND PHASE (IWTPHA12) FOR EACH TRANSMIT CH.}
{ NOTE: THE 12 IN IWTAMP12 AND IWTPHA12 REFERS TO 12 BITS}

    {FOR I:=1 TO NCHAN DO}
    {CALL MEASUREWEIGHT( IWTAMP12[I], IWTPHA12[I] ) ;}

MEASIW (IWTAMP12[1],IWTAMP12[2],IWTAMP12[3],IWTAMP12[4],
        IWTPHA12[1],IWTPHA12[2],IWTPHA12[3],IWTPHA12[4] ) ;

{ CONVERT 12 BIT MEASUREMENTS TO 8 BIT RANGE FOR PURPOSES OF SETTING WEIGHTS}
{ WITH 8-BIT DIGITAL TO ANALOG CONVERTERS}

{ NOTE: 12 BIT RANGE IS STATES    1,2,3,.............,4096}
{        8 BIT RANGE IS STATES    1,2,3,....256}

{ THE MOST SIGNIFICANT BIT FOR THE TRANSMIT WEIGHT MEASUREMENTS IS (MSBMEAWT=4096)}

{ RMSBMEAW := EXP(NBMEAWT * (LN (2.) ) ) ; }
  RMSBMEAW := 4096 ;
```

SUBSTITUTE SHEET

```
{ MSBMEAWT := round(RMSBMEAW) ;

  THE MOST SIGNIFICANT BIT FOR THE TRANSMIT WEIGHT SETTINGS IS (MSBSETWT=256) }

{ RMSBSETW := EXP(NBSETWT * (LN (2.) ) ) ; }
  RMSBSETW := 256 ;
  MSBSETWT := round(RMSBSETW) ;

{ COMPUTE SCALE FACTOR TO CONVERT 12-BIT RANGE TO 8-BIT RANGE}

  FAC12TO8 := RMSBSETW / MSBMEAWT ;

{ CONVERT THE 12-BIT TRANSMIT WEIGHT DATA TO 8-BIT DATA AND PRINT-OUT}

  FOR I:= 1 TO NCHAN  DO

    BEGIN

      IWTAMP8[I] := round( IWTAMP12[I] * FAC12TO8) ;

      IF IWTAMP8[I] < 1 THEN  IWTAMP8[I] := 1  ;

      IWTPHA8[I] := round( IWTPHA12[I] * FAC12TO8) ;

      IF IWTPHA8[I] < 1 THEN  IWTPHA8[I] := 1  ;

      WRITELN('CHANNEL', I, ' AMPLITUDE=', IWTAMP8[I],' PHASE=', IWTPHA8[I]) ;

{ STORE THE 8-BIT DATA IN TEMPORARY WORK ARRAYS}
      IWORKAM8[I] := IWTAMP8[I] ;
      IWORKPH8[I] := IWTPHA8[I]          }

    END;
```

SUBSTITUTE SHEET

```
{  DETERMINE MAXIMUM WEIGHT AMPLITUDE BEFORE NULLING }

   MAXAMP8 :=0 ;

   FOR I := 1 TO NCHAN  DO

       BEGIN

          IF IWTAMP8[I] > MAXAMP8  THEN

                MAXAMP8 :=IWTAMP8[I]      {     ;      }

          END;

{  COPY MAXAMP8 TO A REAL VARIABLE (RMAXAMP8) }

   RMAXAMP8 := MAXAMP8 ;

{  PRINT-OUT THE MAXIMUM WEIGHT AMPLITUDE OVER 8-BIT RANGE}

   WRITELN('MAXIMUM WEIGHT AMPLITUDE OVER 8-BIT RANGE=', RMAXAMP8) ;

{  MEASURE INITIAL E-FIELD POWER AT DESIRED NULL POSITION (RECEIVE PROBE CHANNEL 2)}

   MEASUREP (IWTAMP8[1],IWTAMP8[2],IWTAMP8[3],IWTAMP8[4],
             IWTPHA8[1],IWTPHA8[2],IWTPHA8[3],IWTPHA8[4], DNPOWER) ;

   WRITELN('INITIAL E-FIELD POWER AT DESIRED NULL POSITION=',DNPOWER) ;

{  READ-IN THE MAXIMUM NUMBER OF STATES TO DITHER TRANSMIT WEIGHT AMPLITUDE}

   WRITELN('ENTER MAXIMUM NUMBER OF STATES TO DITHER TRANSMIT WEIGHT AMPLITUDE') ;

   READLN (MDELAMP) ;
```

SUBSTITUTE SHEET

```
{  READ-IN THE MAXIMUM NUMBER OF STATES TO DITHER TRANSMIT WEIGHT PHASE}

   WRITELN('ENTER MAXIMUM NUMBER OF STATES TO DITHER TRANSMIT WEIGHT PHASE');

   READLN (MDELPHA) ;

   writeln('MDELAMP=',MDELAMP,'  MDELPHA=',MDELPHA) ;

{  BEGIN GRADIENT SEARCH: }

   FOR ITER := 1 TO JSMAX  DO    {Start ITER Loop}

       BEGIN

   SUMDF :=0.0 ;

       WRITELN ('ITERATION NUMBER=',ITER);

{  COMPUTE WEIGHT-DITHERING STATES +-AMPLITUDE,  +-PHASE}

       FOR K := 1 TO NCHAN  DO    {Start K Loop For Weight Dithering}

           BEGIN

{  AMPLITUDE SECTION: }

           IAMPP8 := IWTAMP8[K] + MDELAMP ;

           writeln('IAMPP8=',IAMPP8)  ;

{  MAKE SURE WEIGHT AMPLITUDE DOES NOT EXCEED MOST SIGNIFICANT BIT (256) }

           IF IAMPP8 > MSBSETWT THEN

               BEGIN
```

SUBSTITUTE SHEET

```
                IAMPP8 := MSBSETWT ;

            END;

        IAMPM8 := IWTAMP8[K] - MDELAMP ;

    writeln('IAMPM8=',IAMPM8) ;

{   MAKE SURE WEIGHT AMPLITUDE STATE IS NOT LESS THAN THE LEAST SIGNIFICANT BIT [1]}

        IF IAMPM8 < 1  THEN

            BEGIN

                IAMPM8 := 1 ;

            END;

{   PHASE SECTION:}

        IPHAP8 := IWTPHA8[K] + MDELPHA ;

{   MAKE SURE WEIGHT PHASE DOES NOT EXCEED MOST SIGNIFICANT BIT (256) }

        IF IPHAP8 > MSBSETWT  THEN

            BEGIN

                IPHAP8 := MSBSETWT ;

            END;

    writeln('IPHAP8=',IPHAP8) ;

        IPHAM8 := IWTPHA8[K] - MDELPHA ;
```

```
{    MAKE SURE WEIGHT PHASE STATE IS NOT LESS THAN THE LEAST SIGNIFICANT BIT [1]}

          IF IPHAM8  <   1   THEN

                    BEGIN

                    IPHAM8  :=  1 ;

                    END;

     writeln('IPHAM8=',IPHAM8) ;

{    NOW, DITHER THE TRANSMIT WEIGHTS UP AND DOWN IN AMPLITUDE AND PHASE}

{    AMPLITUDE SECTION:}

{    DITHER WEIGHT AMPLITUDE UP:}

          IWTAMP8[K] := IAMPP8 ;

{    SET THE TRANSMIT WEIGHTS WITH KTH WEIGHT DITHERED UP IN AMPLITUDE}

{    CALL SETWEIGHTS( IWTAMP8(1 2 3 ... NCHAN) , IWTPHA8(1 2 3 ... NCHAN) }

{    *MEASURE CURRENT E-FIELD POWER AT TUMOR SITE (RECEIVE PROBE CHANNEL 1)}
{    notation in PWR_TPA for example is PA for +Amplitude}
{         CALL MEASUREPOWER(  measure PWR_TPA, the E-field probe power at the tumor site)}
{    *MEASURE INITIAL E-FIELD POWER AT DESIRED NULL POSITION (RECEIVE PROBE CHANNEL 2)}
{         CALL MEASUREPOWER(  measure PWR_NPA, the E-field probe power at the desired null pos.)}

MEASUREP (IWTAMP8[1],IWTAMP8[2],IWTAMP8[3],IWTAMP8[4],
          IWTPHA8[1],IWTPHA8[2],IWTPHA8[3],IWTPHA8[4],PWR_NPA)  ;
```

SUBSTITUTE SHEET

```
    WRITELN('POWER WITH KTH WEIGHT DITHERED UP IN AMPLITUDE=',PWR_NPA) ;

{   DITHER WEIGHT AMPLITUDE DOWN:}

            IWTAMP8[K] := IAMPM8 ;

{   SET THE TRANSMIT WEIGHTS WITH KTH WEIGHT DITHERED DOWN IN AMPLITUDE}

    {CALL SETWEIGHTS( IWTAMP8(1 2 3 ... NCHAN) , IWTPHA8(1 2 3 ... NCHAN)}

{   *MEASURE CURRENT E-FIELD POWER AT TUMOR SITE (RECEIVE PROBE CHANNEL 1)}
{   notation in PWR_TMA for example is MA for -Amplitude}
{   CALL MEASUREPOWER(  measure PWR_TMA, the E-field probe power at the tumor site) }
{   *MEASURE INITIAL E-FIELD POWER AT DESIRED NULL POSITION (RECEIVE PROBE CHANNEL 2)}
{   CALL MEASUREPOWER(  measure PWR_NMA, the E-field probe power at the desired null pos.) }

MEASUREP (IWTAMP8[1],IWTAMP8[2],IWTAMP8[3],IWTAMP8[4],
          IWTPHA8[1],IWTPHA8[2],IWTPHA8[3],IWTPHA8[4], PWR_NMA) ;

    WRITELN('POWER WITH KTH WEIGHT DITHERED DOWN IN AMPLITUDE=',PWR_NMA) ;

{   RESET KTH WEIGHT AMPLITUDE BACK TO STATE SET BEFORE THIS DITHERING WAS PERFORMED}

            IWTAMP8[K] := IWORKAM8[K] ;

{   PHASE SECTION:}

{   DITHER WEIGHT PHASE UP:}

            IWTPHA8[K] := IPHAP8 ;

{   SET THE TRANSMIT WEIGHTS WITH KTH WEIGHT DITHERED UP IN PHASE}

    {  CALL SETWEIGHTS( IWTAMP8(1 2 3 ... NCHAN) , IWTPHA8(1 2 3 ... NCHAN) }
```

SUBSTITUTE SHEET

```
{ *MEASURE CURRENT E-FIELD POWER AT TUMOR SITE (RECEIVE PROBE CHANNEL 1)}
{  notation in PWR_TPP for example is PP for +Phase}
{    CALL MEASUREPOWER( measure PWR_TPP, the E-field probe power at the tumor site)}
{ *MEASURE INITIAL E-FIELD POWER AT DESIRED NULL POSITION (RECEIVE PROBE CHANNEL 2)}
{    CALL MEASUREPOWER( measure PWR_NPP, the E-field probe power at the desired null pos.)}

MEASUREP (IWTAMP8[1],IWTAMP8[2],IWTAMP8[3],IWTAMP8[4],
          IWTPHA8[1],IWTPHA8[2],IWTPHA8[3],IWTPHA8[4], PWR_NPP) ;

WRITELN('POWER WITH KTH WEIGHT DITHERED UP IN PHASE=',PWR_NPP) ;

{ DITHER WEIGHT PHASE DOWN:}

            IWTPHA8[K] := IPHAM8 ;

{ SET THE TRANSMIT WEIGHTS WITH KTH WEIGHT DITHERED DOWN IN PHASE}

{  CALL SETWEIGHTS( IWTAMP8(1 2 3 ... NCHAN) , IWTPHA8(1 2 3 ... NCHAN) }

{ *MEASURE CURRENT E-FIELD POWER AT TUMOR SITE (RECEIVE PROBE CHANNEL 1) }
{  notation in PWR_TMP for example is MP for -Phase}
{    CALL MEASUREPOWER( measure PWR_TMP, the E-field probe power at the tumor site)}
{ *MEASURE INITIAL E-FIELD POWER AT DESIRED NULL POSITION (RECEIVE PROBE CHANNEL 2)}
{    CALL MEASUREPOWER( measure PWR_NMP, the E-field probe power at the desired null pos.)}

MEASUREP (IWTAMP8[1],IWTAMP8[2],IWTAMP8[3],IWTAMP8[4],
          IWTPHA8[1],IWTPHA8[2],IWTPHA8[3],IWTPHA8[4], PWR_NMP) ;

WRITELN('POWER WITH KTH WEIGHT DITHERED DOWN IN PHASE=',PWR_NMP) ;

{ RESET KTH WEIGHT PHASE BACK TO STATE SET BEFORE THIS DITHERING WAS PERFORMED}

writeln('reset kth phase weight') ;

            IWTPHA8[K] := IWORKPH8[K] ;
```

```
writeln('KTH PHASE WEIGHT IS NOW=',IWTPHA8[K]) ;

{ COMPUTE POWER DIFFERENCES DUE TO WEIGHT DITHERING }

    writeln('compute power differences') ;

        DFANJ[K] := PWR_NPA - PWR_NMA ;

        DFPNJ[K] := PWR_NPP - PWR_NMP ;

    writeln('DFANJ[K]=',DFANJ[K],' DFPNJ[K]=',DFPNJ[K]) ;

{ COMPUTE NORMALIZING FACTOR }

    writeln('MDELAMP=',MDELAMP,' MDELPHA=',MDELPHA) ;
        SUMDF := SUMDF + SQR(DFANJ[K]/MDELAMP) + SQR(DFPNJ[K]/MDELPHA) ;
    writeln('SUMDF=',SUMDF)

        END;        {End of K Loop For Weight Dithering}

{ END OF WEIGHT DITHERING AND POWER DIFFERENCING LOOP}

        FACDEN := SQRT(SUMDF) ;

{ END OF WEIGHT DITHERING AND POWER DIFFERENCING SECTION}

{ COMPUTE GRADIENT SEARCH DIRECTIONS}

{ START GRADIENT SEARCH DIRECTION LOOP}

    FOR N :=1 TO NCHAN DO

        BEGIN    {Begin N Loop For Computing Search Directions}

{ THE NEXT TWO LINES ARE FOR FIGURE OF MERIT (POWER) MINIMIZATION}
```

SUBSTITUTE SHEET

```
        RANJ[N] := -DFANJ[N]/MDELAMP/FACDEN ;

        RPNJ[N] := -DFPNJ[N]/MDELPHA/FACDEN ;

        writeln('N=',N,' RANJ[N]=',RANJ[N],' RPNJ[N]=',RPNJ[N]) ;

{       COMPUTE ACTUAL WEIGHT INCREMENTS (NUMBER OF STATES) }

        RNAMPINC := MDELAMP * RANJ[N] ;
        NAMPINC  := round(RNAMPINC) ;

        RNPHAINC := MDELPHA * RPNJ[N] ;
        NPHAINC  := round(RNPHAINC) ;

        writeln('N=',N,' NAMPINC=',NAMPINC,' NPHAINC=',NPHAINC) ;

{       COMPUTE UPDATED WEIGHTS:}

{       AMPLITUDE SECTION:}

        IWTAMP8[N] := IWTAMP8[N] + NAMPINC ;

{       MAKE SURE WEIGHT AMPLITUDE DOES NOT EXCEED MOST SIGNIFICANT BIT (256)}

        IF IWTAMP8[N] > MSBSETWT  THEN

            BEGIN

            IWTAMP8[N] := MSBSETWT ;

            END;

{       MAKE SURE WEIGHT AMPLITUDE STATE IS NOT LESS THAN THE LEAST SIGNIFICANT BIT [1] }
```

```
         IF IWTAMP8[N] < 1  THEN

             BEGIN

                 IWTAMP8[N] := 1 ;

             END;

{ PHASE SECTION: }

         IWTPHA8[N] := IWTPHA8[N] + NPHAINC ;

{ MAKE SURE WEIGHT PHASE DOES NOT EXCEED MOST SIGNIFICANT BIT (256)}

         IF IWTPHA8[N] > MSBSETWT  THEN

             BEGIN

                 IWTPHA8[N] := MSBSETWT ;

             END;

{ MAKE SURE WEIGHT PHASE STATE IS NOT LESS THAN THE LEAST SIGNIFICANT BIT [1] }

         IF IWTPHA8[N] < 1  THEN

             BEGIN

                 IWTPHA8[N] := 1 ;

             END;

{ END GRADIENT SEARCH DIRECTIONS LOOP}

         END;   {End N Loop For Gradient Search Directions}
```

SUBSTITUTE SHEET

```
{ FIND NEW MAXIMUM AMPLITUDE}

  NEWMAXA8 := 0 ;

  FOR K:= 1 TO NCHAN  DO

    BEGIN

      IF IWTAMP8[K] > NEWMAXA8   THEN

        BEGIN

          NEWMAXA8 := IWTAMP8[K] ;

        END;

    END;

{ MAKE SURE TRANSMIT WEIGHT AMPLITUDES DO NOT EXCEED INITIAL MAXIMUM AMPLITUDE}

  FOR  K:= 1 TO NCHAN  DO

    BEGIN

      IWTAMP8[K] := round( IWTAMP8[K] * RMAXAMP8 / NEWMAXA8) {  ;  }

    END;

{ SET THE UPDATED (ADAPTIVE) TRANSMIT WEIGHTS AT ITERATION NUMBER ITER}

{ CALL SETWEIGHTS( IWTAMP8(1 2 3 ... NCHAN) , IWTPHA8(1 2 3 ... NCHAN) }

{ MEASURE ADAPTIVE E-FIELD POWER AT TUMOR SITE (RECEIVE PROBE CHANNEL 1)}
{ CALL MEASUREPOWER( measure TAPOWER, the E-field probe power at the tumor site)}
```

SUBSTITUTE SHEET

```
{   MEASURE ADAPTIVE E-FIELD POWER AT DESIRED NULL POSITION (RECEIVE PROBE CHANNEL 2)}
{   CALL MEASUREPOWER( measure DNAPOWER, the E-field probe power at the desired null pos.)}

MEASUREP (IWTAMP8[1],IWTAMP8[2],IWTAMP8[3],IWTAMP8[4],
          IWTPHA8[1],IWTPHA8[2],IWTPHA8[3],IWTPHA8[4], DNAPOWER ) ;

WRITELN('ITERATION no.=',ITER,'  POWER=',DNAPOWER)      ;

{   PRINT OUT ADAPTIVE WEIGHTS }

    FOR K:= 1 TO NCHAN  DO

        BEGIN

        WRITELN('CH. no.',K,'  AMP=',IWTAMP8[K],'  PHASE=',IWTPHA8[K]) {   ;   }

        END;

{FILL-IN NEW VALUES FOR WORK ARRAYS}

    FOR K := 1 TO NCHAN  DO

        BEGIN

        IWORKAM8[K] := IWTAMP8[K]     ;

        IWORKPH8[K] := IWTPHA8[K]

        END

{END OF GRADIENT SEARCH LOOP}

    END;    {End ITER loop}
```

SUBSTITUTE SHEET

```
{ END OF GRADIENT SEARCH}
   writeln('final adaptive weights')  ;
{ PRINT OUT ADAPTIVE WEIGHTS }
   FOR K:= 1 TO NCHAN  DO
     BEGIN
     WRITELN('CH. no.',K,'  AMP=',IWTAMP8[K],'  PHASE=',IWTPHA8[K])  {  ;  }
     END;
END.
```

SAMPLE OUTPUT

```
enter number of iterations in gradient search
JSMAX= 5
CHANNEL    1  AMPLITUDE=    125   PHASE=    1
CHANNEL    2  AMPLITUDE=    125   PHASE=    1
CHANNEL    3  AMPLITUDE=    125   PHASE=    1
CHANNEL    4  AMPLITUDE=    125   PHASE=    1
MAXIMUM WEIGHT AMPLITUDE OVER 8-BIT RANGE= 1.2500000000000E+0002
INITIAL E-FIELD POWER AT DESIRED NULL POSITION= 2.2483000000000E+0004
ENTER MAXIMUM NUMBER OF STATES TO DITHER TRANSMIT WEIGHT AMPLITUDE
ENTER MAXIMUM NUMBER OF STATES TO DITHER TRANSMIT WEIGHT PHASE
MDELAMP=    20  MDELPHA=    20
ITERATION NUMBER=    1
IAMPP8=   145
IAMPM8=   105
IPHAP8=    21
IPHAM8=     1
POWER WITH KTH WEIGHT DITHERED UP IN AMPLITUDE= 2.5043000000000E+0004
POWER WITH KTH WEIGHT DITHERED DOWN IN AMPLITUDE= 2.0723000000000E+0004
POWER WITH KTH WEIGHT DITHERED UP IN PHASE= 2.2883000000000E+0004
POWER WITH KTH WEIGHT DITHERED DOWN IN PHASE= 2.2483000000000E+0004
reset kth phase weight
KTH PHASE WEIGHT IS NOW=    1
compute power differences
DFANJ[K]= 4.3200000000000E+0003    DFPNJ[K]= 4.0000000000000E+0002
MDELAMP=    20  MDELPHA=    20
SUMDF= 4.7055999999999E+0004
IAMPP8=   145
IAMPM8=   105
IPHAP8=    21
IPHAM8=     1
POWER WITH KTH WEIGHT DITHERED UP IN AMPLITUDE= 2.4483000000000E+0004
POWER WITH KTH WEIGHT DITHERED DOWN IN AMPLITUDE= 2.1283000000000E+0004
POWER WITH KTH WEIGHT DITHERED UP IN PHASE= 1.8923000000000E+0004
```

SUBSTITUTE SHEET

```
POWER WITH KTH WEIGHT DITHERED DOWN IN PHASE= 2.2483000000000E+0004
reset kth phase weight
KTH PHASE WEIGHT IS NOW=            1
compute power differences
DFANJ[K]= 3.200000000000E+0003   DFPNJ[K]=-3.560000000000E+0003
MDELAMP=       20  MDELPHA=       20
SUMDF= 1.0434000000000E+0005
IAMPP8=      145
IAMPM8=      105
IPHAP8=       21
IPHAM8=        1
POWER WITH KTH WEIGHT DITHERED UP IN AMPLITUDE= 2.4243000000000E+0004
POWER WITH KTH WEIGHT DITHERED DOWN IN AMPLITUDE= 2.1523000000000E+0004
POWER WITH KTH WEIGHT DITHERED UP IN PHASE= 1.9963000000000E+0004
POWER WITH KTH WEIGHT DITHERED DOWN IN PHASE= 2.2483000000000E+0004
reset kth phase weight
KTH PHASE WEIGHT IS NOW=            1
compute power differences
DFANJ[K]= 2.7200000000000E+0003   DFPNJ[K]=-2.5200000000000E+0003
MDELAMP=       20  MDELPHA=       20
SUMDF= 1.3871200000000E+0005
IAMPP8=      145
IAMPM8=      105
IPHAP8=       21
IPHAM8=        1
POWER WITH KTH WEIGHT DITHERED UP IN AMPLITUDE= 2.2883000000000E+0004
POWER WITH KTH WEIGHT DITHERED DOWN IN AMPLITUDE= 2.2883000000000E+0004
POWER WITH KTH WEIGHT DITHERED UP IN PHASE= 2.1243000000000E+0004
POWER WITH KTH WEIGHT DITHERED DOWN IN PHASE= 2.2483000000000E+0004
reset kth phase weight
KTH PHASE WEIGHT IS NOW=            1
compute power differences
DFANJ[K]= 0.0000000000000E+0000   DFPNJ[K]=-1.2400000000000E+0003
MDELAMP=       20  MDELPHA=       20
SUMDF= 1.4255600000000E+0005
```

SUBSTITUTE SHEET

```
N=    1    RANJ[N]=-5.7208557949563E-0001    RPNJ[N]=-5.2970886990336E-0002
N=    1    NAMPINC=    -11  NPHAINC=    -1
N=    2    RANJ[N]=-4.2376709592269E-0001    RPNJ[N]= 4.7144089421399E-0001
N=    2    NAMPINC=    -8   NPHAINC=     9
N=    3    RANJ[N]=-3.6020203153428E-0001    RPNJ[N]= 3.3716588803912E-0001
N=    3    NAMPINC=    -7   NPHAINC=     7
N=    4    RANJ[N]= 0.0000000000000E+0000    RPNJ[N]= 1.6420974967004E-0001
N=    4    NAMPINC=     0   NPHAINC=     3
ITERATION no.=    1   POWER= 1.7502000000000E+0004
CH. no.    1   AMP=   114   PHASE=     1
CH. no.    2   AMP=   117   PHASE=    10
CH. no.    3   AMP=   118   PHASE=     8
CH. no.    4   AMP=   125   PHASE=     4
ITERATION NUMBER=         2
IAMPP8=    134
IAMPM8=     94
IPHAP8=     21
IPHAM8=      1
POWER WITH KTH WEIGHT DITHERED UP IN AMPLITUDE= 1.9622000000000E+0004
POWER WITH KTH WEIGHT DITHERED DOWN IN AMPLITUDE= 1.6182000000000E+0004
POWER WITH KTH WEIGHT DITHERED UP IN PHASE= 1.7902000000000E+0004
POWER WITH KTH WEIGHT DITHERED DOWN IN PHASE= 1.7502000000000E+0004
reset kth phase weight
KTH PHASE WEIGHT IS NOW=           1
compute power differences
DFANJ[K]= 3.4400000000000E+0003    DFPNJ[K]= 4.0000000000000E+0002
MDELAMP=     20  MDELPHA=        20
SUMDF= 2.9984000000000E+0004
IAMPP8=    137
IAMPM8=     97
IPHAP8=     30
IPHAM8=      1
POWER WITH KTH WEIGHT DITHERED UP IN AMPLITUDE= 1.9182000000000E+0004
POWER WITH KTH WEIGHT DITHERED DOWN IN AMPLITUDE= 1.6622000000000E+0004
POWER WITH KTH WEIGHT DITHERED UP IN PHASE= 1.4302000000000E+0004
```

SUBSTITUTE SHEET

POWER WITH KTH WEIGHT DITHERED DOWN IN PHASE= 1.9203000000000E+0004
reset kth phase weight
KTH PHASE WEIGHT IS NOW=　　　10
compute power differences
DFANJ[K]= 2.5600000000000E+0003　　DFPNJ[K]=-4.9010000000000E+0003
MDELAMP=　　20　MDELPHA=　　20
SUMDF= 1.0641750250000E+0005
IAMPP8=　　138
IAMPM8=　　98
IPHAP8=　　28
IPHAM8=　　1
POWER WITH KTH WEIGHT DITHERED UP IN AMPLITUDE= 1.8982000000000E+0004
POWER WITH KTH WEIGHT DITHERED DOWN IN AMPLITUDE= 1.6822000000000E+0004
POWER WITH KTH WEIGHT DITHERED UP IN PHASE= 1.5262000000000E+0004
POWER WITH KTH WEIGHT DITHERED DOWN IN PHASE= 1.8475000000000E+0004
reset kth phase weight
KTH PHASE WEIGHT IS NOW=　　　8
compute power differences
DFANJ[K]= 2.1600000000000E+0003　　DFPNJ[K]=-3.2130000000000E+0003
MDELAMP=　　20　MDELPHA=　　20
SUMDF= 1.4388992500000E+0005
IAMPP8=　　145
IAMPM8=　　105
IPHAP8=　　24
IPHAM8=　　1
POWER WITH KTH WEIGHT DITHERED UP IN AMPLITUDE= 1.7902000000000E+0004
POWER WITH KTH WEIGHT DITHERED DOWN IN AMPLITUDE= 1.7902000000000E+0004
POWER WITH KTH WEIGHT DITHERED UP IN PHASE= 1.6382000000000E+0004
POWER WITH KTH WEIGHT DITHERED DOWN IN PHASE= 1.7739000000000E+0004
reset kth phase weight
KTH PHASE WEIGHT IS NOW=　　　4
compute power differences
DFANJ[K]= 0.0000000000000E+0000　　DFPNJ[K]=-1.3570000000000E+0003
MDELAMP=　　20　MDELPHA=　　20
SUMDF= 1.4849354750000E+0005

SUBSTITUTE SHEET

```
N=    1    RANJ[N]=-4.4634909195497E-0001    RPNJ[N]=-5.19010572040067E-0002
N=    1    NAMPINC=    -9  NPHAINC=    -1
N=    2    RANJ[N]=-3.3216676610603E-0001    RPNJ[N]= 6.3591770390283E-0001
N=    2    NAMPINC=    -7  NPHAINC=    13
N=    3    RANJ[N]=-2.8026570890196E-0001    RPNJ[N]= 4.1689524199167E-0001
N=    3    NAMPINC=    -6  NPHAINC=    8
N=    4    RANJ[N]= 0.0000000000000E+0000    RPNJ[N]= 1.7607433656480E-0001
N=    4    NAMPINC=    0  NPHAINC=    4
ITERATION no. =  2  POWER= 1.2671000000000E+0004
CH. no.   1   AMP=   105   PHASE=    1
CH. no.   2   AMP=   110   PHASE=    23
CH. no.   3   AMP=   112   PHASE=    16
CH. no.   4   AMP=   125   PHASE=    8
ITERATION NUMBER=    3
IAMPP8=   125
IAMPM8=   85
IPHAP8=   21
IPHAM8=   1
POWER WITH KTH WEIGHT DITHERED UP IN AMPLITUDE= 1.4431000000000E+0004
POWER WITH KTH WEIGHT DITHERED DOWN IN AMPLITUDE= 1.1711000000000E+0004
POWER WITH KTH WEIGHT DITHERED UP IN PHASE= 1.3071000000000E+0004
POWER WITH KTH WEIGHT DITHERED DOWN IN PHASE= 1.2671000000000E+0004
reset kth phase weight
KTH PHASE WEIGHT IS NOW=    1
compute power differences
DFANJ[K]= 2.7200000000000E+0003  DFPNJ[K]= 4.0000000000000E+0002
MDELAMP=    20  MDELPHA=    20
SUMDF= 1.8896000000000E+0004
IAMPP8=   130
IAMPM8=   90
IPHAP8=   43
IPHAM8=   3
POWER WITH KTH WEIGHT DITHERED UP IN AMPLITUDE= 1.4071000000000E+0004
POWER WITH KTH WEIGHT DITHERED DOWN IN AMPLITUDE= 1.2071000000000E+0004
POWER WITH KTH WEIGHT DITHERED UP IN PHASE= 9.9910000000000E+0003
```

```
POWER WITH KTH WEIGHT DITHERED DOWN IN PHASE= 1.6151000000000E+0004
reset kth phase weight
KTH PHASE WEIGHT IS NOW=           23
compute power differences
DFANJ[K]= 2.0000000000000E+0003      DFPNJ[K]=-6.1600000000000E+0003
MDELAMP=         20    MDELPHA=          20
SUMDF= 1.2376000000000E+0005
IAMPP8=        132
IAMPM8=         92
IPHAP8=         36
IPHAM8=          1
POWER WITH KTH WEIGHT DITHERED UP IN AMPLITUDE= 1.3911000000000E+0004
POWER WITH KTH WEIGHT DITHERED DOWN IN AMPLITUDE= 1.2231000000000E+0004
POWER WITH KTH WEIGHT DITHERED UP IN PHASE= 1.0751000000000E+0004
POWER WITH KTH WEIGHT DITHERED DOWN IN PHASE= 1.4636000000000E+0004
reset kth phase weight
KTH PHASE WEIGHT IS NOW=           16
compute power differences
DFANJ[K]= 1.6800000000000E+0003      DFPNJ[K]=-3.8850000000000E+0003
MDELAMP=         20    MDELPHA=          20
SUMDF= 1.6854906250000E+0005
IAMPP8=        145
IAMPM8=        105
IPHAP8=         28
IPHAM8=          1
POWER WITH KTH WEIGHT DITHERED UP IN AMPLITUDE= 1.3071000000000E+0004
POWER WITH KTH WEIGHT DITHERED DOWN IN AMPLITUDE= 1.3071000000000E+0004
POWER WITH KTH WEIGHT DITHERED UP IN PHASE= 1.1711000000000E+0004
POWER WITH KTH WEIGHT DITHERED DOWN IN PHASE= 1.3196000000000E+0004
reset kth phase weight
KTH PHASE WEIGHT IS NOW=            8
compute power differences
DFANJ[K]= 0.0000000000000E+0000      DFPNJ[K]=-1.4850000000000E+0003
MDELAMP=         20    MDELPHA=          20
SUMDF= 1.7406212500000E+0005
```

```
N= 1   RANJ[N]=-3.2597685677754E-0001   RPNJ[N]=-4.7937773055521E-0002
N= 1   NAMPINC=     -7   NPHAINC=     -1
N= 2   RANJ[N]=-2.3968865527760E-0001   RPNJ[N]= 7.3824170505502E-0001
N= 2   NAMPINC=     -5   NPHAINC=     15
N= 3   RANJ[N]=-2.0133864683319E-0001   RPNJ[N]= 4.6559562080175E-0001
N= 3   NAMPINC=     -4   NPHAINC=      9
N= 4   RANJ[N]= 0.0000000000000E+0000   RPNJ[N]= 1.7796898246862E-0001
N= 4   NAMPINC=      0   NPHAINC=      4
ITERATION no.=    3   POWER= 8.5630000000000E+0003
CH. no.    1   AMP=   98   PHASE=    1
CH. no.    2   AMP=  105   PHASE=   38
CH. no.    3   AMP=  108   PHASE=   25
CH. no.    4   AMP=  125   PHASE=   12
ITERATION NUMBER=    4
IAMPP8=  118
IAMPM8=   78
IPHAP8=   21
IPHAM8=    1
POWER WITH KTH WEIGHT DITHERED UP IN AMPLITUDE= 1.0043000000000E+0004
POWER WITH KTH WEIGHT DITHERED DOWN IN AMPLITUDE= 7.8830000000000E+0003
POWER WITH KTH WEIGHT DITHERED UP IN PHASE= 8.9630000000000E+0003
POWER WITH KTH WEIGHT DITHERED DOWN IN PHASE= 8.5630000000000E+0003
reset kth phase weight
KTH PHASE WEIGHT IS NOW=    1
compute power differences
DFANJ[K]= 2.1600000000000E+0003   DFPNJ[K]= 4.0000000000000E+0002
MDELAMP=     20   MDELPHA=     20
SUMDF= 1.2064000000000E+0004
IAMPP8=  125
IAMPM8=   85
IPHAP8=   58
IPHAM8=   18
POWER WITH KTH WEIGHT DITHERED UP IN AMPLITUDE= 9.7630000000000E+0003
POWER WITH KTH WEIGHT DITHERED DOWN IN AMPLITUDE= 8.1630000000000E+0003
POWER WITH KTH WEIGHT DITHERED UP IN PHASE= 6.4830000000000E+0003
```

```
POWER WITH KTH WEIGHT DITHERED DOWN IN PHASE= 1.1443000000000E+0004
reset kth phase weight
KTH PHASE WEIGHT IS NOW=          38
compute power differences
DFANJ[K]= 1.6000000000000E+0003    DFPNJ[K]=-4.9600000000000E+0003
MDELAMP=          20    MDELPHA=          20
SUMDF= 7.9967999999999E+0004
IAMPP8=    128
IAMPM8=     88
IPHAP8=     45
IPHAM8=      5
POWER WITH KTH WEIGHT DITHERED UP IN AMPLITUDE= 9.6430000000000E+0003
POWER WITH KTH WEIGHT DITHERED DOWN IN AMPLITUDE= 8.2830000000000E+0003
POWER WITH KTH WEIGHT DITHERED UP IN PHASE= 7.0030000000000E+0003
POWER WITH KTH WEIGHT DITHERED DOWN IN PHASE= 1.0923000000000E+0004
reset kth phase weight
KTH PHASE WEIGHT IS NOW=          25
compute power differences
DFANJ[K]= 1.3600000000000E+0003    DFPNJ[K]=-3.9200000000000E+0003
MDELAMP=          20    MDELPHA=          20
SUMDF= 1.2300800000000E+0005
IAMPP8=    145
IAMPM8=    105
IPHAP8=     32
IPHAM8=      1
POWER WITH KTH WEIGHT DITHERED UP IN AMPLITUDE= 8.9630000000000E+0003
POWER WITH KTH WEIGHT DITHERED DOWN IN AMPLITUDE= 8.9630000000000E+0003
POWER WITH KTH WEIGHT DITHERED UP IN PHASE= 7.7630000000000E+0003
POWER WITH KTH WEIGHT DITHERED DOWN IN PHASE= 9.3440000000000E+0003
reset kth phase weight
KTH PHASE WEIGHT IS NOW=          12
compute power differences
DFANJ[K]= 0.0000000000000E+0000    DFPNJ[K]=-1.5810000000000E+0003
MDELAMP=          20    MDELPHA=          20
SUMDF= 1.2925690250000E+0005
```

SUBSTITUTE SHEET

```
N=     1    RANJ[N]=-3.00397893778774E-0001   RPNJ[N]=-5.56292395903322E-0002
N=     1    NAMPINC=   -6   NPHAINC=    -1
N=     2    RANJ[N]=-2.2251695836129E-0001    RPNJ[N]= 6.89802570919999E-0001
N=     2    NAMPINC=   -4   NPHAINC=    14
N=     3    RANJ[N]=-1.89139414607100E-0001   RPNJ[N]= 5.4516654798516E-0001
N=     3    NAMPINC=   -4   NPHAINC=    11
N=     4    RANJ[N]= 0.0000000000000E+0000    RPNJ[N]= 2.19874569480755E-0001
N=     4    NAMPINC=    0   NPHAINC=     4
ITERATION no.=    4   POWER= 5.290000000000E+0003
CH. no.    1    AMP=    92   PHASE=     1
CH. no.    2    AMP=   101   PHASE=    52
CH. no.    3    AMP=   104   PHASE=    36
CH. no.    4    AMP=   125   PHASE=    16
ITERATION NUMBER=     5
IAMPP8=  112
IAMPM8=   72
IPHAP8=   21
IPHAM8=    1
POWER WITH KTH WEIGHT DITHERED UP IN AMPLITUDE= 6.53000000000E+0003
POWER WITH KTH WEIGHT DITHERED DOWN IN AMPLITUDE= 4.85000000000000E+0003
POWER WITH KTH WEIGHT DITHERED UP IN PHASE= 5.69000000000E+0003
POWER WITH KTH WEIGHT DITHERED DOWN IN PHASE= 5.290000000000E+0003
reset kth phase weight
KTH PHASE WEIGHT IS NOW=       1
compute power differences
DFANJ[K]= 1.6800000000000E+0003   DFPNJ[K]= 4.0000000000000E+0002
MDELAMP=    20   MDELPHA=      20
SUMDF= 7.4559999999999E+0003
IAMPP8=  121
IAMPM8=   81
IPHAP8=   72
IPHAM8=   32
POWER WITH KTH WEIGHT DITHERED UP IN AMPLITUDE= 6.33000000000E+0003
POWER WITH KTH WEIGHT DITHERED DOWN IN AMPLITUDE= 5.05000000000000E+0003
POWER WITH KTH WEIGHT DITHERED UP IN PHASE= 3.77000000000E+0003
```

SUBSTITUTE SHEET

```
POWER WITH KTH WEIGHT WEIGHT DITHERED DOWN IN PHASE= 7.6100000000000E+0003
reset kth phase weight
KTH PHASE WEIGHT IS NOW=            52
compute power differences
DFANJ[K]= 1.2800000000000E+0003    DFPNJ[K]=-3.8400000000000E+0003
MDELAMP=            20  MDELPHA=            20
SUMDF= 4.8415999999999E+0004
IAMPP8=    124
IAMPM8=     84
IPHAP8=     56
IPHAM8=     16
POWER WITH KTH WEIGHT DITHERED UP IN AMPLITUDE= 6.2100000000000E+0003
POWER WITH KTH WEIGHT DITHERED DOWN IN AMPLITUDE= 5.1700000000000E+0003
POWER WITH KTH WEIGHT DITHERED UP IN PHASE= 4.1700000000000E+0003
POWER WITH KTH WEIGHT DITHERED DOWN IN PHASE= 7.2100000000000E+0003
reset kth phase weight
KTH PHASE WEIGHT IS NOW=            36
compute power differences
DFANJ[K]= 1.0400000000000E+0003    DFPNJ[K]=-3.0400000000000E+0003
MDELAMP=            20  MDELPHA=            20
SUMDF= 7.4223999999999E+0004
IAMPP8=    145
IAMPM8=    105
IPHAP8=     36
IPHAM8=      1
POWER WITH KTH WEIGHT DITHERED UP IN AMPLITUDE= 5.6900000000000E+0003
POWER WITH KTH WEIGHT DITHERED DOWN IN AMPLITUDE= 5.6900000000000E+0003
POWER WITH KTH WEIGHT DITHERED UP IN PHASE= 4.6500000000000E+0003
POWER WITH KTH WEIGHT DITHERED DOWN IN PHASE= 6.2950000000000E+0003
reset kth phase weight
KTH PHASE WEIGHT IS NOW=            16
compute power differences
DFANJ[K]= 0.0000000000000E+0000    DFPNJ[K]=-1.6450000000000E+0003
MDELAMP=            20  MDELPHA=            20
SUMDF= 8.0989062499999E+0004
```

```
N=  1   RANJ[N]=-2.9516584387132E-0001   RPNJ[N]=-7.0277581874123E-0002
N=  1   NAMPINC=    -6  NPHAINC=      -1
N=  2   RANJ[N]=-2.2488826199720E-0001   RPNJ[N]= 6.7466478599158E-0001
N=  2   NAMPINC=    -4  NPHAINC=      13
N=  3   RANJ[N]=-1.8272171287272E-0001   RPNJ[N]= 5.3410962224334E-0001
N=  3   NAMPINC=    -4  NPHAINC=      11
N=  4   RANJ[N]= 0.0000000000000E+0000   RPNJ[N]= 2.8901655545733E-0001
N=  4   NAMPINC=     0  NPHAINC=       6
ITERATION no.=   5   POWER= 2.8040000000000E+0003
CH. no.  1   AMP=  86   PHASE=    1
CH. no.  2   AMP=  97   PHASE=   65
CH. no.  3   AMP= 100   PHASE=   47
CH. no.  4   AMP= 125   PHASE=   22
final adaptive weights
CH. no.  1   AMP=  86   PHASE=    1
CH. no.  2   AMP=  97   PHASE=   65
CH. no.  3   AMP= 100   PHASE=   47
CH. no.  4   AMP= 125   PHASE=   22
```

SUBSTITUTE SHEET

APPENDIX D

```
{ COPYRIGHT M.I.T. LINCOLN LABORATORY 1991, ALL RIGHTS RESERVED}
{ PROGRAM FOCUSGS.P (PASCAL VERSION BY ALAN J. FENN)}
{ THIS SUBROUTINE PERFORMS A GRADIENT SEARCH FOR THE}
{ ADAPTIVE FOCUSING WEIGHTS (PHASE ONLY)}
{ BASED ON MAXIMIZING THE POWER RECEIVED BY AN E-FIELD PROBE}
{ AT A DESIRED FOCUS (TUMOR) POSITION. }
PROGRAM FOCUSGS (INPUT,OUTPUT) ;
{ PROGRAM INPUT OR FIXED PARAMETERS}

{ NCHAN IS THE NUMBER OF ADAPTIVE TRANSMIT CHANNELS (=4)}
{ NETUMOR IS THE NUMBER OF E-FIELD TUMOR-SITE PROBES (=1)}
{ NEPROBE IS THE NUMBER OF E-FIELD NULLING PROBES (=1)}
{ JSMAX IS THE MAXIMUM NUMBER OF GRADIENT ITERATIONS (=200)}
{ NBSETWT IS THE NUMBER OF BITS USED IN SETTING THE TRANSMIT WEIGHTS (=8)}
{ NBMEAWT IS THE NUMBER OF BITS USED IN MEASURING THE TRANSMIT WEIGHTS (=12)}
{ NBPROBE IS THE NUMBER OF BITS USED IN MEASURING THE E-FIELD PROBE POWER (=12)}

{ PROGRAM OUTPUT}

{ IWTAMP8 IS THE ADAPTIVE NULLING WEIGHT VECTOR AMPLITUDE}
{ IWTPHA8 IS THE ADAPTIVE NULLING WEIGHT VECTOR PHASE}

{ This computer program is intended to be used in the following manner:}

{ Initially, the phased array should be turned on and the}
{ transmit weights are set to some nominal values. Assume that there are}
{ two E-field probes, one invasive at the desired tumor position and}
{ one noninvasive on the skin surface. The output power of the two E-field}
{ probes should be measured and be printed, saved, or displayed on the screen }
{ for reference purposes.}
{ This focusing program can do both amplitude and phase dithering if }
{ desired by uncommenting the read statement for the amplitude dither}
{ parameter and then commenting the line of code where the amplitude}
```

```
{  dither parameter is set equal to zero}
{  Currently, this program will only dither the transmit phase weights}

{  DECLARE INTEGER AND REAL ARRAYS WITH APPROPRIATE DIMENSIONS}

VAR

IWTAMP12 : ARRAY [1..4] OF INTEGER;
IWTPHA12 : ARRAY [1..4] OF INTEGER;
IWTAMP8  : ARRAY [1..4] OF INTEGER;
IWTPHA8  : ARRAY [1..4] OF INTEGER;
IWORKAM8 : ARRAY [1..4] OF INTEGER;
IWORKPH8 : ARRAY [1..4] OF INTEGER;

DFANJ    : ARRAY [1..4] OF REAL;
DFPNJ    : ARRAY [1..4] OF REAL;
RANJ     : ARRAY [1..4] OF REAL;
RPNJ     : ARRAY [1..4] OF REAL;

{  DECLARE INTEGER AND REAL VARIABLES}

MAXAMP8,NBSETWT,NBMEAWT,NBPROBE             : INTEGER;
MSBMEAWT,MSBSETWT,MSBPROBE                  : INTEGER;
I,K,N,MDELAMP,MDELPHA,ITER,JSMAX            : INTEGER;
NCHAN,IAMPP8,IPHAP8,IAMPM8,IPHAM8           : INTEGER;
NAMPINC,NPHAINC,NEWMAXA8                    : INTEGER;
NETUMOR,NEPROBE                            : INTEGER;

FAC12TO8,FACDEN,SUMDF                       : REAL;
TPOWER,DNPOWER,TAPOWER,DNAPOWER            : REAL;
PWR_TPA,PWR_NPA,PWR_TMA,PWR_NMA            : REAL;
PWR_TPP,PWR_NPP,PWR_TMP,PWR_NMP            : REAL;
RMSBMEAW,RMSBSETW,RNAMPINC,RNPHAINC         : REAL;
RMAXAMP8                                    : REAL;

{  NOTE: Define  MEASUREPOWER Procedure}
```

SUBSTITUTE SHEET

```
PROCEDURE MEASUREP (IA1,IA2,IA3,IA4,IP1,IP2,IP3,IP4 : INTEGER ;
                    VAR POWER : REAL) ; {E-FIELD PROBE POWER MEASUREMENT PROCEDURE}

VAR
     IA01,IA02,IA03,IA04,IP01,IP02,IP03,IP04 : INTEGER ;
     POWERA,POWERP                           : REAL   ;

BEGIN

     {8-bit weight data}

     IA01 := 71 ;
     IA02 := 85 ;
     IA03 := 91 ;
     IA04 := 125 ;

     IP01 := 1 ;
     IP02 := 100 ;
     IP03 := 74 ;
     IP04 := 42 ;

{ Polynomial Function Definition }

POWERA := SQR(IA1-IA01)+SQR(IA2-IA02)+SQR(IA3-IA03)+SQR(IA4-IA04) ;
POWERP := SQR(IP1-IP01)+SQR(IP2-IP02)+SQR(IP3-IP03)+SQR(IP4-IP04) ;

POWER := -POWERA - POWERP      {   ;   }

END;

PROCEDURE MEASIW (VAR  IWA1,IWA2,IWA3,IWA4,IWP1,IWP2,IWP3,IWP4 : INTEGER) ;

{THIS PROCEDURE MEASURES THE INITIAL WEIGHTS}
{artificially sets them for now}
```

SUBSTITUTE SHEET

```
BEGIN

{12-bit data}

IWA1 := 2000 ;
IWA2 := 2000 ;
IWA3 := 2000 ;
IWA4 := 2000 ;

IWP1 := 1 ;
IWP2 := 1 ;
IWP3 := 1 ;
IWP4 := 1        {  ;  }

END;

PROCEDURE SETWTS ;  {procedure to set weights}

BEGIN

{NON-FUNCTIONING FOR NOW}

END;

BEGIN   {BEGIN THE MAIN PROGRAM}

{    FIXED DATA FOR SYSTEM}

     NCHAN := 4 ;

{    NUMBER OF BITS TO SET WEIGHTS, MEASURE WEIGHTS, MEASURE E-FIELD PROBE}
     NBSETWT:=8 ;
     NBMEAWT:=12 ;
```

```
     NBPROBE:=12 ;

     NETUMOR:=1 ;
     NEPROBE:=1 ;
     JSMAX  :=25 ;    {number of iterations in gradient search}

     WRITELN('enter number of iterations in gradient search') ;

     READLN (JSMAX) ;

     WRITELN('JSMAX=',JSMAX) ;

{    END OF DATA}


{    MEASURE INITIAL E-FIELD POWER AT TUMOR SITE (RECEIVE PROBE CHANNEL 1)}
{       CALL MEASUREPOWER( measure TPOWER, the E-field probe power at the tumor site)}
{    MEASURE INITIAL E-FIELD POWER AT DESIRED NULL POSITION (RECEIVE PROBE CHANNEL 2)}
{       CALL MEASUREPOWER( measure DNPOWER, the E-field probe power at the desired null pos.)}

{    MEASURE TRANSMIT WEIGHTS AMPLITUDE (IWTAMP12) AND PHASE (IWTPHA12) FOR EACH TRANSMIT CH.}
{    NOTE: THE 12 IN IWTAMP12 AND IWTPHA12 REFERS TO 12 BITS}

     {FOR I:=1 TO NCHAN DO}
     {CALL MEASUREWEIGHT( IWTAMP12[I], IWTPHA12[I]  ) ;}

MEASIW (IWTAMP12[1],IWTAMP12[2],IWTAMP12[3],IWTAMP12[4],
        IWTPHA12[1],IWTPHA12[2],IWTPHA12[3],IWTPHA12[4] ) ;

{    CONVERT 12 BIT MEASUREMENTS TO 8 BIT RANGE FOR PURPOSES OF SETTING WEIGHTS}
{       WITH 8-BIT DIGITAL TO ANALOG CONVERTERS}

{    NOTE: 12 BIT RANGE IS STATES   1,2,3,............,4096}
{          8 BIT RANGE IS STATES    1,2,3,....256}
```

SUBSTITUTE SHEET

```
{ THE MOST SIGNIFICANT BIT FOR THE TRANSMIT WEIGHT MEASUREMENTS IS (MSBMEAWT=4096)}

{ RMSBMEAW := EXP(NBMEAWT * (LN (2.) ) ) ; }
  RMSBMEAW := 4096 ;
  MSBMEAWT := round(RMSBMEAW) ;

{ THE MOST SIGNIFICANT BIT FOR THE TRANSMIT WEIGHT SETTINGS IS (MSBSETWT=256)}

{ RMSBSETW := EXP(NBSETWT * (LN (2.) ) ) ; }
  RMSBSETW := 256 ;
  MSBSETWT := round(RMSBSETW) ;

{ COMPUTE SCALE FACTOR TO CONVERT 12-BIT RANGE TO 8-BIT RANGE}

  FAC12TO8 := RMSBSETW / MSBMEAWT ;

{ CONVERT THE 12-BIT TRANSMIT WEIGHT DATA TO 8-BIT DATA AND PRINT-OUT}

  FOR I:= 1 TO NCHAN  DO

    BEGIN

      IWTAMP8[I] := round( IWTAMP12[I] * FAC12TO8) ;

      IF IWTAMP8[I] < 1 THEN  IWTAMP8[I] := 1 ;

      IWTPHA8[I] := round( IWTPHA12[I] * FAC12TO8) ;

      IF IWTPHA8[I] < 1 THEN  IWTPHA8[I] := 1 ;

      WRITELN('CHANNEL', I, ' AMPLITUDE=', IWTAMP8[I],' PHASE=', IWTPHA8[I]) ;

{ STORE THE 8-BIT DATA IN TEMPORARY WORK ARRAYS}
      IWORKAM8[I] := IWTAMP8[I] ;
```

SUBSTITUTE SHEET

```
          IWORKPH8[I] := IWTPHA8[I]       {       ;       }
          END;
{

{ DETERMINE MAXIMUM WEIGHT AMPLITUDE BEFORE FOCUSING}

    MAXAMP8 :=0 ;

    FOR I := 1 TO NCHAN  DO

        BEGIN

        IF IWTAMP8[I] > MAXAMP8   THEN

            MAXAMP8 :=IWTAMP8[I]    {    ;    }

        END;
{

{ COPY MAXAMP8 TO A REAL VARIABLE (RMAXAMP8) }

    RMAXAMP8 := MAXAMP8 ;
{

{ PRINT-OUT THE MAXIMUM WEIGHT AMPLITUDE OVER 8-BIT RANGE}

    WRITELN('MAXIMUM WEIGHT AMPLITUDE OVER 8-BIT RANGE=', RMAXAMP8) ;

{MEASURE INITIAL E-FIELD POWER AT DESIRED FOCUS (TUMOR) POSITION (RECEIVE PROBE CHANNEL 2)}

    MEASUREP (IWTAMP8[1],IWTAMP8[2],IWTAMP8[3],IWTAMP8[4],
              IWTPHA8[1],IWTPHA8[2],IWTPHA8[3],IWTPHA8[4], TPOWER) ;

    WRITELN('INITIAL E-FIELD POWER AT DESIRED FOCUS (TUMOR) POSITION=',TPOWER) ;
{

{ READ-IN THE MAXIMUM NUMBER OF STATES TO DITHER TRANSMIT WEIGHT AMPLITUDE}
```

SUBSTITUTE SHEET

```
WRITELN('A BASIC ASSUMPTION IS THAT NO AMPLITUDE FOCUSING IS NEEDED,') ;
WRITELN('SO THE NUMBER OF STATES TO DITHER AMPLITUDE IS EQUAL TO ZERO (0)') ;
{WRITELN('ENTER MAXIMUM NUMBER OF STATES TO DITHER TRANSMIT WEIGHT AMPLITUDE');}

{  READLN (MDELAMP) ; }

MDELAMP := 0 ;  {set amplitude dither to zero}

READ-IN THE MAXIMUM NUMBER OF STATES TO DITHER TRANSMIT WEIGHT PHASE}

WRITELN('ENTER MAXIMUM NUMBER OF STATES TO DITHER TRANSMIT WEIGHT PHASE');
READLN (MDELPHA) ;

writeln('MDELAMP=',MDELAMP,'  MDELPHA=',MDELPHA) ;

{ BEGIN GRADIENT SEARCH: }

FOR ITER := 1 TO JSMAX  DO      {Start ITER Loop}
          BEGIN
SUMDF :=0.0 ;

WRITELN ('ITERATION NUMBER=',ITER);

{ COMPUTE WEIGHT-DITHERING STATES +-AMPLITUDE,  +-PHASE}

FOR K := 1 TO NCHAN  DO     {Start K Loop For Weight Dithering}

               BEGIN

{ AMPLITUDE SECTION: }
```

SUBSTITUTE SHEET

```
     IAMPP8 := IWTAMP8[K] + MDELAMP ;

     writeln('IAMPP8=',IAMPP8) ;

{ MAKE SURE WEIGHT AMPLITUDE DOES NOT EXCEED MOST SIGNIFICANT BIT (256) }

     IF IAMPP8 > MSBSETWT THEN

          BEGIN

          IAMPP8 := MSBSETWT ;

          END;

     IAMPM8 := IWTAMP8[K] - MDELAMP ;

     writeln('IAMPM8=',IAMPM8) ;

{ MAKE SURE WEIGHT AMPLITUDE STATE IS NOT LESS THAN THE LEAST SIGNIFICANT BIT [1]}

     IF IAMPM8 < 1  THEN

          BEGIN

          IAMPM8 := 1 ;

          END;

{ PHASE SECTION:}

     IPHAP8 := IWTPHA8[K] + MDELPHA ;

{ MAKE SURE WEIGHT PHASE DOES NOT EXCEED MOST SIGNIFICANT BIT (256)}

     IF IPHAP8 > MSBSETWT  THEN
```

SUBSTITUTE SHEET

```
                BEGIN

                    IPHAP8 := MSBSETWT ;

                END;

            IPHAM8 := IWTPHA8[K] - MDELPHA ;

{ MAKE SURE WEIGHT PHASE STATE IS NOT LESS THAN THE LEAST SIGNIFICANT BIT [1]}

            IF IPHAM8 < 1  THEN

                BEGIN

                    IPHAM8 := 1 ;

                END;

        writeln('IPHAM8=',IPHAM8) ;

{ NOW, DITHER THE TRANSMIT WEIGHTS UP AND DOWN IN AMPLITUDE AND PHASE}

{ AMPLITUDE SECTION:}

{ DITHER WEIGHT AMPLITUDE UP:}

            IWTAMP8[K] := IAMPP8 ;

{ SET THE TRANSMIT WEIGHTS WITH KTH WEIGHT DITHERED UP IN AMPLITUDE}

{ CALL SETWEIGHTS( IWTAMP8(1 2 3 ... NCHAN) , IWTPHA8(1 2 3 ... NCHAN) }
```

writeln('IPHAP8=',IPHAP8) ;

SUBSTITUTE SHEET

```
{ *MEASURE CURRENT E-FIELD POWER AT TUMOR SITE (RECEIVE PROBE CHANNEL 1)}
{ notation in PWR_TPA for example is PA for +Amplitude}
{   CALL MEASUREPOWER(  measure PWR_TPA, the E-field probe power at the tumor site)}
{ *MEASURE INITIAL E-FIELD POWER AT DESIRED NULL POSITION (RECEIVE PROBE CHANNEL 2)}
{   CALL MEASUREPOWER(  measure PWR_NPA, the E-field probe power at the desired null pos.)}

MEASUREP (IWTAMP8[1],IWTAMP8[2],IWTAMP8[3],IWTAMP8[4],
          IWTPHA8[1],IWTPHA8[2],IWTPHA8[3],IWTPHA8[4], PWR_TPA)  ;

WRITELN('POWER WITH KTH WEIGHT DITHERED UP IN AMPLITUDE=',PWR_TPA) ;

{ DITHER WEIGHT AMPLITUDE DOWN:}

                IWTAMP8[K] := IAMPM8  ;

{ SET THE TRANSMIT WEIGHTS WITH KTH WEIGHT DITHERED DOWN IN AMPLITUDE}

     {CALL SETWEIGHTS( IWTAMP8(1 2 3 ... NCHAN) , IWTPHA8(1 2 3 ... NCHAN) }

{ *MEASURE CURRENT E-FIELD POWER AT TUMOR SITE (RECEIVE PROBE CHANNEL 1)}
{ notation in PWR_TMA for example is MA for -Amplitude}
{   CALL MEASUREPOWER(  measure PWR_TMA, the E-field probe power at the tumor site) }
{ *MEASURE INITIAL E-FIELD POWER AT DESIRED NULL POSITION (RECEIVE PROBE CHANNEL 2)}
{   CALL MEASUREPOWER(  measure PWR_NMA, the E-field probe power at the desired null pos.) }

MEASUREP (IWTAMP8[1],IWTAMP8[2],IWTAMP8[3],IWTAMP8[4],
          IWTPHA8[1],IWTPHA8[2],IWTPHA8[3],IWTPHA8[4], PWR_TMA)  ;

WRITELN('POWER WITH KTH WEIGHT DITHERED DOWN IN AMPLITUDE=',PWR_TMA) ;

{ RESET KTH WEIGHT AMPLITUDE BACK TO STATE SET BEFORE THIS DITHERING WAS PERFORMED}

                IWTAMP8[K] := IWORKAM8[K]  ;

{ PHASE SECTION:}
```

SUBSTITUTE SHEET

```
{ DITHER WEIGHT PHASE UP:}

        IWTPHA8[K] := IPHAP8 ;

{ SET THE TRANSMIT WEIGHTS WITH KTH WEIGHT DITHERED UP IN PHASE}

{ CALL SETWEIGHTS( IWTAMP8(1 2 3 ... NCHAN) , IWTPHA8(1 2 3 ... NCHAN) }

{ *MEASURE CURRENT E-FIELD POWER AT TUMOR SITE (RECEIVE PROBE CHANNEL 1)}
{ notation in PWR_TPP for example is PP for +Phase}
{      CALL MEASUREPOWER( measure PWR_TPP, the E-field probe power at the tumor site)}
{ *MEASURE INITIAL E-FIELD POWER AT DESIRED NULL POSITION (RECEIVE PROBE CHANNEL 2)}
{      CALL MEASUREPOWER( measure PWR_NPP, the E-field probe power at the desired null pos.)}

MEASUREP (IWTAMP8[1],IWTAMP8[2],IWTAMP8[3],IWTAMP8[4],
          IWTPHA8[1],IWTPHA8[2],IWTPHA8[3],IWTPHA8[4], PWR_TPP) ;

WRITELN('POWER WITH KTH WEIGHT DITHERED UP IN PHASE=',PWR_TPP) ;

{ DITHER WEIGHT PHASE DOWN:}

        IWTPHA8[K] := IPHAM8 ;

{ SET THE TRANSMIT WEIGHTS WITH KTH WEIGHT DITHERED DOWN IN PHASE}

{ CALL SETWEIGHTS( IWTAMP8(1 2 3 ... NCHAN) , IWTPHA8(1 2 3 ... NCHAN) }

{ *MEASURE CURRENT E-FIELD POWER AT TUMOR SITE (RECEIVE PROBE CHANNEL 1) }
{ notation in PWR_TMP for example is MP for -Phase}
{      CALL MEASUREPOWER( measure PWR_TMP, the E-field probe power at the tumor site)}
{ *MEASURE INITIAL E-FIELD POWER AT DESIRED NULL POSITION (RECEIVE PROBE CHANNEL 2)}
{      CALL MEASUREPOWER( measure PWR_NMP, the E-field probe power at the desired null pos.)}

MEASUREP (IWTAMP8[1],IWTAMP8[2],IWTAMP8[3],IWTAMP8[4],
          IWTPHA8[1],IWTPHA8[2],IWTPHA8[3],IWTPHA8[4], PWR_TMP) ;
```

```
    WRITELN('POWER WITH KTH WEIGHT DITHERED DOWN IN PHASE=',PWR_TMP) ;

{ RESET KTH WEIGHT PHASE BACK TO STATE SET BEFORE THIS DITHERING WAS PERFORMED}

    writeln('reset kth phase weight') ;

                IWTPHA8[K] := IWORKPH8[K] ;

    writeln('KTH PHASE WEIGHT IS NOW=',IWTPHA8[K]) ;

{ COMPUTE POWER DIFFERENCES DUE TO WEIGHT DITHERING }

    writeln('compute power differences') ;

                DFANJ[K] := PWR_TPA - PWR_TMA ;

                DFPNJ[K] := PWR_TPP - PWR_TMP ;

    writeln('DFANJ[K]=',DFANJ[K],'  DFPNJ[K]=',DFPNJ[K]) ;

{ COMPUTE NORMALIZING FACTOR }

    writeln('MDELAMP=',MDELAMP,'  MDELPHA=',MDELPHA) ;

    IF MDELAMP > 0 THEN
        BEGIN
            SUMDF := SUMDF + SQR(DFANJ[K]/MDELAMP) + SQR(DFPNJ[K]/MDELPHA) ;
        END
    ELSE
        BEGIN
            SUMDF := SUMDF + SQR(DFPNJ[K]/MDELPHA) ;
        END;
    writeln('SUMDF=',SUMDF)

        END;      {End of K Loop For Weight Dithering}
```

SUBSTITUTE SHEET

```
{    END OF WEIGHT DITHERING AND POWER DIFFERENCING LOOP}

          FACDEN := SQRT(SUMDF) ;

{    END OF WEIGHT DITHERING AND POWER DIFFERENCING SECTION}

{    COMPUTE GRADIENT SEARCH DIRECTIONS}

{    START GRADIENT SEARCH DIRECTION LOOP}

          FOR N :=1 TO NCHAN  DO

          BEGIN    {Begin N Loop For Computing Search Directions}

{    THE NEXT TWO LINES ARE FOR FIGURE OF MERIT (POWER) MAXIMIZATION}

          IF MDELAMP > 0 THEN
               BEGIN
                    RANJ[N] := DFANJ[N]/MDELAMP/FACDEN ;
               END
          ELSE
               BEGIN
                    RANJ[N] := 0.0
               END;

          RPNJ[N] := DFPNJ[N]/MDELPHA/FACDEN ;

          writeln('N=',N,'  RANJ[N]=',RANJ[N],'  RPNJ[N]=',RPNJ[N]) ;

{    COMPUTE ACTUAL WEIGHT INCREMENTS (NUMBER OF STATES)}

          RNAMPINC := MDELAMP * RANJ[N] ;
          NAMPINC  := round(RNAMPINC) ;

          RNPHAINC := MDELPHA * RPNJ[N] ;
```

```
        NPHAINC    := round(RNPHAINC) ;

        writeln('N=',N,'  NAMPINC=',NAMPINC,'   NPHAINC=',NPHAINC) ;

{ COMPUTE UPDATED WEIGHTS:}

{ AMPLITUDE SECTION:}

        IWTAMP8[N] := IWTAMP8[N] + NAMPINC ;

{ MAKE SURE WEIGHT AMPLITUDE DOES NOT EXCEED MOST SIGNIFICANT BIT (256)}

        IF IWTAMP8[N] > MSBSETWT  THEN

                BEGIN

                IWTAMP8[N] := MSBSETWT ;

                END;

{ MAKE SURE WEIGHT AMPLITUDE STATE IS NOT LESS THAN THE LEAST SIGNIFICANT BIT [1] }

        IF IWTAMP8[N] < 1  THEN

                BEGIN

                IWTAMP8[N] := 1 ;

                END;

{ PHASE SECTION: }

        IWTPHA8[N] := IWTPHA8[N] + NPHAINC ;
```

```
{ MAKE SURE WEIGHT PHASE DOES NOT EXCEED MOST SIGNIFICANT BIT (256)}

         IF IWTPHA8[N] > MSBSETWT  THEN

             BEGIN

             IWTPHA8[N] := MSBSETWT ;

             END;

{ MAKE SURE WEIGHT PHASE STATE IS NOT LESS THAN THE LEAST SIGNIFICANT BIT [1] }

         IF IWTPHA8[N] < 1  THEN

             BEGIN

             IWTPHA8[N] := 1 ;

             END;

{ END GRADIENT SEARCH DIRECTIONS LOOP}

     END;   {End N Loop For Gradient Search Directions}

{ FIND NEW MAXIMUM AMPLITUDE}

     NEWMAXA8 := 0 ;

         FOR K:= 1 TO NCHAN  DO

             BEGIN

             IF IWTAMP8[K] > NEWMAXA8  THEN
```

−177−

```
        BEGIN

        WRITELN('CH. no.',K,'  AMP=',IWTAMP8[K],'  PHASE=',IWTPHA8[K]) {  ;  }

        END;

{FILL-IN NEW VALUES FOR WORK ARRAYS}

        FOR K := 1 TO NCHAN   DO

            BEGIN

            IWORKAM8[K] := IWTAMP8[K]  ;

            IWORKPH8[K] := IWTPHA8[K]

            END

{END OF GRADIENT SEARCH LOOP}

        END;    {End ITER loop}

{  END OF GRADIENT SEARCH}

        writeln('final adaptive weights')  ;

{  PRINT OUT ADAPTIVE WEIGHTS }

        FOR K:= 1 TO NCHAN   DO

            BEGIN

            WRITELN('CH. no.',K,'  AMP=',IWTAMP8[K],'  PHASE=',IWTPHA8[K]) {  ;  }
```

SUBSTITUTE SHEET

-178-

END;

END.

SUBSTITUTE SHEET

SAMPLE OUTPUT

enter number of iterations in gradient search
JSMAX=   5
CHANNEL   1 AMPLITUDE=   125 PHASE=   1
CHANNEL   2 AMPLITUDE=   125 PHASE=   1
CHANNEL   3 AMPLITUDE=   125 PHASE=   1
CHANNEL   4 AMPLITUDE=   125 PHASE=   1
MAXIMUM WEIGHT AMPLITUDE OVER 8-BIT RANGE= 1.2500000000000E+0002
INITIAL E-FIELD POWER AT DESIRED FOCUS (TUMOR) POSITION=-2.2483000000000E+0004
A BASIC ASSUMPTION IS THAT NO AMPLITUDE FOCUSING IS NEEDED,
SO THE NUMBER OF STATES TO DITHER AMPLITUDE IS EQUAL TO ZERO (0)
ENTER MAXIMUM NUMBER OF STATES TO DITHER TRANSMIT WEIGHT PHASE
MDELAMP=   0 MDELPHA=   20
ITERATION NUMBER=   1
IAMPP8=   125
IAMPM8=   125
IPHAP8=   21
IPHAM8=   1
POWER WITH KTH WEIGHT DITHERED UP IN AMPLITUDE=-2.2483000000000E+0004
POWER WITH KTH WEIGHT DITHERED DOWN IN AMPLITUDE=-2.2483000000000E+0004
POWER WITH KTH WEIGHT DITHERED UP IN PHASE=-2.2883000000000E+0004
POWER WITH KTH WEIGHT DITHERED DOWN IN PHASE=-2.2483000000000E+0004
reset kth phase weight
KTH PHASE WEIGHT IS NOW=   1
compute power differences
DFANJ[K]= 0.0000000000000E+0000 DFPNJ[K]=-4.0000000000000E+0002
MDELAMP=   0 MDELPHA=   20
SUMDF= 4.0000000000000E+0002
IAMPP8=   125
IAMPM8=   125
IPHAP8=   21
IPHAM8=   1
POWER WITH KTH WEIGHT DITHERED UP IN AMPLITUDE=-2.2483000000000E+0004
POWER WITH KTH WEIGHT DITHERED DOWN IN AMPLITUDE=-2.2483000000000E+0004

SUBSTITUTE SHEET

```
POWER WITH KTH WEIGHT DITHERED UP IN PHASE=-1.89230000000000E+0004
POWER WITH KTH WEIGHT DITHERED DOWN IN PHASE=-2.24830000000000E+0004
reset kth phase weight
KTH PHASE WEIGHT IS NOW=        1
compute power differences
DFANJ[K]= 0.00000000000000E+0000    DFPNJ[K]= 3.56000000000000E+0003
MDELAMP=        0    MDELPHA=        20
SUMDF= 3.20840000000000E+0004
IAMPP8=      125
IAMPM8=      125
IPHAP8=       21
IPHAM8=        1
POWER WITH KTH WEIGHT DITHERED UP IN AMPLITUDE=-2.24830000000000E+0004
POWER WITH KTH WEIGHT DITHERED DOWN IN AMPLITUDE=-2.24830000000000E+0004
POWER WITH KTH WEIGHT DITHERED UP IN PHASE=-1.99630000000000E+0004
POWER WITH KTH WEIGHT DITHERED DOWN IN PHASE=-2.24830000000000E+0004
reset kth phase weight
KTH PHASE WEIGHT IS NOW=        1
compute power differences
DFANJ[K]= 0.00000000000000E+0000    DFPNJ[K]= 2.52000000000000E+0003
MDELAMP=        0    MDELPHA=        20
SUMDF= 4.79599999999999E+0004
IAMPP8=      125
IAMPM8=      125
IPHAP8=       21
IPHAM8=        1
POWER WITH KTH WEIGHT DITHERED UP IN AMPLITUDE=-2.24830000000000E+0004
POWER WITH KTH WEIGHT DITHERED DOWN IN AMPLITUDE=-2.24830000000000E+0004
POWER WITH KTH WEIGHT DITHERED UP IN PHASE=-2.12430000000000E+0004
POWER WITH KTH WEIGHT DITHERED DOWN IN PHASE=-2.24830000000000E+0004
reset kth phase weight
KTH PHASE WEIGHT IS NOW=        1
compute power differences
DFANJ[K]= 0.00000000000000E+0000    DFPNJ[K]= 1.24000000000000E+0003
MDELAMP=        0    MDELPHA=        20
```

```
SUMDF= 5.180399999999E+0004
N= 1  RANJ[N]= 0.00000000000000E+0000  RPNJ[N]=-8.78715623737828E-0002
N= 1  NAMPINC=  0   NPHAINC=  -2
N= 2  RANJ[N]= 0.00000000000000E+0000  RPNJ[N]= 7.82056905127707E-0001
N= 2  NAMPINC=  0   NPHAINC=  16
N= 3  RANJ[N]= 0.00000000000000E+0000  RPNJ[N]= 5.53590842955118E-0001
N= 3  NAMPINC=  0   NPHAINC=  11
N= 4  RANJ[N]= 0.00000000000000E+0000  RPNJ[N]= 2.72401843358877E-0001
N= 4  NAMPINC=  0   NPHAINC=  5
ITERATION no.= 1   POWER=-1.77010000000000E+0004
CH. no.  1  AMP=  125  PHASE=  1
CH. no.  2  AMP=  125  PHASE=  17
CH. no.  3  AMP=  125  PHASE=  12
CH. no.  4  AMP=  125  PHASE=  6
ITERATION NUMBER= 2
IAMPP8=  125
IAMPM8=  125
IPHAP8=   21
IPHAM8=    1
POWER WITH KTH WEIGHT DITHERED UP IN AMPLITUDE=-1.77010000000000E+0004
POWER WITH KTH WEIGHT DITHERED DOWN IN AMPLITUDE=-1.77010000000000E+0004
POWER WITH KTH WEIGHT DITHERED UP IN PHASE=-1.81010000000000E+0004
POWER WITH KTH WEIGHT DITHERED DOWN IN PHASE=-1.77010000000000E+0004
reset kth phase weight
KTH PHASE WEIGHT IS NOW=          1
compute power differences
DFANJ[K]= 0.00000000000000E+0000  DFPNJ[K]=-4.0000000000000E+0002
MDELAMP=      0   MDELPHA=       20
SUMDF= 4.00000000000000E+0002
IAMPP8=  125
IAMPM8=  125
IPHAP8=   37
IPHAM8=    1
POWER WITH KTH WEIGHT DITHERED UP IN AMPLITUDE=-1.77010000000000E+0004
POWER WITH KTH WEIGHT DITHERED DOWN IN AMPLITUDE=-1.77010000000000E+0004
```

-182-

```
POWER WITH KTH WEIGHT DITHERED UP IN PHASE=-1.47810000000000E+0004
POWER WITH KTH WEIGHT DITHERED DOWN IN PHASE=-2.06130000000000E+0004
reset kth phase weight
KTH PHASE WEIGHT IS NOW=          17
compute power differences
DFANJ[K]= 0.00000000000000E+0000   DFPNJ[K]= 5.83200000000000E+0003
MDELAMP=          0    MDELPHA=          20
SUMDF= 8.54305999999999E+0004
IAMPP8=       125
IAMPM8=       125
IPHAP8=        32
IPHAM8=         1
POWER WITH KTH WEIGHT DITHERED UP IN AMPLITUDE=-1.77010000000000E+0004
POWER WITH KTH WEIGHT DITHERED DOWN IN AMPLITUDE=-1.77010000000000E+0004
POWER WITH KTH WEIGHT DITHERED UP IN PHASE=-1.56210000000000E+0004
POWER WITH KTH WEIGHT DITHERED DOWN IN PHASE=-1.91860000000000E+0004
reset kth phase weight
KTH PHASE WEIGHT IS NOW=          12
compute power differences
DFANJ[K]= 0.00000000000000E+0000   DFPNJ[K]= 3.56500000000000E+0003
MDELAMP=          0    MDELPHA=          20
SUMDF= 1.17203622500000E+0005
IAMPP8=       125
IAMPM8=       125
IPHAP8=        26
IPHAM8=         1
POWER WITH KTH WEIGHT DITHERED UP IN AMPLITUDE=-1.77010000000000E+0004
POWER WITH KTH WEIGHT DITHERED DOWN IN AMPLITUDE=-1.77010000000000E+0004
POWER WITH KTH WEIGHT DITHERED UP IN PHASE=-1.66610000000000E+0004
POWER WITH KTH WEIGHT DITHERED DOWN IN PHASE=-1.80860000000000E+0004
reset kth phase weight
KTH PHASE WEIGHT IS NOW=           6
compute power differences
DFANJ[K]= 0.00000000000000E+0000   DFPNJ[K]= 1.42500000000000E+0003
MDELAMP=          0    MDELPHA=          20
```

SUBSTITUTE SHEET

```
SUMDF= 1.22280185000000E+0005
N=  1  RANJ[N]= 0.00000000000000E+0000  RPNJ[N]=-5.71941950487310E-0002
N=  1  NAMPINC=  0  NPHAINC=  -1
N=  2  RANJ[N]= 0.00000000000000E+0000  RPNJ[N]= 8.33891363810500E-0001
N=  2  NAMPINC=  0  NPHAINC=  17
N=  3  RANJ[N]= 0.00000000000000E+0000  RPNJ[N]= 5.09743263371820E-0001
N=  3  NAMPINC=  0  NPHAINC=  10
N=  4  RANJ[N]= 0.00000000000000E+0000  RPNJ[N]= 2.03754319861100E-0001
N=  4  NAMPINC=  0  NPHAINC=  4
ITERATION no.=   2   POWER=-1.37560000000000E+0004
CH. no.=  1   AMP= 125   PHASE=  1
CH. no.=  2   AMP= 125   PHASE=  34
CH. no.=  3   AMP= 125   PHASE=  22
CH. no.=  4   AMP= 125   PHASE=  10
ITERATION NUMBER=   3
IAMPP8= 125
IAMPM8= 125
IPHAP8=  21
IPHAM8=   1
POWER WITH KTH WEIGHT DITHERED UP IN AMPLITUDE=-1.37560000000000E+0004
POWER WITH KTH WEIGHT DITHERED DOWN IN AMPLITUDE=-1.37560000000000E+0004
POWER WITH KTH WEIGHT DITHERED UP IN PHASE=-1.41560000000000E+0004
POWER WITH KTH WEIGHT DITHERED DOWN IN PHASE=-1.37560000000000E+0004
reset kth phase weight
KTH PHASE WEIGHT IS NOW=                        1
compute power differences
DFANJ[K]= 0.00000000000000E+0000   DFPNJ[K]=-4.00000000000000E+0002
MDELAMP=       0  MDELPHA=          20
SUMDF= 4.00000000000000E+0002
IAMPP8= 125
IAMPM8= 125
IPHAP8=  54
IPHAM8=  14
POWER WITH KTH WEIGHT DITHERED UP IN AMPLITUDE=-1.37560000000000E+0004
POWER WITH KTH WEIGHT DITHERED DOWN IN AMPLITUDE=-1.37560000000000E+0004
```

```
POWER WITH KTH WEIGHT DITHERED UP IN PHASE=-1.15160000000000E+0004
POWER WITH KTH WEIGHT DITHERED DOWN IN PHASE=-1.67960000000000E+0004
reset kth phase weight
KTH PHASE WEIGHT IS NOW=          34
compute power differences
DFANJ[K]= 0.00000000000000E+0000   DFPNJ[K]= 5.28000000000000E+0003
MDELAMP=          0   MDELPHA=          20
SUMDF= 7.00959999999999E+0004
IAMPP8=     125
IAMPM8=     125
IPHAP8=      42
IPHAM8=       2
POWER WITH KTH WEIGHT DITHERED UP IN AMPLITUDE=-1.37560000000000E+0004
POWER WITH KTH WEIGHT DITHERED DOWN IN AMPLITUDE=-1.37560000000000E+0004
POWER WITH KTH WEIGHT DITHERED UP IN PHASE=-1.20760000000000E+0004
POWER WITH KTH WEIGHT DITHERED DOWN IN PHASE=-1.62360000000000E+0004
reset kth phase weight
KTH PHASE WEIGHT IS NOW=          22
compute power differences
DFANJ[K]= 0.00000000000000E+0000   DFPNJ[K]= 4.16000000000000E+0003
MDELAMP=          0   MDELPHA=          20
SUMDF= 1.13360000000000E+0005
IAMPP8=     125
IAMPM8=     125
IPHAP8=      30
IPHAM8=       1
POWER WITH KTH WEIGHT DITHERED UP IN AMPLITUDE=-1.37560000000000E+0004
POWER WITH KTH WEIGHT DITHERED DOWN IN AMPLITUDE=-1.37560000000000E+0004
POWER WITH KTH WEIGHT DITHERED UP IN PHASE=-1.28760000000000E+0004
POWER WITH KTH WEIGHT DITHERED DOWN IN PHASE=-1.44130000000000E+0004
reset kth phase weight
KTH PHASE WEIGHT IS NOW=          10
compute power differences
DFANJ[K]= 0.00000000000000E+0000   DFPNJ[K]= 1.53700000000000E+0003
MDELAMP=          0   MDELPHA=          20
```

SUBSTITUTE SHEET

```
SUMDF= 1.1926592250000E+0005
N=  1  RANJ[N]= 0.0000000000000E+0000  RPNJ[N]=-5.7912432871831E-0002
N=  1  NAMPINC=           0  NPHAINC=          -1
N=  2  RANJ[N]= 0.0000000000000E+0000  RPNJ[N]= 7.6444411390817E-0001
N=  2  NAMPINC=           0  NPHAINC=          15
N=  3  RANJ[N]= 0.0000000000000E+0000  RPNJ[N]= 6.0228930186705E-0001
N=  3  NAMPINC=           0  NPHAINC=          12
N=  4  RANJ[N]= 0.0000000000000E+0000  RPNJ[N]= 2.2252852331001E-0001
N=  4  NAMPINC=           0  NPHAINC=           4
ITERATION no.=    3  POWER=-1.0657000000000E+0004
CH. no.=  1  AMP=  125  PHASE=   1
CH. no.=  2  AMP=  125  PHASE=  49
CH. no.=  3  AMP=  125  PHASE=  34
CH. no.=  4  AMP=  125  PHASE=  14
ITERATION NUMBER=    4
IAMPP8=  125
IAMPM8=  125
IPHAP8=   21
IPHAM8=    1
POWER WITH KTH WEIGHT DITHERED UP IN AMPLITUDE=-1.0657000000000E+0004
POWER WITH KTH WEIGHT DITHERED DOWN IN AMPLITUDE=-1.0657000000000E+0004
POWER WITH KTH WEIGHT DITHERED UP IN PHASE=-1.1057000000000E+0004
POWER WITH KTH WEIGHT DITHERED DOWN IN PHASE=-1.0657000000000E+0004
reset kth phase weight
KTH PHASE WEIGHT IS NOW=           1
compute power differences
DFANJ[K]= 0.0000000000000E+0000  DFPNJ[K]=-4.0000000000000E+0002
MDELAMP=           0  MDELPHA=          20
SUMDF= 4.0000000000000E+0002
IAMPP8=  125
IAMPM8=  125
IPHAP8=   69
IPHAM8=   29
POWER WITH KTH WEIGHT DITHERED UP IN AMPLITUDE=-1.0657000000000E+0004
POWER WITH KTH WEIGHT DITHERED DOWN IN AMPLITUDE=-1.0657000000000E+0004
```

SUBSTITUTE SHEET

```
POWER WITH KTH WEIGHT DITHERED UP IN PHASE=-9.0170000000000E+0003
POWER WITH KTH WEIGHT DITHERED DOWN IN PHASE=-1.3097000000000E+0004
reset kth phase weight
KTH PHASE WEIGHT IS NOW=            49
compute power differences
DFANJ[K]= 0.0000000000000E+0000    DFPNJ[K]= 4.0800000000000E+0003
MDELAMP=          0   MDELPHA=          20
SUMDF= 4.2015999999999E+0004
IAMPP8=     125
IAMPM8=     125
IPHAP8=      54
IPHAM8=      14
POWER WITH KTH WEIGHT DITHERED UP IN AMPLITUDE=-1.0657000000000E+0004
POWER WITH KTH WEIGHT DITHERED DOWN IN AMPLITUDE=-1.0657000000000E+0004
POWER WITH KTH WEIGHT DITHERED UP IN PHASE=-9.4570000000000E+0003
POWER WITH KTH WEIGHT DITHERED DOWN IN PHASE=-1.2657000000000E+0004
reset kth phase weight
KTH PHASE WEIGHT IS NOW=            34
compute power differences
DFANJ[K]= 0.0000000000000E+0000    DFPNJ[K]= 3.2000000000000E+0003
MDELAMP=          0   MDELPHA=          20
SUMDF= 6.7615999999999E+0004
IAMPP8=     125
IAMPM8=     125
IPHAP8=      34
IPHAM8=       1
POWER WITH KTH WEIGHT DITHERED UP IN AMPLITUDE=-1.0657000000000E+0004
POWER WITH KTH WEIGHT DITHERED DOWN IN AMPLITUDE=-1.0657000000000E+0004
POWER WITH KTH WEIGHT DITHERED UP IN PHASE=-9.9370000000000E+0003
POWER WITH KTH WEIGHT DITHERED DOWN IN PHASE=-1.1554000000000E+0004
reset kth phase weight
KTH PHASE WEIGHT IS NOW=            14
compute power differences
DFANJ[K]= 0.0000000000000E+0000    DFPNJ[K]= 1.6170000000000E+0003
MDELAMP=          0   MDELPHA=          20
```

SUBSTITUTE SHEET

```
SUMDF= 7.4152722499999E+0004
N=     1  RANJ[N]= 0.00000000000000E+0000  RPNJ[N]=-7.34457119975A9E-0002
N=     1  NAMPINC=               0  NPHAINC=      -1
N=     2  RANJ[N]= 0.00000000000000E+0000  RPNJ[N]= 7.49146262375000E-0001
N=     2  NAMPINC=               0  NPHAINC=      15
N=     3  RANJ[N]= 0.00000000000000E+0000  RPNJ[N]= 5.87565698039E-0001
N=     3  NAMPINC=               0  NPHAINC=      12
N=     4  RANJ[N]= 0.00000000000000E+0000  RPNJ[N]= 2.96904290750009E-0001
N=     4  NAMPINC=               0  NPHAINC=       6
ITERATION no.  =       4  POWER=-8.23600000000000E+0003
CH. no.       1   AMP=     125  PHASE=       1
CH. no.       2   AMP=     125  PHASE=      64
CH. no.       3   AMP=     125  PHASE=      46
CH. no.       4   AMP=     125  PHASE=      20
ITERATION NUMBER=       5
IAMPP8=     125
IAMPM8=     125
IPHAP8=      21
IPHAM8=       1
POWER WITH KTH WEIGHT DITHERED UP IN AMPLITUDE=-8.23600000000000E+0003
POWER WITH KTH WEIGHT DITHERED DOWN IN AMPLITUDE=-8.23600000000000E+0003
POWER WITH KTH WEIGHT DITHERED UP IN PHASE=-8.63600000000000E+0003
POWER WITH KTH WEIGHT DITHERED DOWN IN PHASE=-8.23600000000000E+0003
reset kth phase weight
KTH PHASE WEIGHT IS NOW=                 1
compute power differences
DFANJ[K]= 0.00000000000000E+0000  DFPNJ[K]=-4.00000000000000E+0002
MDELAMP=               0  MDELPHA=               20
SUMDF= 4.00000000000000E+0002
IAMPP8=     125
IAMPM8=     125
IPHAP8=      84
IPHAM8=      44
POWER WITH KTH WEIGHT DITHERED UP IN AMPLITUDE=-8.23600000000000E+0003
POWER WITH KTH WEIGHT DITHERED DOWN IN AMPLITUDE=-8.23600000000000E+0003
```

```
POWER WITH KTH WEIGHT DITHERED UP IN PHASE=-7.1960000000000E+0003
POWER WITH KTH WEIGHT DITHERED DOWN IN PHASE=-1.0076000000000E+0004
reset kth phase weight
KTH PHASE WEIGHT IS NOW=            64
compute power differences
DFANJ[K]= 0.0000000000000E+0000   DFPNJ[K]= 2.8800000000000E+0003
MDELAMP=           0   MDELPHA=          20
SUMDF= 2.1136000000000E+0004
IAMPP8=       125
IAMPM8=       125
IPHAP8=        66
IPHAM8=        26
POWER WITH KTH WEIGHT DITHERED UP IN AMPLITUDE=-8.2360000000000E+0003
POWER WITH KTH WEIGHT DITHERED DOWN IN AMPLITUDE=-8.2360000000000E+0003
POWER WITH KTH WEIGHT DITHERED UP IN PHASE=-7.5160000000000E+0003
POWER WITH KTH WEIGHT DITHERED DOWN IN PHASE=-9.7560000000000E+0003
reset kth phase weight
KTH PHASE WEIGHT IS NOW=            46
compute power differences
DFANJ[K]= 0.0000000000000E+0000   DFPNJ[K]= 2.2400000000000E+0003
MDELAMP=           0   MDELPHA=          20
SUMDF= 3.3680000000000E+0004
IAMPP8=       125
IAMPM8=       125
IPHAP8=        40
IPHAM8=         1
POWER WITH KTH WEIGHT DITHERED UP IN AMPLITUDE=-8.2360000000000E+0003
POWER WITH KTH WEIGHT DITHERED DOWN IN AMPLITUDE=-8.2360000000000E+0003
POWER WITH KTH WEIGHT DITHERED UP IN PHASE=-7.7560000000000E+0003
POWER WITH KTH WEIGHT DITHERED DOWN IN PHASE=-9.4330000000000E+0003
reset kth phase weight
KTH PHASE WEIGHT IS NOW=            20
compute power differences
DFANJ[K]= 0.0000000000000E+0000   DFPNJ[K]= 1.6770000000000E+0003
MDELAMP=           0   MDELPHA=          20
```

```
SUMDF= 4.0710822499999E+0004
N= 1  RANJ[N]= 0.0000000000000E+0000   RPNJ[N]=-9.9123141423090E-0002
N= 1  NAMPINC=        0  NPHAINC=       -2
N= 2  RANJ[N]= 0.0000000000000E+0000   RPNJ[N]= 7.1368661824625E-0001
N= 2  NAMPINC=        0  NPHAINC=       14
N= 3  RANJ[N]= 0.0000000000000E+0000   RPNJ[N]= 5.5508959196930E-0001
N= 3  NAMPINC=        0  NPHAINC=       11
N= 4  RANJ[N]= 0.0000000000000E+0000   RPNJ[N]= 4.1557377041630E-0001
N= 4  NAMPINC=        0  NPHAINC=        8
ITERATION no.=     5  POWER=-6.6410000000000E+0003
CH. no.   1  AMP=  125  PHASE=   1
CH. no.   2  AMP=  125  PHASE=  78
CH. no.   3  AMP=  125  PHASE=  57
CH. no.   4  AMP=  125  PHASE=  28
final adaptive weights
CH. no.   1  AMP=  125  PHASE=   1
CH. no.   2  AMP=  125  PHASE=  78
CH. no.   3  AMP=  125  PHASE=  57
CH. no.   4  AMP=  125  PHASE=  28
```

−190−

CLAIMS

1.   A hyperthermia applicator for inducing a temperature rise in a
target, comprising

         a plurality of electric field radiators;

         a source of electric field radiation coupled to each
electric field radiator through a controllable transmit weighting
network coupled to a respective electric field radiator, each
weighting network controlling the phase and amplitude of the
electric field radiation transmitted by the respective electric
field radiator in response to a respective feedback signal;

         at least one electric field probe for detecting electric
field radiation from the plurality of radiators; and

         a controller coupled to the electric field probes for
receiving the detected electric field radiation and generating
the respective feedback signals, and for adjusting the
feedback signal in response to the detected electric field
radiation so that the detected electric field radiation is
minimized at the electric field probe.

2.   The apparatus of Claim 1, wherein the plurality of electric
field radiators comprises a phased-array of electric field
transmit elements.

3.   The apparatus of Claim 2, wherein the phased-array of
electric field transmit elements comprises an annular array for
surrounding the target.

4.   The apparatus of Claims 1, 2, or 3 wherein the electric field
probes comprise a plurality of probe elements disposed non-
invasively along the perimeter of the target.

SUBSTITUTE SHEET

5. The apparatus of Claims 1, 2, 3, or 4 further comprising

at least one secondary electric field probe for detecting electric field radiation;

wherein the controller adjusts the feedback signals in response to the electric field radiation detected by the secondary electric field probe so that the electric field radiation is maximized at the secondary electric field probe.

6. The apparatus of Claim 5, wherein the plurality of electric field radiators comprises a phased-array of electric field transmit elements, and the secondary electric field probe is disposed at the desired focus of the phased-array.

7. The apparatus of Claim 6, wherein

the secondary electric field probe comprises at least one probe element disposed invasively within the target at the desired focus of the electric field energy.

8. The apparatus of Claims 1, 2, 3, 4, 5, 6 or 7 wherein the controller performs a matrix inversion to generate the feedback signal.

9. The apparatus of Claim 8, wherein the controller comprises

a receiver coupled to the electric field probes for receiving voltages $v_1^i, v_2^i, \cdots, v_N^i$ due to the mth and nth electric field radiator at the ith electric field probe;

means for forming a cross correlation R_{mn}^i of the received voltages, the cross correlation being given by

$$R_{mn}^i = E(v_m^i v_n^{i*}) \qquad ,$$

SUBSTITUTE SHEET

-192-

where • means complex conjugate and $E(\cdot)$ means mathematical expectation;

means for forming a channel correlation matrix R given by

$$R=\sum_{i=1}^{N_{aux}} R_i \quad ,$$

5   where N_{aux} is the number of electric field probes, R_i is the sample correlation matrix observed at the ith electric field probe; and

means for generating an adapted transmit weight vector w_a given by

$$w_a = R^{-1} w_q \quad ,$$

10   where generally the transmit weight vector $w = (w_1, w_2, ..., w_N)^T$ represents the transmit weights of each of N controllable weighting networks, and w_q represents the quiescent transmit weight vector;

wherein the controller adjusts the feedback signal in 15   response to the adapted transmit weight vector w_a.

10.   The apparatus of Claim 1, 2, 3, 4, 5, 6 or 7 wherein the controller performs a gradient search algorithm to generate the feedback signal.

11.   The apparatus of Claim 10, wherein the controller comprises

SUBSTITUTE SHEET

-193-

a receiver coupled to the electric field probes for receiving voltage amplitudes $|v_{1j}^i|, |v_{2j}^i|, \cdots, |v_{Nj}^i|$ due to the mth and nth electric field radiator at the ith electric field probe for the jth configuration of the transmit weights w_{nj};

means for calculating a figure of merit F_{nj} from the received voltage amplitudes given by

$$F_{nj} = \sum_{i=1}^{N_{aux}} |v_{nj}^i|^2$$

where N_{aux} is the number of electric field probes,

means for dithering the transmit weights w_{nj} by a small amount in amplitude, ΔA_{nj}, and phase, $\Delta \Phi_{nj}$;

means for determining the figure of merit differences ΔF_{Anj} and $\Delta F_{\Phi nj}$ caused by dithering the amplitude and phase, respectively,

means for determining gradient search directions search directions r_{Anj} and $r_{\Phi nj}$ given by

$$r_{Anj} = -\frac{\dfrac{\Delta F_{Anj}}{\Delta A}}{\sqrt{\sum_{n=1}^{N} [(\dfrac{\Delta F_{Anj}}{\Delta A})^2 + (\dfrac{\Delta F_{\Phi nj}}{\Delta \Phi})^2]}}$$

and

$$r_{\Phi nj} = -\frac{\dfrac{\Delta F_{\Phi nj}}{\Delta \Phi}}{\sqrt{\sum_{n=1}^{N} [(\dfrac{\Delta F_{Anj}}{\Delta A})^2 + (\dfrac{\Delta F_{\Phi nj}}{\Delta \Phi})^2]}}$$

SUBSTITUTE SHEET

respectively, and

means for generating the new transmit weight $w_{n,(j+1)}$ for the $(j+1)$th configuration where the amplitude component of the new weight is given by

$$A_{n,j+1} = A_{n,j} + \Delta A r_{A,n,j}$$

5   and the phase component of the new weight is given by

$$\Phi_{n,j+1} = \Phi_{n,j} + \Delta \Phi r_{\Phi,n,j} \ .$$

12.   A method for inducing a temperature rise in a target, comprising the steps of:

surrounding a target with an annular phased array of electric field radiators;

10   coupling a source of electric field radiation to each electric field radiator through a controllable transmit weighting network coupled to a respective electric field radiator;

controlling the phase and amplitude of the electric field radiation transmitted by the respective electric field radiator

15   with each weighting network in response to a respective feedback signal;

detecting electric field radiation from the annular phased array of radiators with a plurality of electric field probe elements disposed non-invasively along the perimeter

20   of the target; and

receiving the detected electric field radiation and generating the respective feedback signals for adjusting the controllable transmit weighting network in response to the

detected electric field radiation so that the detected electric field radiation is minimized at the electric field probe elements.

13.   A hyperthermia applicator for inducing a temperature rise in a target within a body, comprising

a plurality of electric field radiators;

a plurality of controllable transmit weighting networks, each such network coupled to a respective electric field radiator, each weighting network controlling the phase and amplitude of the electric field radiation transmitted by the respective electric field radiator in response to a respective feedback signal;

a source of electric field radiation coupled to each electric field radiator through a respective weighting network;

at least one electric field probe disposed outside the body for detecting electric field radiation from the plurality of radiators; and

a controller coupled to the electric field probes for receiving the detected electric field radiation outside the body and generating the respective feedback signals, and for adjusting the feedback signals in response to the detected electric field radiation outside the body so that the electric field radiation is controlled at the target inside the body.

14.   The apparatus of Claim 13, wherein the plurality of electric field radiators comprises a phased-array of electric field transmit elements.

15.   The apparatus of Claim 13 or 14, wherein the electric field transmit elements comprises an array of monopole antenna elements.

SUBSTITUTE SHEET

-196-

16.· The apparatus of Claim 15, further comprising an RF reflecting
groundplane surface for mounting the monopole antenna
elements, wherein the monopole antenna elements are
perpendicularly mounted to the same side of the RF reflecting
ground plane, wherein the body containing the target is
disposed on the same side of the ground plane as the monopole
antenna elements.

17. The apparatus of Claim 16 wherein the ground plane comprises
an aperture through which the body containing the target is
disposed to allow positioning the target on the same side of the
ground plane as the monopole antenna elements.

18. The apparatus of Claim 16 or 17 further comprising an RF
reflecting screen mounted perpendicular to the groundplane
surface behind the monopole antenna elements to reflect RF
energy from the monopole antenna elements toward the target.

19. The apparatus of Claim 18 wherein the RF reflecting screen is
positioned between 1/8 to 1/2 wavelength from the monopole
antenna elements.

20. The apparatus of Claim 15, 16, 17, 18 or 19 further comprising
an enclosure surrounding the monopole antenna elements and

SUBSTITUTE SHEET

providing a vessel for enclosing a bolus of fluid between the monopole antenna elements and the body.

21. The apparatus of Claim 20 wherein the vessel comprises a bolus of deionized water.

22. The apparatus of Claim 15, 16, 17, 18, 19, 20, or 21 wherein the monopole antenna elements are arranged in a circular arc of substantially constant radius.

23. The apparatus of Claim 22 wherein the body containing the target is a cranium and the radius is substantially the distance from the monopole antenna array to the center of the cranium.

24. The apparatus of Claim 22 wherein the body containing the target is a cranium and the radius is substantially the distance from the monopole antenna array to the target within the cranium.

25. The apparatus of Claim 22, 23, or 24 wherein the monopole antenna elements resonate at between 800 and 1000 MHz.

26. The apparatus of Claim 13, 14, 15, 16, 17, 18, 19, 20, 21, 22, 23, 24, or 25 wherein the electric field probes comprise a plurality of probe elements disposed non-invasively along the

SUBSTITUTE SHEET

-198-

perimeter of the body between the elements of the phased-array and the target.

27.   The apparatus of Claim 26 wherein the controller comprises means for adjusting the feedback signals to minimize the difference in the electric field detected by adjacent electric field probes and thereby provide uniform electric field radiation into the body.

28.   The apparatus of Claim 27, wherein the adjusting means performs a gradient search algorithm to adjust the feedback signals.

29.   The apparatus of Claim 27, wherein the adjusting means performs a matrix inversion algorithm to adjust the feedback signals.

30.   The apparatus of Claim 26, wherein the controller comprises means for adjusting the feedback signals to provide a particular electric field pattern across the electric field probe array and thereby focus radiation into the target.

SUBSTITUTE SHEET
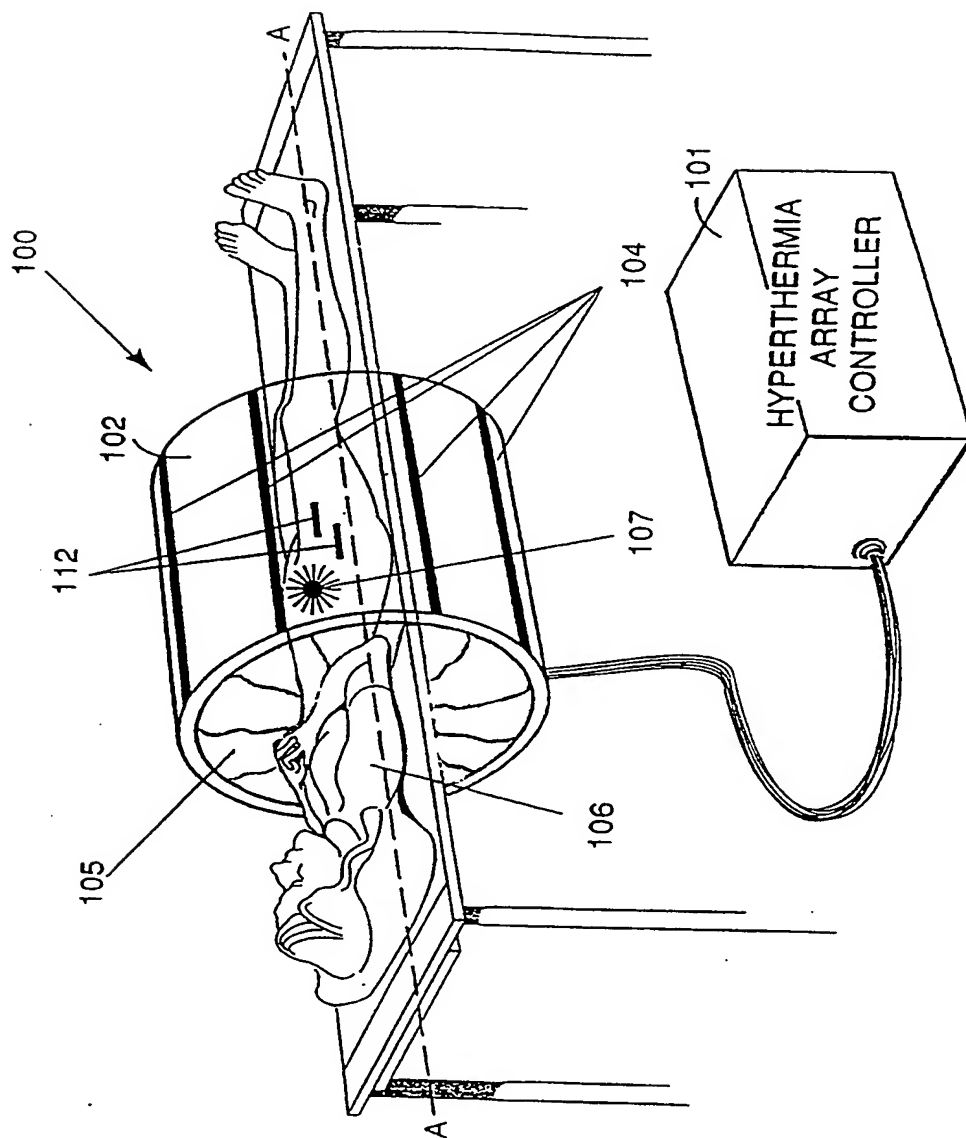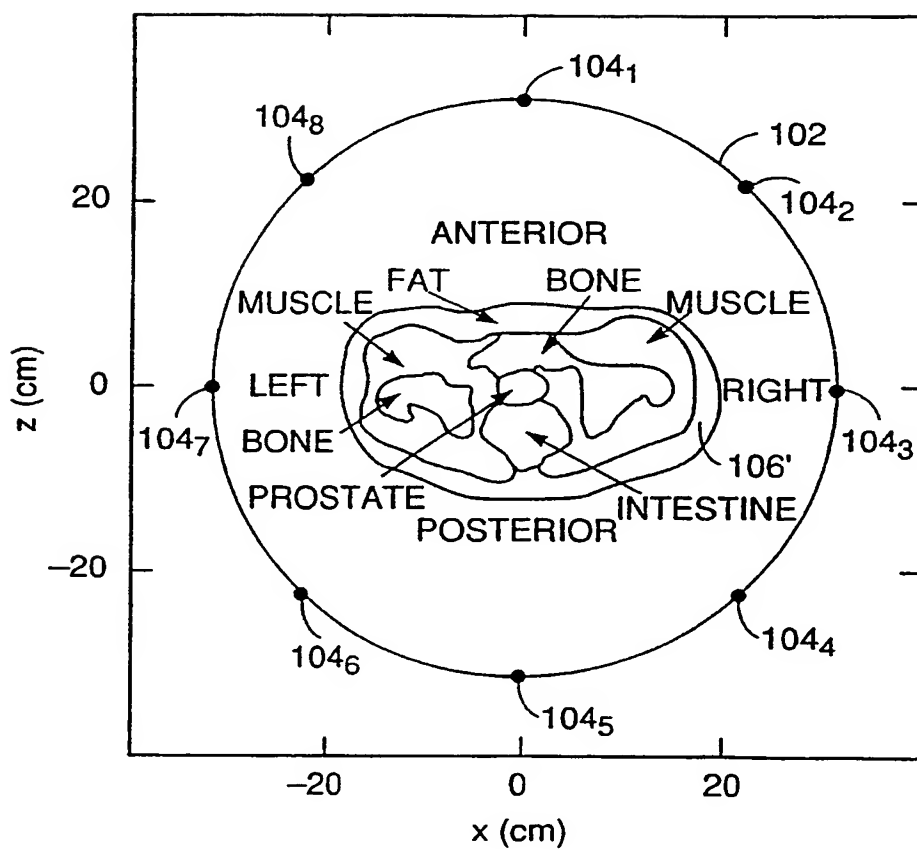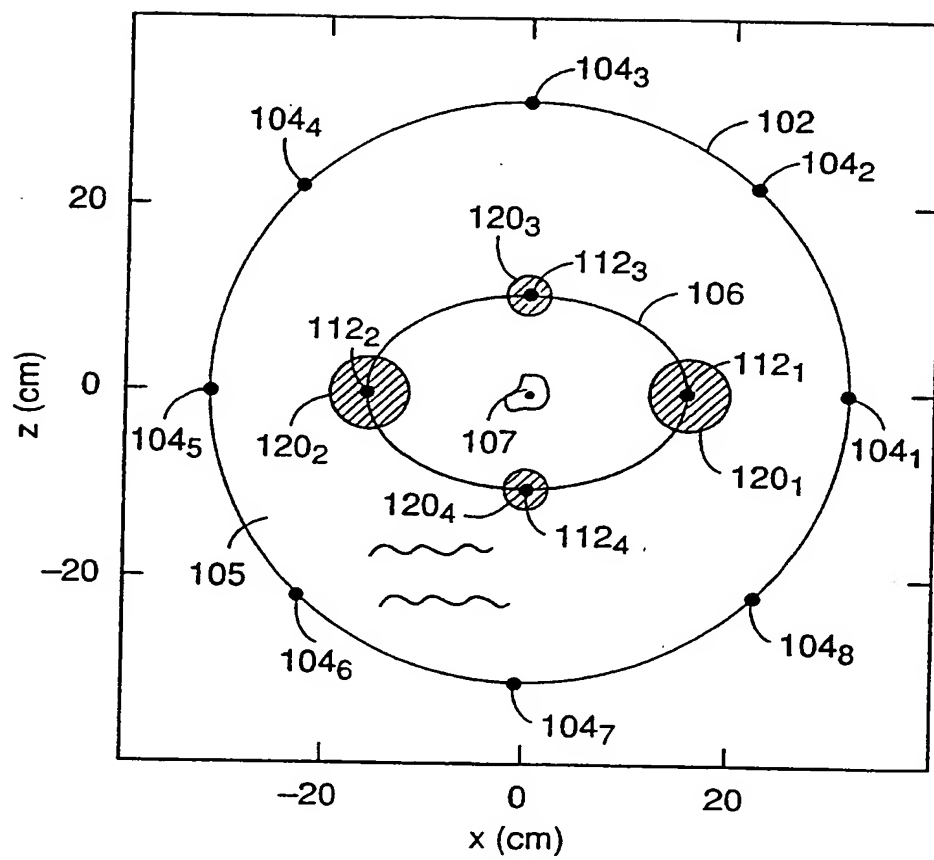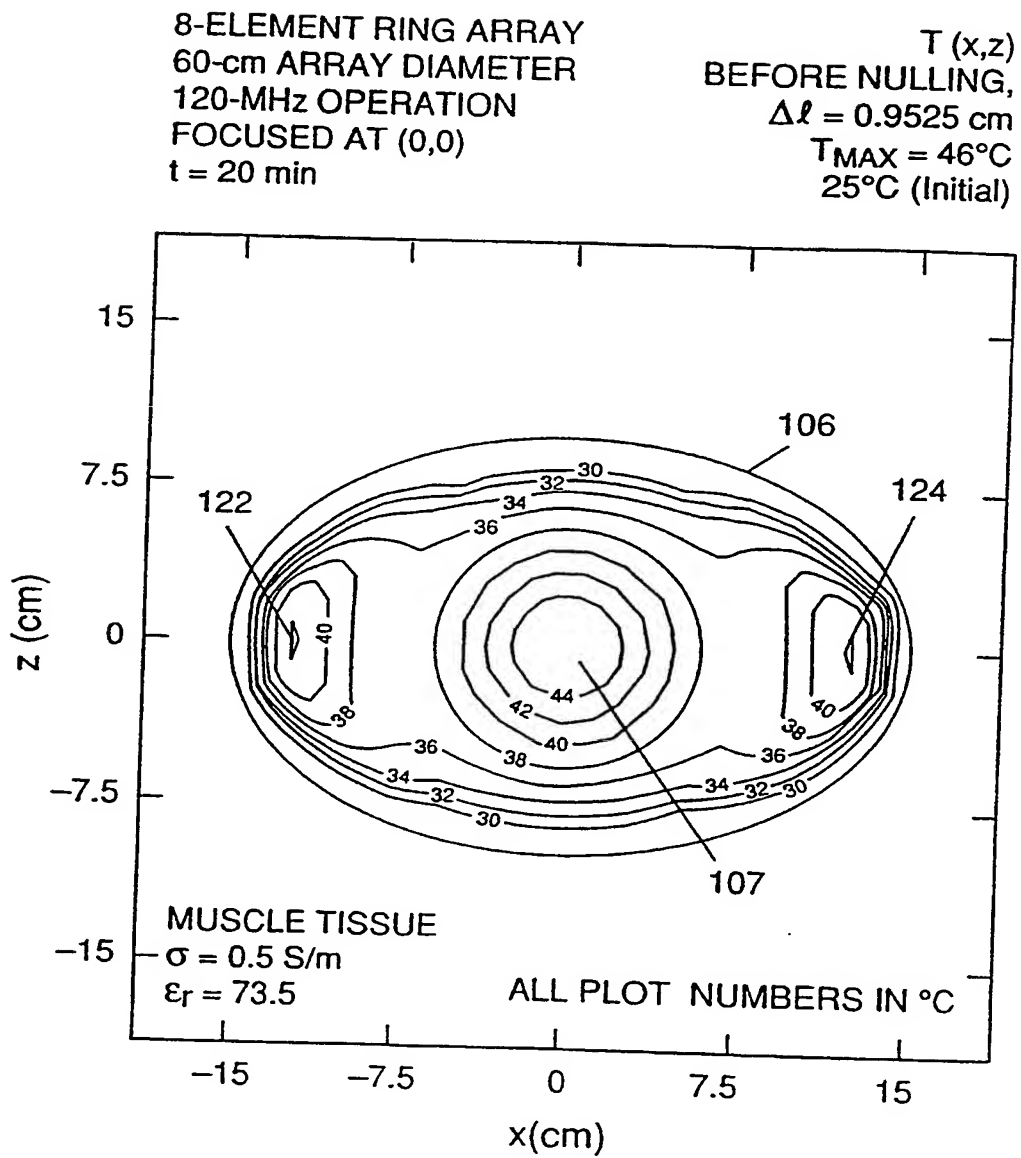
Fig. 1

Fig. 2

Fig. 3

8-ELEMENT RING ARRAY
60-cm ARRAY DIAMETER
120-MHz OPERATION
FOCUSED AT (0,0)
t = 20 min

$T (x,z)$
BEFORE NULLING,
$\Delta \ell = 0.9525$ cm
$T_{MAX} = 46°C$
25°C (Initial)

MUSCLE TISSUE
$\sigma = 0.5$ S/m
$\varepsilon_r = 73.5$

ALL PLOT NUMBERS IN °C

Fig. 4

Fig. 5

Fig. 6

Fig. 7

Fig. 8

FROM
RECEIVER
114

INPUT VOLTAGE VECTOR
$(v_1^i, v_2^i, \ldots v_N^i)$

$v_m^i v_n^{i*}$ 280

CHANNEL
CORRELATION

R_{mn}

$$R = \sum_{i=1}^{J_{aux}} R_i$$ 282

CORRELATION
MATRIX

TRANSMIT
QUIESCENT
WEIGHT VECTOR

R

w_q

$R^{-1}w_q$ 284

ADAPTED TRANSMIT
WEIGHT VECTOR

w_a
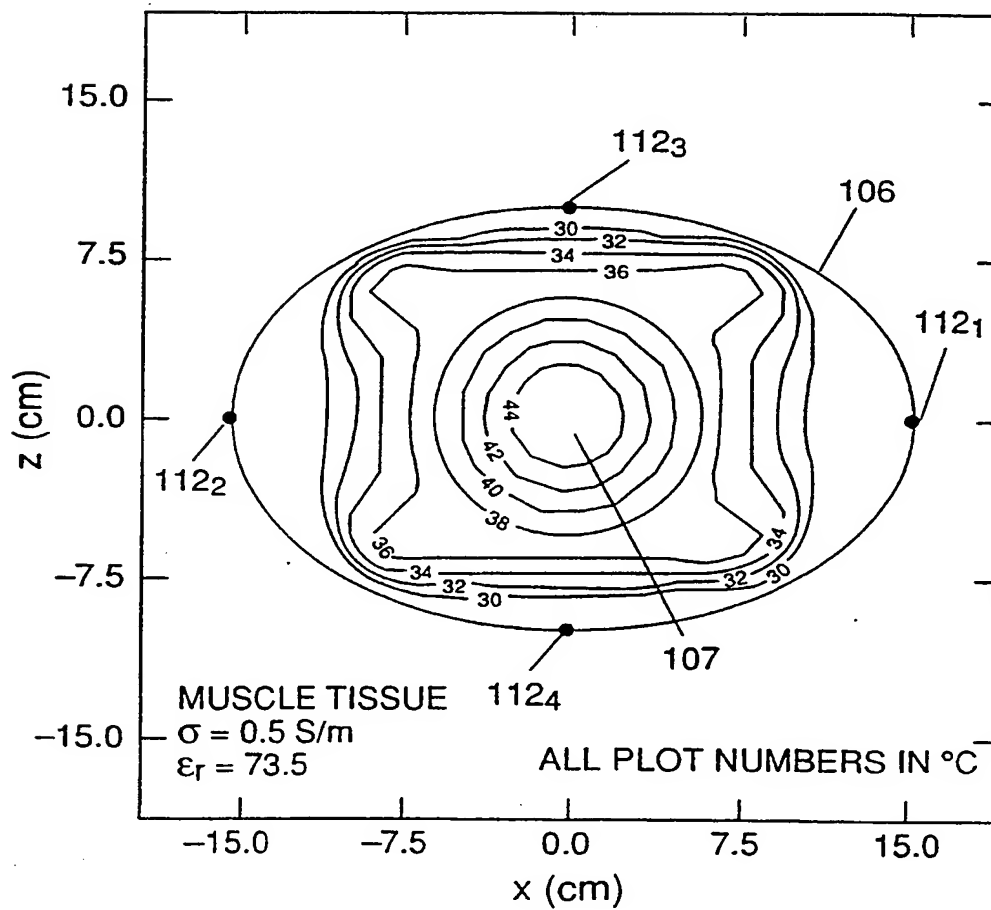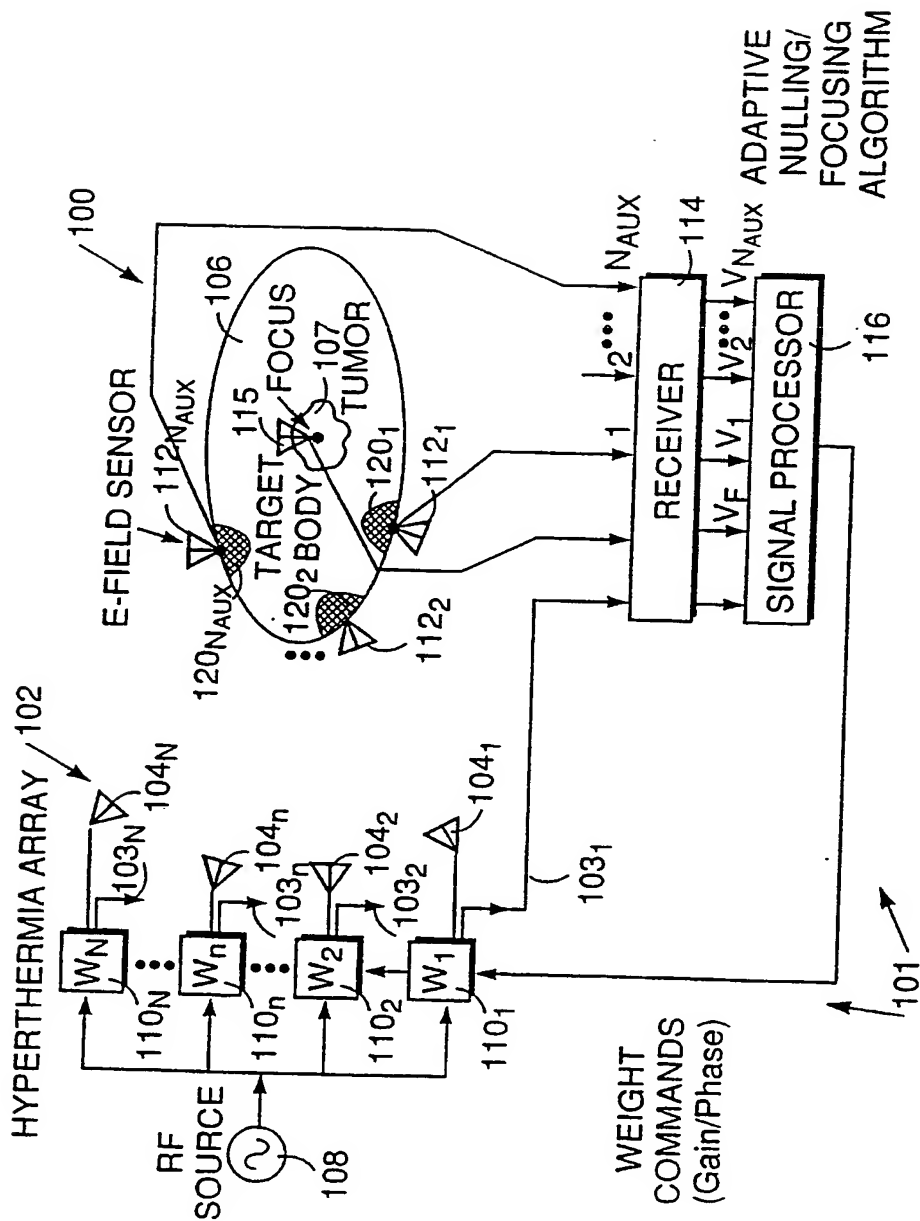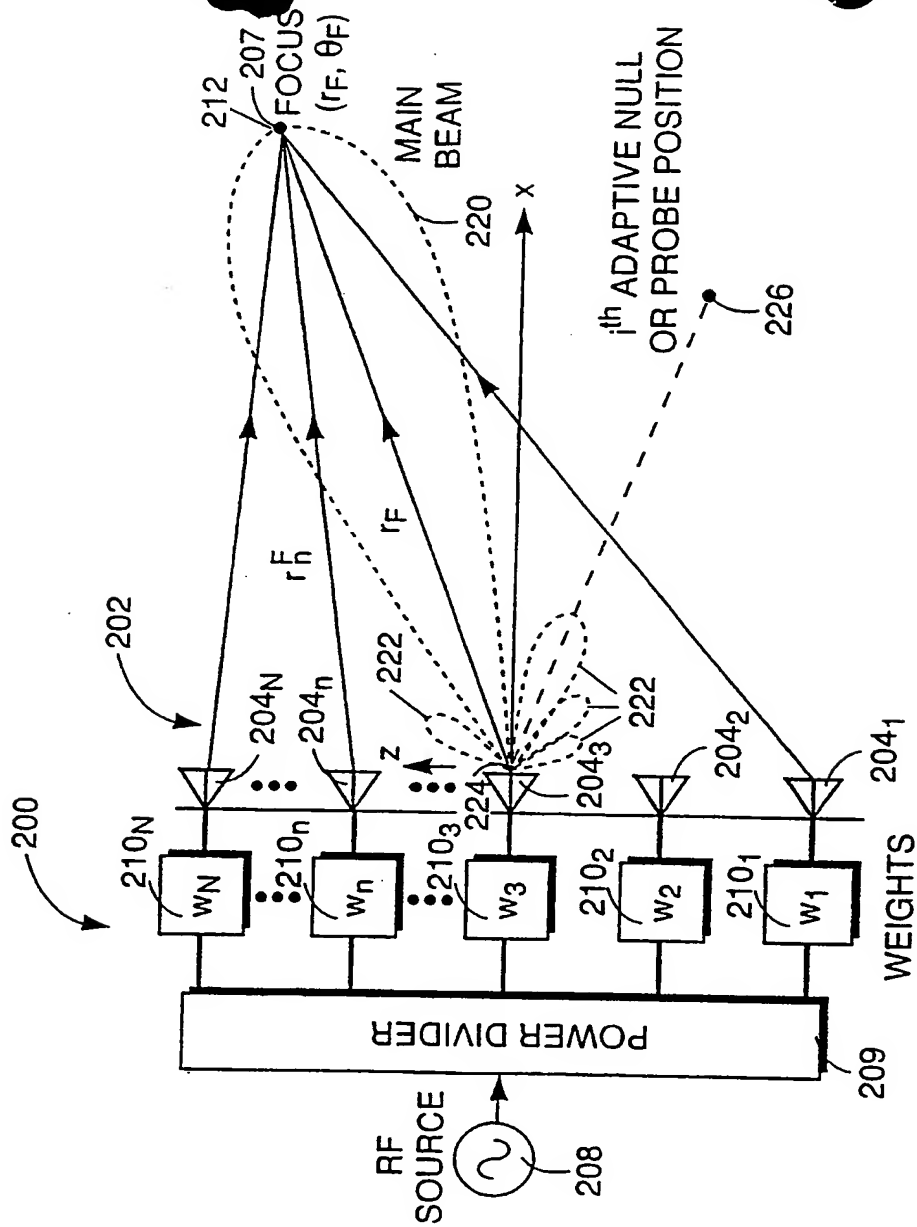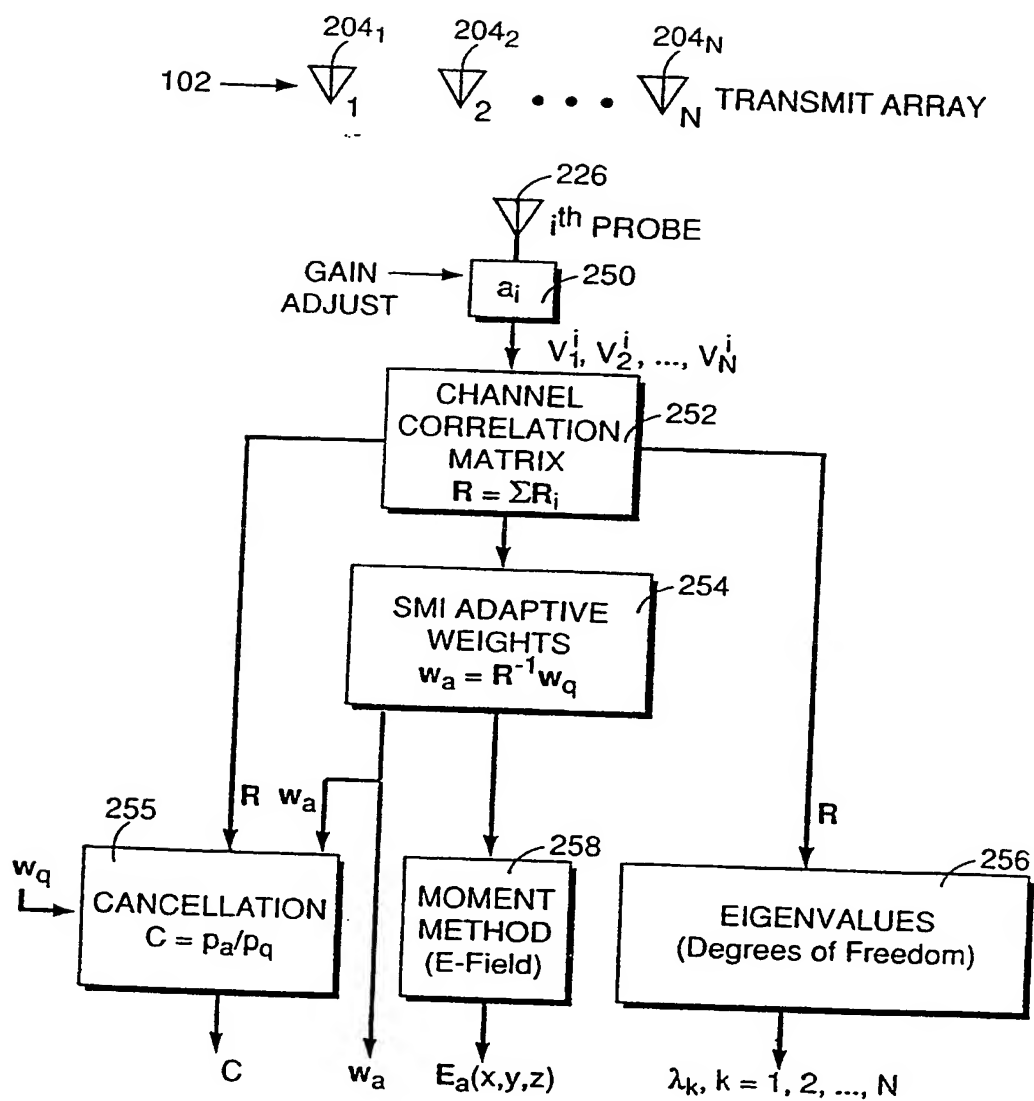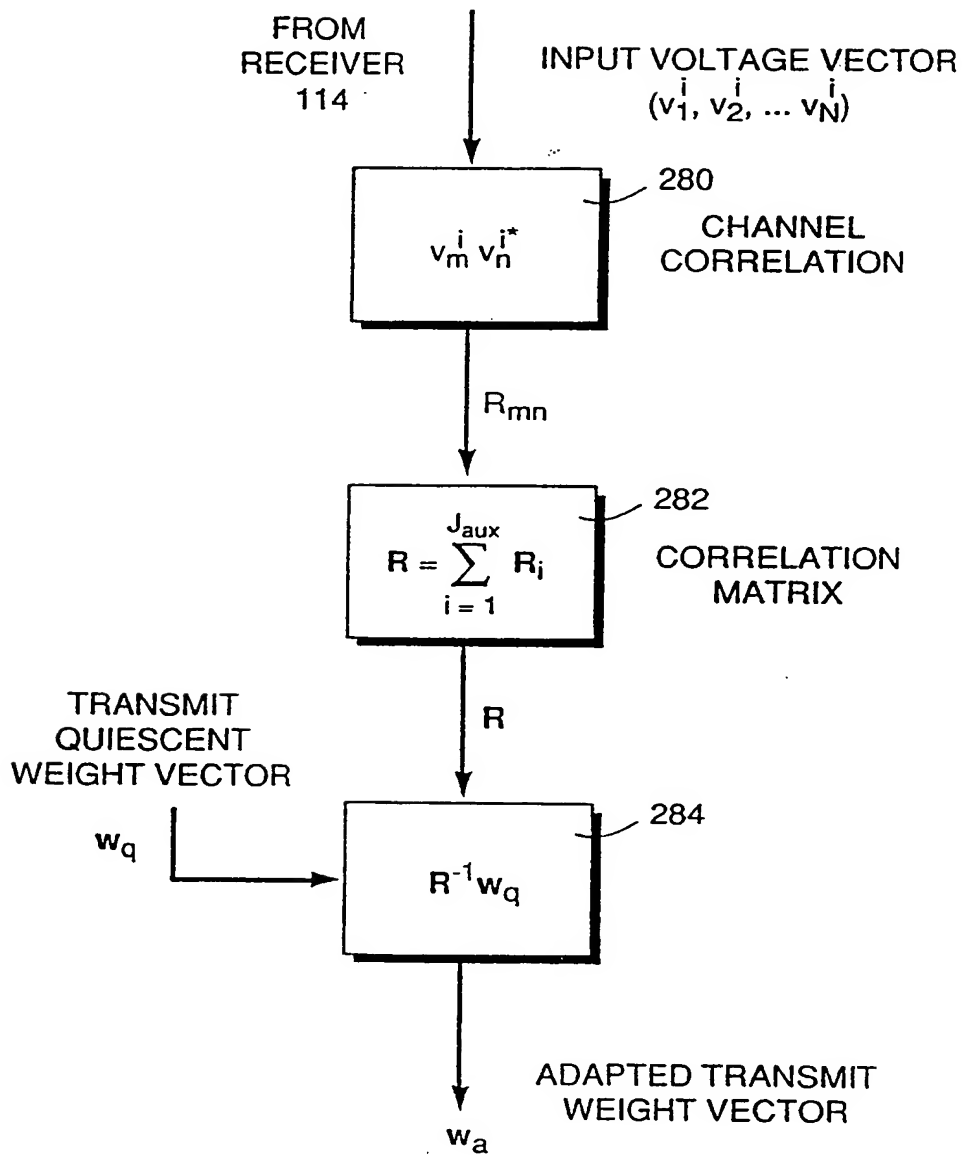
Fig. 9
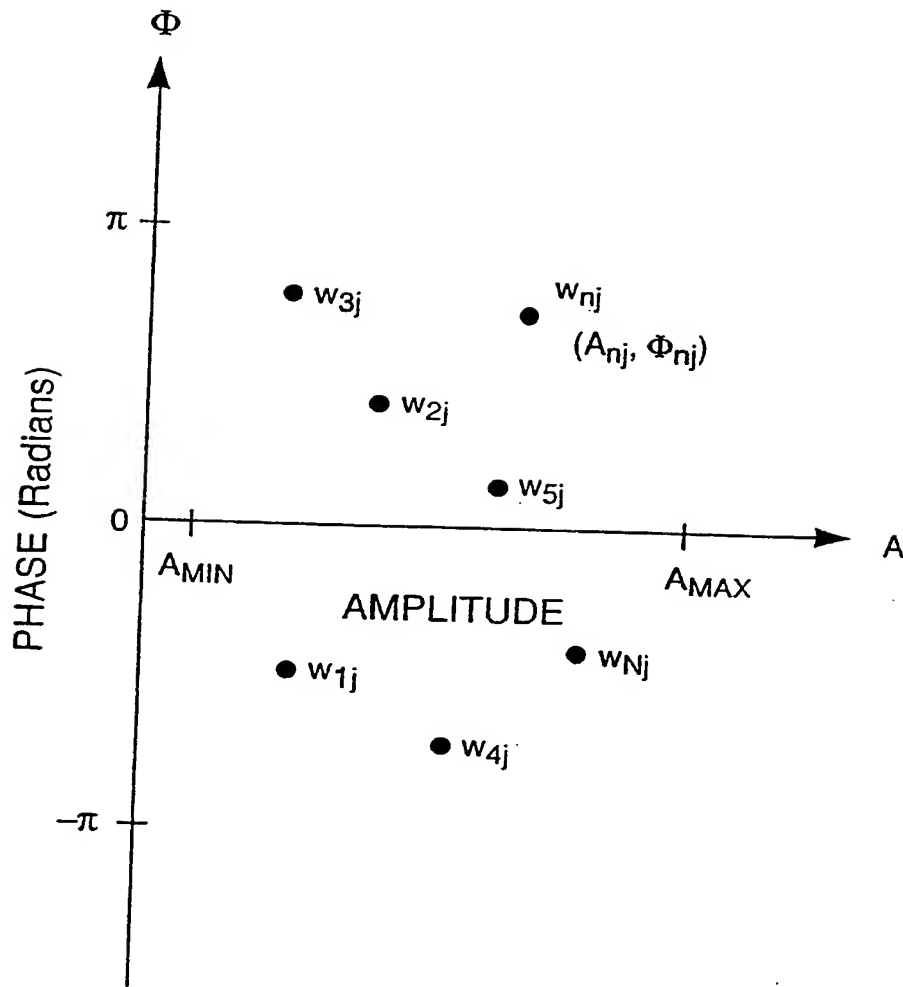
Fig. 10
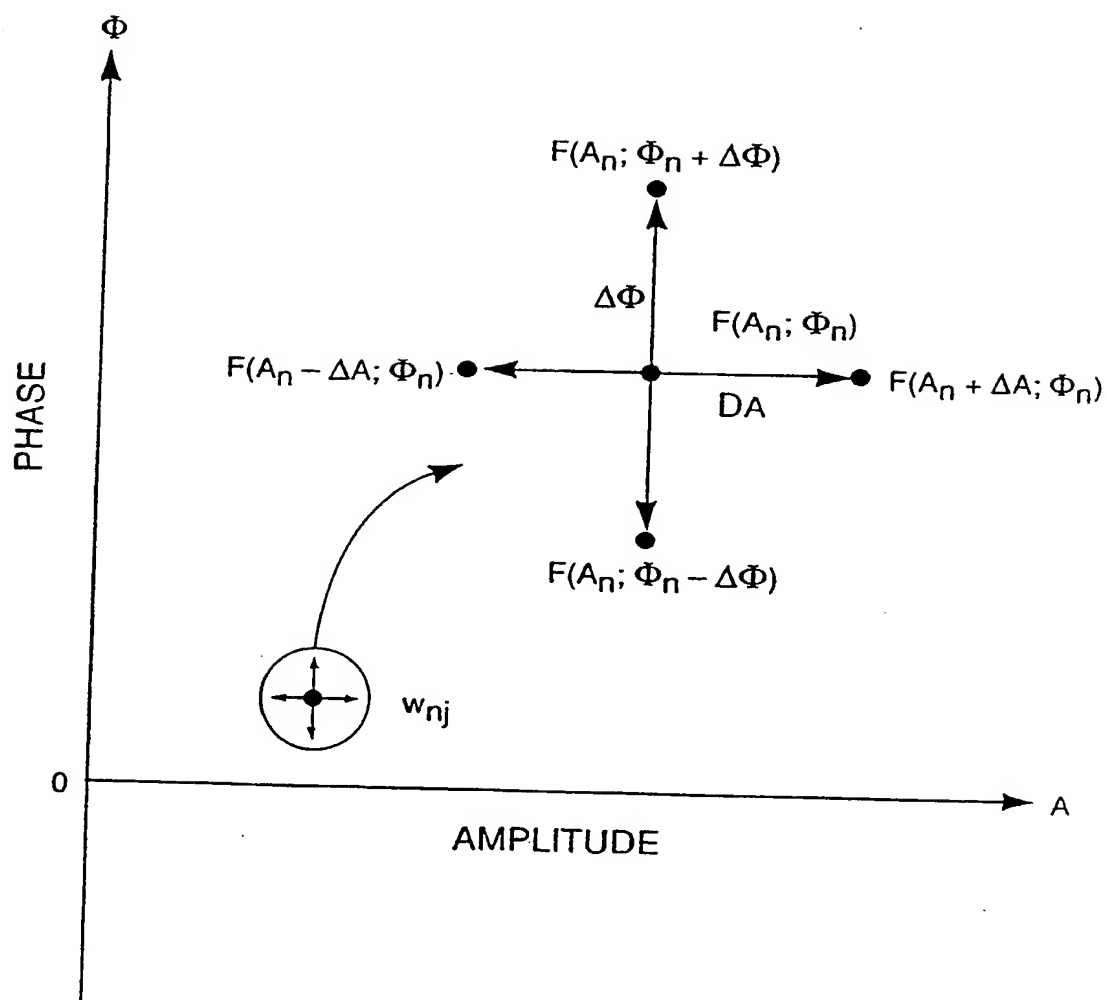
Fig. 11

GRADIENT SEARCH SYSTEM BLOCK DIAGRAM

$$F_{nj} = p_{nj}^{rec} = \sum_{i=1}^{N_{aux}} |v_{nj}^i|^2$$

Fig. 12

200

202

TRANSMIT
ARRAY

250_N

w_N

Z_L

204_N

$(\mu, \varepsilon, \sigma)$

250_m

w_m

Z_L

204_m
mth
ELEMENT

j^{th}
PROBE
$\pm V_j^{o.c.}$

$Z_{m,n}$

Z_n^j

226

250_n

w_n

Z_L

204_n

nth
ELEMENT

L_p

250_1

w_1

Z_L

204_1

Fig. 13

Fig. 14

R = RESISTOR
C = CAPACITOR
P = POWER
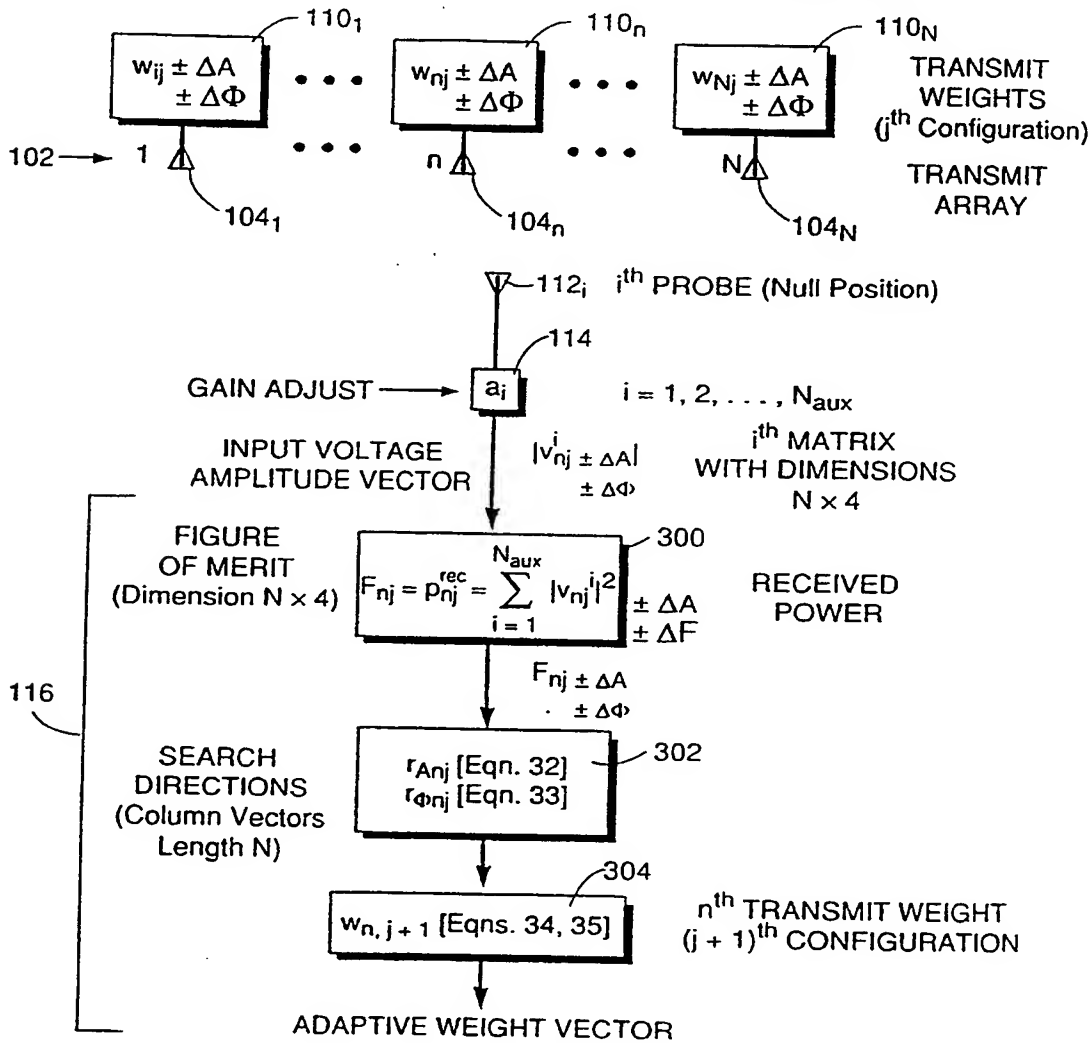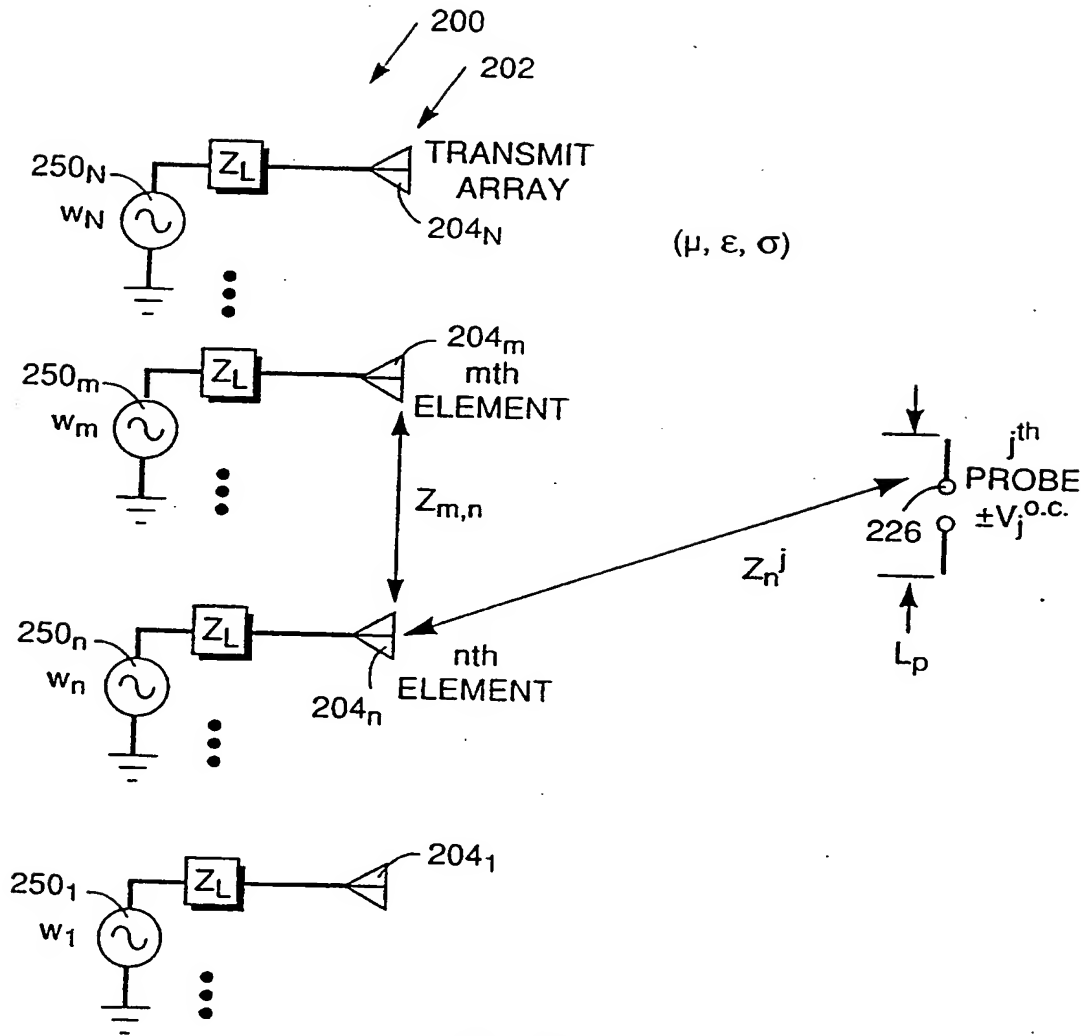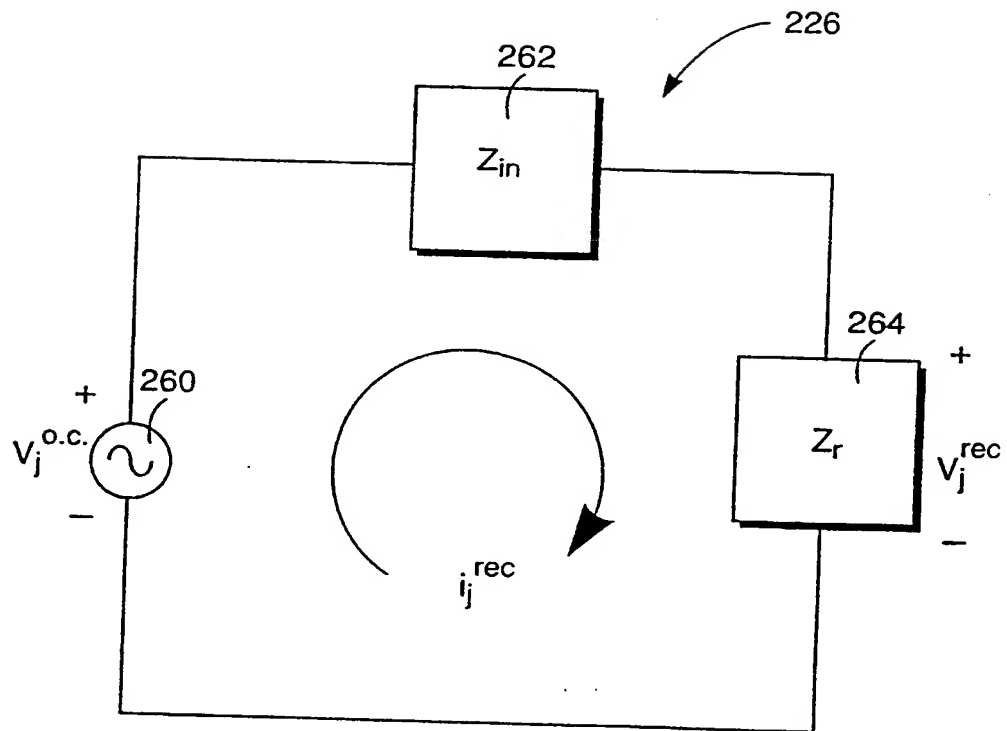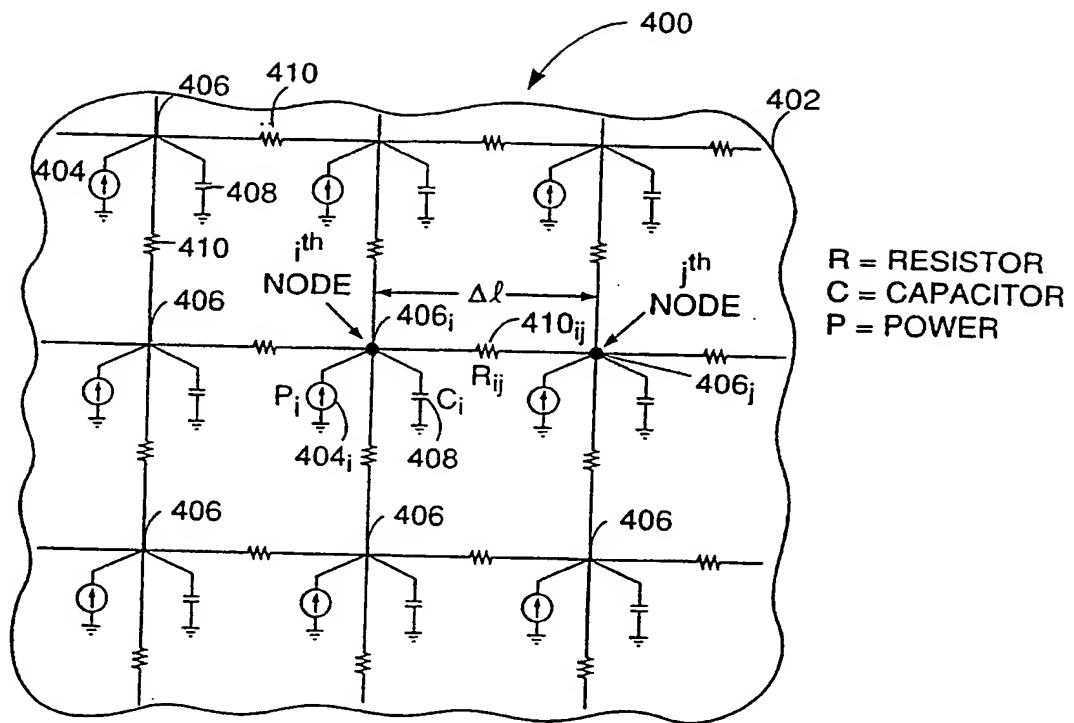
$R = \dfrac{1}{k\Delta\ell}$ [°C / W], k = THERMAL CONDUCTIVITY

$C = \rho C_p (\Delta\ell)^3$ [J/°C], ρ = DENSITY, C_P = SPECIFIC HEAT

$P = SAR \, \rho \, (\Delta\ell)^3$ [W], $SAR = \dfrac{\sigma}{2\rho}|E|^2$ (Specific Absorption Rate)

σ = ELECTRICAL CONDUCTIVITY

|E| = MAGNITUDE OF ELECTRIC FIELD

Fig. 15
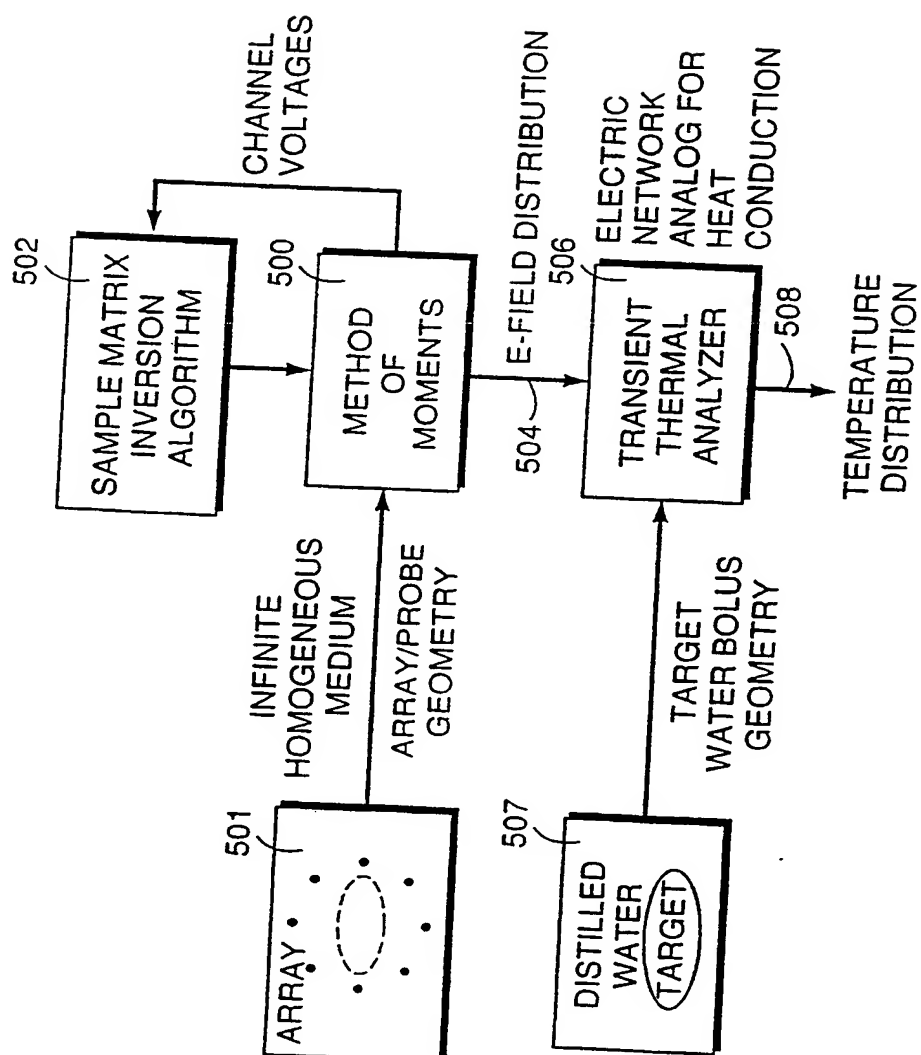
Fig. 16(a)

PARAMETER	PHANTOM MUSCLE TISSUE	DISTILLED WATER
DIELECTRIC CONSTANT @ 100 MHz	73.5	80.0
ELECTRICAL CONDUCTIVITY @ 100 MHz	0.5 S/m	0.0001 S/m
DENSITY	970.0 kg/m^3	1000.0 kg/m^3
SPECIFIC HEAT	3516.0 J/kg °C	4200.0 J/kg °C
THERMAL CONDUCTIVITY	0.544 W/m °C	0.6019 W/m °C

Table 1

Fig. 16(b)

Fig. 17

Fig. 18

E-FIELD BEFORE NULLING

8-ELEMENT DIPOLE RING ARRAY
60-cm ARRAY DIAMETER
120-MHz OPERATION
FOCUSED AT (0,0)

107

106

MUSCLE TISSUE
$\sigma = 0.5$ S/m
$\varepsilon_r = 73.5$

ALL PLOT NUMBERS IN dB

z (cm)

x (cm)
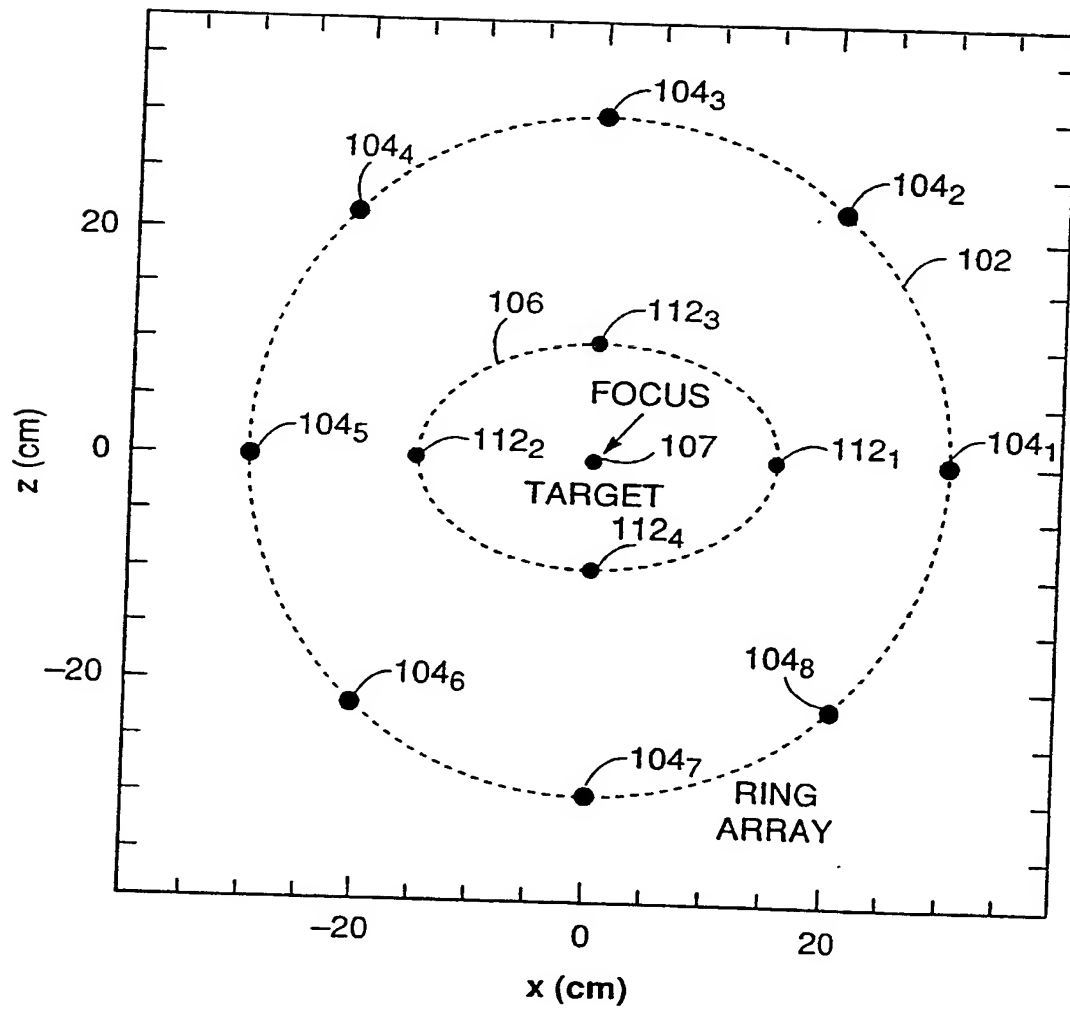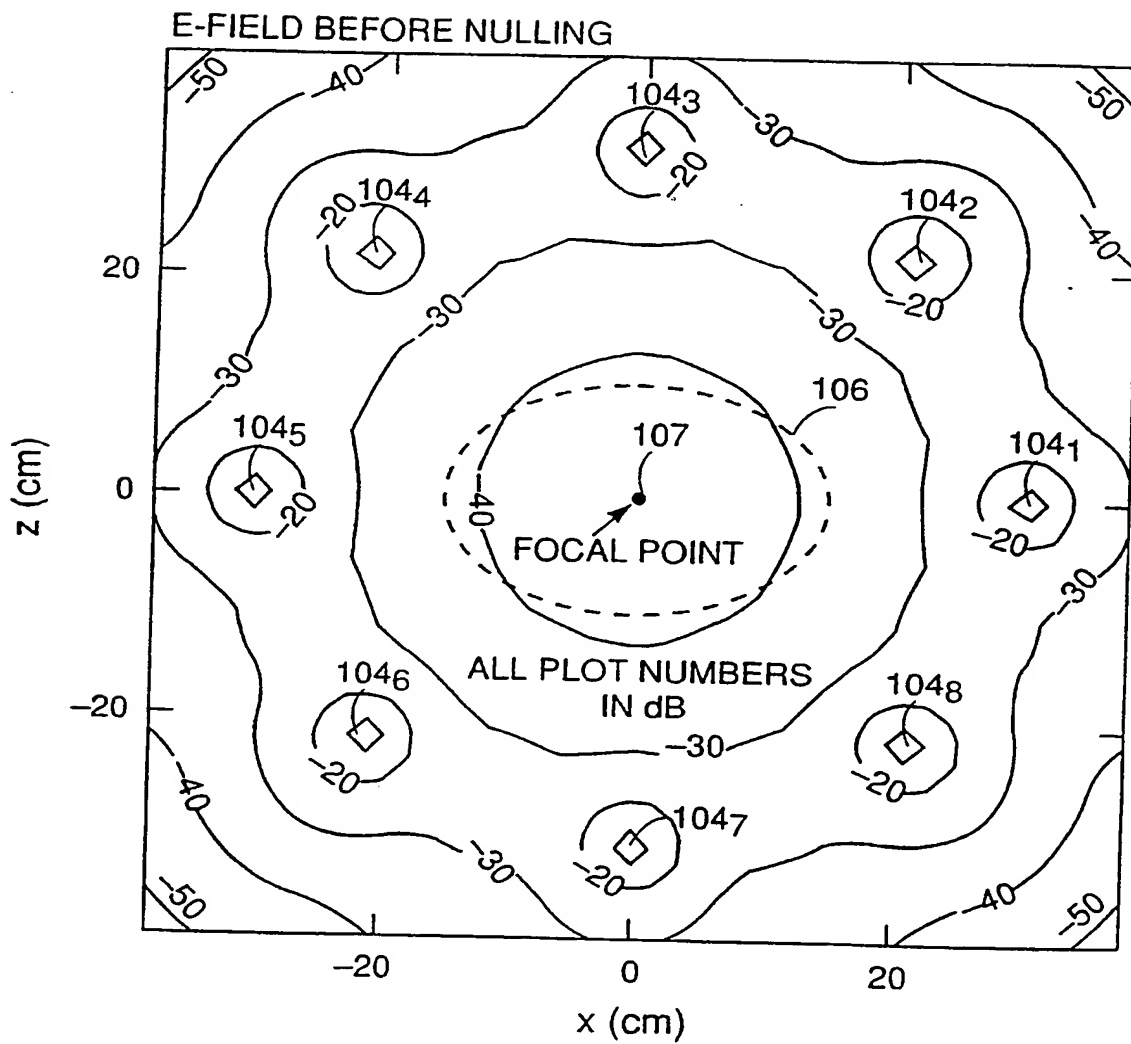
Fig. 19
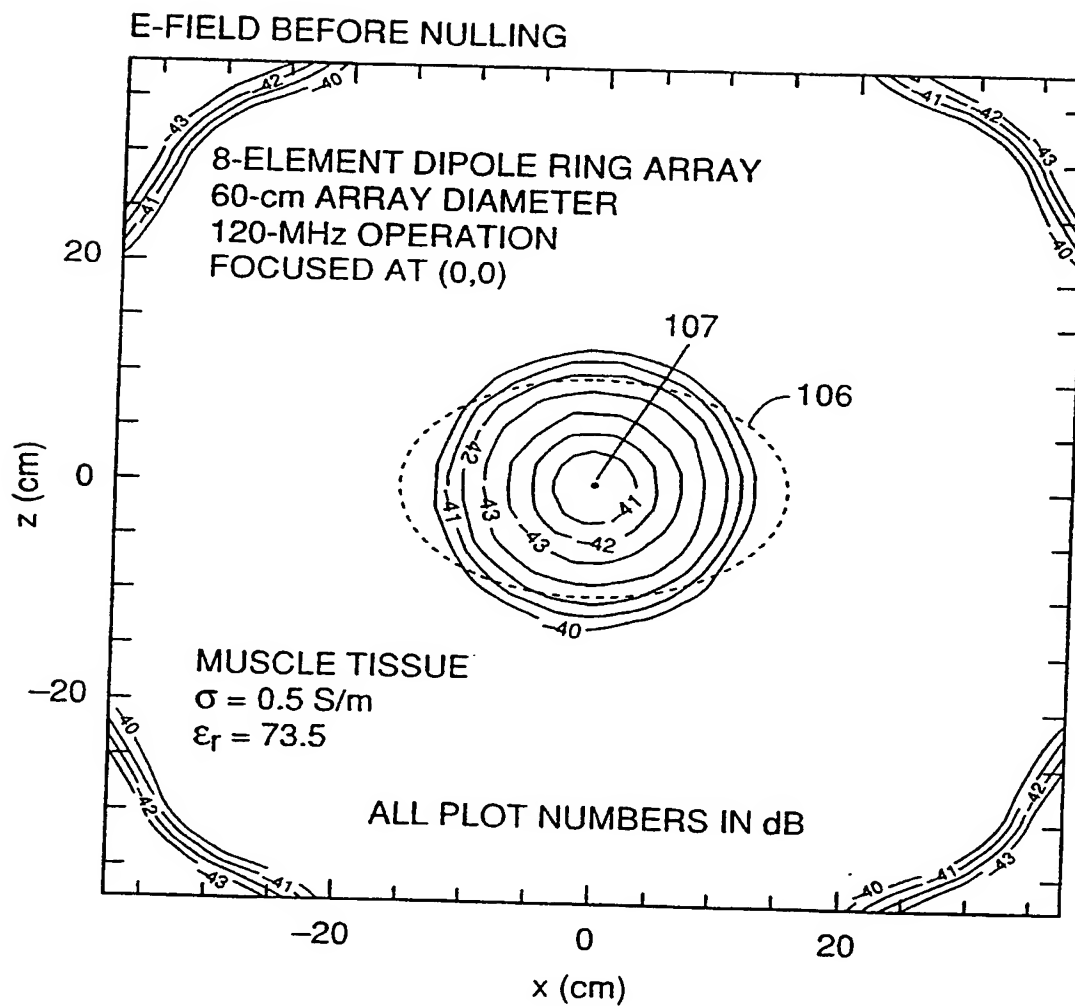
BEFORE NULLING
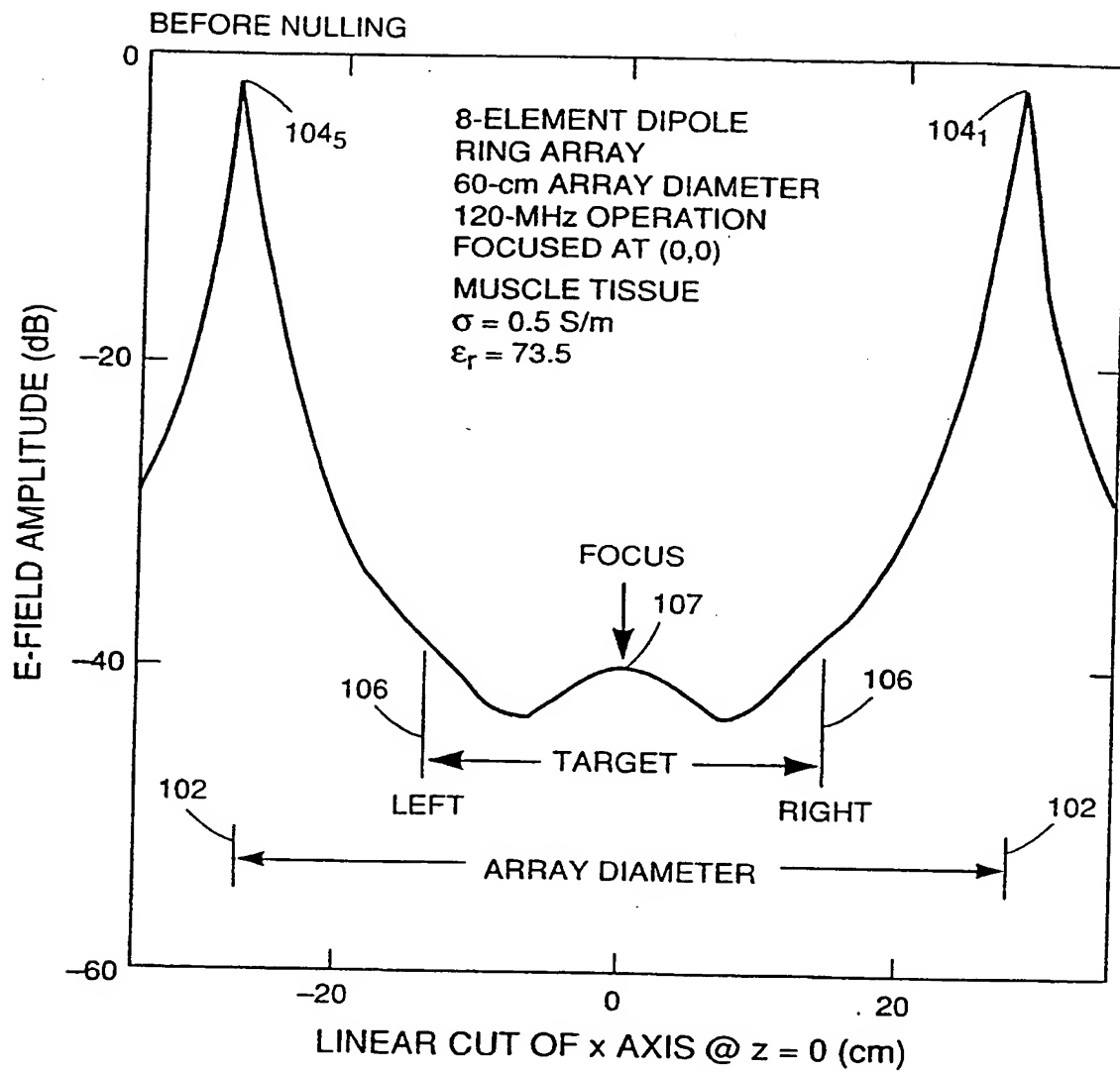
Fig. 20
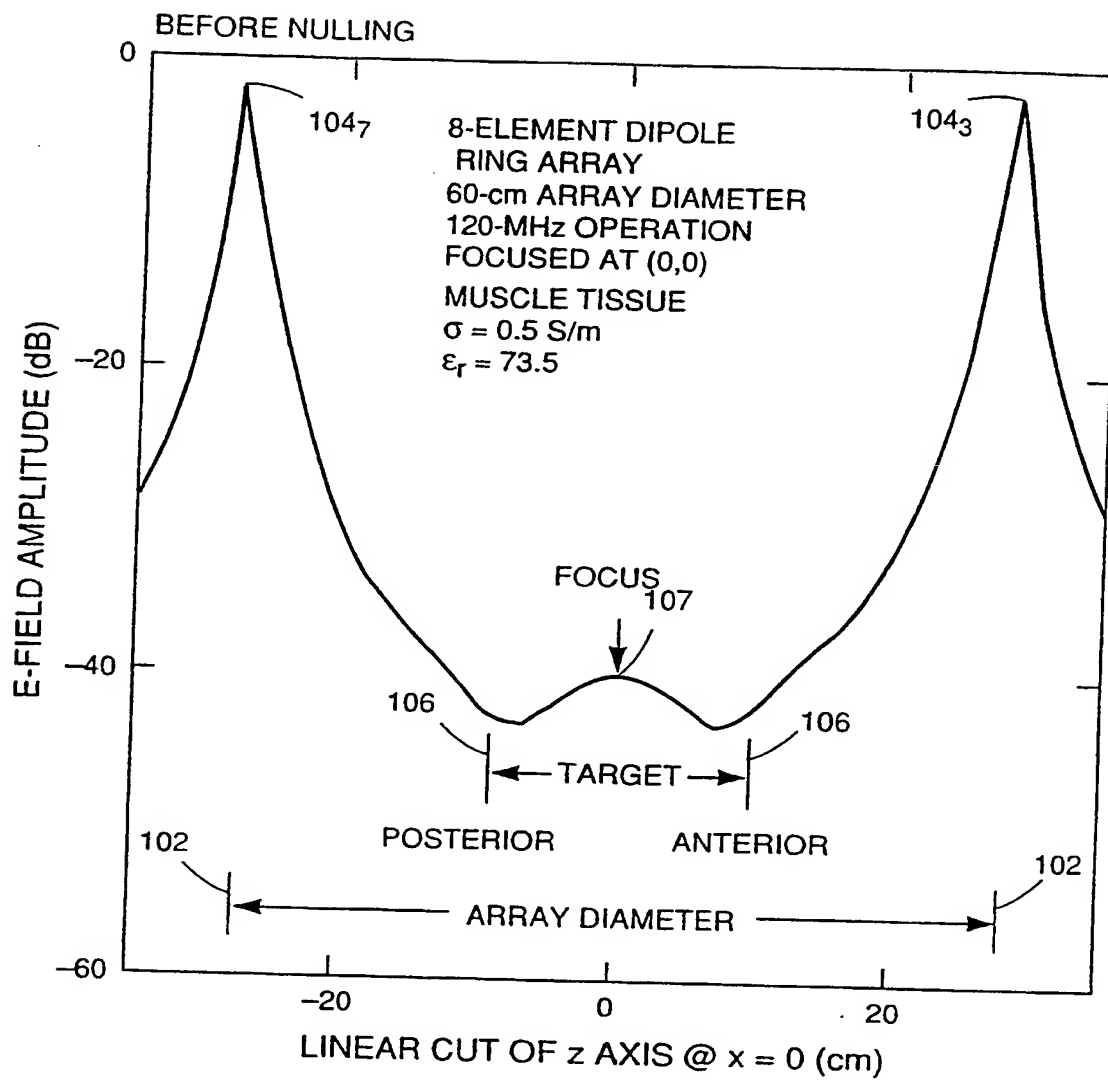
BEFORE NULLING

Fig. 21

E-FIELD AFTER NULLING; 4 AUXILIARIES

Fig. 22

Fig. 23

8-ELEMENT DIPOLE RING ARRAY
60-cm ARRAY DIAMETER
120-MHz OPERATION
FOCUSED AT (0,0)

MUSCLE TISSUE
$\sigma = 0.5$ S/m
$\varepsilon_r = 73.5$

BEFORE NULLING
AFTER NULLING
(4 Auxiliaries)
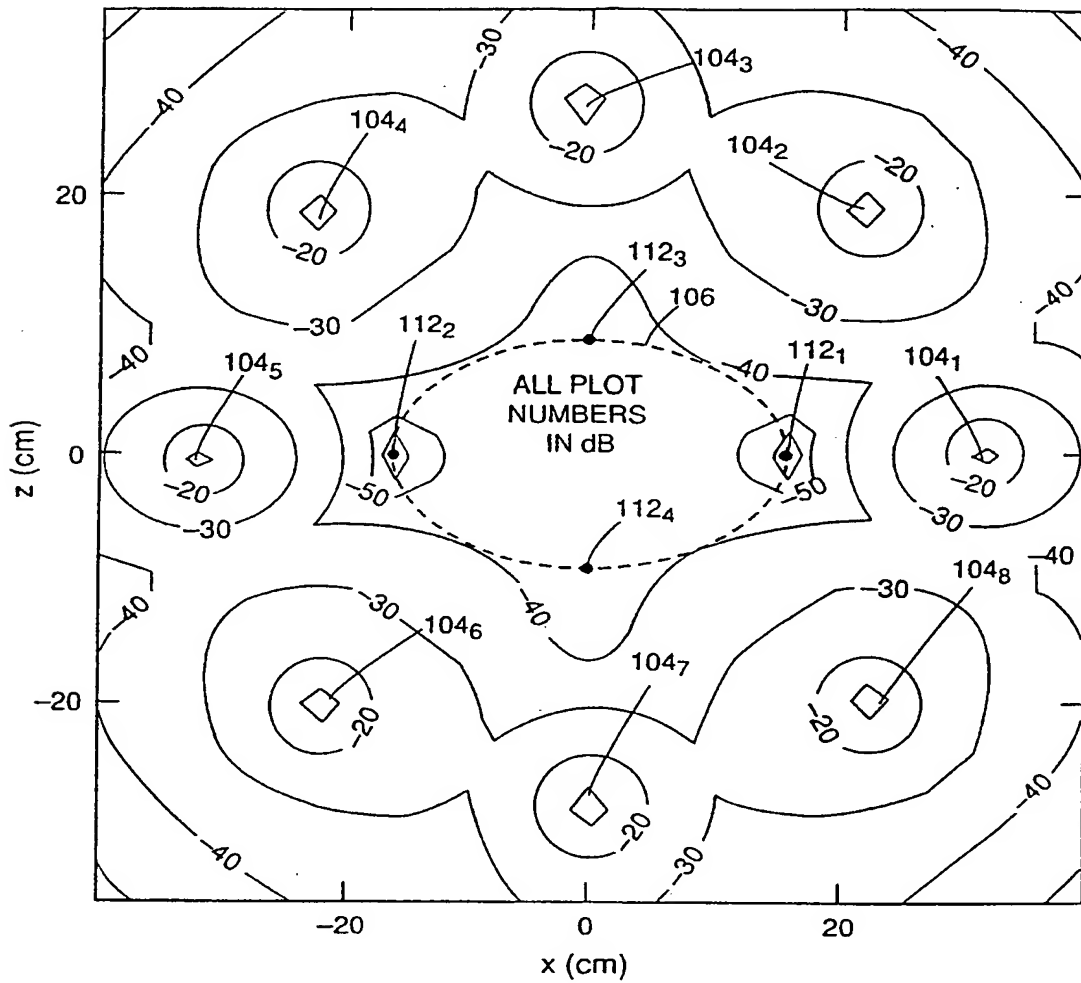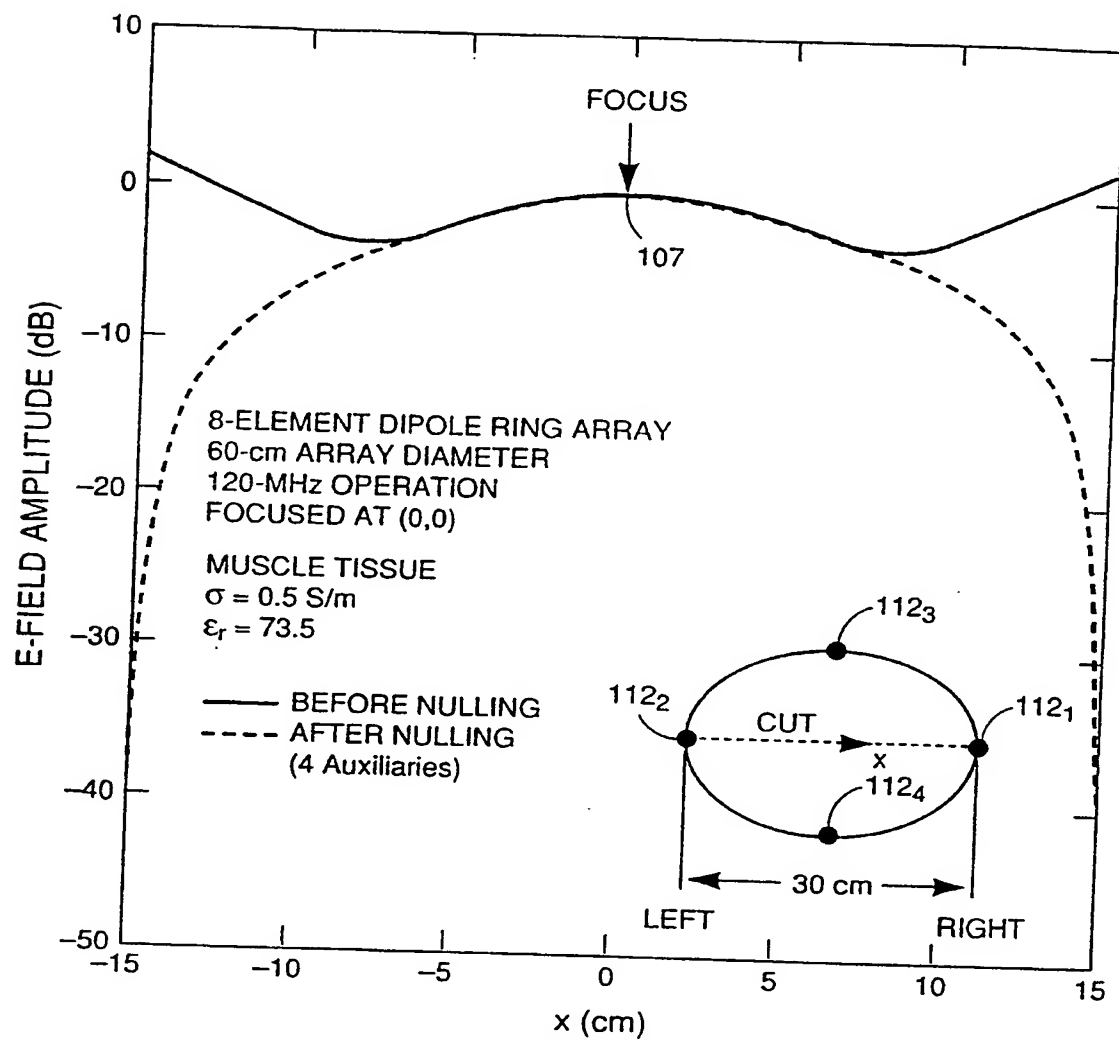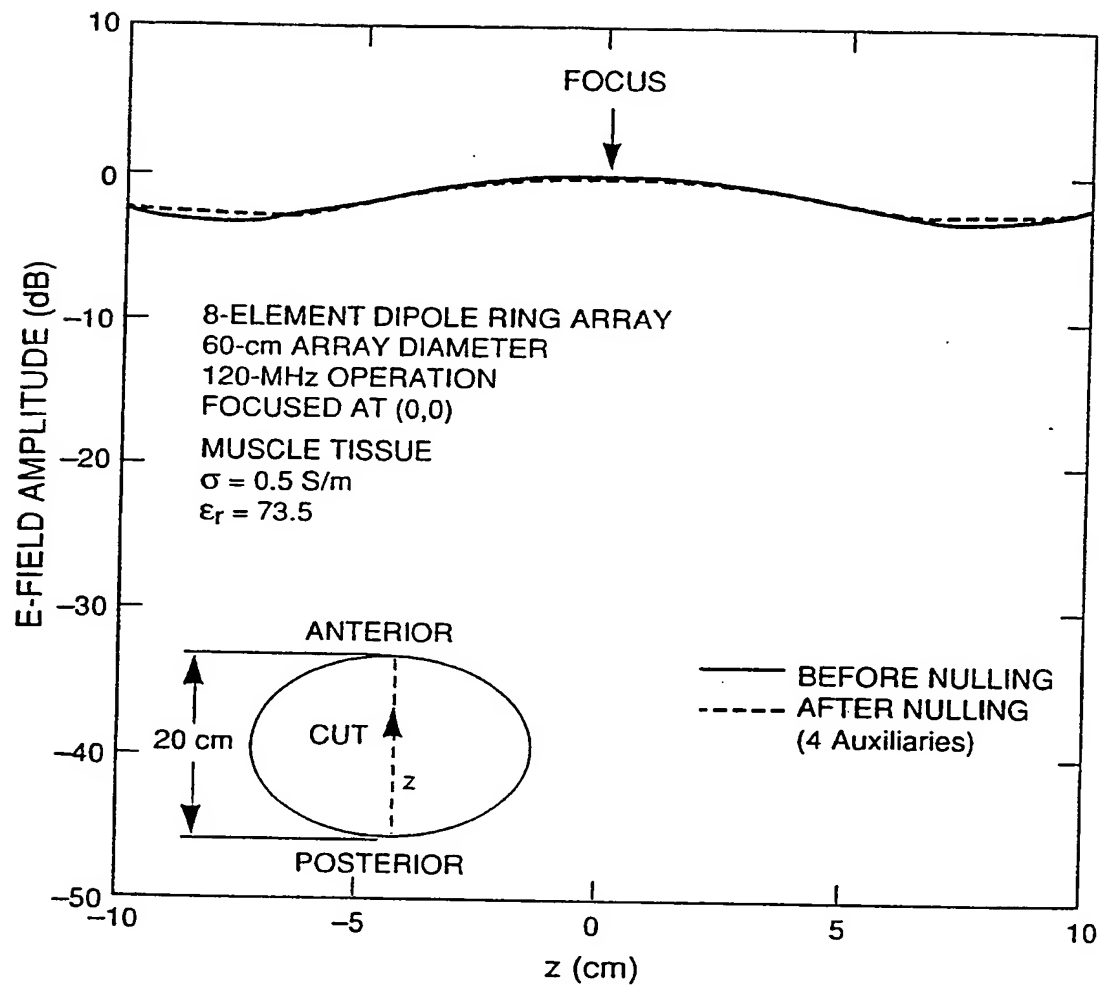
Fig. 24
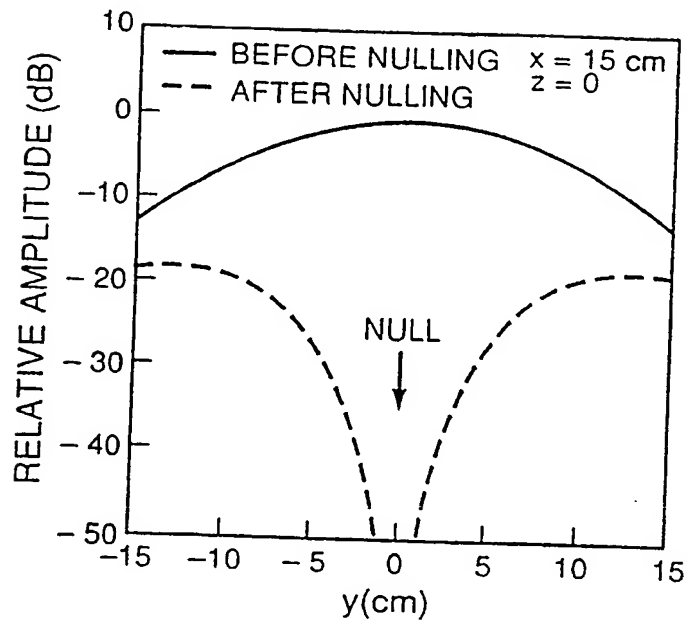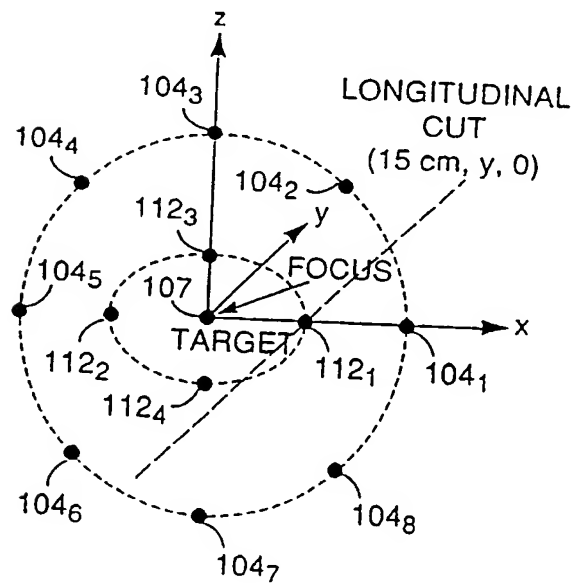
Fig. 25(a)

Fig. 25(b)

SUBSTITUTE SHEET

SIMULATED E-FIELD BEFORE AND AFTER NULLING

LONGITUDINAL CUT

8 TRANSMIT CHANNELS
4 AUXILIARIES
120 MHz, ε_r = 73.5, σ = 0.5 S/m

Fig. 26(b)

Fig. 26(a)

Fig. 27 (a)

Fig. 27 (b)

Fig. 28

8-ELEMENT DIPOLE RING ARRAY
60-cm ARRAY DIAMETER
120-MHz OPERATION
FOCUSED AT (0,0)
t = 20 min

$T(x,z)$
BEFORE NULLING
$T_{MAX} = 46°C$
25°C (Initial)

MUSCLE TISSUE
σ = 0.5 S/m
ε_r = 73.5

ALL PLOT NUMBERS IN °C

z (cm)

x (cm)
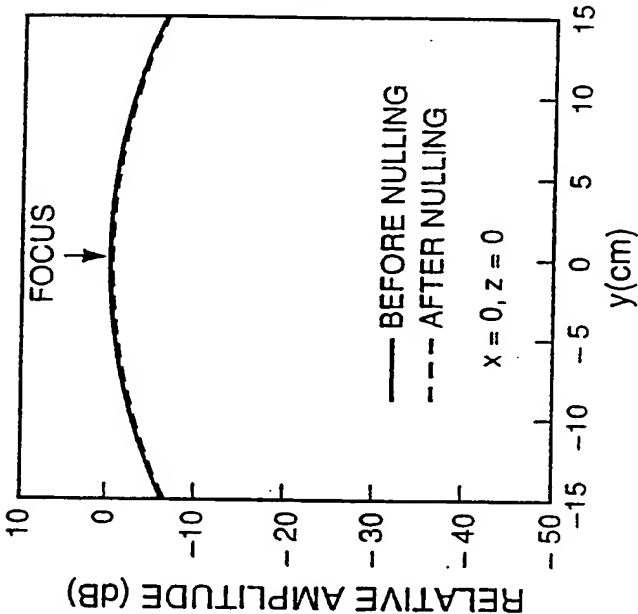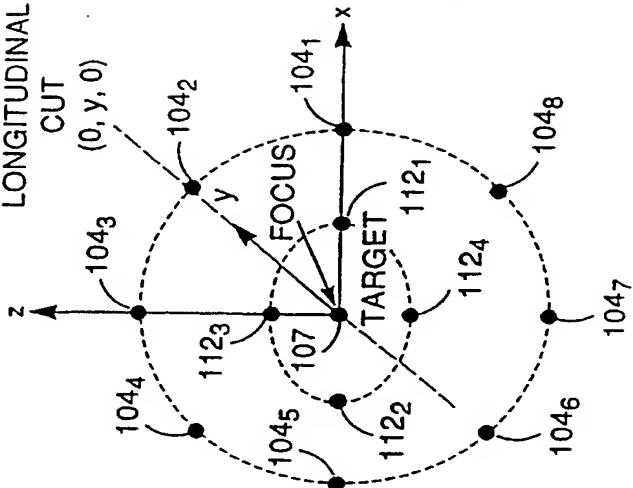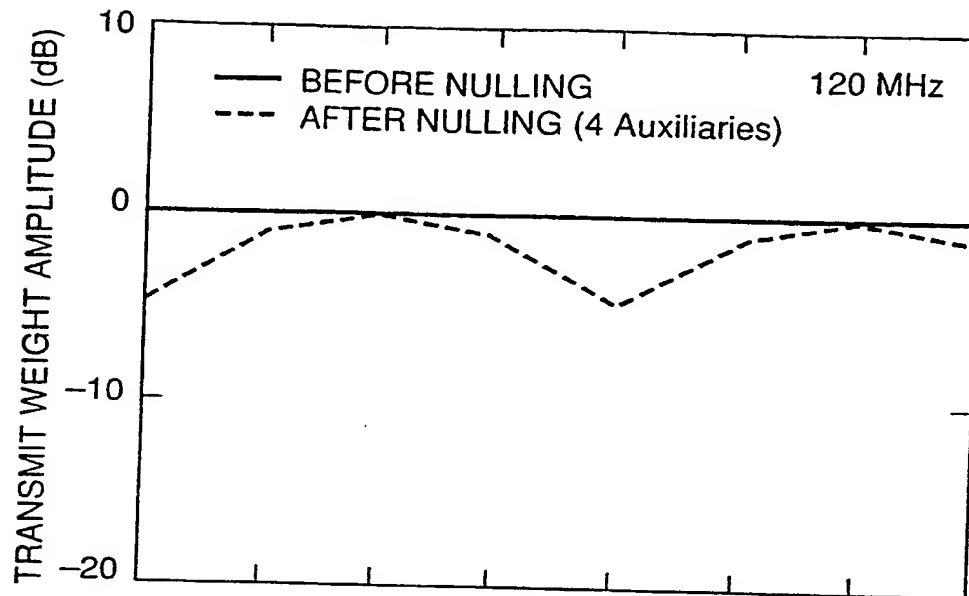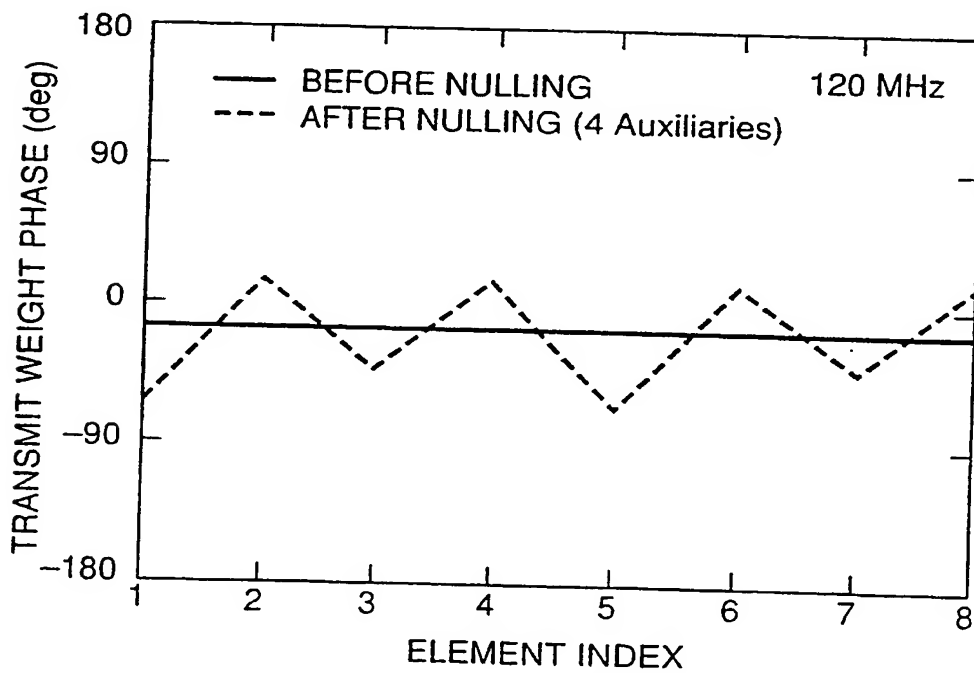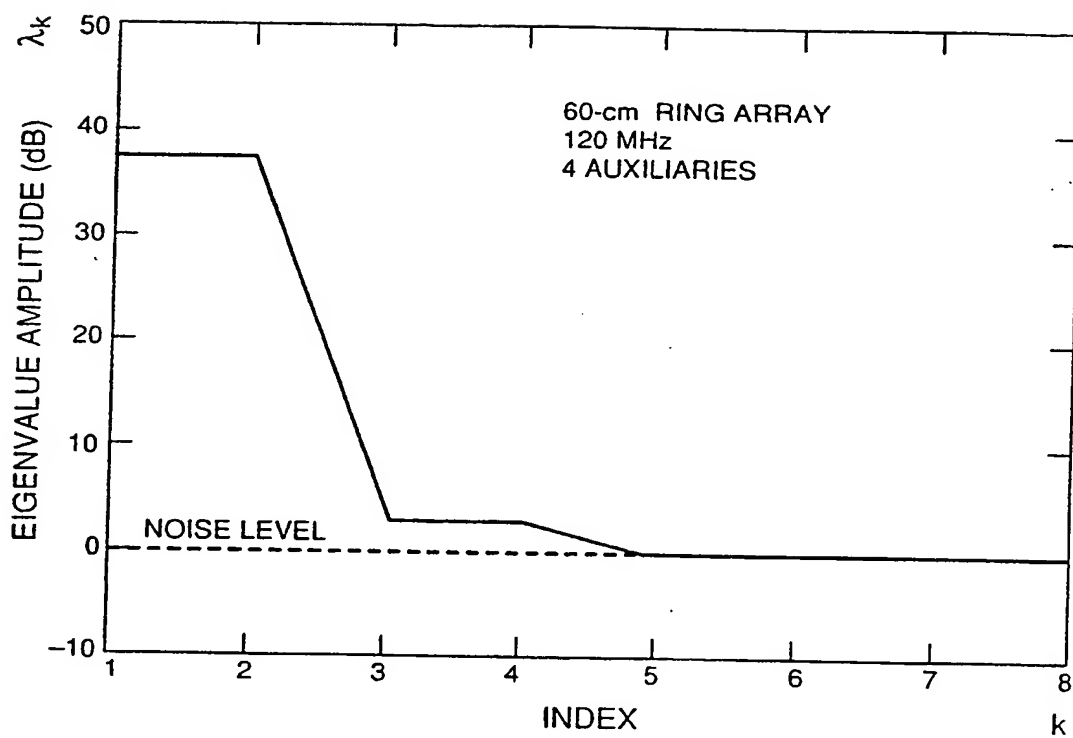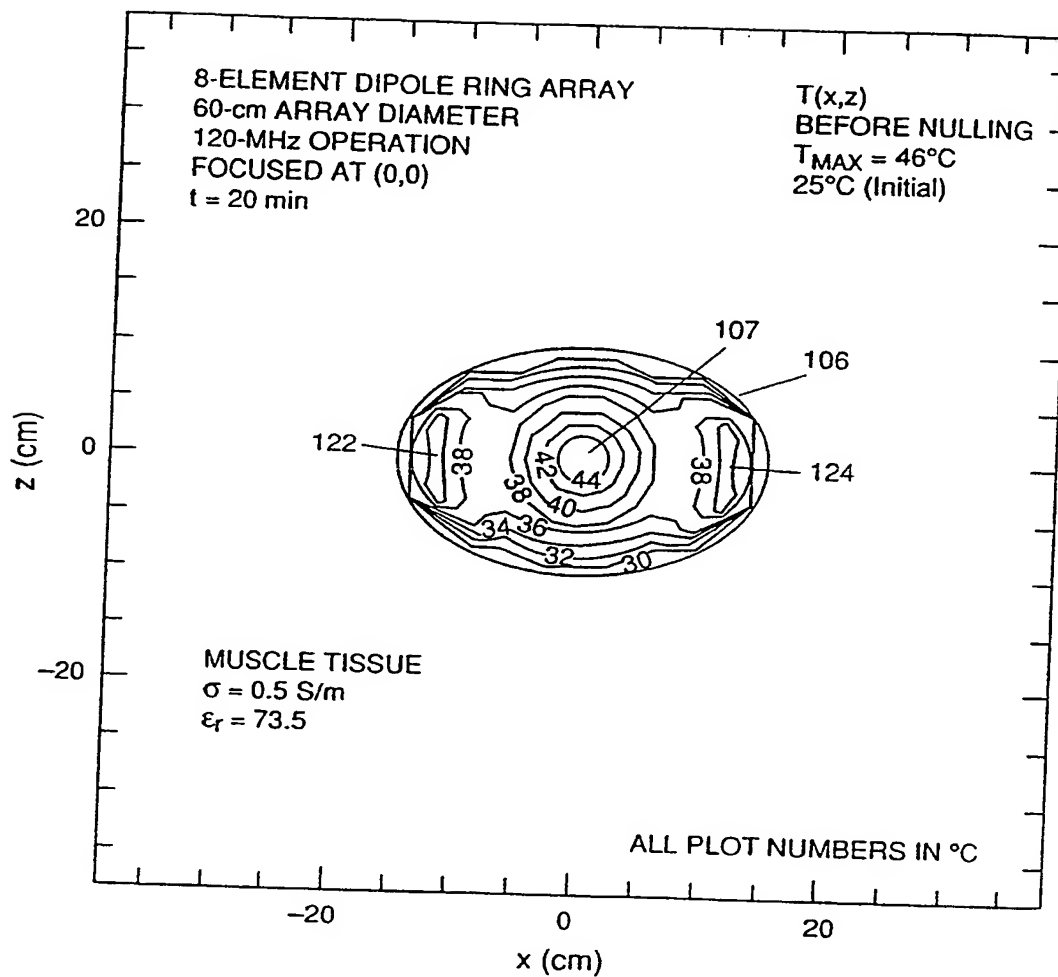
Fig. 29
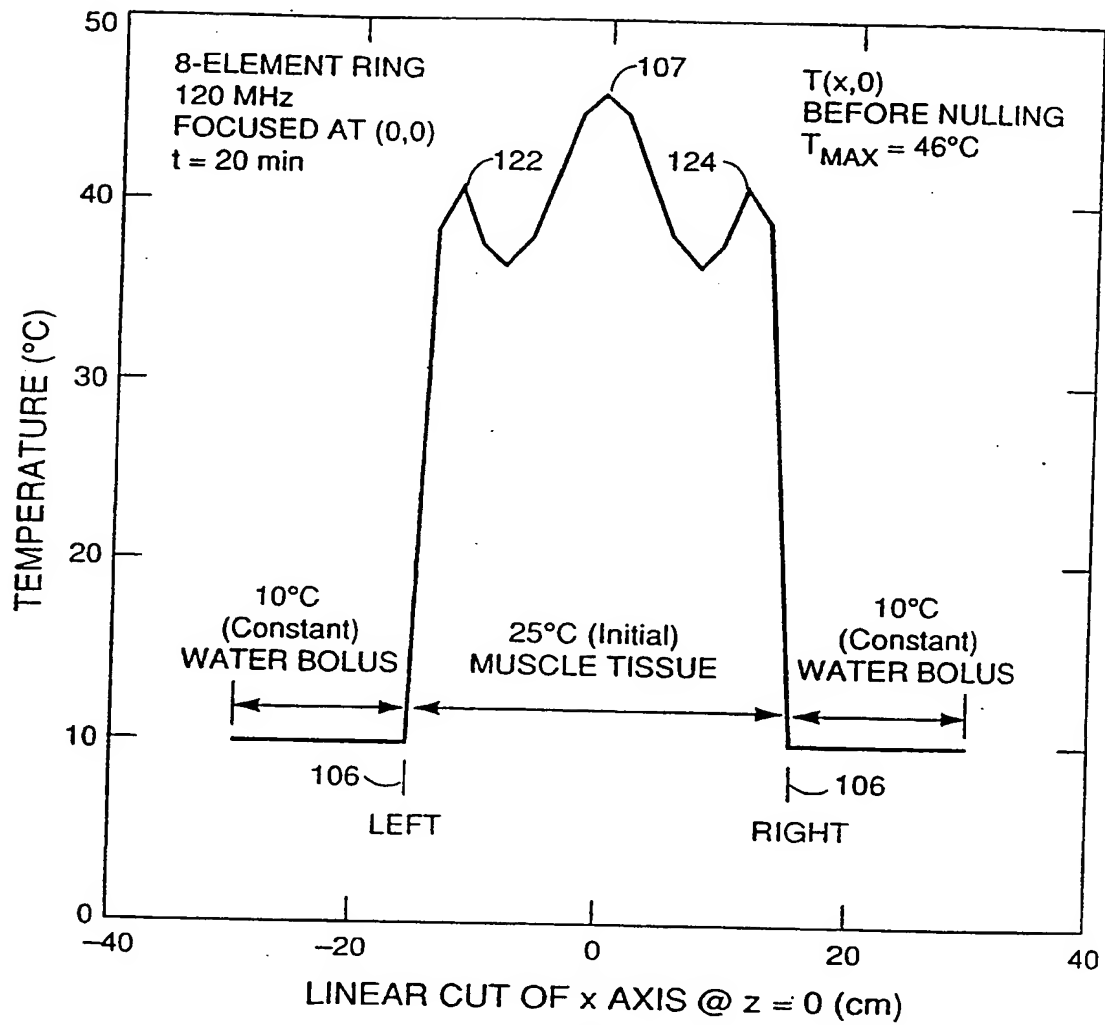
Fig. 30
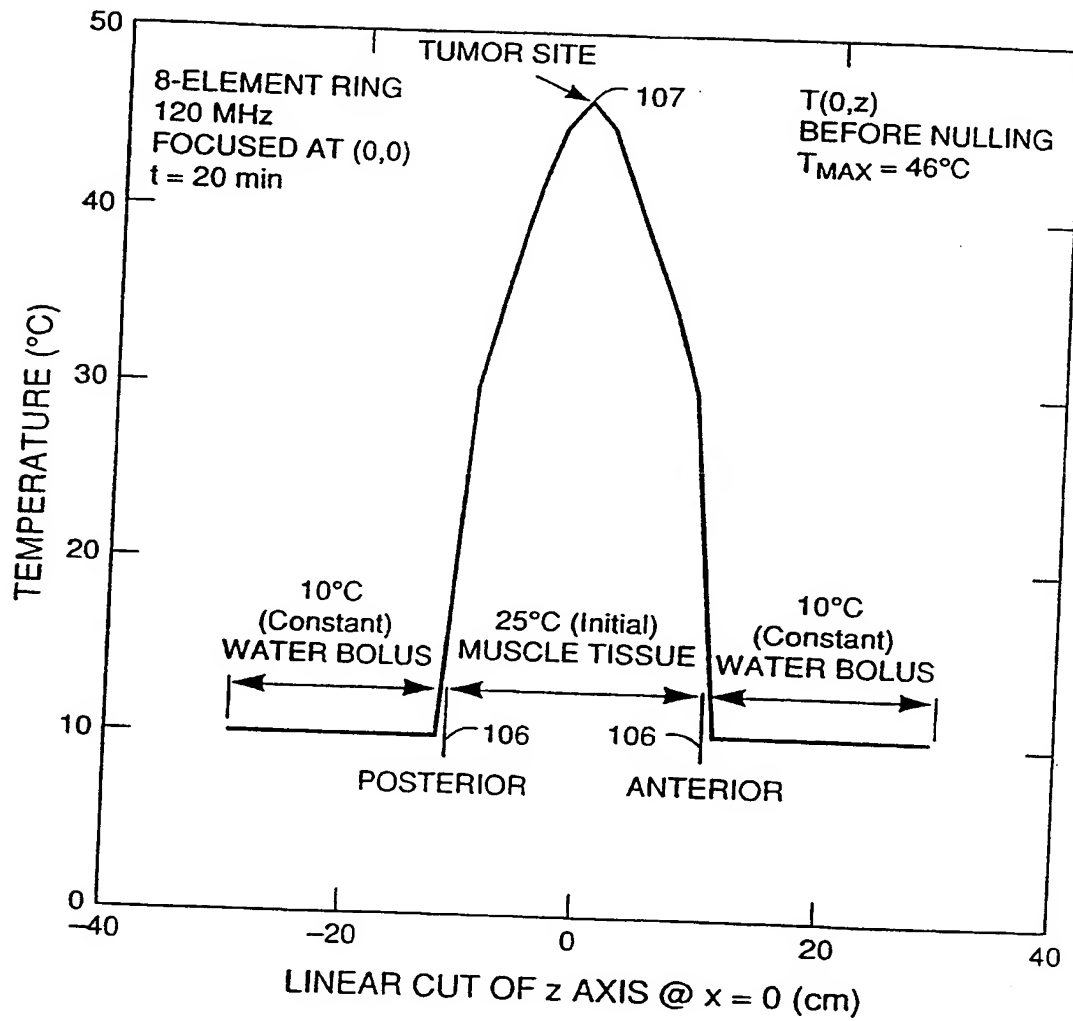
Fig. 31

Fig. 32

Fig. 33
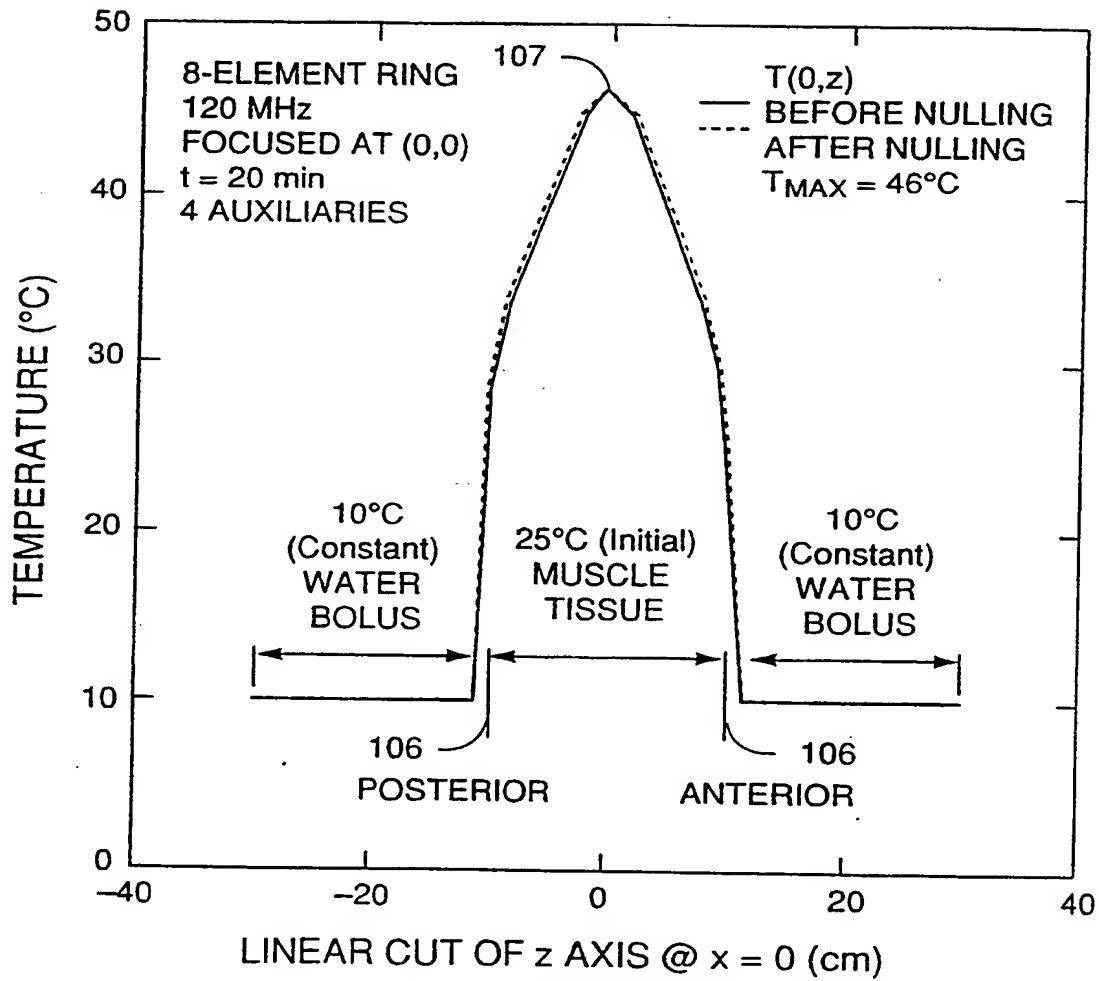
Fig. 34
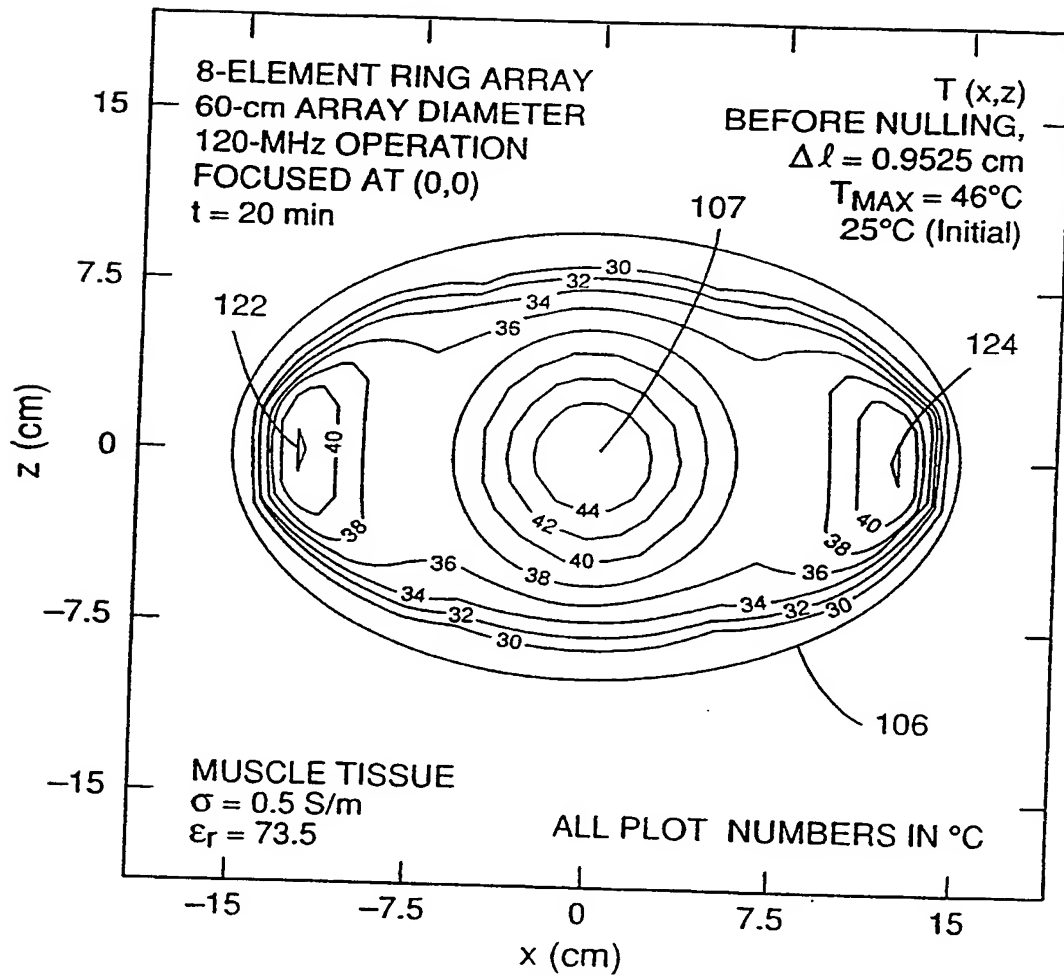
Fig. 35
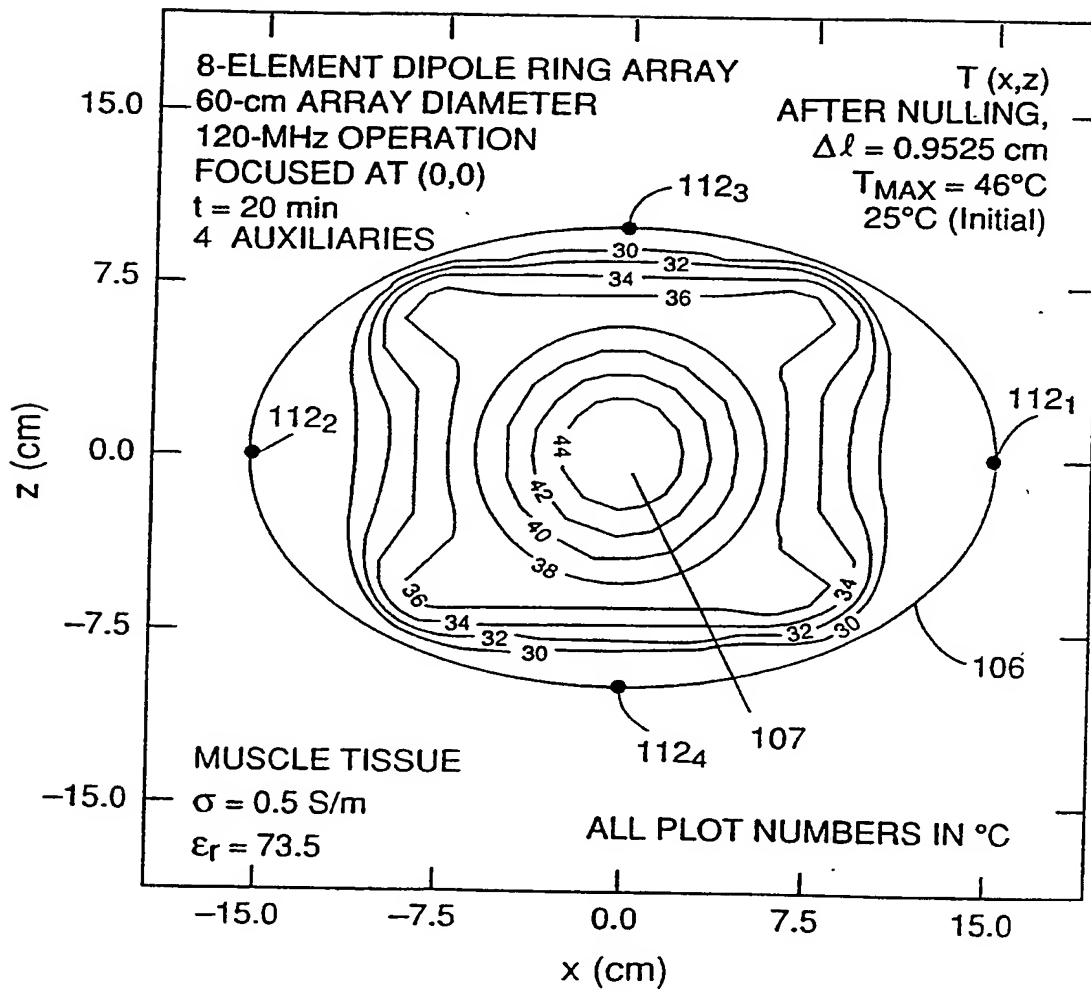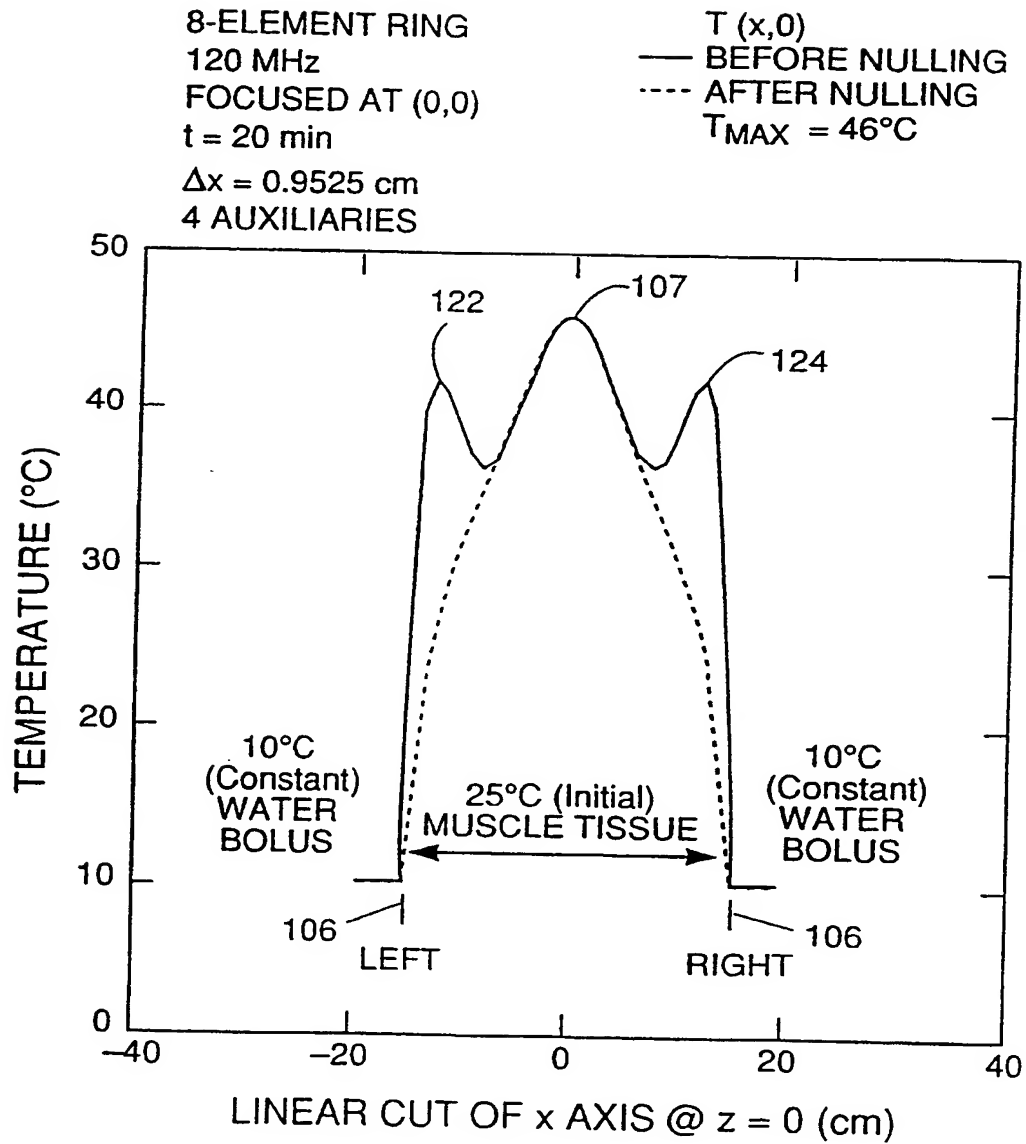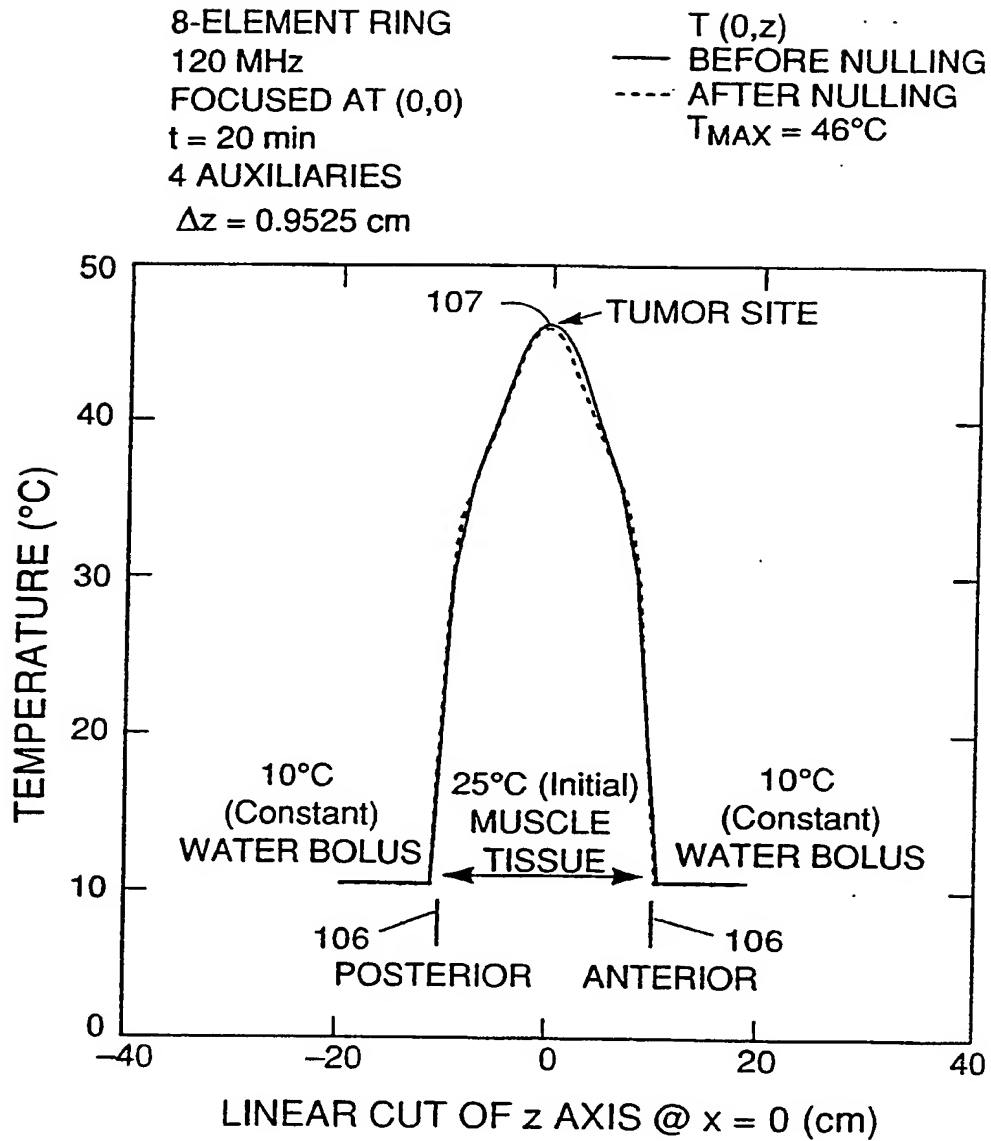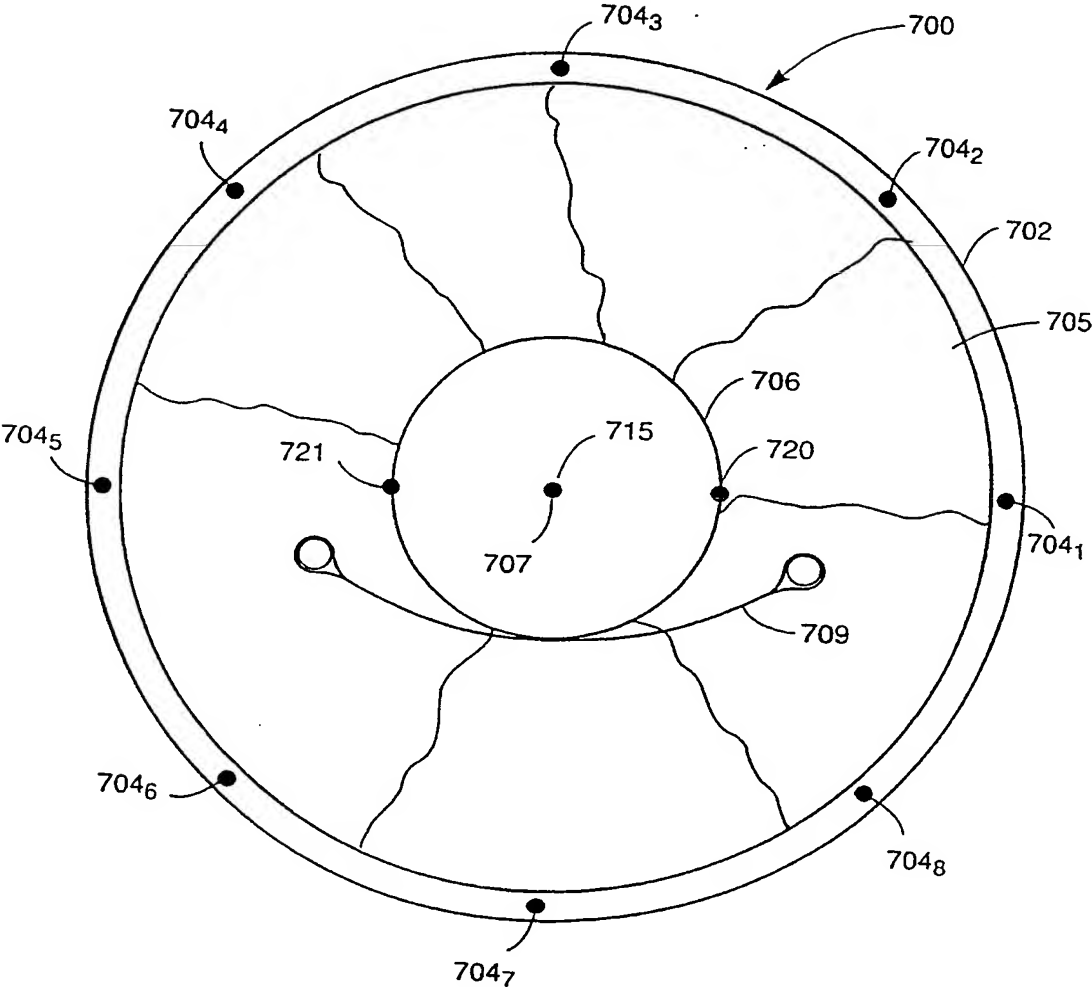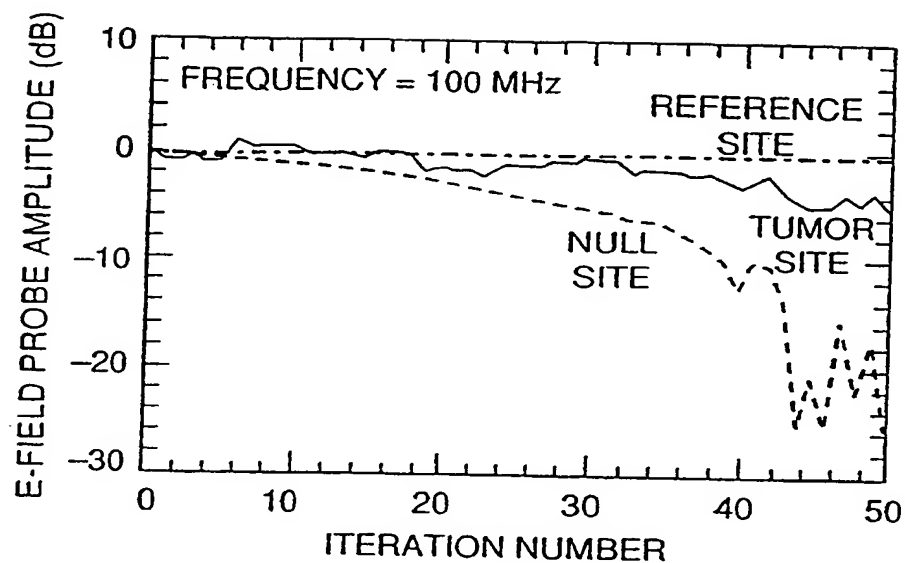
8-ELEMENT DIPOLE RING ARRAY
60-cm ARRAY DIAMETER
120-MHz OPERATION
FOCUSED AT (0,0)
t = 20 min
4 AUXILIARIES

T (x,z)
AFTER NULLING,
$\Delta \ell$ = 0.9525 cm
T_{MAX} = 46°C
25°C (Initial)

MUSCLE TISSUE
σ = 0.5 S/m
ε_r = 73.5

ALL PLOT NUMBERS IN °C

z (cm)

x (cm)

Fig. 36

8-ELEMENT RING
120 MHz
FOCUSED AT (0,0)
t = 20 min

Δx = 0.9525 cm
4 AUXILIARIES

T (x,0)
—— BEFORE NULLING
---- AFTER NULLING
T_{MAX} = 46°C

Fig. 37

8-ELEMENT RING
120 MHz
FOCUSED AT (0,0)
t = 20 min
4 AUXILIARIES
$\Delta z = 0.9525$ cm

T (0,z)
—— BEFORE NULLING
---- AFTER NULLING
$T_{MAX} = 46°C$

Fig. 38

Fig. 39

EXPERIMENTAL CONFIGURATION
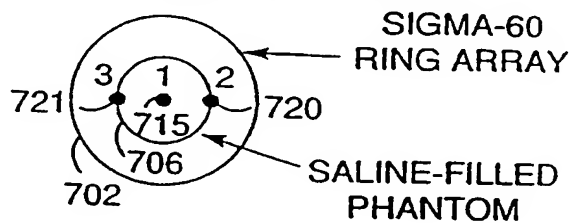
POSITION	COMMENT	PROBE
1	TUMOR SITE	EP-500
2	NULL SITE	EP-100
3	REF. SITE	EP-400

Fig. 40

SUBSTITUTE SHEET

Fig. 41

BEEF
HIND LEG CUT
24 lbs

WIDTH = 38 cm
HEIGHT = 23 cm } FRONT FACE
THICKNESS = 15 cm
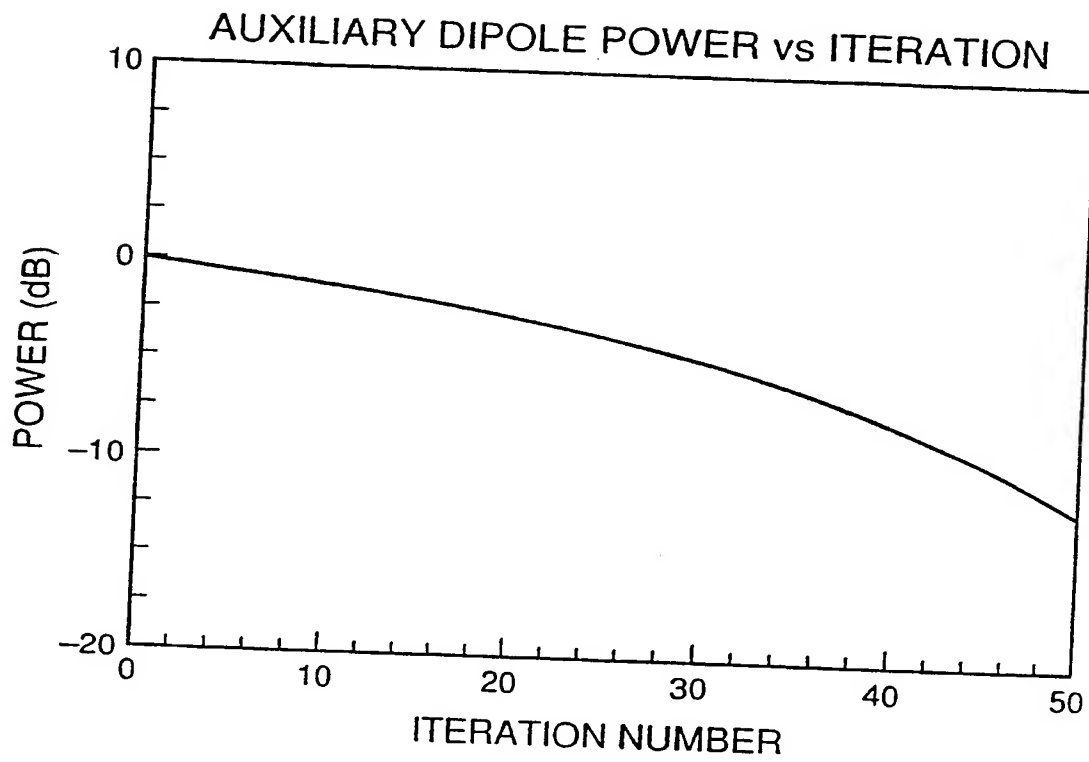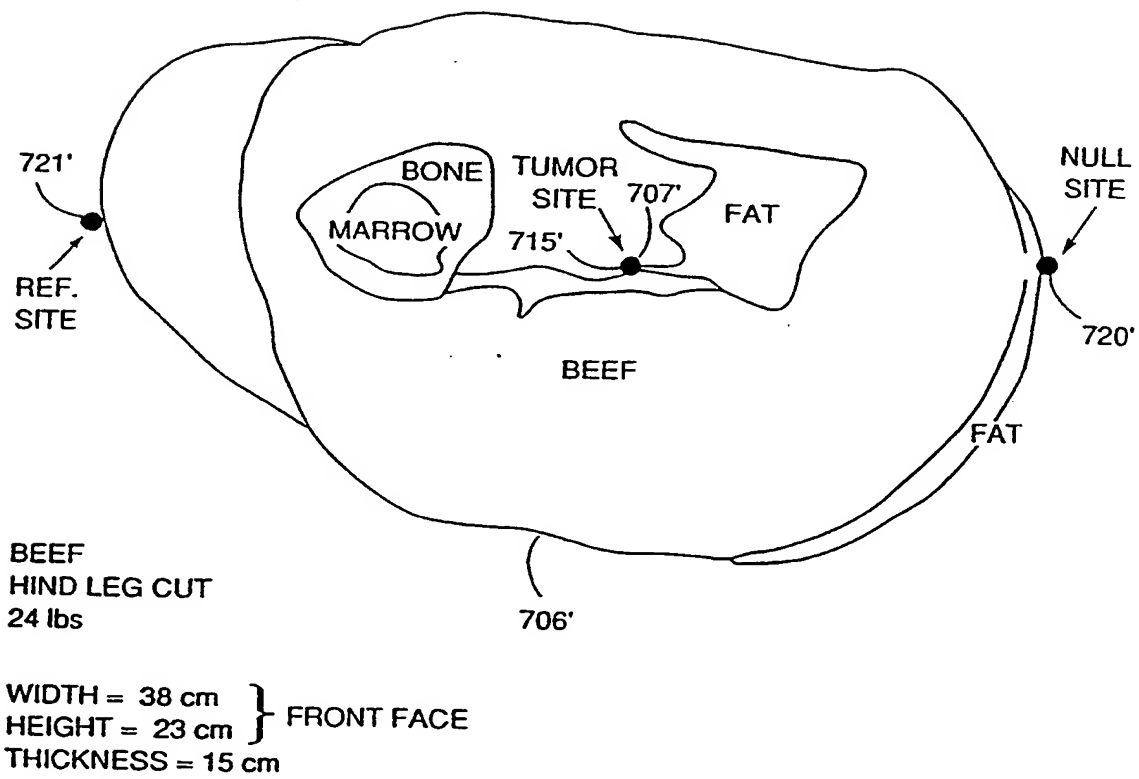
Fig. 42

SUBSTITUTE SHEET

EXPERIMENTAL CONFIGURATION
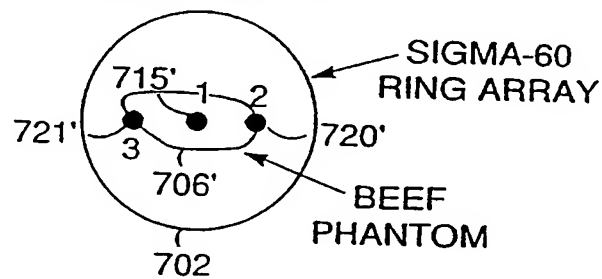
POSITION	COMMENT	PROBE
1	TUMOR SITE	EP-500
2	NULL SITE	EP-100
3	REF. SITE	EP-400

Fig. 43

SUBSTITUTE SHEET
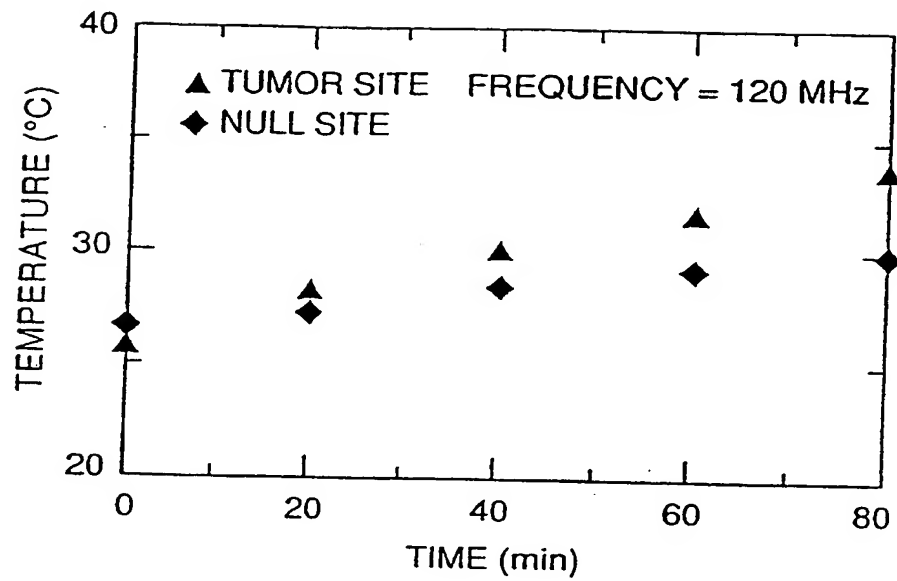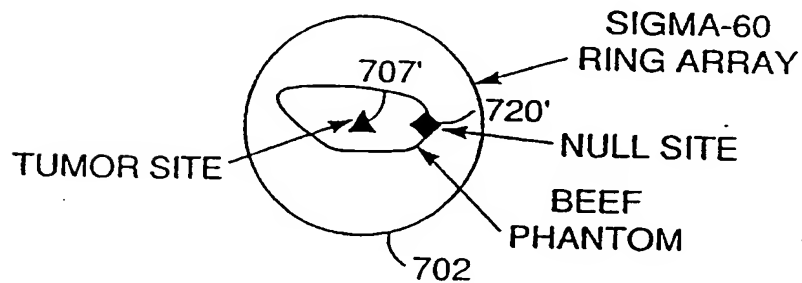
EXPERIMENTAL CONFIGURATION

Fig. 44
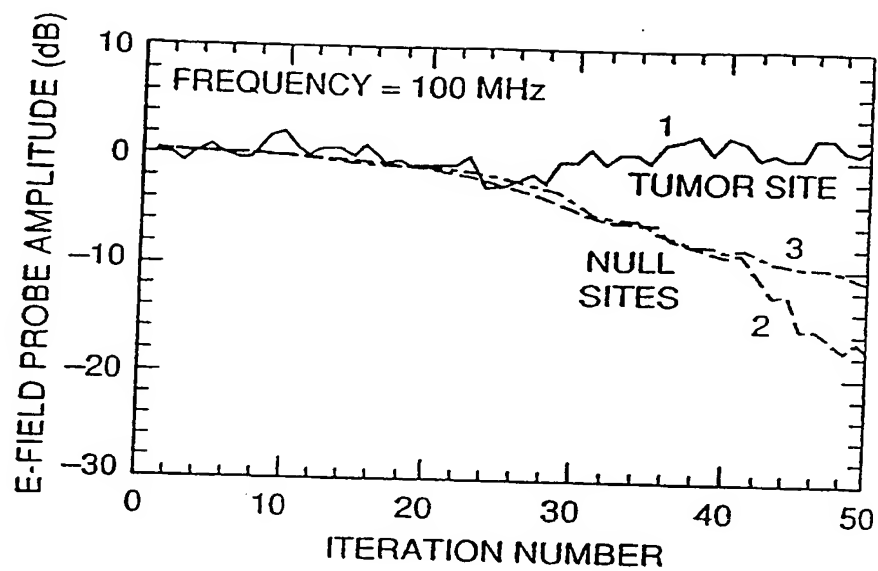
EXPERIMENTAL CONFIGURATION
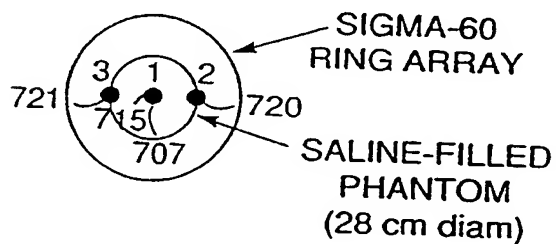
POSITION	COMMENT	PROBE
1	TUMOR SITE	EP-500
2	NULL SITE	EP-100
3	NULL SITE	EP-100

Fig. 45

SUBSTITUTE SHEET

FREQUENCY = 100 MHz   PHASE FOCUSING

PROBE MODEL # EP-100

(Graph: E-FIELD PROBE AMPLITUDE (dB) vs ITERATION NUMBER)

EXPERIMENTAL CONFIGURATION

SIGMA-60 RING ARRAY

720 — FOCUS

SALINE-FILLED PHANTOM (28 cm diam)
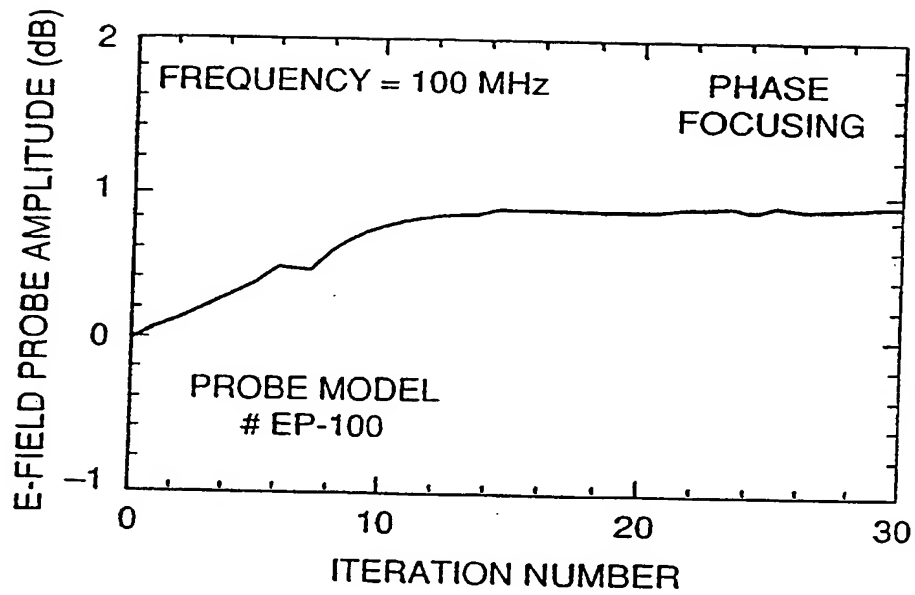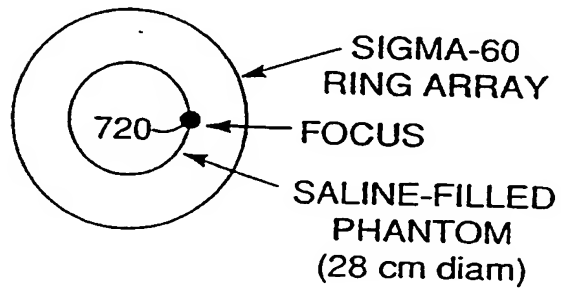
Fig. 46
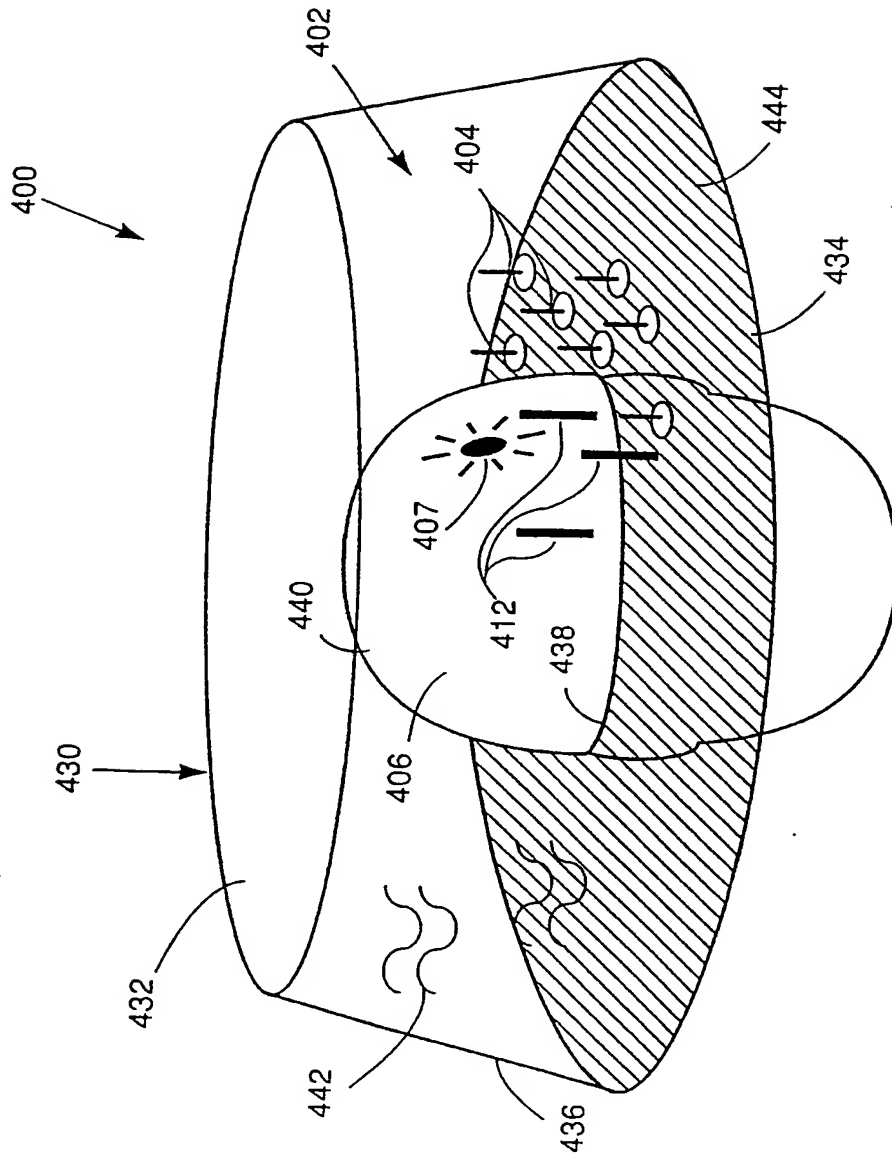
Fig. 47
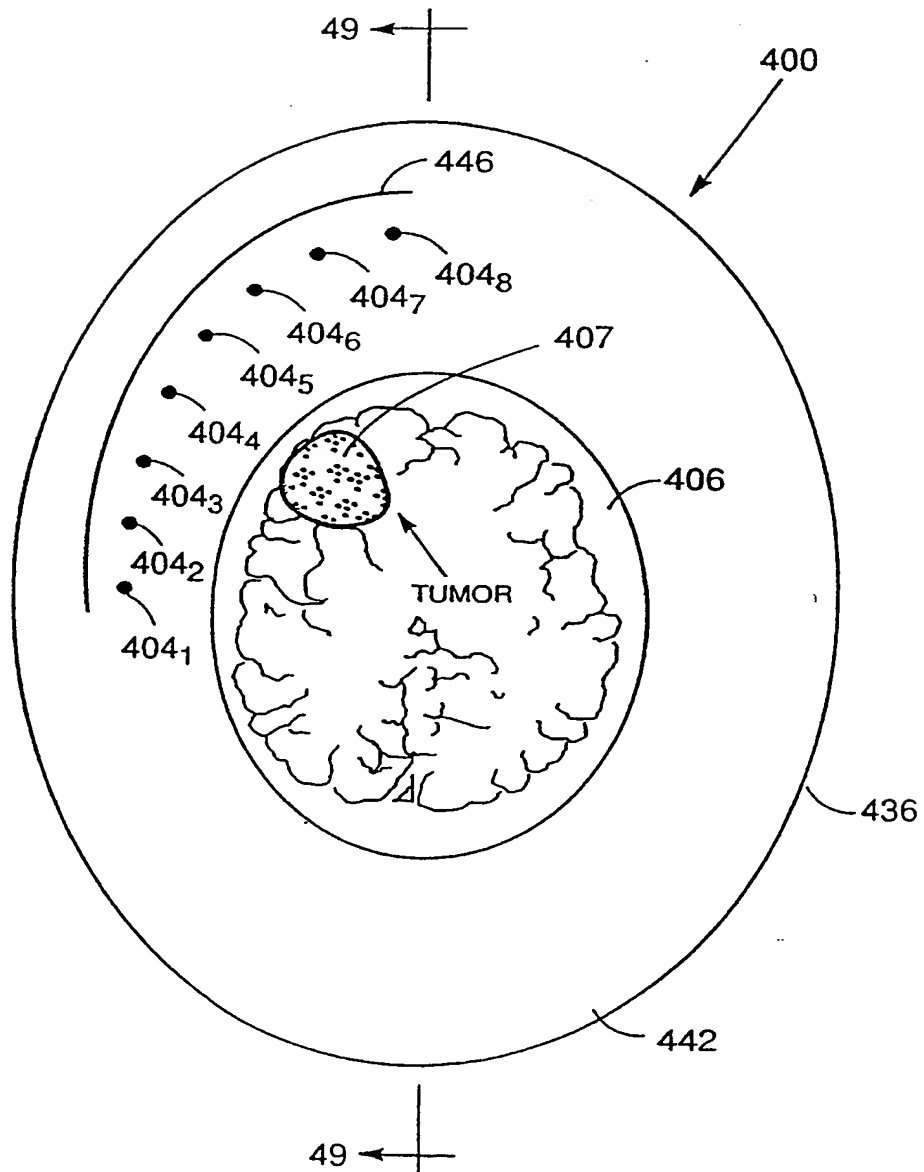
Fig. 48

SUBSTITUTE SHEET
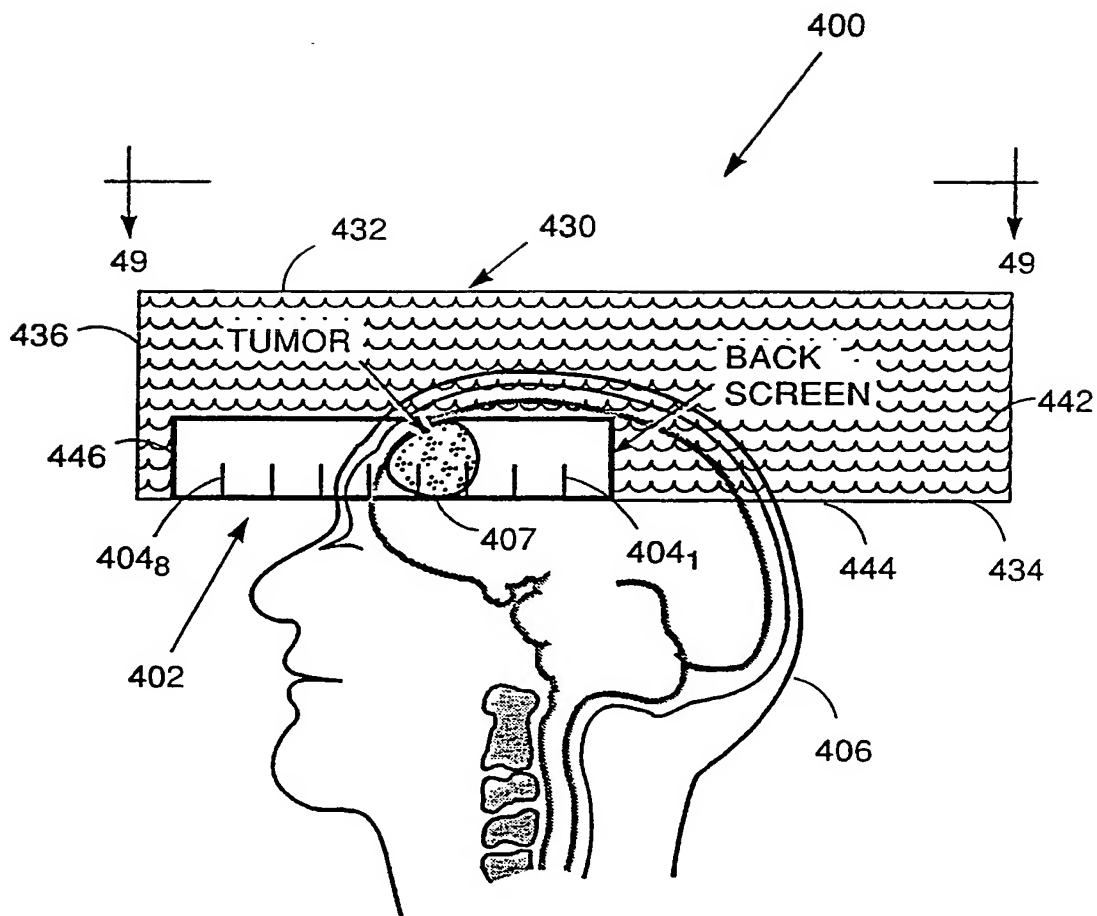
Fig. 49
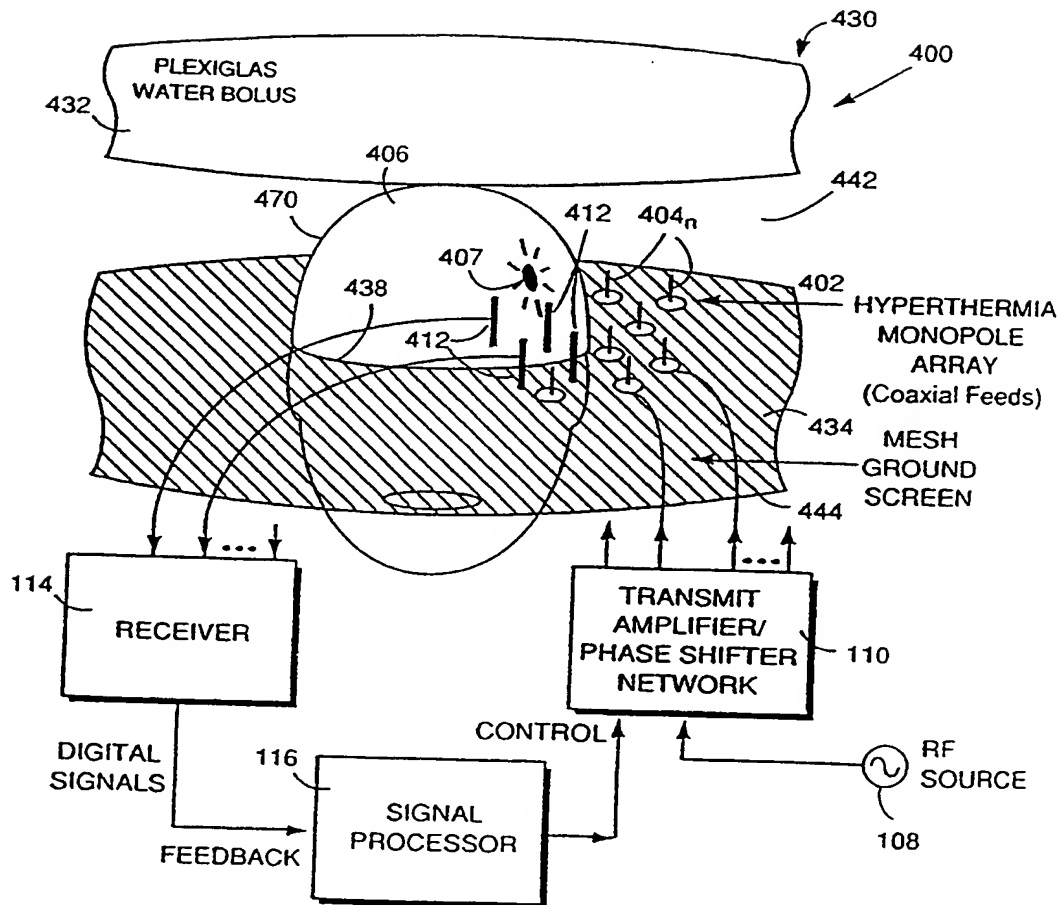
Fig. 50

SUBSTITUTE SHEET
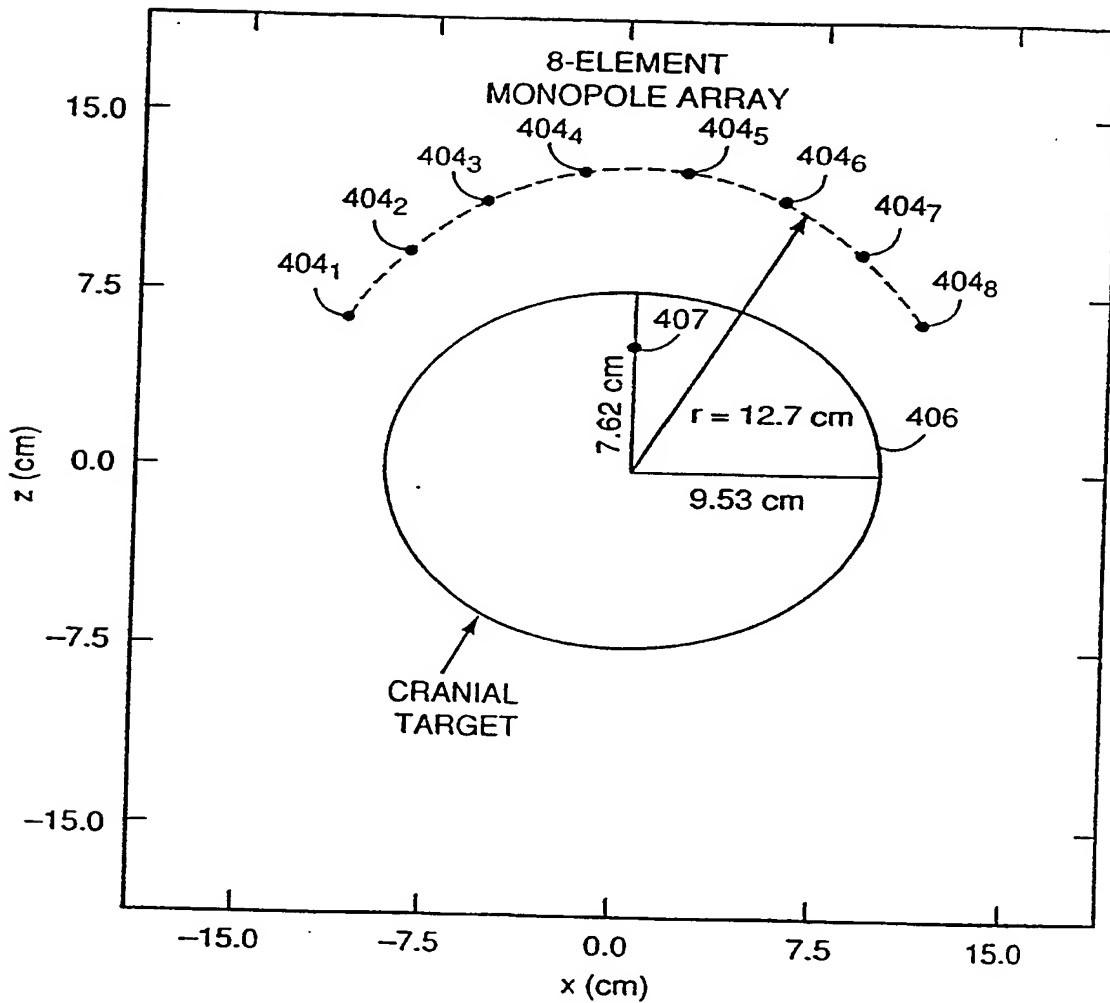
Fig. 51
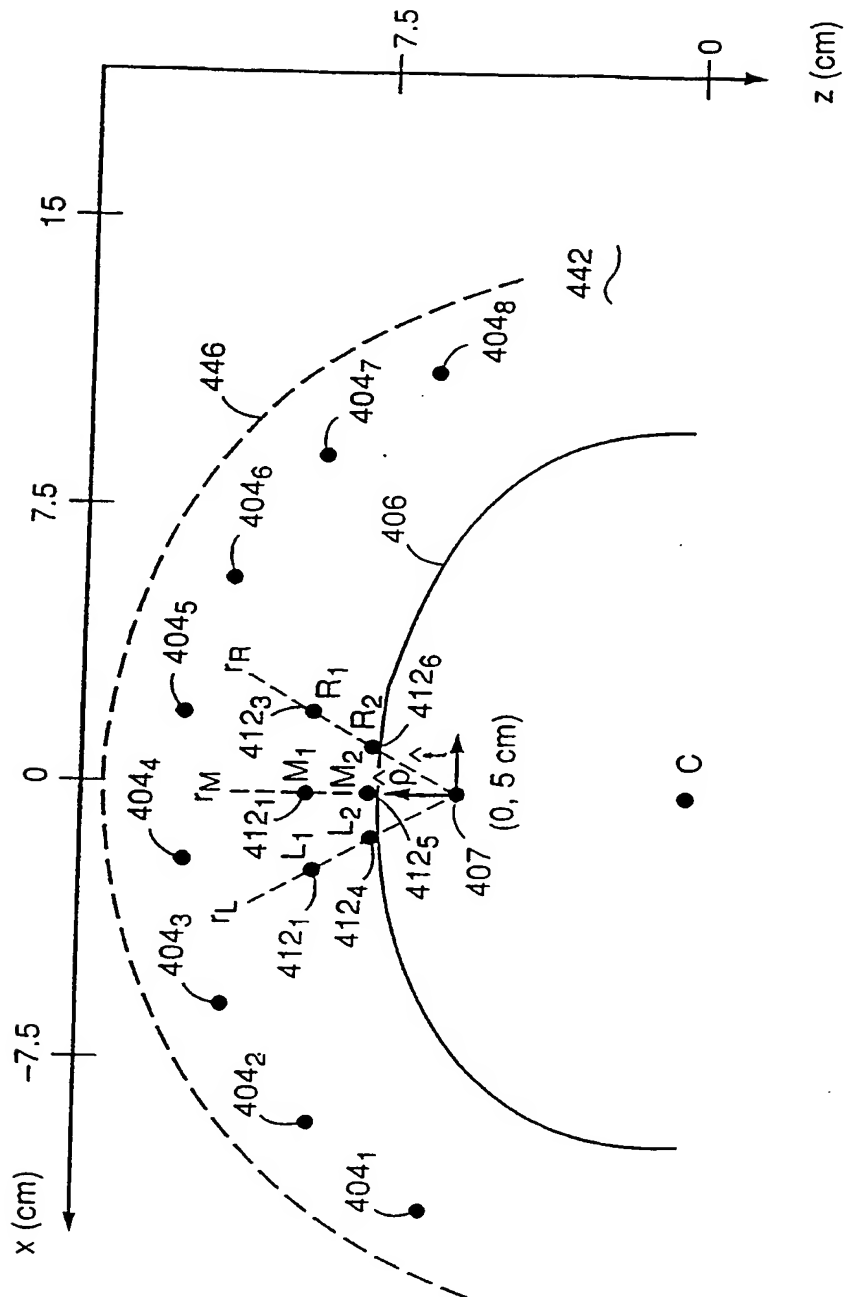
Fig. 52
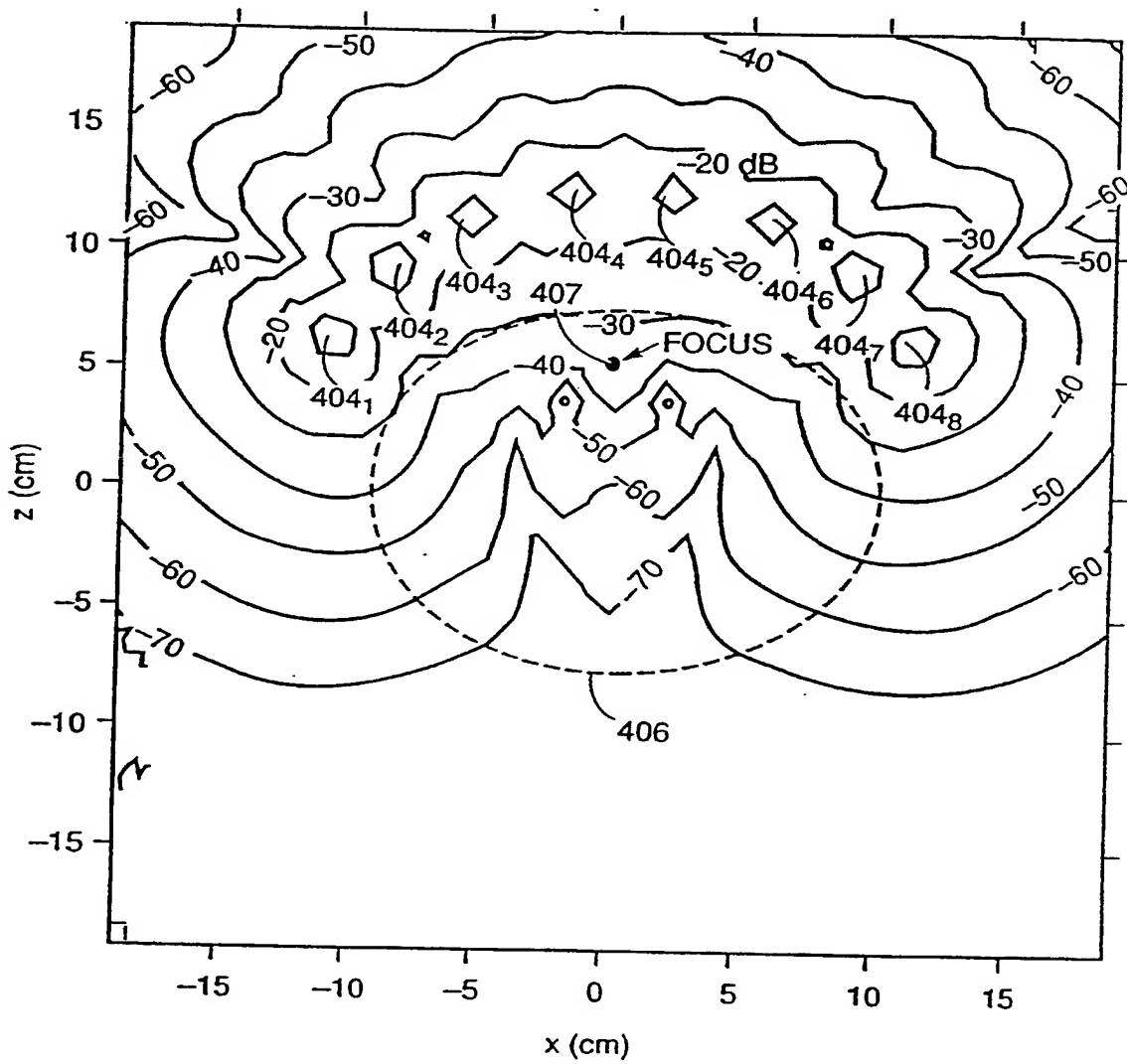
Fig. 53

FOCUS AT z = 5.08 cm, 915 MHz, ε_r = 50, σ = 1.3 S/m

MONOPOLE ARRAY
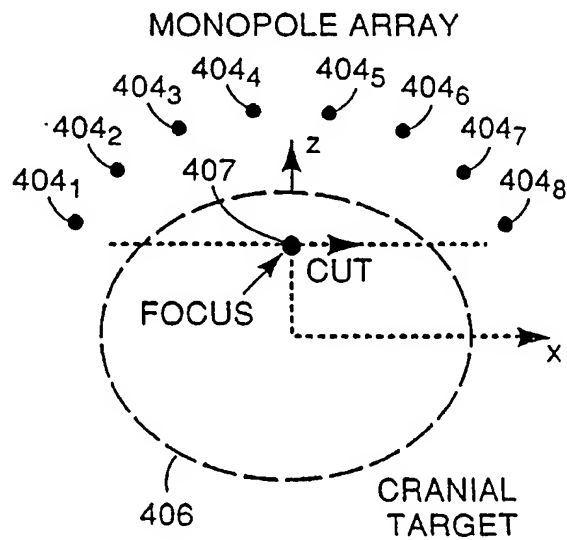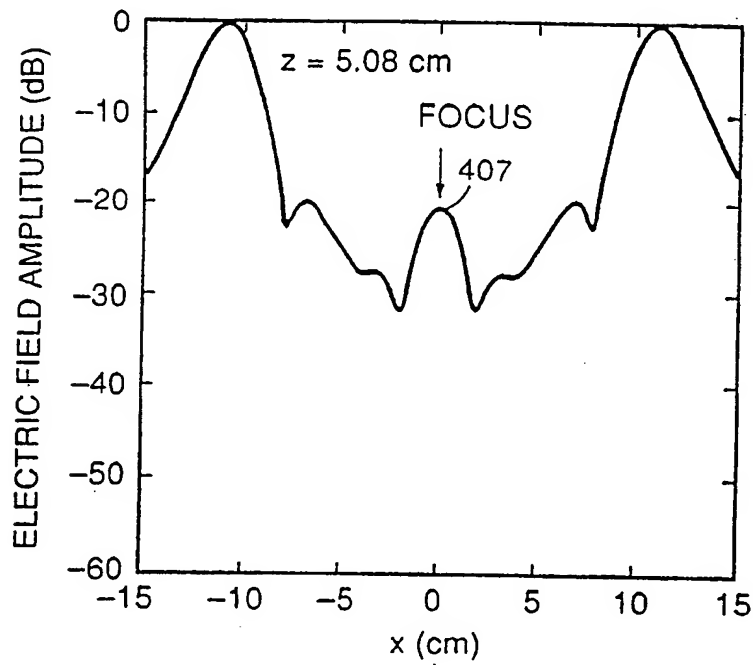
Fig. 54

SUBSTITUTE SHEET
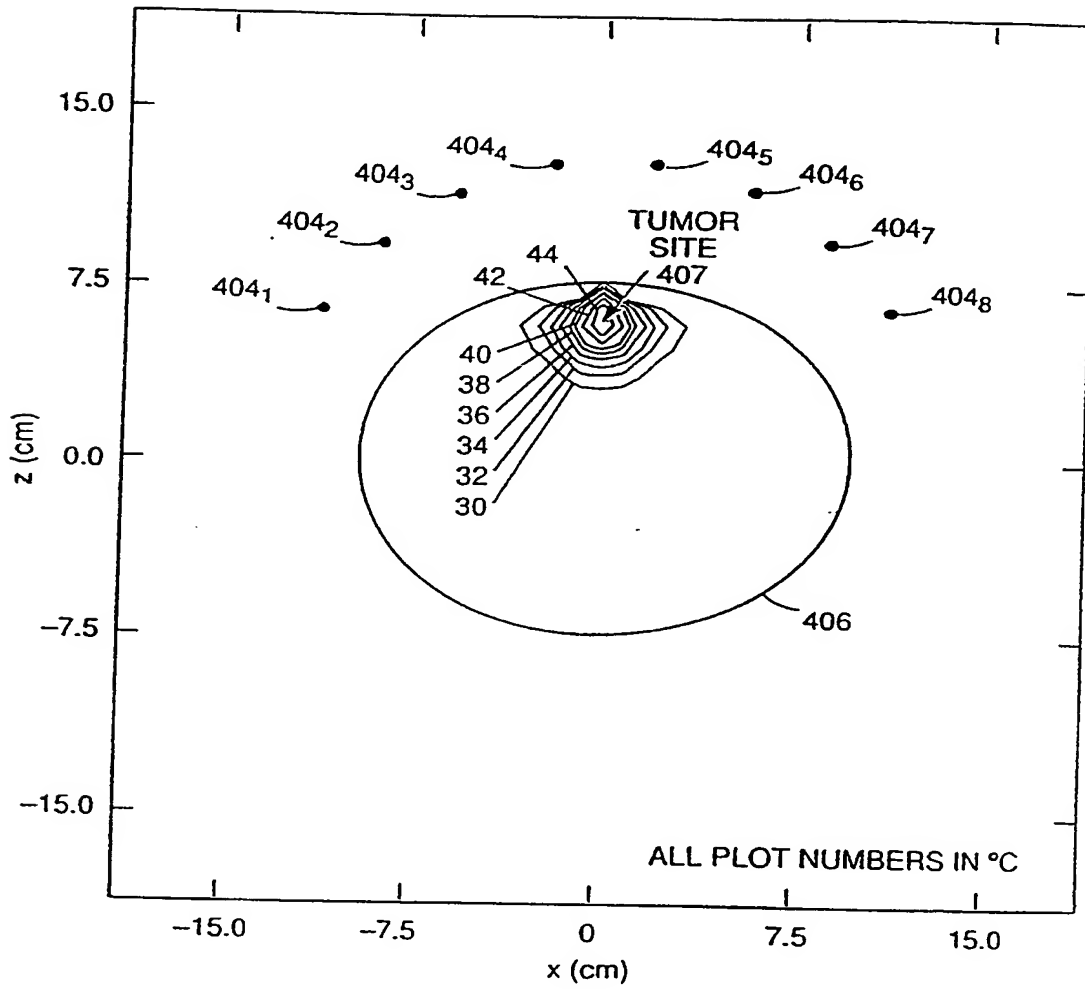
Fig. 55
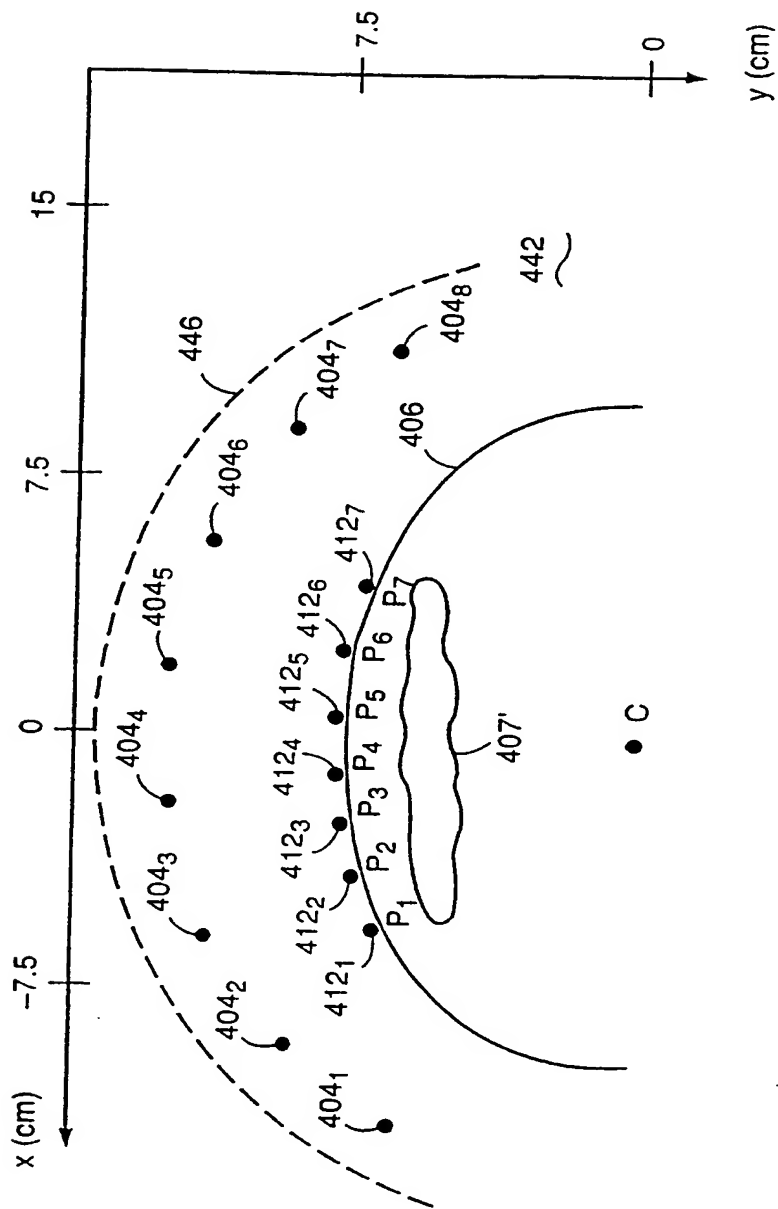
Fig. 56
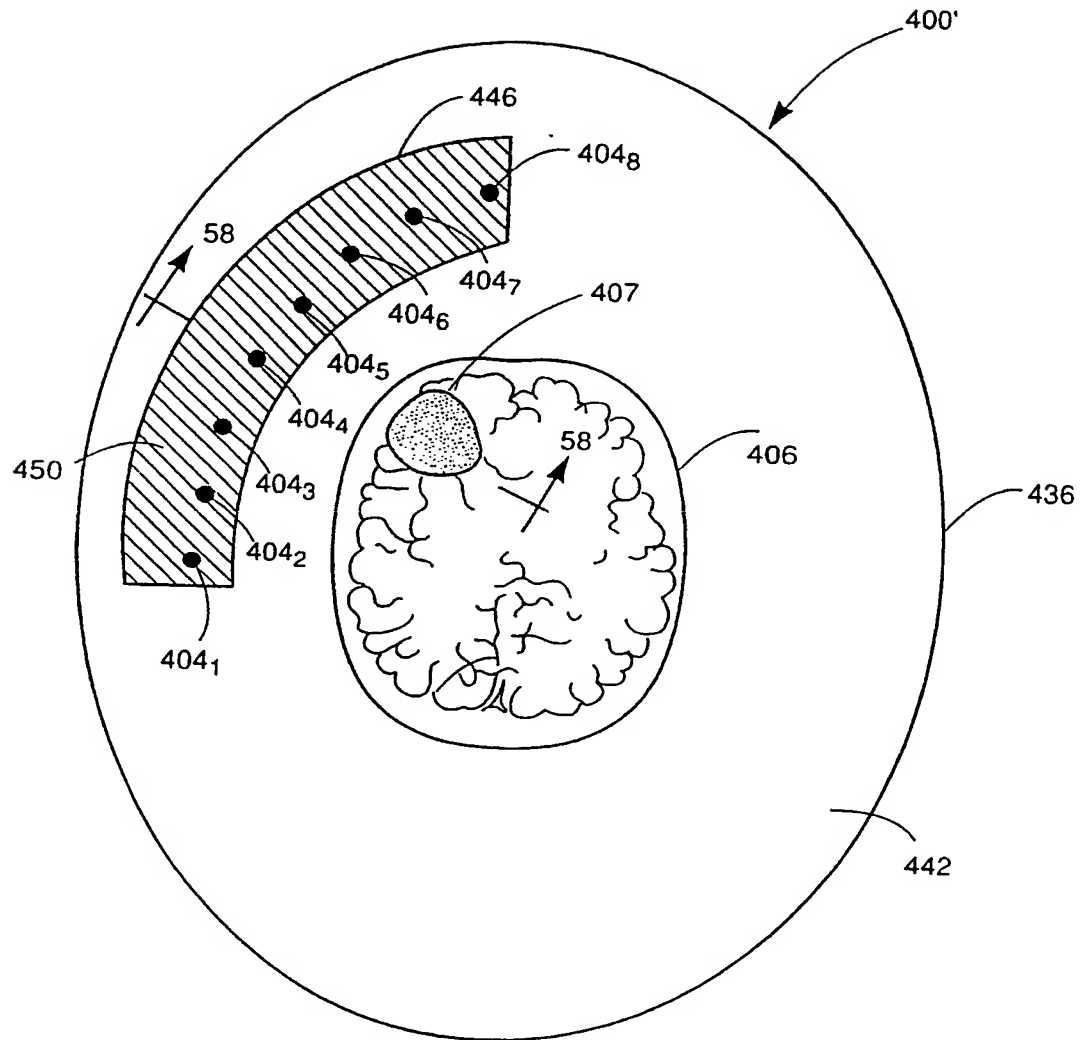
Fig. 57
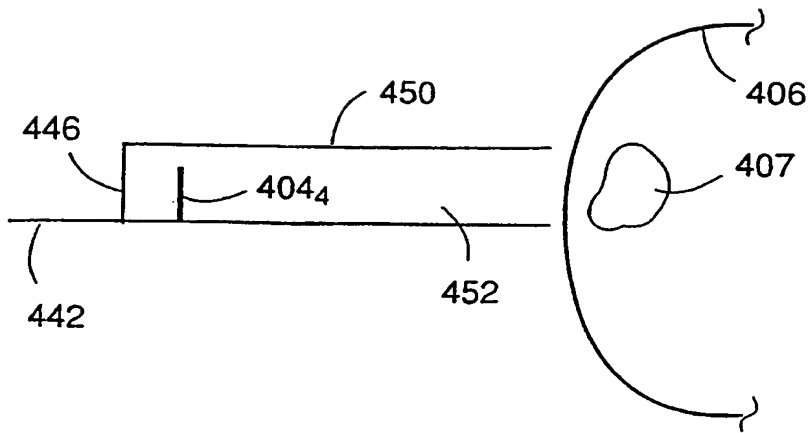
Fig. 58A
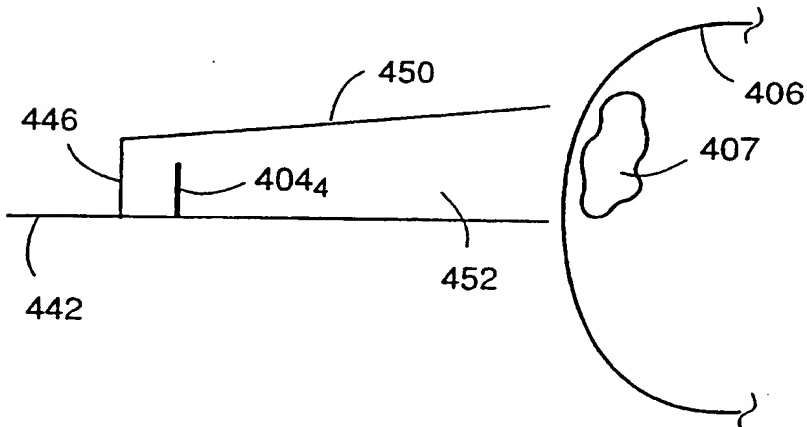
Fig. 58B
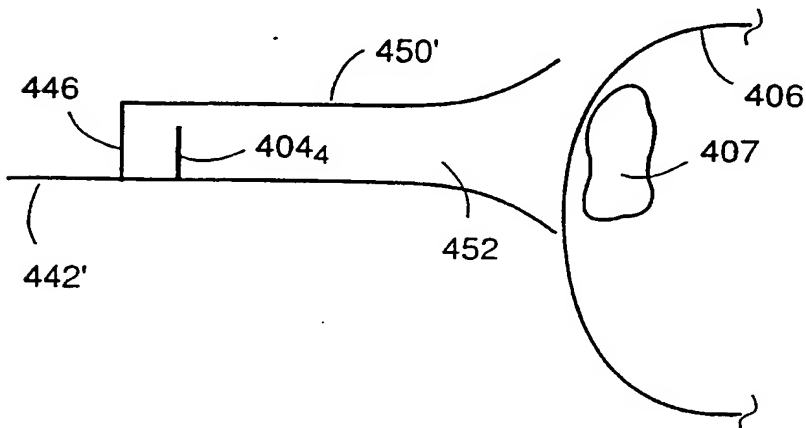
Fig. 58C
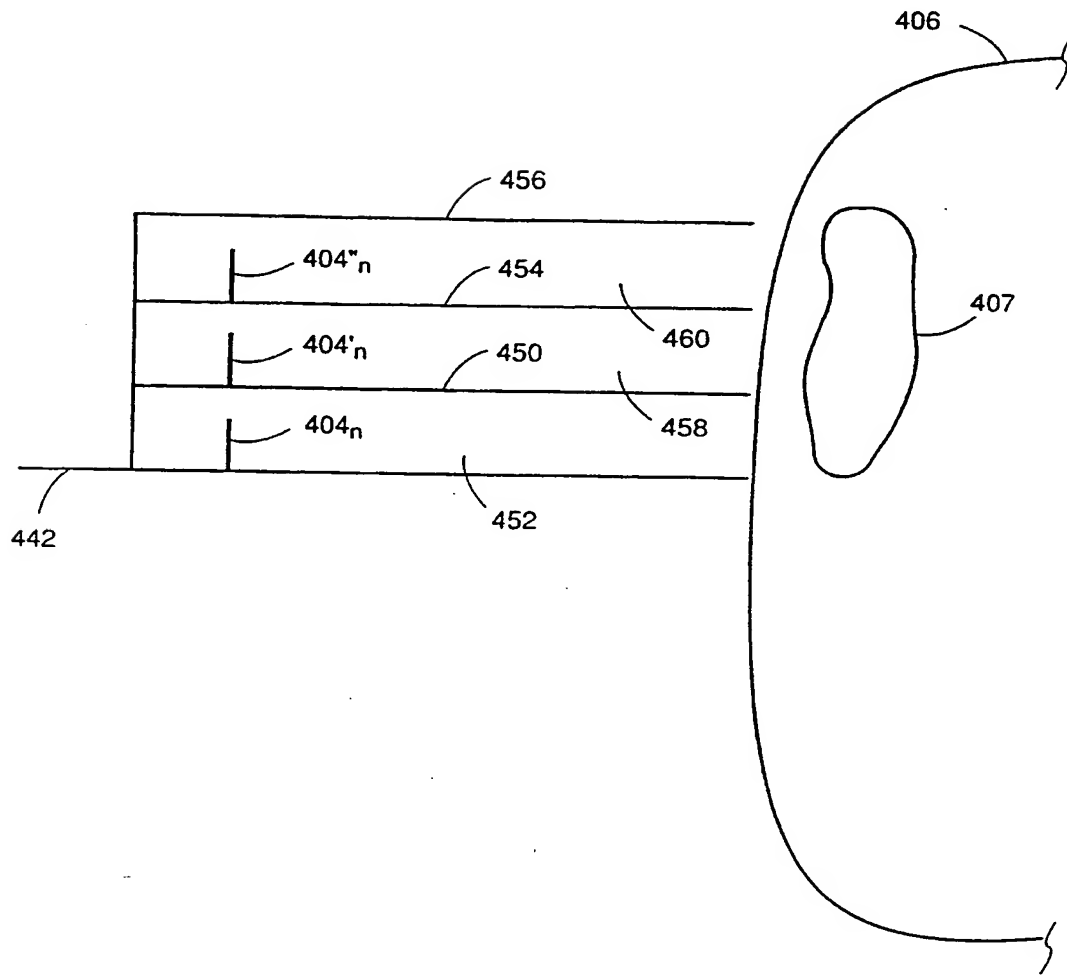
Fig. 59
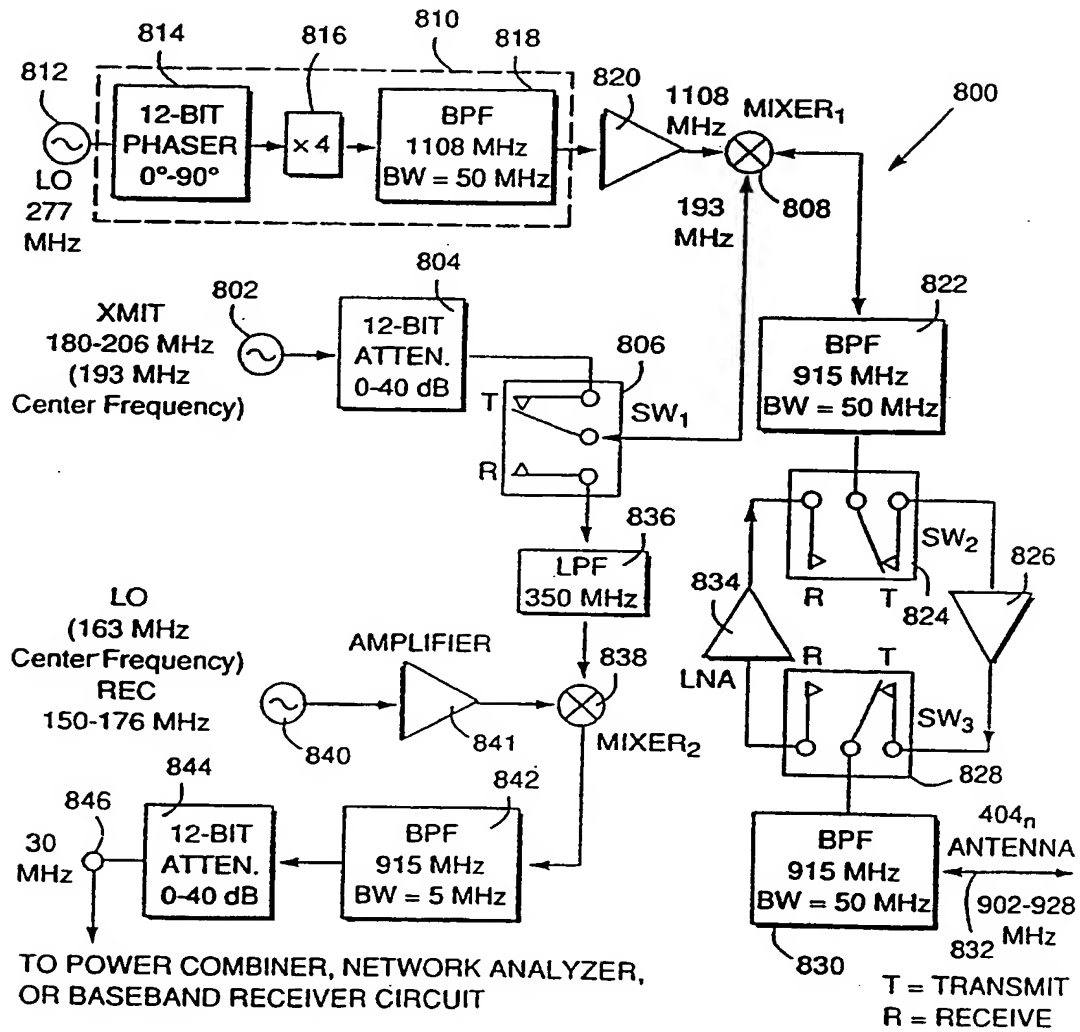
Fig. 60

I. CLASSIFICATION OF SUBJECT MATTER (if several classification symbols apply, indicate all)[6]

According to International Patent Classification (IPC) or to both National Classification and IPC

Int.Cl. 5 A61N5/02

II. FIELDS SEARCHED

Minimum Documentation Searched[7]

Classification System	Classification Symbols
Int.Cl. 5	A61N

Documentation Searched other than Minimum Documentation
to the Extent that such Documents are Included in the Fields Searched[8]

III. DOCUMENTS CONSIDERED TO BE RELEVANT[9]

Category[°]	Citation of Document,[11] with indication, where appropriate, of the relevant passages[12]	Relevant to Claim No.[13]
X	US,A,4 638 813 (TURNER) 27 January 1987 see column 6, line 15 - column 8, line 14	1-4 12-14, 20,21,25
A	see column 14, line 13 - column 15, line 26 ---	5-7
X	US,A,4 951 688 (KEREN) 28 August 1990 see the whole document ---	1-4, 12-14
X	US,A,4 974 587 (TURNER ET AL.) 4 December 1990 see column 4, line 21 - column 6, line 66 ---	13,20, 21,30
X	EP,A,0 256 524 (M/A-COM, INC.) 24 February 1988 see the whole document ---	1,2, 13-14
	-/--	

° Special categories of cited documents :[10]

"A" document defining the general state of the art which is not considered to be of particular relevance

"E" earlier document but published on or after the international filing date

"L" document which may throw doubts on priority claim(s) or which is cited to establish the publication date of another citation or other special reason (as specified)

"O" document referring to an oral disclosure, use, exhibition or other means

"P" document published prior to the international filing date but later than the priority date claimed

"T" later document published after the international filing date or priority date and not in conflict with the application but cited to understand the principle or theory underlying the invention

"X" document of particular relevance; the claimed invention cannot be considered novel or cannot be considered to involve an inventive step

"Y" document of particular relevance; the claimed invention cannot be considered to involve an inventive step when the document is combined with one or more other such documents, such combination being obvious to a person skilled in the art.

"&" document member of the same patent family

IV. CERTIFICATION

Date of the Actual Completion of the International Search	Date of Mailing of this International Search Report
08 OCTOBER 1992	2 2. 10. 92

International Searching Authority	Signature of Authorized Officer
EUROPEAN PATENT OFFICE	LEMERCIER D.L.L.

Category°	Citation of document, with indication, where appropriate, of the relevant passages	Relevant to Claim No.
A	IEEE TRANSACTIONS ON MICROWAVE THEORY AND TECHTNIQUES vol. 39, no. 5, May 1991, USA pages 798 - 808 JOHNSON ET AL. 'An experimental adaptive nulling receiver utilizing the sample matrix inversion algorithm with channel equalization' cited in the application see the whole document ---	8,29
A	EP,A,0 167 670 (SIEMENS) 15 January 1986 see page 3, line 4 - page 4, line 4 ---	13-17
A	DE,A,3 831 016 (REINBOLD) 15 March 1990 see column 3, line 56 - column 4, line 11 ---	15
A	GB,A,624 409 (GRELL) 8 June 1949 see the whole document ---	18
P,A	US,A,5 101 836 (LEE) 7 April 1992 see the whole document ---	20-25
A	WO,A,8 001 461 (TURNER) 24 July 1980 see page 11, line 34 - page 12, line 9 -----	1,5,12,13

III. DOCUMENTS CONSIDERED TO BE RELEVANT (CONTINUED FROM THE SECOND SHEET)

This annex lists the patent family members relating to the patent documents cited in the above-mentioned international search report.
The members are as contained in the European Patent Office EDP file on
The European Patent Office is in no way liable for these particulars which are merely given for the purpose of information. 08/10/92

Patent document cited in search report	Publication date	Patent family member(s)		Publication date
US-A-4638813	27-01-87	US-A-	4462412	31-07-84
		US-A-	4798215	17-01-89
		DE-A-	3176954	26-01-89
		EP-A,B	0048750	07-04-82
		EP-A,B	0208058	14-01-87
		WO-A-	8102841	15-10-81
		US-A-	5097844	24-03-92
		US-A-	4672980	16-06-87
		US-A-	4589423	20-05-86
		US-A-	4586516	06-05-86
US-A-4951688	28-08-90	None		
US-A-4974587	04-12-90	None		
EP-A-0256524	24-02-88	US-A-	4815479	28-03-89
		JP-A-	63073974	04-04-88
EP-A-0167670	15-01-86	US-A-	4682600	28-07-87
DE-A-3831016	15-03-90	None		
GB-A-624409		None		
US-A-5101836	07-04-92	None		
WO-A-8001461	24-07-80	US-A-	4271848	09-06-81
		EP-A-	0022824	28-01-81
		US-A-	4403618	13-09-83